Interactions between macroalgae and the sediment microbial community: Nutrient cycling within shallow coastal bays

---

A Dissertation

Presented to

The Faculty of the School of Marine Science

The College of William and Mary in Virginia

In Partial Fulfillment

Of the requirements for the Degree of

Doctor of Philosophy

By

Amber Kay Hardison

2009

APPROVAL SHEET

This dissertation is submitted in partial fulfillment of

the requirements for the degree of

Doctor of Philosophy

_____

Amber K. Hardison

Approved, by the Committee, November 2009

_____

Iris C. Anderson, Ph.D
Co-Advisor

_____

Elizabeth A. Canuel, Ph.D
Co-Advisor

_____

Mark Luckenbach, Ph.D

_____

Carl Friedrichs, Ph.D

_____

Karen J. McGlathery, Ph.D
University of Virginia
Charlottesville, Virginia

TABLE OF CONTENTS

ACKNOWLEDGEMENTS v

LIST OF TABLES vi

LIST OF FIGURES vii

ABSTRACT ix

CHAPTER 1: INTRODUCTION 2
Literature Cited 13

CHAPTER 2: AN EXPERIMENTAL APPARATUS FOR LABORATORY AND FIELD-BASED PERFUSION OF SEDIMENT POREWATER WITH DISSOLVED TRACERS 20
Abstract 21
Introduction 22
Methods 25
Results & Discussion 35
References 48

CHAPTER 3: BENTHIC ALGAE DETERMINE SEDIMENT ORGANIC MATTER COMPOSITION IN SHALLOW PHOTIC SEDIMENTS 69
Abstract 70
Introduction 72
Methods 74
Results 81
Discussion 86
Literature Cited 96

CHAPTER 4: CARBON AND NITROGEN DYNAMICS IN SHALLOW PHOTIC SYSTEMS: INTERACTIONS BETWEEN MACRO- AND MICROALGAL COMMUNITIES 121
Abstract 123
Introduction 125
Methods 127
Results 137
Discussion 141
Literature Cited 149

CHAPTER 5: FATE OF MACROALGAE IN BENTHIC SYSTEMS: CARBON AND NITROGEN CYCLING WITHIN THE MICROBIAL COMMUNITY 175
ABSTRACT 176
INTRODUCTION 177
METHODS 179
RESULTS 187
DISCUSSION 194
LITERATURE CITED 204

CHAPTER 6: SYNTHESIS 226
Literature Cited 230

APPENDIX A: CHAPTER 2 SF_6 DATA..... 235

APPENDIX B: CHAPTER 2 STABLE ISOTOPE DATA..... 236

APPENDIX C: CHAPTER 2 RHODAMINE DATA..... 238

APPENDIX D: CHAPTER 3 BULK, THAA CONCENTRATION DATA..... 241

APPENDIX E: CHAPTER 3 PLFA CONCENTRATION DATA..... 249

APPENDIX F: CHAPTER 4 BULK, THAA ISOTOPE DATA..... 263

APPENDIX G: CHAPTER 4 PLFA ISOTOPE DATA..... 266

APPENDIX H: CHAPTER 5 BULK, THAA ISOTOPE DATA..... 278

APPENDIX I: CHAPTER 5 PLFA ISOTOPE DATA..... 279

VITA 285

LIST OF TABLES

CHAPTER 3
Table 3-1: Parameters measured concurrently at Hog Island Bay field sites and in mesocosms. 104
Table 3-2: Results of two-factor repeated measures ANOVA. 105
Table 3-3 Mole percent individual amino acids of THAA. 106

CHAPTER 4
Table 4-1: Results of two-factor repeated measures ANOVA. 156
Table 4-2: Uptake and loss rates for label into bulk, THAA, and PLFA. 157
Table 4-3: Isotope inventory in macroalgae and sediments..... 158

CHAPTER 5
Table 5-1: Environmental parameters measured in the field and in the mesocosms..... 210
Table 5-2: Bulk sediment characterization parameters and statistical results from repeated measures ANOVA..... 211
Table 5-3: Statistical results for repeated measures ANOVA of isotopic enrichments. 212
Table 5-4. Fraction (%) of excess isotope (^{13}C or ^{15}N) in THAA, D-Ala, and PLFA out of excess isotope in bulk sediment. 213

LIST OF FIGURES

CHAPTER 2
Figure 2-1. Perfusionator diagram. 53
Figure 2-2. Plumbing schematic for field deployment. 55
Figure 2-3. Rhodamine WT concentrations for the laboratory test of the perfusionator. 57
Figure 2-4. SF_6 concentrations during outdoor mesocosm array experiment. 59
Figure 2-5. Bulk sediment isotopic enrichments for surface sediments (0-1 cm) during outdoor mesocosm array experiment. 61
Figure 2-6. SF6 concentrations during field deployment of the perfusionator. 63
Figure 2-7. Bulk sediment isotopic enrichments for surface sediments (0-1 cm) during the field deployment of the perfusionator. 65
Figure 2-8. Isotopic enrichment (δ15N) for porewater NH4+ during the field deployment of the perfusionator. 67

CHAPTER 3
Figure 3-1. Study site. 107
Figure 3-2. Macroalgal biomass (a) and benthic chlorophyll *a* concentrations for surface (0-1 cm) sediments (a). 109
Figure 3-3. Total nitrogen (a) and total organic carbon (b) concentrations and C/N (c) in surface (0-1 cm) sediments. 111
Figure 3-4. THAA (a) and total PLFA (b) concentrations in surface (0-1 cm) sediments. 113
Figure 3-5. Composition as mole percent of THAA for select HAA. 115
Figure 3-6. Concentrations of select algal and bacterial PLFA. 117
Figure 3-7. Score and loading results for PC1 and PC2 from PCA analyses. 119

CHAPTER 4
Figure 4-1. Map of study site. 159
Figure 4-2. Macroalgal biomass and isotopic enrichment. 161
Figure 4-3. Benthic chlorophyll *a* concentrations in a) Surface Water and b) Pore Water treatments. 163
Figure 4-4. Bulk sediment isotopes. 165
Figure 4-5. PLFA isotopic enrichments. 167
Figure 4-6. The bacteria-to-algae ratio (BAR). 169
Figure 4-7. THAA isotopic enrichments. 171
Figure 4-8. D-alanine isotopic enrichments. 173

CHAPTER 5
Figure 5-1. Study sites. 214

Figure 5-2. Bulk sediment isotopic enrichments for HIB (solid lines) and IWB (dotted lines)..... 216
Figure 5-3. Amino acid isotopic enrichments for HIB (solid line) and IWB (dotted line). 218
Figure 5-4. The ratio of excess ^{13}C (a) or ^{15}N (b) in D-Ala/L-Ala. 220
Figure 5-5. PLFA isotopic enrichments. 222
Figure 5-6. Proposed mechanism for microbial processing of dead macroalgal biomass within the sediments. 224

CHAPTER 6
Figure 6-1. Conceptual diagram summarizing macroalgal and sediment microbial interactions in a shallow coastal system. ……233

ABSTRACT

Ephemeral macroalgal blooms are considered a symptom of eutrophication in shallow coastal lagoons, but their influence on nutrient cycling dynamics in these systems is not fully understood. From 2006-2008, I conducted a series of experiments to determine the influence of living and senescent macroalgae on sediment carbon (C) and nitrogen (N) cycling in coastal lagoons along the Delmarva Peninsula, USA. In particular, I focused on how macroalgae affect the microbial community at the sediment-water interface of shallow subtidal sediments because this complex consortium of autotrophic (e.g. benthic microalgae, BMA) and heterotrophic (e.g. bacteria) organisms plays a critical role in nutrient cycling within these systems. To more accurately address microbial uptake of nutrients and organic matter from porewater and surface water sources, I designed and tested the "perfusionator," an experimental apparatus which allowed for continuous and homogenous perfusion of sediment porewater with dissolved tracers. I used the perfusionator in an outdoor mesocosm study to investigate the influence of benthic micro- and macroalgae on sediment organic matter quantity and quality using bulk and molecular level (total hydrolyzable amino acids, THAA; phospholipid linked fatty acids, PLFA) analyses. In a companion study, I further quantified C and N cycling by explicitly tracking C and N uptake into the sediments in the presence and absence of macroalgae using a dual stable isotope ($H^{13}CO_3^-$, $^{15}NH_4^+$) tracer approach in combination with isotope analyses of THAA and PLFA. Together, the studies demonstrated that BMA activity, which was dominated by diatoms according to PLFA biomarkers, increased storage of C and N in surface sediments, relative to dark treatments without BMA. BMA also increased the lability of sediment organic matter, which in turn resulted in observed increases in bacterial PLFA concentrations and isotopic incorporation. Efficient shuttling of C and N between BMA and bacteria in this system served as a mechanism for retention of C and N within the sediments. Macroalgae fundamentally altered sediment C and N cycling by decreasing sediment organic matter buildup. Macroalgae also sequestered C and N, but sediment C and N uptake decreased by ~40% when macroalgae were present. This was likely due to shading of the sediment surface by macroalgae, which decreased BMA production, which in turn decreased bacterial production. Although macroalgae are capable of sequestering significant amounts of nutrients, storage of C and N as macroalgal biomass is only temporary, as these blooms often exhibit a bloom and die-off cycle. In the final portion of this project, I traced C and N from senescing macroalgae into relevant sediment pools. A macroalgal die-off was simulated by the addition of freeze-dried macroalgae, pre-labeled with ^{13}C and ^{15}N, to sediment mesocosms. Bulk sediments took up label immediately following the die-off, and macroalgal C and N were retained in the sediments for >2 weeks. Approximately 6 to 50% and 2 to 9% of macroalgal N and C, respectively, were incorporated into the sediments. Label from the macroalgae appeared first in bacterial and then BMA biomarkers, suggesting that shuttling of macroalgal C and N between these communities may serve as a mechanism for retention of some macroalgal nutrients within the sediments. Together, these experiments suggest that ephemeral macroalgae diminish C and N uptake by the sediment microbial community, which may substantially impact the response of coastal bays to increased nutrient loading.

Interactions between macroalgae and the sediment microbial community: Nutrient cycling within shallow coastal bays

CHAPTER 1: INTRODUCTION

Eutrophication and primary producers in coastal lagoons

Projected changes in land use and population densities in coastal regions indicate that delivery of nutrients to coastal systems will increase considerably over the coming decades; consequently, nutrient pollution is a significant and urgent threat to the health of coastal systems globally (Nixon 1995, Howarth et al. 2000, NRC 2000). A great deal of research attempting to predict the response of coastal systems to nutrient enrichment has focused on relatively deep estuaries where primary production is dominated by phytoplankton (Cloern 2001). Less attention has been paid, however, to shallow coastal lagoons and estuaries, common to the East and Gulf coasts of the U.S. and constituting at least 13% of the world's coastline (Boynton et al. 1996). These shallow lagoons, typically 2-5 m deep, provide important societal and ecosystem functions. Coastal bays sustain recreational and commercial fisheries, support travel and tourism, and serve as an estuarine filter to incoming land-derived nutrients. Given their widespread global distribution and the important services that they perform, these bays require increased attention as the threat from anthropogenic changes along the coastal margin escalates.

Because most of the seafloor in coastal bays lies within the photic zone, benthic autotrophs such as seagrasses, macroalgae, and benthic microalgae (BMA) often dominate production. In many cases, as nutrient loading increases, the contribution from ephemeral macroalgae, phytoplankton, and epiphytes increases, whereas the importance of slow-growing perennial macrophytes such as seagrass decreases (Sand-Jensen & Borum 1991, Valiela et al. 1992, Duarte 1995, Hauxwell et al. 2001, Valiela & Cole 2002). For example, in Waquoit Bay, MA, ephemeral populations of green (*Cladophora*)

and red (*Gracilaria*) macroalgae replaced *Zostera marina* seagrass when nutrient (nitrogen) loading increased six-fold (Hauxwell et al. 2003). The mechanisms underlying this shift in autotrophic community structure relate to differences among plant types in nutrient uptake and growth strategies (Sand-Jensen & Borum 1991, Nielsen et al. 1996). BMA often contribute significantly to primary production within these shallow systems; however, their role as community structures shift in response to nutrient over-enrichment is not well understood.

The deleterious effects of macroalgae are not limited to replacement of seagrasses. When present in dense accumulations, macroalgal blooms have been associated with decreased diversity and biomass within the faunal and fish communities (Holmquist 1997, Hauxwell et al. 1998, Raffaelli 2000, Bowen & Valiela 2001, Deegan et al. 2002), which limits food available for upper trophic levels (i.e. birds, predatory fish, epibenthic crustaceans; Raffaelli 2000). Dense blooms have also interfered with recreational and commercial activities in coastal bays, as macroalgae can foul trawl nets, reduce waterway access, clog boat motors, and create beach debris (Raffaelli et al. 1998). A shift to macroalgal dominance is of important biogeochemical consequence as well, since coastal bays are hypothesized to function as a nutrient filter (McGlathery et al. 2007). The lagoons remove, transform, and retain nutrients, thereby buffering the immediate effects of external nutrient loading on water quality. This function is facilitated primarily by autotrophs because a significant fraction of nutrients, regardless of the level of eutrophication, passes through the autotrophic community (Sand-Jensen & Nielsen 2004). Macroalgae may potentially impact this filtering role directly by taking up, storing, and releasing nutrients and indirectly by competing with other autotrophs for

limiting resources (i.e. light, nutrients), thereby altering their role in the estuarine filter. The mechanisms by which increased eutrophication and the related shift to macroalgal dominance may impact the ability of lagoons to act as filters are currently unknown. My dissertation research aims to describe the influence of benthic macroalgae on nutrient cycling in temperate coastal bays in order to understand how increased nutrient loading (and the dominance of ephemeral macroalgae) might influence the ability of a shallow photic system to function as nutrient filters.

Benthic algae and nutrient cycling

A common symptom of eutrophication in shallow coastal bays is proliferation of ephemeral macroalgae, which often grow through a "boom-and-bust" cycle; biomass peaks in spring and then precipitously declines in mid- to late-summer, likely because high temperatures and self-shading negatively affect algal productivity (Peckol & Rivers 1995, McGlathery et al. 1997, Valiela et al. 1997, Bintz et al. 2003, Brush & Nixon 2003). These blooms, which can attain biomass up to 10 kg wet weight m^{-2} (Morand & Briand 1996), have been described in a variety of temperate and tropical locations (Harlin & Thornemiller 1981, Lapointe 1989, Lavery & Mccomb 1991, Sfriso et al. 1992, Valiela et al. 1997, Goshorn et al. 2001, McGlathery et al. 2001, Villares & Carballeira 2003). Macroalgae may directly and indirectly affect the ability of coastal bays to serve as nutrient filters by regulating the flows of carbon (C) and nitrogen (N) through the system, whether through uptake, storage, release, transformation, or competition with other autotrophs.

Macroalgae are extremely efficient at nutrient uptake and can store a significant fraction of nutrients (Thybo-Christesen et al. 1993, McGlathery et al. 1996, Pedersen et al. 2004). In Waquoit Bay, MA, macroalgal stored N was of the same magnitude as the annual N load from the watershed (Valiela et al. 1997). Thybo-Christesen and colleagues (1993) found that macroalgae in a shallow Danish bay took up ~95% of available N and 85% of available phosphorus. The ability of macroalgae to take up and store nutrients in excess of their growth demands is so effective that waters of heavily loaded coastal systems can actually appear oligotrophic (low nutrient, low chlorophyll concentrations), when macroalgae are present (Thybo-Christesen et al. 1993, Peckol et al. 1994). Due to the capabilities of macroalgae to efficiently sequester nutrients and to grow in dense accumulations, it is expected that ephemeral macroalgae may compete with BMA for nutrients and/or light (Valiela et al. 1997, McGlathery et al. 2001, Tyler et al. 2003).

BMA and autotrophic bacteria (e.g. cyanobacteria) are limited by bottom-up forcings such as light and nutrients (Hillebrand & Sommer 2000, Stutes et al. 2006) as well as top-down control by grazers; however, light availability is thought to be the primary factor regulating BMA community growth (Heip et al. 1995). Macroalgae have been shown to "self-shade;" light is attenuated within the layers of an algal mat (Peckol & Rivers 1996), affecting overall mat metabolism (Brush & Nixon 2003). Self-shading has been suggested as a possible cause for mid-summer macroalgal mat crashes that have been observed in numerous systems (e.g. Sfriso et al. 1992, McGlathery et al. 2001). Thus, shading of plants such as seagrass below dense macroalgal mats has been suggested as a mechanism by which macroalgal blooms have contributed to global

seagrass declines (Hauxwell et al. 2001). It is also likely that shading of the sediment surface by macroalgae will reduce BMA production.

Since macroalgae reside at the sediment surface, they can potentially influence nutrients available at the sediment-water interface, a zone of intense biogeochemical activity, mediated by autotrophic and heterotrophic microbes. However, to date, few studies have focused directly on the influence of macroalgae on nutrient cycling within the sediment microbial community. Benthic flux studies have revealed that macroalgae play a major role regulating nutrient cycling at the sediment surface. For example, McGlathery and colleagues (2001) used dissolved inorganic carbon (DIC) fluxes to document that BMA production increased following a macroalgal decline, suggesting competition between macroalgae and BMA, possibly for light and/or nutrients. Dalsgaard (2003) measured lower denitrification rates in the presence of macroalgae, presumably because macroalgae out-competed sediment denitrifiers for water column nitrate. Tyler and colleagues (2003) found that macroalgal uptake resulted in an uncoupling of sediment-water column interactions by controlling the exchange of dissolved inorganic nitrogen (DIN) as well as dissolved organic nitrogen (DON) between the sediments and water column. While measurements of benthic fluxes provide information about the net results of processes occurring at the sediment-water interface, it has been difficult to further describe the microbial "black box" within the sediments using flux data alone.

My work builds upon these studies to more explicitly track C and N within the sediments. In Chapter 3, I examined the influence of benthic micro- and macroalgae on C and N storage within the sediments, and in Chapter 4, I directly tracked the uptake and cycling of C and N by BMA and sediment bacteria in the presence and absence of living

macroalgae. At the sediment-water interface of these shallow systems, nutrients in the water column as well as the sediment porewater are available for uptake by benthic autotrophs. Thus, for the experiment that I describe in Chapters 3 and 4, I designed an experimental apparatus that allowed the introduction of dissolved nutrients simultaneously via the surface water and porewater. In Chapter 2, I describe the "perfusionator," an innovative apparatus that allows continual long-term perfusion of sediment porewater with dissolved tracers in a mesocosm or a field setting.

Fate of macroalgal biomass

By definition, ephemeral macroalgal blooms cannot serve as a permanent reservoir for C and N. Consequently, understanding the fate of macroalgal C and N following a die-off, rather than the uptake of the nutrients alone, is critical when evaluating nutrient cycling processes within coastal bays. Studies of macroalgal bloom decay have demonstrated rapid breakdown of biomass, resulting in release of both inorganic and organic nutrients to the water column (Buchsbaum et al. 1991, Tyler et al. 2001, Castaldelli et al. 2003, Garcia-Robledo et al. 2008), supporting phytoplankton and bacterial metabolism (Sfriso et al. 1992, Valiela et al. 1997, McGlathery et al. 2001, Nedergaard et al. 2002).

Fewer studies have focused on macroalgal decay within the sediments (Nedergaard et al. 2002, Lomstein et al. 2006, Rossi 2007, Garcia-Robledo et al. 2008), where heterotrophic bacterial densities are significantly higher than in the water column (Deming & Baross 1993, Schmidt et al. 1998, Ducklow 2000). In addition, most of the

sediment studies have been conducted in low or no light environments even though light is typically available to shallow sediments where macroalgal die-offs occur, and sediment biogeochemistry is largely affected by BMA activity (Underwood & Kromkamp 1999). While nutrients associated with senescent macroalgal blooms are recycled and can have a positive feedback on phytoplankton production in the water column, nutrients released during macroalgal decay in the sediments may support BMA and bacterial production, which intercept the return of nutrients to the overlying water column. If shallow-water sediments, thus, behave as a nutrient "filter" the response by phytoplankton may be reduced, and benthic production could effectively buffer the system from further eutrophication. In Chapter 5, I tracked macroalgal C and N after a simulated macroalgal die-off in order to better quantify the input and retention of macroalgae-associated nutrients in the sediments.

Approach

In order to determine how ephemeral macroalgal blooms altered sediment organic matter (C, N pools), I used a number of geochemical tools to distinguish the various organic matter sources to the sediments. Stable isotopes and biomarkers are tools that can be used separately or in combination to study the cycling of organic matter. Natural abundance levels of stable isotopes are useful for discriminating between sources in systems characterized by a limited number of sources, each with distinct stable isotopic signatures (e.g. Cloern et al. 2002). Deliberate addition of stable isotope labels is another approach for following the flow of specific sources through transformation pathways. In

this approach, a substrate that is highly enriched in the heavier isotope is added to the system. This "label" is then tracked through various pools to quantify the flow of the label through the system. Laboratory and field-based isotope label additions have lent insight into a variety of nutrient cycling processes (e.g. Bronk et al. 1994, Middelburg et al. 2000, Naldi & Wheeler 2002, Tobias et al. 2003, Veuger et al. 2007). I used stable isotope tracers in Chapter 2 to test the performance of the perfusionator apparatus at delivering dissolved tracers to the microbial community living at the sediment surface and in Chapters 4 and 5 to track C and N uptake into bulk sediments.

Biomarkers are organic compounds that have source specificity due to inherent structural characteristics and, like stable isotopes, often allow resolution between organic matter sources (Killops & Killops 1993). Lipids, a class of biomarkers that includes fatty acids and sterols, have been used in a number of systems to determine sediment organic matter sources over various temporal and spatial scales (e.g. Canuel & Martens 1993, Yunker & Macdonald 1995, Zimmerman & Canuel 2000, Schefuss et al. 2004). Phospholipid-linked fatty acids (PLFA) are particularly useful for studying active microbial populations because they are a component of both bacterial and eukaryotic cell walls and they represent viable organic matter since they turn over rapidly after cell death (Parkes 1987). Hydrolyzable amino acids (HAA), a class of organic compounds found in proteins, are often used to describe the degradation state of organic matter (Dauwe & Middelburg 1998); however, their application as specific biomarkers is limited due to low source specificity. A noted exception is that amino acids can be present as D- and L-stereoisomers, and D-AA can be used as bacterial biomarkers since they are only

produced by bacteria. In Chapter 3, I combined bulk and molecular-level (biomarker) analyses to characterize the sediment organic matter of my experimental system.

Compound-specific isotope analysis (CSIA), measuring the isotopic composition of a particular biomarker, is perhaps one of the most powerful geochemical tools available to unambiguously trace C and N through a system. CSIA is commonly used in microbial ecology because it provides the best tool for tracing C and N into microbial biomarkers (Bouillon & Boschker 2006); quantitative separation of bacteria and BMA from sediments is otherwise impossible. Deliberately adding isotopic tracers and following them into biomarkers affords the possibility to directly link microbial identity (biomarker) with activity (isotope assimilation). CSIA of PLFA, and recently, HAA, have allowed for explicit tracking of C and N into specific pools within the sediment microbial community (Boschker & Middelburg 2002, Veuger et al. 2005, Veuger et al. 2007). I applied the same methodology to my experiments presented in Chapters 4 and 5 to measure the uptake and cycling of C and N by the sediment microbial community.

Study Sites

This study focused primarily on Hog Island Bay, Virginia, a coastal lagoon located along the Delmarva Peninsula, within the Virginia Coast Reserve, a Long-Term Ecological Research site. The coastal bays along the Delmarva Peninsula are typical of temperate lagoons along the U.S. coast. They are shallow, on average less than 2 m deep at mean low water, and are characterized by benthic autotrophs such as seagrass, macroalgae, and BMA (Goshorn et al. 2001, McGlathery et al. 2001, Volkman et al.

2008). The coastal lagoons of the Delmarva Peninsula exist along a eutrophication gradient (Giordano et al. Submitted), with greater development and agriculture contributing to elevated nutrient loads in the northern lagoons compared to the southern lagoons. Hog Island Bay is located at the less degraded end of that gradient, with lower nutrient (N) loadings (14 kg N ha^{-1} y^{-1}; Anderson et al. In press) due to less development (Stanhope et al. 2009). As a result, macroalgae are present locally and only dominant during brief portions of the year (McGlathery et al. 2001). In chapter 5, as a contrast to Hog Island Bay, sediments and macroalgae were also collected from Isle of Wight Bay, Maryland, located at the more degraded end of the eutrophication gradient, with N loads of 65 kg N ha^{-1} y^{-1} (Boynton et al. 1996) due to extensive development within its watershed and inputs from the highly impacted St. Martin's River (Wazniak et al. 2004). As a result, ephemeral macroalgal blooms are present in high densities in Isle of Wight Bay, and it ranks among Maryland's more degraded lagoons (Wazniak et al. 2004).

Literature Cited

Anderson IC, Stanhope JW, Hardison AK, McGlathery KJ (In press) Sources and fates of nitrogen in Virginia Coastal Bays. In: Kennish MJ, Paerl HW (eds) Coastal Lagoons: Critical Habitats of Environmental Change. Taylor and Francis

Bintz JC, Nixon SW, Buckley BA, Granger SL (2003) Impacts of temperature and nutrients on coastal lagoon plant communities. Estuaries 26:765-776

Boschker HTS, Middelburg JJ (2002) Stable isotopes and biomarkers in microbial ecology. FEMS Microbiology Ecology 40:85-95

Bouillon S, Boschker HTS (2006) Bacterial carbon sources in coastal sediments: a cross-system analysis based on stable isotope data of biomarkers. Biogeosciences 3:175-185

Bowen JL, Valiela I (2001) The ecological effects of urbanization of coastal watersheds: historical increases in nitrogen loads and eutrophication of Waquoit Bay estuaries. Canadian Journal of Fish and Aquatic Science 58:1489-1500

Boynton WR, Hagy JD, Murray L, Stokes C, Kemp WM (1996) A comparative analysis of eutrophication patterns in a temperate coastal lagoon. Estuaries 19:408-421

Bronk DA, Glibert PM, Ward BB (1994) Nitrogen Uptake, Dissolved Organic Nitrogen Release, and New Production. Science 265:1843-1846

Brush MJ, Nixon SW (2003) Biomass layering and metabolism in mats of the macroalga Ulva lactuca L. Estuaries 26:916-926

Buchsbaum R, Valiela I, Swain T, Dzierzeski M, Allen S (1991) Available and refractory nitrogen in detritus of coastal vascular plants and macroalgae. Marine Ecology Progress Series 72:131-143

Canuel EA, Martens CS (1993) Seasonal-Variations in the Sources and Alteration of Organic-Matter Associated with Recently-Deposited Sediments. Organic Geochemistry 20:563-577

Castaldelli G, Welsh DT, Flachi G, Zucchini G, Colombo G, Rossi R, Fano EA (2003) Decomposition dynamics of the bloom forming macroalga Ulva rigida C. Agardh determined using a C-14-carbon radio-tracer technique. Aquatic Botany 75:111-122

Cloern JE (2001) Our evolving conceptual model of the coastal eutrophication problem. Marine Ecology Progress Series 210:223-253

Cloern JE, Canuel EA, Harris D (2002) Stable carbon and nitrogen isotope composition of aquatic and terrestrial plants of the San Francisco Bay estuarine system. Limnology and Oceanography 47:713-729

Dalsgaard T (2003) Benthic primary production and nutrient cycling in sediments with benthic microalgae and transient accumulation of macroalgae. Limnology and Oceanography 48:2138-2150

Dauwe B, Middelburg JJ (1998) Amino acids and hexosamines as indicators of organic matter degradation state in North Sea sediments. Limnology and Oceanography 43:782-798

Deegan LA, Wright A, Ayvazian SG, Finn JT, Golden H, Rand Merson R, Harrison J (2002) Nitrogen loading alters seagrass ecosystem structure and support of higher trophic levels. Aquatic Conservation: Marine and Freshwater Ecosystems 12:193-212

Deming JW, Baross JA (1993) The Early Diagenesis of Organic Matter: Bacterial Activity. In: Engel MH, Macko SA (eds) Organic Geochemistry. Plenum Press, New York, p 119-144

Duarte CM (1995) Submerged Aquatic Vegetation in Relation to Different Nutrient Regimes. Ophelia 41:87-112

Ducklow H (2000) Bacterial Production and Biomass in the Oceans. In: Kirchman DL (ed) Microbial Ecology of the Oceans. Wiley-Liss, Inc., New York, p 85-120

Garcia-Robledo E, Corzo A, de Lomas JG, van Bergeijk SA (2008) Biogeochemical effects of macroalgal decomposition on intertidal microbenthos: a microcosm experiment. Marine Ecology-Progress Series 356:139-151

Giordano JCP, Brush MJ, Anderson IC (Submitted) Extending the Delmarva eutrophication gradient into Virginia's coastal lagoons: watershed modeling and nitrogen source tracking. Estuaries and Coasts

Goshorn D, McGinty M, Kennedy C, Jordan C, Wazniak C, Schwenke K, Coyne K (2001) An examination of benthic macroalgae communities as indicators of nutrients in middle atlantic coastal estuaries -- Maryland component Final Report 1998-1999, Maryland Department of Natural Resources, Annapolis, MD

Harlin MM, Thornemiller M (1981) Nutrient enrichment of seagrass beds in a Rhode Island coastal lagoon. Marine Biology 65:221.

Hauxwell J, Cebrian J, Furlong C, Valiela I (2001) Macroalgal canopies contribute to eelgrass (*Zostera marina*) decline in temperate estuarine ecosystems. Ecology 82:1007-1022

Hauxwell J, Cebrian J, Valiela I (2003) Eelgrass *Zostera marina* loss in temperate estuaries: relationship to land-derived nitrogen loads and effect of light limiataion imposed by algae. Marine Ecology Progress Series 247:59-73

Hauxwell J, McClelland J, Behr PJ, Valiela I (1998) Relative importance of grazing and nutrient controls of macroalgal biomass in three temperate shallow estuaries. Estuaries 21:347-360

Heip C, Goosen NK, Herman P, Kromkamp JC, Middelburg JJ, Soetaert K (1995) Production and consumption of biological particles in temperate tidal estuaries. Oceanography and Marine Biology Annual Reviews 33

Hillebrand H, Sommer U (2000) Marine microbenthic community structure regulated by nitrogen loading and grazing pressure. Marine Ecology Progress Series 204:27-38

Holmquist JG (1997) Disturbance and gap formation in a marine benthic mosaic: influence of shifting macroalgal patches on seagrass structure and mobile invertebrates. Marine Ecology-Progress Series 158:121-130

Howarth RW, Anderson D, Cloern JE, Elfring C, Hopkinson C, Lapointe B, Malone T, Marcus N, McGlathery KJ, Sharpley A, Walker D (2000) Nutrient pollution of coastal rivers, bays, and seas. Issues in Ecology 7:1-14

Killops SD, Killops VJ (1993) An Introduction to Organic Geochemistry, Vol. John Wiley & Sons, Inc., New York

Lapointe BE (1989) Macroalgal Production and Nutrient Relations in Oligotrophic Areas of Florida Bay. Bulletin of Marine Science 44:312-323

Lavery PS, Mccomb AJ (1991) Macroalgal Sediment Nutrient Interactions and Their Importance to Macroalgal Nutrition in a Eutrophic Estuary. Estuarine Coastal and Shelf Science 32:281-295

Lomstein BA, Guldberg LB, Neubauer ATA, Hansen J, Donnelly A, Herbert RA, Viaroli P, Giordani G, Azzoni R, de Wit R, Finster K (2006) Benthic decomposition of Ulva lactuca: A controlled laboratory experiment. Aquatic Botany 85:273-283

McGlathery K, Sundback K, Anderson I (2007) Eutrophication in shallow coastal bays and lagoons: the role of plants in the coastal filter. Marine Ecology-Progress Series 348:1-18.

McGlathery KJ, Anderson IC, Tyler AC (2001) Magnitude and variability of benthic and pelagic metabolism in a temperate coastal lagoon. Marine Ecology-Progress Series 216:1-15

McGlathery KJ, Krause-Jensen D, Rysgaard S, Christensen PB (1997) Patterns of ammonium uptake within dense mats of the filamentous macroalga Chaetomorpha linum. Aquatic Botany 59:99-115

McGlathery KJ, Pedersen MF, Borum J (1996) Changes in intracellular nitrogen pools and feedback controls on nitrogen uptake in Chaetomorpha linum (chlorophyta). Journal of Phycology 32:393-401

Middelburg JJ, Barranguet C, Boschker HTS, Herman PMJ, Moens T, Heip CHR (2000) The fate of intertidal microphytobenthos carbon: An in situ C-13-labeling study. Limnology and Oceanography 45:1224-1234

Morand P, Briand X (1996) Excessive growth of macroalgae: A symptom of environmental disturbance. Botanica Marina 39:491-516

Naldi M, Wheeler PA (2002) N-15 measurements of ammonium and nitrate uptake by Ulva fenestrata (chlorophyta) and Gracilaria pacifica (rhodophyta): Comparison of net nutrient disappearance, release of ammonium and nitrate, and N-15 accumulation in algal tissue. Journal of Phycology 38:135-144

Nedergaard RI, Risgaard-Petersen N, Finster K (2002) The importance of sulfate reduction associated with *Ulva lactuca* thalli during decomposition: a mesocosm approach. Journal of Experimental Marine Biology and Ecology 275:15-29

Nielsen SL, Enriquez S, Duarte CM, SandJensen K (1996) Scaling maximum growth rates across photosynthetic organisms. Functional Ecology 10:167-175

Nixon SW (1995) Coastal Marine Eutrophication - a Definition, Social Causes, and Future Concerns. Ophelia 41:199-219

NRC (2000) National Research Council. Clean coastal waters: understanding and reducing the effects of nutrient pollution, Vol. National Academy Press, Washington, DC

Parkes RJ (1987) Analysis of microbial communities within sediments using biomarkers. In: Hetcher M, Gray RTG, Jones JG (eds) Ecology of Microbial Communities. Cambridge University Press, Cambridge, p 147-177

Peckol P, Demeoanderson B, Rivers J, Valiela I, Maldonado M, Yates J (1994) Growth, Nutrient-Uptake Capacities and Tissue Constituents of the Macroalgae Cladophora-Vagabunda and Gracilaria-Tikvahiae Related to Site-Specific Nitrogen Loading Rates. Marine Biology 121:175-185

Peckol P, Rivers JS (1995) Physiological-Responses of the Opportunistic Macroalgae Cladophora-Vagabunda (L) Vandenhoek and Gracilaria-Tikvahiae (Mclachlan) to Environmental Disturbances Associated with Eutrophication. Journal of Experimental Marine Biology and Ecology 190:1-16

Peckol P, Rivers JS (1996) Contribution by macroalgal mats to primary production of a shallow embayment under high and low nitrogen-loading rates. Estuarine Coastal and Shelf Science 43:311-325

Pedersen MF, Nielsen SL, Banta GT (2004) Interactions between vegetation and nutrient dynamics in coastal marine ecosystems: An introduction. In: Nielsen SL, Banta GT, Pedersen MF (eds) Estuarine Nutrient Cycling: The Influence of Primary Producers. Kluwer, Dordrecht

Raffaelli D (2000) Interactions between macro-algal mats and invertebrates in the Ythan estuary, Aberdeenshire, Scotland. Helgoland Marine Research 54:71-79

Raffaelli DG, Raven JH, Poole LJ (1998) Ecological impact of green macroalgal blooms. Oceanography and Marine Biology - an Annual Review 36

Rossi F (2007) Recycle of buried macroalgal detritus in sediments: use of dual-labelling experiments in the field. Marine Biology 150:1073-1081

Sand-Jensen K, Borum J (1991) Interactions among phytoplankton, periphyton, and macrophytes in temperate freshwaters and estuaries. Aquatic Botany 41:137-175

Sand-Jensen K, Nielsen SL (2004) Estuarine Primary Producers. In: Nielsen SL, Banta GT, Pedersen M (eds) Estuarine Nutrient Cycling: The Influence of Primary Producers. Kluwer Academic Publishers, Netherlands, p 17-57

Schefuss E, Versteegh GJM, Jansen JHF, Damste JSS (2004) Lipid biomarkers as major source and preservation indicators in SE Atlantic surface sediments. Deep-Sea Research Part I-Oceanographic Research Papers 51:1199-1228

Schmidt JL, Deming JW, Jumars PA, Keil RG (1998) Constancy of bacterial abundance in surficial marine seciments. Limnology and Oceanography 43:976-982

Sfriso A, Pavoni B, Marcomini A, Raccanelli S, Orio AA (1992) Particulate Matter Deposition and Nutrient Fluxes onto the Sediments of the Venice Lagoon. Environmental Technology 13:473-483

Stanhope JW, Anderson IC, Reay WG (2009) Base flow nutrient discharges from lower Delmarva Peninsula watersheds of Virginia. Journal of Environmental Quality 38:2070-2083

Stutes AL, Cebrian J, Corcoran AA (2006) Effects of nutrient enrichment and shading on sediment primary production and metabolism in eutrophic estuaries. Marine Ecology-Progress Series 312:29-43

Thybo-Christesen M, Rasmussen MB, Blackburn TH (1993) Nutrient Fluxes and Growth of Cladophora-Sericea in a Shallow Danish Bay. Marine Ecology-Progress Series 100:273-281

Tobias CR, Cieri M, Peterson BJ, Deegan LA, Vallino J, Hughes J (2003) Processing watershed-derived nitrogen in a well-flushed New England estuary. Limnology and Oceanography 48:1766-1778

Tyler AC, McGlathery KJ, Anderson IC (2001) Macroalgae mediation of dissolved organic nitrogen fluxes in a temperate coastal lagoon. Estuarine Coastal and Shelf Science 53:155-168

Tyler AC, McGlathery KJ, Anderson IC (2003) Benthic algae control sediment-water column fluxes of organic and inorganic nitrogen compounds in a temperate lagoon. Limnology and Oceanography 48:2125-2137

Underwood GJC, Kromkamp J (1999) Primary production by phytoplankton and microphytobenthos in estuaries. Advances in Ecological Research, Vol 29 29:93-153

Valiela I, Cole ML (2002) Comparative evidence that salt marshes and mangroves may protect seagrass meadows from land-derived nitrogen loads. Ecosystems 5:92-102

Valiela I, Foreman K, Lamontagne M, Hersh D, Costa J, Peckol P, Demeoandreson B, Davanzo C, Babione M, Sham CH, Brawley J, Lajtha K (1992) Couplings of Watersheds and Coastal Waters - Sources and Consequences of Nutrient Enrichment in Waquoit Bay, Massachusetts. Estuaries 15:443-457

Valiela I, McClelland J, Hauxwell J, Behr PJ, Hersh D, Foreman K (1997) Macroalgal blooms in shallow estuaries: Controls and ecophysiological and ecosystem consequences. Limnology and Oceanography 42:1105-1118

Veuger B, Eyre BD, Maher D, Middelburg JJ (2007) Nitrogen incorporation and retention by bacteria, algae, and fauna in a subtropical intertidal sediment: An in situ N-15-labeling study. Limnology and Oceanography 52:1930-1942

Veuger B, Middelburg JJ, Boschker HTS, Houtekamer M (2005) Analysis of N-15 incorporation into D-alanine: A new method for tracing nitrogen uptake by bacteria. Limnology and Oceanography-Methods 3:230-240

Villares R, Carballeira A (2003) Seasonal variation in the concentrations of nutrients in two green macroalgae and nutrient levels in sediments in the Rias Baixas (NW Spain). Estuarine Coastal and Shelf Science 58:887-900

Volkman JK, Revill AT, Holdsworth DG, Fredericks D (2008) Organic matter sources in an enclosed coastal inlet assessed using lipid biomarkers and stable isotopes. Organic Geochemistry 39:689-710

Wazniak C, Hall M, Cain C, Wilson D, Jesien R, Thomas J, Carruthers T, dennison W (2004) State of the Maryland Coastal Bays, Maryland Department of Natural Resources, Annapolis, MD

Yunker MB, Macdonald RW (1995) Composition and Origins of Polycyclic Aromatic-Hydrocarbons in the Mackenzie River and on the Beaufort Sea Shelf. Arctic 48:118-129

Zimmerman AR, Canuel EA (2000) A geochemical record of eutrophication and anoxia in Chesapeake Bay sediments: anthropogenic influence on organic matter composition (vol 69, pg 117, 2000). Marine Chemistry 72:77-77

CHAPTER 2: AN EXPERIMENTAL APPARATUS FOR LABORATORY AND FIELD-BASED PERFUSION OF SEDIMENT POREWATER WITH DISSOLVED TRACERS

Amber Hardison[1], Craig Tobias[2], Jennifer Stanhope[1], Elizabeth Canuel[1], Iris Anderson[1]

Submitted to *Estuaries and Coasts*, September 2009

[1]Virginia Institute of Marine Sciences

College of William and Mary

P.O. Box 1346

Gloucester Point, VA 23062

amber@vims.edu

[2]Department of Marine Sciences

University of Connecticut

Groton, CT 06340

Abstract

The water-sediment interface is a dynamic zone where the benthic and pelagic environments are linked through exchange and recycling of organic matter and nutrients. However, it is often difficult to measure rate processes in this zone. To that end, we designed an experimental apparatus for continuous and homogenous perfusion of sediment porewater with dissolved conservative (SF_6, Rhodamine WT dye) and isotopic ($H^{13}CO_3^-$ and $^{15}NH_4^+$) tracers to study nitrogen and carbon cycling by the sediment microbial community of shallow illuminated sediments. The perfusionator consists of a 60 cm I.D. x 60 cm height cylinder that includes a reservoir for porewater at the base of the sediment column. Porewater amended with conservative and stable isotopic tracers was pumped through a mixing reservoir and upward through the overlying sediments. We tested the perfusionator in a laboratory setting, as part of an outdoor mesocosm array, and buried in coastal sediments. Conservative and isotopic tracers demonstrated that the porewater tracers were distributed homogenously through the sediment column in all settings. The perfusionator was designed to introduce dissolved stable isotope tracers, but is capable of delivering any dissolved ionic, organic, or gaseous constituent. We see potentially wide application of this technique in the aquatic and marine sciences in laboratory and field settings.

Key Words: stable isotopes, mesocosms, porewater advection, water-sediment interface, sediment column

Introduction

Shallow coastal systems are characterized by sediment-water exchange between benthic and pelagic compartments. Understanding the physical and biological mechanisms responsible for this exchange is critical for describing how these ecosystems currently function and predicting how their function may change in response to future environmental change. Porewater within subtidal sediments contains a suite of dissolved substances (e.g. nutrients, organic matter, gases, toxins, salts, metals) that can play a critical role in regulating metabolic processes taking place within the sediments and resultant fluxes to the overlying water. Sediment porewater characterization has been the focus of research for decades, and recently developed technologies (e.g. micro-electrodes, -optodes, and –biosensors; see Stockdale et al. 2009, Reimers 2007, for recent reviews) now allow for routine analysis of micro-scale spatial and temporal heterogeneity of dissolved substances within the sediments, often with minimal sediment disturbance. However, in order to evaluate the role that dissolved porewater constituents play in sediment biogeochemical processes, explicit tracing of solutes/nutrients by experimental manipulation must be accomplished to identify mechanisms underlying observed profiles and fluxes.

A number of laboratory and field-based methods have been applied to alter the concentrations of dissolved substances in porewaters and/or to introduce tracers. Direct introduction of dissolved solutes to sediments in the laboratory have most often involved amended slurries (Parkes et al. 1993; Trimmer et al. 2003; Veuger et al. 2005) or direct syringe injections of tracer into small sediment cores (Anderson et al. 2003; Boschker et

al. 1998; Bühring et al. 2006). Field-based introduction of tracers to the sediments have included one-time surface spray application (Middelburg et al. 2000) or syringe injections (Veuger et al. 2006, 2007) into intertidal sediments at low tide. When possible (e.g. with nutrients, iron, organic matter), the solutes have been added as particulates that are sprinkled onto or buried within the sediment surface and subsequently dissolve (Armitage et al. 2006; Enoksson 1993; Franke et al. 2006; Mutchler et al. 2004). While suitable for certain studies of nutrient cycling and trophic transfer, these methods offer a number of challenges. Slurries, for example, disrupt naturally occurring physical, chemical, and biological gradients in the sediments, which may confound interpretation of results. Injection into sediment cores or addition of particulate material directly to the sediment surface likely results in patchy distribution of the dissolved substances within the porewater and function only as a short-term amendment. Spray-on or syringe injections into sediments provide reasonable measurements of rates operating on short timescales in laboratory or field studies involving intertidal sediments, but they are not amenable to use in subtidal systems, because sediments are never exposed.

As an alternative, introduction of dissolved constituents by advection of amended porewater through sediment cores (columns) has been applied in numerous physical and biogeochemical studies (Girguis et al. 2005; McGlathery et al. 1998; Polerecky et al. 2005; Rao et al. 2007). With this technique, the dissolved constituents are likely more homogenously distributed in the sediment porewaters than the previous techniques allow, but this approach is limited to small-scale core studies. Further, the unidirectional flow through the sediments in the laboratory may not best represent the complex circulation

patterns present in some systems, which is essential for maintaining reactive redox interfaces (Huettel et al. 1996; Janssen et al. 2005; Reimers et al. 2004). This study builds on past designs of sediment advection columns to create a versatile apparatus that delivers porewater tracer through sediments at expanded spatial and temporal scales for the purpose of examining sediment biogeochemical cycles.

The purpose of this study was to focus on the microbial community living at the sediment-water interface of shallow subtidal sediments. This complex community of autotrophic (e.g. benthic microalgae, BMA) and heterotrophic (e.g. bacteria) organisms can assimilate nutrients and organic matter from surface water and porewater sources (Cahoon 1999; MacIntyre et al. 1996; Veuger et al. 2007). Developing mechanistic models of benthic-pelagic coupling in this zone depends on identifying sources of carbon (C) and/or nitrogen (N) for sediment autotrophs and heterotrophs, and tracking the processing and recycling through those compartments. Because it is difficult to separate microbial biomass from the sediment matrix, recent studies have adopted the use of stable isotopes incorporated into microbial biomarkers as a tool for tracking nutrients supporting sediment microbial production in the BMA and bacterial compartments (Boschker et al. 1998; Boschker and Middelburg 2002; Tobias et al. 2003). Tracking C and N uptake from the water column by sediment microbes using isotopes has been accomplished by a variety of approaches including laboratory core incubations (Dornblaser et al. 1994; Jönsson 1991; Nielsen 1992) and small (Hughes et al. 2000; Kaldy et al. 2006) and large-scale (Gribsholt et al. 2007; Tobias et al. 2003a) field studies. However, porewater is also an important source of dissolved nutrients and

organic matter that support sediment microbes, and quantifying the exchange of C and N between porewater and the sediment microbial community is a key step towards understanding ecosystem functions of shallow sediments. Given the methodological challenges posed by existing porewater manipulation techniques, we developed an approach to more accurately address microbial uptake of porewater substrates. Our approach involves perfusing intact sediments with isotopically-labeled porewater, resulting in continuous, uniform introduction of labeled constituents to the sediment microbial community. This approach provides a novel method for addition of dissolved tracers via the porewater. To address the need for larger-scale laboratory and field experiments, we used a large mesocosm, which provided a balance between more realistic experimental conditions and our need to contain the isotopic tracers to achieve adequate enrichment of target pools. Here we describe the "perfusionator", an innovative apparatus that allows continual long-term perfusion of sediment porewater with dissolved tracers in a mesocosm or a field setting.

Methods

Perfusionator Design

The perfusionator was fabricated from a cylindrical translucent fiberglass tank (60 cm diameter x 60 cm height; Solar Components, Inc.) with a false bottom (Fig. 1). At the base of the tank was a 23-L reservoir for storage of feed water, or, seawater amended with dissolved tracers. This reservoir was capped by a false bottom, and sediment and

water were added above the false bottom. Feed water was stored in an external tank and supplied to the reservoir through a standpipe. Water from the reservoir was subsequently perfused up through the sediment column, providing a mechanism for delivery of dissolved constituents to the water-sediment interface.

The false bottom was a perforated (0.64 cm hole diameter) PVC disc (0.32 cm thick) covered with silt mesh (Geotextile, 50 US Standard sieve opening) which provided a filter through which only water and dissolved constituents could pass. The false bottom was supported by seven 10.2 cm tall columns of 7.6 cm I.D. PVC pipe, perforated to enable water circulation within the reservoir. The seal between the false bottom and the tank walls was made water-tight by sandwiching the edge of the perforated plastic disc inside a ring of flexible insulation pipe foam (1.6 cm I.D. x 6.4 cm O.D.) before pressing the disc into place. This seal was also lined with non-toxic 100% silicone sealant above and below the disc/foam junction with the wall.

Seawater amended with dissolved tracers (isotopically-labeled nutrients: ammonium as $(^{15}NH_4)_2SO_4$; bicarbonate as $NaH^{13}CO_3$) was continuously introduced into the perfusionator reservoir from an external source via a PVC standpipe (1.3 cm I.D.) which extended ~125 cm vertically from the false bottom. The bottom of the standpipe was connected by an elbow joint to porous PVC pipe (1.3 cm I.D.; 2.5 mm screen) situated on the floor of the reservoir. The porous PVC was configured in a cross-shape to distribute the feed water across the length of the tank, allowing for controlled introduction of feed water into the reservoir (Fig. 1). All PVC joints were sealed with Teflon tape and PVC

glue. Depending on the experimental requirements, the rate of feed water delivery into the standpipe could be regulated via a variety of methods such as gravimetric flow, a medical grade IV dripper, or a peristaltic pump. Before adding sediments to the tank, we found that it was essential to fill the perfusionator reservoir and cross-pipe completely with seawater to avoid trapping air inside the perfusionator which would subsequently be pumped through the sediments.

To ensure adequate mixing of the feed water within the reservoir before perfusion through the sediments, an electric-powered mini-jet pump (Aquatic Ecosystems, Inc.) was installed to circulate the reservoir water. In case of pump failure, a second mini-jet pump was included, and the pumps were alternated every three days. This minimized the potential impact of a broken pump since pumps could not be replaced without disruption of the sediments during the experiment. The mini-pumps were encased in 7.6 cm I.D. PVC wellscreen (2.5 mm screen) closed on both ends except at the output nozzle with Cap Plugs and wrapped in silt mesh to minimize any sediment introduction through the intake, which would decrease the lifetime of the pumps.

Perfusionator testing

We conducted a series of tests to determine the effectiveness of the perfusionator at delivering dissolved tracers homogenously through the sediment porewater. We used both conservative (Rhodamine WT dye (RWT), sulfur hexafluoride (SF_6)) and non-

conservative ($H^{13}CO_3^-$, $^{15}NH_4^+$) tracers in a laboratory setting, an outdoor mesocosm array, and in subtidal sediments in the field.

Laboratory

We tested the perfusionator system in the laboratory initially to ensure homogenous introduction of the feed water into the sediments by tracking RWT dye as it flowed through the perfusionator from an external feed tank. RWT is a fluorescent dye that is used commonly as a hydrodynamic surface water tracer (Lin et al. 2003; Shiau et al. 1993; Smart and Laidlaw 1977). The perfusionator was filled with rinsed all purpose play sand to a depth of 16 cm. The RWT dye solution was introduced to the perfusionator reservoir by an IV dripper at a drip rate equivalent to 8.5 L porewater day^{-1}, or a porewater residence time of ~2.7 days. Porewater (5 mL per sample) was collected from each of nine locations across the sediment surface over six days. The sampling locations were divided into "edge" and "center" positions to account for edge effects that could result from a leaky seal at the false bottom-wall interface. Each location was sampled at 2 depths (6 cm and 15 cm below the sediment surface) using a stainless steel push-point sampler (2 cm screen; MHE Products) connected to a peristaltic pump (6 mL min^{-1}). Surface water samples were also collected each time porewater was sampled. Samples were collected in glass culture tubes, covered with Parafilm and refrigerated until analysis.

Outdoor mesocosm array

The second application of the perfusionator was a stable isotope tracer experiment set up in a flow-through outdoor mesocosm array located at the Virginia Institute of Marine Science (VIMS) Eastern Shore Lab in Wachapreague, Virginia. We tested the effectiveness of the perfusionator at delivering dissolved tracers homogenously to the sediment surface using both conservative (SF_6) and non-conservative ($H^{13}CO_3^-$, $^{15}NH_4^+$) tracers. The perfusionators were filled with sediments (fine sand) to a depth of 15 cm. Sediments were collected using multiple sediment cores from a shallow subtidal field site in Hog Island Bay, VA, and then transferred directly to the perfusionators, taking care to minimize disturbance of the natural vertical sediment horizons. The sediments contained macrofauna such as worms and clams as indicated by the presence of burrows, siphons, tubes, and fecal pellets. The perfusionators were placed in water baths under a large greenhouse frame covered with 30% shade cloth to regulate temperature and light conditions. They were connected to a flow-through, filtered (1 μm) seawater system and were allowed to equilibrate for two weeks before beginning the experiment. Feed water was pumped from an adjacent creek, through a series of sand, bag (10 μm), and cartridge (5 and 1 μm) filters, amended with $NaH^{13}CO_3$ and $(^{15}NH_4)_2SO_4$ dissolved in deionized water, and homogenized in a mixing chamber before being pumped through the standpipe into the perfusionator reservoir at a rate of ~15 L day^{-1}, or a porewater residence time of ~1.8 days. Fine-scale control of the flow rate into each perfusionator was achieved using an IV dripper located at each stand pipe that was calibrated daily. The water column above the sediments was also connected to the flow-through filtered seawater system and was stirred continuously with a mini-jet pump to keep the water column well mixed and

prevent buildup of artificial gradients. The mesocosm array consisted of 24 perfusionators all receiving isotope tracer (^{15}N and ^{13}C) divided amongst several experimental treatments. We do not present the full results of our experimental manipulations here, but instead focus on the effectiveness of the perfusionator design in delivering tracer through the sediments via porewater.

Sulfur hexafluoride (SF_6), $^{15}NH_4^+$, and $H^{13}CO_3^-$ were supplied to the feed water by dedicated metering pumps. SF_6 is an inert gas, detectable at very low concentrations and often used as a physical gas exchange and water mass tracer (Emery and Thomson 2001; Watson and Ledwell 1988). Because gas exchange is trivial within sediments, the SF_6 proved a reliable conservative tracer for tracking the perfusion of porewater. The distribution of SF_6 concentrations in porewater was used to assess the homogeneity of tracer distribution in the sediments. Porewater SF_6 was measured once in four of the 24 perfusionators. The SF_6 solution was prepared as described in Tobias et al. (2009). Briefly, the SF_6 tracer solution was prepared in a 40-L Tedlar (SKC Inc.) plastic sample bag that was floated in a tub of water to provide thermal stability. First, the bag was filled approximately half way by pumping in 20 L deionized water with a peristaltic pump, and the remaining air headspace was forced out of the bag through a port at the top of the bag until no air headspace remained. Then the headspace was refilled with approximately 10 L of pure SF_6 that was transferred to the bag from a pressurized tank. The mixture was agitated repeatedly and allowed to equilibrate for approximately 24 hours before the tracer experiment began, thereby creating a solution nearly saturated with SF_6 at 1 atm pressure. The SF_6-saturated (~0.25 – 0.30 mmol L^{-1}) tracer solution

was pumped using a metering pump through Norprene tubing into the perfusionator feed water line at a constant rate of 1 mL min^{-1}. Feed water flow past the point of mixing ranged from 300 – 500 ml min^{-1} generating an SF_6 concentration delivered to the mesocosm on the order of 500 nM. After 2 days of SF_6 introduction to the feed lines, sediment porewater was sampled simultaneously at 10 grid locations across the sediment surface at a depth of 5 cm using stainless steel push-point samplers (2 cm screen) connected to a peristaltic pump (2-3 mL min^{-1}) into N_2-sparged serum vials.

Isotopic tracers ($(^{15}NH_4)_2SO_4$ and $NaH^{13}CO_3$) were added from separate stock solutions to the perfusionator feed water continuously for two weeks. This enrichment phase was followed by a four week period of unlabeled $NaHCO_3$ and $(NH_4)_2SO_4$ addition. Surface sediments (0-1 cm) from three mesocosms were sampled for bulk isotope analysis using an acrylic core (5.7 cm I.D.) before beginning the isotope additions (control), during the isotope additions (Days 1, 3, 7, 14), and after stopping the isotope additions (Days 21, 42). Samples were stored at -80ºC in pre-combusted glass jars until analysis. A different region of the sediment surface was sampled each day to avoid re-sampling any sediments.

Field deployment

The final application of the perfusionator was in the field. We buried four perfusionators at a sandy, shallow (~0.5 m water depth at mean low water) subtidal site in the York River adjacent to VIMS (Fig. 2). We tested the effectiveness of the perfusionator at delivering dissolved tracers homogenously to the sediment surface using the same

conservative (SF_6) and non-conservative ($H^{13}CO_3^-$, $^{15}NH_4^+$) tracers that were applied to the mesocosm experiment described above. Each perfusionator was placed in a hole in the sediments that was created using a suction sampler. The perfusionators were filled with sediments (sand, ~10 cm deep) collected from the site and allowed to equilibrate for 20 days before beginning the experiment. To minimize disruption of surface water movement over the sediment surface, the wall of the perfusionator (Fig. 1) was shortened to 25cm for the field application such that only ~5 cm of the wall extended above the sediment-water interface. The feed water was supplied from a porewater well that was installed adjacent to the buried perfusionators at approximately the same depth as the perfusionator reservoir. Porewater from the well was pumped (dotted gray lines, Fig. 2) with a peristaltic pump to a mixing chamber on the shore (~20 m distance) where isotopic and SF_6 tracers were added, as described in the outdoor mesocosm array experiment. The tracer-amended porewater (feed water) was then pumped (solid black lines, Fig. 2) back to the buried perfusionators, where it was introduced through the standpipe to the perfusionator reservoir. The feed water pumping rate was ~29 L day^{-1}; or a porewater residence time of ~0.15 day. Flow rates into the perfusionators were controlled using a peristaltic pump that was calibrated daily. Tracer addition occurred for 12 days. During the tracer period, translucent fiberglass lids were secured with rebar stakes on top of the perfusionator walls to minimize hydrodynamic disturbance. The lids, however, were perforated to allow for water exchange during that period. The lids from two of the perfusionators were removed at the end of the addition period while the other two lids remained in place to assess the effect of hydraulic energy on the retention of isotopes within the sediments.

On the final day of tracer addition, porewater SF_6 was sampled simultaneously at 10 grid locations across the sediment surface at a depth of 5 cm using stainless steel push-point samplers (2 cm screen) connected to a peristaltic pump as performed in the mesocosm study.

Surface sediments (0-1 cm) were sampled for bulk isotope analysis using an acrylic core (5.7 cm I.D.) before beginning the isotope additions (control), during the addition phase (Days 7, 12), and after stopping the isotope additions (Days 14, 19, 26, 33, 42). Samples were stored in pre-combusted glass jars at -80ºC until analysis. As done in the mesocosm study, a different region of the sediment surface was sampled each day to avoid re-sampling any sediments. In addition to the sediment samples, porewater samples were taken for measurement of ^{15}N-isotopic enrichment of NH_4^+. Porewater was collected from ~6 cm depth at five locations across the sediment surface using stainless steel push point samplers (2 cm screen; MHE products) connected to a peristaltic pump (~10 mL min-1). The sub-samples from each mesocosm were filtered through 2.7 mm GFD and 0.7 mm GFF filters, composited, and stored in a high density polyethylene bottle at -20°C until analysis.

Analytical Methods

RWT concentrations were measured using a Shimadzu UV-1601 UV-Visible Spectrophotometer (absorption wavelength = 550 nm; Shiau et al. 1993; Smart and

Laidlaw 1977). A calibration curve was prepared using different proportions of the feed water mixed with deionized water and used to determine sample RWT concentrations. Concentrations were expressed as percent of the feed water (source) concentration, which was designated as 100%. Two-sample T-tests were used to test for differences in RWT concentration by depth (6 vs. 15 cm; $\alpha = 0.05$) and by horizontal sampling position (central vs. edge; $\alpha = 0.05$). SF_6 concentrations were measured with a Shimadzu 8A gas chromatograph fitted with an electron capture detector, a packed molecular sieve 5A column, and using N_2 carrier gas. Sample SF_6 peaks were calibrated against serial dilutions of a 1ppm SF_6 standard, and SF_6 concentrations were calculated from the ideal gas law and sample volumes.

For bulk isotope measurements, sediments were freeze-dried, ground and homogenized, acidified with 10% HCl to remove inorganic C (Hedges and Stern 1984), and analyzed for $^{13}C/^{12}C$ and $^{15}N/^{14}N$ using an elemental analyzer coupled to an isotope ratio mass spectrometer (EA-IRMS; Thermo Delta V Plus). Isotopic values are presented as delta values ($\delta^{13}C$ or $\delta^{15}N$) in units of per mil (‰) relative to Vienna Pee Dee Belemnite (VPDB, C) and air (N) standards:

$$\delta X = [R_{sample} / R_{standard} - 1]*1000 \quad (1)$$

where X is either ^{15}N or ^{13}C, R = $^{15}N/^{14}N$ or $^{13}C/^{12}C$. For porewater $\delta^{15}N\text{-}NH_4^+$ analysis, NH_4^+ was trapped using an alkaline diffusion acid trap according to Holmes et al. 1998. Pre-combusted GFD (1 cm) filter discs were acidified with 2M $KHSO_4$ and sandwiched

between two 2 mm polypropylene filters. The acid filter sandwich and approximately 0.5g MgO were added to a porewater volume sufficient to contain 2 mmoles N as NH_4^+. The sample was diffused for 1 week, and the sandwich dried in a dessicator containing high concentration H_2SO_4 for 48 hours. The GFD discs were wrapped in tin capsules, and analyzed for $^{15}N/^{14}N$ using the EA-IRMS.

Results & Discussion

Laboratory testing

During the lab-based Rhodamine test, RWT first appeared in porewater sampled 15 cm below the sediment surface on Day 1 (0.7 ± 0.3% of source solution; Fig. 3; error represents 1 SE) and increased through the final sampling day (57 ± 2%). RWT was subsequently detected at 6 cm on Day 4 (16 ± 4%), although at lower concentrations than at 15 cm (45 ± 4%) on that day, confirming that deeper sediments had been exposed longer to reservoir water than the shallow sediments. Concentrations at 6 cm continued to increase through the final sampling day (31 ± 7%). Concentrations at 15 cm were consistently higher than at 6 cm throughout the experiment ($p < 0.05$; $df = 89$). No dye was measurable in the surface water until the final day. The sampling locations were distributed to account for edge effects that could result from a leaky seal at the false bottom-wall interface (see inset, Fig. 3). There were no significant differences between "edge" and "central" sampling positions for either depth ($p > 0.05$, $df = 41$ for 6 cm and $p > 0.05$, $df = 48$ for 15 cm; see inset, Fig. 3), which suggested that the seal along the false

bottom and tank wall edge was water-tight. No additional "hot spots" of dye were apparent, indicating relatively even distribution throughout the sediments. RWT dye has limited use as a conservative tracer in sediments due to losses from sorption to sediments, photochemical degradation, or microbial decomposition (Lin et al. 2003). In our lab-based perfusionator test, we used rinsed play sand, which we assumed had negligible organic content, so we expected minor losses due to sorption and decomposition, although some sorption may have accounted for the higher concentrations at 15 cm compared with 6 cm and delayed appearance in the water column. While sorption and photodegradation limit the use of RWT for estimating transport parameters in natural systems, these processes were minimized in our laboratory test and did not lessen the utility of using RWT for assessing homogenous dispersal of tracer under controlled conditions. RWT was not used in the subsequent perfusionator tests in natural settings.

Mesocosm testing

In the outdoor mesocosm array test, we used 24 perfusionators for a 58-day experiment that investigated sediment microbial uptake and retention of dissolved inorganic nutrients from water column and porewater sources using stable isotope tracers. With a few exceptions, the perfusionators worked well. Four of the 24 false bottoms were breached by overlying sediment, rendering the perfusionators unusable, and 2 of the 48 mini-jet pumps were faulty by the end of the experiment. More precise fitting of the false bottom into the tank will correct the likelihood of a failure, and our perfusionator design

minimized the effect of a broken pump within the reservoir by alternating between two pumps every three days.

Subsurface SF_6 distributions measured 5 cm below the sediment surface are shown in Figure 4 as contour plots for each perfusionator. Mean concentrations of SF_6 varied between perfusionators (45 ± 9, 90 ± 13, 67 ± 13, 189 ± 29, nM for tanks a, b, c, d, respectively; error represents SE, n = 10); however, the within-tank variability was similar among tanks (CV = 61, 46, 62, 49 %, respectively). Within-tank distribution of tracer was heterogeneous, but values were generally within a factor of 2-3. We identified the location of the standpipe for each perfusionator in Figure 4 to assess whether the standpipes leaked, which would be indicated by localized maxima in SF_6 concentrations centered around the standpipes. The absence of "hot spots" suggests that leaking or other influences from the standpipe, edge, or biotubes were minimal.

For the mesocosm array experiment, non-conservative tracers ($H^{13}CO_3^-$, $^{15}NH_4^+$) introduced through the porewater were incorporated into the sediment microbial community as indicated by enrichments in bulk surface sediment $\delta^{15}N$ and $\delta^{13}C$ (Fig. 5). $\delta^{15}N$ values increased throughout the label addition period, reached a maximum of 20086 ± 3665 ‰ by Day 14, and declined until Day 42 (11502 ± 1842). The high levels of ^{15}N were necessary because of a concurrent study that was trying to track N into the large and exchangeable N_2 fraction. $\delta^{13}C$ values were lower than $\delta^{15}N$ but followed similar patterns (r^2 = 0.97). $\delta^{13}C$ values increased throughout the label addition period, reached a maximum of 1601 ± 251 ‰ by Day 14 and declined until Day 42 (679 ± 91 ‰). The

isotopic enrichment trajectories show the incorporation of isotopic label during the tracer portion (through Day 14) of the experiment, and the dilution of the isotopic label after the isotopically-labeled NH_4^+ and HCO_3^- were replaced with unlabelled stock (after Day 14).

Together, the conservative (SF_6) and non-conservative (isotopic) tracers demonstrated that the perfusionator provided a reliable approach for distributing dissolved tracers via the porewater throughout the sediment column in a laboratory or mesocosm setting. The SF_6 and isotopic tests were conducted using sediments (fine sand) collected from the field and transferred directly to the mesocosm chamber. The sediments collected from the field remained relatively intact during placement in the mesocosms and included organic and inorganic components typical of estuarine sediments (e.g. macro- and meiofauna, BMA, bacteria, shell fragments). The SF_6 distributions showed some heterogeneity horizontally across the sediments, but concentrations within a mesocosm varied within a factor of 2-3, which was quite low considering the naturally-occurring heterogeneity of the sediments (Fig. 4). Despite the presence of worm tubes and clams, no channeling was evident. Absolute SF_6 concentrations between tanks differed by a factor of 4 even though each tank received SF_6 from the same feed line. We attribute these differences to three possible sources of variability: 1) variable exposure of the feed water solution containing SF_6 to air in the standpipe and the feed lines, leading to re-equilibration of the SF_6 solution with air, 2) small differences in the flow rates at each stand pipe which would translate into logarithmic changes in gas exchange (especially gases such as SF_6 that are very insoluble; see Tobias et al. (2009) and references therein) and 3) changes in SF_6 solubility associated with diel temperature variability of the feed water reservoir. Given

the highly insoluble nature of SF_6 and the presence of a headspace in the standpipe, these between-tank differences are not unexpected, and the SF_6 provides a worst-case representation for subsurface heterogeneity of tracer.

The incorporation of the isotopic tracers into the surface sediments suggested a more homogenous delivery of inorganic tracers than the SF_6 might indicate. Active uptake of C and N by the microbial community at the sediment surface caused the isotopic enrichment of the bulk sediments to increase steadily throughout the labeling period. The enrichment trajectories, and between-mesocosm variation in sediment enrichments on the order of ~ 30%, indicate consistent delivery of the isotopic tracers to the surface sediments. Further, active uptake and cycling of the introduced tracers by the sediment microbial community was demonstrated by the retention of label in the bulk sediments following the end of the isotopic addition period (Day 14). Some variability (CV ~ 30%) between replicates at any given time point was evident, which could be attributed to natural heterogeneity of the microbial community processing the C and N, and/or disproportionate delivery of the tracers to each replicate. Because variability over time was larger than variability at a given time point, any inconsistencies associated with the tracer delivery were small relative to the overall enrichment patterns that we observed over time due to autotrophic/heterotrophic uptake and recycling.

The perfusionator allowed us continuously add the isotope tracer for two weeks, which provided ample opportunity for the target pools to become enriched at detectable levels. Overall, these tracer tests demonstrate the utility of the perfusionator as a system for

delivering dissolved constituents continuously and homogenously through the sediments via the porewater in mesocosm-based experiments, within the limitations of mesocosm studies (Carpenter 1996; 1999; Drenner and Mazumder 1999; Huston 1999; Short 1995).

Field deployment

The field deployment was the ultimate test for the perfusionator because of its exposure to *in situ* conditions. Not only did we use natural, heterogenous sediments as in the mesocosm test, but we also maintained dynamic physical exchange with turbulent surface waters and used porewater as the feed water to which the tracers were added (Fig. 2). We applied the same conservative (SF_6) and non-conservative ($^{15}NH_4^+$, $H^{13}CO_3^-$) tracers as in the mesocosm experiment to assess the effectiveness of the field deployment. SF_6 distributions at 5 cm below the sediment surface for the field deployment are presented as contour plots for each perfusionator (Fig. 6). Mean concentrations for each perfusionator were similar (627 ± 76, 595 ± 74, 650 ± 91, 590 ± 195 nM for perfusionators a, b, c, d, respectively; error represents SE, n = 10). Within-chamber variability was similar among perfusionators a, b, and c (CV = 38, 39, 44%), however replicate d was more variable (CV = 104%). We believe the high variability in perfusionator d reflects unintentional collection of surface water with some of the porewater sippers, which would have resulted in artificially low SF_6 concentrations at those locations since the atmosphere-equilibrated surface water contains no SF_6. This was verified by increased concentrations of dissolved oxygen measured in split samples run on the IRMS for gas isotopes used in a concurrent study (data not presented here). Accordingly, the SF_6 tracer distribution for

tank d likely did not accurately reflect the porewater distribution. On the other hand, within-tank distributions of tracer for tanks a, b, and c were within a factor of 2, which was similar to the variability observed in the mesocosm array experiment. The location of the standpipe was indicated for each perfusionator to assess for leakage from the standpipe as described for the mesocosm experiment (Fig. 6). The absence of "hot spots" suggests that leaking or other influences from the standpipe, edge, or biotubes were minimal.

For the bulk sediment isotopic values, we were unable to identify differences between the perfusionators that were covered vs. uncovered following the labeling period, so the average values of all four perfusionators are presented as mean ± SE (Fig. 7). Unlike the SF_6 data, the bulk sediment isotopic enrichments for perfusionator d were consistent with the other three perfusionators, which further suggests that sampling error caused the differences we observed in the SF_6 data, rather than a failure of the perfusionator. Generally, the patterns of isotope uptake during the labeling period and loss during the post-labeling period were similar for the mesocosm array and the field deployment tests, although the isotopic enrichments were lower in the field experiment (Fig. 7). $\delta^{15}N$ values increased throughout the label addition period, reached a maximum of 599 ± 84 ‰ by Day 12, decreased during the post-labeling period to 150 ± 20 ‰ on Day 19 and remained at this level through Day 42. Similar to the mesocosm experiment, $\delta^{13}C$ values were lower than $\delta^{15}N$ but followed similar patterns ($r^2 = 0.83$). $\delta^{13}C$ values increased throughout the label addition period, reached a maximum of 38.9 ± 22 ‰ by Day 12,

decreased during the post-labeling period to -9.75 ± 1.4 ‰ on Day 19, and remained steady through Day 42.

For the field deployment, we also measured $\delta^{15}N$ enrichments of porewater NH_4^+ (Fig. 8). Unlike the SF_6 measurements, which showed the within-perfusionator dissolved tracer distribution for one day (Day 12), $\delta^{15}N$ of porewater NH_4^+ were measured throughout the experiment, so we were able to track changes over time in NH_4^+ isotopic enrichments encountered by the sediment microbial community. In general, $\delta^{15}N$-NH_4^+ showed the same patterns as the bulk sediments, although NH_4^+ was more enriched than bulk sediments in ^{15}N. Throughout the labeling period, $\delta^{15}N$ increased, peaked on Day 7 at 20273 ± 2310 ‰ and decreased once the labels were turned off to 2084 ± 607 ‰ on Day 42. Porewater $\delta^{15}N$-NH_4^+ peaked on Day 7, just before the end of the labeling period when the bulk sediment isotopic enrichments peaked. Between-perfusionator variability was low, with CV varying from 5 to 36%. Once again, perfusionator d was similar to a, b, and c, suggesting a sampling error caused the high variability in SF_6 values in perfusionator d rather than a failure of the perfusionator. Based on the bulk sediment and NH_4^+ $\delta^{15}N$ data, we estimated conservatively that less than 5% of the sediment ^{15}N enrichment could have been due to residual ^{15}N from porewater NH_4^+.

As in the mesocosm array test, delivery of conservative and isotopic tracers was successful in the field test perfusionators. While more involved logistically than the mesocosm experiments, the field experiment had some important advantages. First, by supplying tracer to the circulating porewater system (Fig. 2), we avoided potential

artifacts associated with introducing oxygenated water into the subsurface. Second, because overlying surface water was exchanged almost instantaneously, no tracer could accumulate in overlying water and serve as a labeled substrate to the sediments from "above." Our mesocosm array could be adapted to account for both of these potential artifacts and remains a suitable design for many experimental manipulations. However, the last and critical advantage the field deployment offered was maintenance of the dynamic nature of the porewater and resuspension in a natural setting, which was not possible in a mesocosm setting. The perfusionators were buried at an active shallow subtidal site where, over the course of the experiment, tidal strengths varied across four neap-spring tidal cycles (tidal ranges from 0.51 to 0.97 m) and daily maximum wind speeds ranged from 4.8 to 16.7 meters per second (NOAA 2008). Thus, the field labeling via sediment porewater provided a more robust and environmentally meaningful design for testing our experimental questions regarding the N and C uptake dynamics of benthic microbes strictly from a sediment source.

The isotopic enrichment levels were exceptionally consistent between replicates in the field experiment (Fig. 7), and replication was better than that achieved in the mesocosm array experiment (Fig. 5). Again, as observed in the mesocosm experiment, the SF_6 maps show a variable picture of tracer delivery to any given region of sediment (Fig. 6). We believe that the subsurface variation in SF_6 for the field perfusionators reflected a snapshot of a temporally dynamic subsurface rather than an inability of the perfusionator system to evenly distribute dissolved tracer. A highly uneven tracer delivery could not have yielded the smooth isotope trajectories in the sediments. Wave action and tidal

pumping were actively moving the porewater (and dissolved tracers) within the sediments, and they were sufficiently strong to move isotopically-labeled particles deeper into the sediments. This movement was likely transient in strength and direction (Huettel et al. 2003) and occurred over sufficiently short timescales such that the sediments in different locations encountered a temporally-smoothed average tracer delivery. This smoothing likely increased the similarities in bulk sediment isotope trajectories (both rising and falling) between perfusionators (Fig. 7). Even though we induced upward flow, the sediment column was not exposed strictly to unidirectional plug flow, which has been critiqued in previous advective sediment column studies for not characterizing porewater movement *in situ* (Huettel et al. 1996; Janssen et al. 2005).

Because of the dynamics in these sediments, composite sampling (rather than point sampling) of the dissolved porewater pools would likely provide a better indication of the average concentrations to which the sediments were exposed. Composite sampling of perfusionator porewater likely explained the low variability in isotopic enrichments of NH_4^+ (Fig. 8). Even so, the porewater samples represented only a snapshot in time of a dynamic environment and likely differed from the average porewater conditions to which the sediments were exposed. This likely contributed to the premature peak in porewater $\delta^{15}N\text{-}NH_4^+$ on Day 7, prior to the end of the isotope addition period on Day 12, when the bulk sediment $\delta^{15}N$ values peaked. Compared to the porewater, solid phase isotopic uptake provides a more integrated representation of the isotopic environment. Nevertheless, the perfusionator appears to be an effective means by which to study responses of solid sediment phases to experimental manipulation. The approach can be

applied to a wide range of shallow sediments to provide *in situ* tracing of biological and physical processing of dissolved substances that is not possible in a setting isolated from the field.

Applications and limitations

The perfusionator offers some important advantages over alternative methods for introducing dissolved constituents to the sediments. First, it provides more control over solute concentrations, isotopic enrichments, and solute distribution than other available amendment methods (e.g. PVC diffusers, fertilizer pellets; Mutchler et al. 2004). Second, we were able to attain a homogenous solute distribution over a large sediment volume, which maximizes the sediments available for sampling while minimizing the influence of wall artifacts associated with mesocosms (Carpenter 1996). Also, it allows addition of amended feedwater for an extended period of time, enabling us to measure slower rate processes than are studied in typical core experiments (Anderson et al. 2003; Bühring et al. 2006), and although not studied here, tracer incorporation into higher trophic levels. Lastly, in the field deployment, we avoid artifacts associated with unidirectional flow which is common to traditional porewater advection studies that utilize sediment columns (Huettel et al. 1996; Reimers et al. 2004).

Our system would be suitable for biogeochemical studies investigating redox chemistry or manipulation of other dissolved porewater constituents such as trace metals, toxins, salts, gases, or nutrients in a setting which allows porewater advection. For example, the

perfusionator would be an ideal system with which to study the effects of extracellular polymeric substances (EPS) excreted by BMA on sediment stability (Tolhurst et al. 2002) or an investigation of seagrass tolerance to trace metal-contaminated groundwater (Marín-Guirao et al. 2005). Additionally, the perfusionator can be used with amended or unamended feed water. Finally, with a simple modification, it can be run as a *diffusionator* rather than a perfusionator by circulating tracer within the perfusionator reservoir and pumping to a waste output in the reservoir.

The perfusionator may not be suitable for every sediment system. The primary limitations relate to sediment grain size and permeability. Vertical advective flow of porewater would be limited in very fine grained sediments (mud, silt) with low permeability. Upward flow of porewater through the sediments was controlled by head pressure or a peristaltic pump operating at a low setting in the current design of the perfusionator. Low-pressure control of flow would likely be insufficient with low-permeability sediments, as back-pressure would build up and restrict flow. Another sediment limitation that should be considered in future applications of the perfusionator is the use of highly bioturbated sediments, which could channelize and disrupt controlled porewater introduction measures. Application of the perfusionator to fine-grained sediments or highly bioturbated sediments would require additional testing and optimization.

In the appropriate environment, the perfusionator provides a new tool for introducing dissolved tracers to the porewater for extended timescales. There are potentially wide

applications for the perfusionator in the aquatic and marine sciences, including laboratory, mesocosm, or field settings.

Acknowledgments

This research was supported by the National Science Foundation (VCR-LTER project DEB 0080381 and DEB 0621014; DEB Ecosystems 0542645 to VIMS and 0542635 to UNCW) and the Environmental Protection Agency (STAR FP916722010). The EPA has not officially endorsed this publication and the views expressed herein may not reflect the views of the EPA. This work would not have been possible without the help of M. Luckenbach, S. Fate, and R. Bonniwell at the VIMS ESL as well as H. Walker, D. Maxey, J. Adamo, S. Salisbury, E. Lerberg, C. Smith, and E. Ferer at VIMS. We are also grateful to K. Duernberger at UNCW for assistance in the lab.

References

Anderson, I.C., K.J.M. McGlathery, and C. Tyler. 2003. Microbial mediation of 'reactive' nitrogen transformations in a temperate lagoon. Marine Ecology Progress Series 246:73–84.

Armitage, A.R., T.A. Frankovich, and J.W. Fourqurean. 2006. Variable responses within epiphytic and benthic microalgal communities to nutrient enrichment. Hydrobiologia 569:423-435.

Boschker, H.T.S., S.C. Nold, P. Wellsbury, D. Bos, W. de Graaf, R. Pel, R.J. Parkes and T.E. Cappenberg. 1998. Direct linking of microbial populations to specific biogeochemical processes by ^{13}C-labelling of biomarkers. Nature 392:801-805.

Boschker, H.T.S. and J.J. Middelburg. 2002. Stable isotopes and biomarkers in microbial ecology. FEMS Microbiology Ecology 40:85-95.

Bühring, S.I., S. Ehrenhauss, A. Kamp, L. Moodley, and U. Witte. 2006. Enhanced benthic activity in sandy sublittoral sediments: Evidence from ^{13}C tracer experiments. Marine Biology Research 2:120-129.

Cahoon, L.B. 1999. The role of benthic microalgae in neritic ecosystems. Oceanography and Marine Biology 37:47-86.

Carpenter, S.R. 1996. Microcosm experiments have limited relevance for community and ecosystem ecology. Ecology 77:677-680.

Carpenter, S.R. 1999. Microcosm experiments have limited relevance for community and ecosystem ecology: Reply. Ecology 80:1085-1088.

Drenner, R.W. and A. Mazumder 1999. Microcosm experiments have limited relevance for community and ecosystem ecology: Comment. Ecology 80:1081-1085.

Dornblaser, M., A.E. Giblin, B. Fry, and B.J. Peterson. 1994. Effects of sulfate concentration in the overlying water on sulfate reduction and sulfur storage in lake sediments. Biogeochemistry 24:129-144.

Emery, W.J. and R.E. Thomson. 2001. Data Analysis Methods in Physical Oceanography, 2nd and Revised Edition. San Diego: Elsevier.

Enoksson, V. 1993. Nutrient recycling by coastal sediments - Effects of added algal material. Marine Ecology-Progress Series 92:245-254.

Franke, U., L. Polerecky, E. Precht and M. Huettel. 2006. Wave tank study of particulate organic matter degradation in permeable sediments. Limnology and Oceanography 51:1084-1096.

Girguis P.R., A.E. Cozen, and E.F. DeLong. 2005. Growth and population dynamics of anaerobic methane-oxidizing archaea and sulfate-reducing bacteria in a continuous-flow bioreactor. Applied and Environmental Microbiology 71:3725-3733.

Gribsholt B., E. Struyf, A. Tramper, L. De Brabandera, N. Brion, S. Van Damme, F. Meire, F. Dehairs, J.J. Middelburg, and H.T.S. Boschker. 2007. Nitrogen assimilation and short term retention in a nutrient-rich tidal freshwater marsh - a whole ecosystem ^{15}N enrichment study. Biogeosciences 4:11-26.

Hedges, J. and J. H. Stern. 1984. Carbon and nitrogen determinations of carbonate-containing solids. Limnology and Oceanography 29:657–663.

Holmes, R.M., J.W. McClelland, D.M. Sigman, B. Fry, and B.J. Peterson. 1998. Measuring ^{15}N-NH_4^+ in marine, estuarine, and fresh waters: An adaptation of the ammonia diffusion method for samples with low ammonium concentrations. Marine Chemistry 60:235-243.

Hughes, J.D., L.A. Deegan, B.J. Peterson, R.M. Holmes, and B. Fry. 2000. Nitrogen flow through the food web in the oligohaline zone of a New England estuary. Ecology 81:433-452.

Huettel, M. H. Roy, E. Precht, and S. Ehrenhauss. 2003. Hydrodynamical impact on biogeochemical processes in aquatic sediments. Hydrobiologia 494:231-236.

Huettel, M., and A. Rusch. 2000. Transport and degradation of phytoplankton in permeable sediments. Limnology and Oceanography 45:534-539.

Huettel, M., W. Ziebis, and S. Forster. 1996. Flow-induced uptake of particulate matter in permeable sediments. Geochimica Cosmochimica Acta 62:613-631.

Huston, M.A. 1999. Microcosm experiments have limited relevance for community and ecosystem ecology: Synthesis of comments. Ecology 80:1088-1089.

Janssen, F., M. Huettel, and U. Witte. 2005. Pore-water advection and solute fluxes in permeable marine sediments (II): Benthic respiration at three sandy sites with different permeabilities (German Bight, North Sea). Limnology and Oceanography 50:779-792.

Jönsson, B. 1991. A ^{14}C-incubation technique for measuring microphytobenthic primary productivity in intact sediment cores. Limnology and Oceanography 36:1485-1492.

Kaldy, J.E., P.M. Eldridge, L.A. Cifuentes, and W.B. Jones. 2006. Utilization of DOC from seagrass rhizomes by sediment bacteria: ^{13}Ctracer experiments and modeling. Marine Ecology Progress Series 317:41–55.

Lin, A.Y.C., J. F. Debroux, J. A. Cunningham and M. Reinhard. 2003. Comparison of rhodamine WT and bromide in the determination of hydraulic characteristics of constructed wetlands. Ecological Engineering 20:75-88.

MacIntyre, H.L., R.J. Geider, and D.C. Miller. 1996. Microphytoenthos: The ecological role of the "Secret Gardent" of unvegetated, shallow-water marine habitats. I. Distribution, abundance, and primary production. Estuaries 19:186-201.

Marín-Guirao, L., A.M. Atucha, J.L. Barba, E.M. López, and A.J. García Fernández. 2005. Effects of mining wastes on a seagrass ecosystem: metal accumulation and bioavailability, seagrass dynamics and associated community structure. Marine Environmental Research 60: 317-337.

McGlathery, K.J., N. Risgaard-Petersen, and P.B. Christensen. 1998. Temporal and spatial variation in nitrogen fixation activity in the eelgrass Zostera marine rhizosphere. Marine Ecology-Progress Series 168:245-258.

Middelburg, J.J., C. Barranguet, H.T.S. Boschker, P.M.J. Herman, T. Moens, and C.H.R. Heip. 2000. The fate of intertidal microphytobenthos carbon: An in situ ^{13}C-labeling study. Limnology and Oceanography 45:1224-1234.

Mutchler, T., M.J. Sullivan, and B. Fry. 2004. Potential of 14N isotope enrichment to resolve ambiguities in coastal trophic relationships. Marine Ecology Progress Series 266:27-33.

Nielsen, L.P. 1992. Denitrification in sediment determined from nitrogen isotope pairing. FEMS Microbiology Ecology 86:357-362.

NOAA 2008. Meteorological Station at Yorktown USCG Training Center, VA. Station ID 8637689. http://www.co-ops.nos.noaa.gov/data_menu.shtml?stn=8637689%20Yorktown%20Uscg%20Training%20Center,%20VA&type=Meteorological+Observations. Accessed 23 September 2009.

Parkes, R.J., N. J. E. Dowling, D. C. White, R. A. Herbert and G. R. Gibson. 1993. Characterization of sulfate-reducing bacterial-populations within marine and estuarine sediments with different rates of sulfate reduction. FEMS Microbiology Ecology 102:235-250.

Polerecky, L., U. Franke, U. Werner, B. Grunwald, and D. de Beer. 2005. High spatial resolution measurements of oxygen consumption rates in permeable sediments. Limnology and Oceanography: Methods 3:75-85.

Rao, A.M.F., M.J. McCarthy, W.S. Gardner, and R.A. Jahnke. 2007. Respiration and denitrification in permeable continental shelf deposits on the South Atlantic Bight: Rates of carbon and nitrogen cycling from sediment column experiments. Continental Shelf Research 27:1801-1819.

Reimers, C.E. 2007. Applications of microelectrodes to problems in chemical oceanography. Chemical Reviews 107:590-600.

Reimers, C.E., H.A. Stecher III, G.L, Taghon, C.M. Fuller, M. Huettel, A. Rusch, N. Ryckelynck, and C. Wild. 2004. *In situ* measurements of advective solute transport in permeable shelf sands. Continental Shelf Research 24:183-201.

Shiau, B.J., D.A. Sabatini and J.H. Harwell. 1993. Influence of Rhodamine WT Properties on Sorption and Transport in Subsurface Media. Ground Water 31:913-920.

Short, F.T., D.M. Burdick and J.E. Kaldy. 1995. Mesocosm experiments quantify the effects of eutrophication on eelgrass, Zostera marina. Limnology and Oceanography 40:740-749.

Smart, P.L. and I.M.S. Laidlaw. 1977. An evaluation of some fluorescent dyes for water tracing. Water Resources Research 13:15–33.

Stockdale, A., W. Davison, and H. Zhang. 2009. Micro-scale biogeochemical heterogeneity in sediments: A review of available technology and observed evidence. Earth-Science Reviews 92:81-97.

Tobias, C.R., J.K. Bohlke, J.W. Harvey, E. Busenberg. 2009. A simple technique for continuous measurement of time-variable gas transfer in surface waters. Limnology and Oceanography-Methods 7:185-195.

Tobias, C.R., M. Cieri, B.J. Peterson, L.A. Deegan, J. Vallino, and J. Hughes. 2003a. Processing watershed-derived nitrogen in a well-flushed New England estuary. Limnology and Oceanography 48:1766-1778.

Tobias, C., A. Giblin, J. McClelland, J. Tucker, and B. Peterson. 2003b. Sediment DIN fluxes and preferential recycling of benthic microalgal nitrogen in a shallow macrotidal estuary. Marine Ecology Progress Series 257:25-36.

Tolhurst, T.J., G. Gust, and D.M. Paterson. 20002. The influence of extracellular polymeric substance (EPS) on cohesive sediment stability. In Fine Sediment Dynamics in the Marine Environment, eds. J.C. Winterwerp and C. Kranenburg, 409-425. Elsevier Science B.V..

Trimmer, M. J. C. Nicholls, and B. Deflandre. 2003. Anaerobic Ammonium Oxidation Measured in Sediments along the Thames Estuary, United Kingdom. Applied and Environmental Microbiology 69:6447-6454.

Veuger, B., J.J. Middelburg, H.T.S. Boschker, and M. Houtekamer. 2005. Analysis of ^{15}N incorporation into D-alanine: A new method for tracing nitrogen uptake by bacteria. Limnology and Oceanography: Methods 3:230-240.

Veuger, B., D. van Oevelen, H.T.S. Boschker, and J.J. Middelburg. 2006. Fate of peptidoglycan in an intertidal sediment: An in situ ^{13}C-labeling study. Limnology and Oceanography 51:1572-1580.

Veuger, B., B.D. Eyre, D. Maher, and J.J. Middelburg. 2007. Nitrogen incorporation and retention by bacteria, algae, and fauna in a subtropical intertidal sediment: An in situ ^{15}N-labeling study. Limnology and Oceanography 52:1930-1942.

Watson, A.J. and J.R. Ledwell. 1988. Purposefully released tracers. Philosophical Transactions of the Royal Society of London A 325:189-200.

Figure 2-1. Perfusionator diagram.

The perfusionator reservoir, located at the bottom of the mesocosm tank, holds porewater that is pumped up through the sediment column. The porewater is introduced (e.g. via an IV dripper) through a PVC standpipe, which is connected to a porous pipe that feeds the reservoir. A mini-jet pump circulates the reservoir water to ensure that it is well mixed. Note that the figure is not drawn to scale.

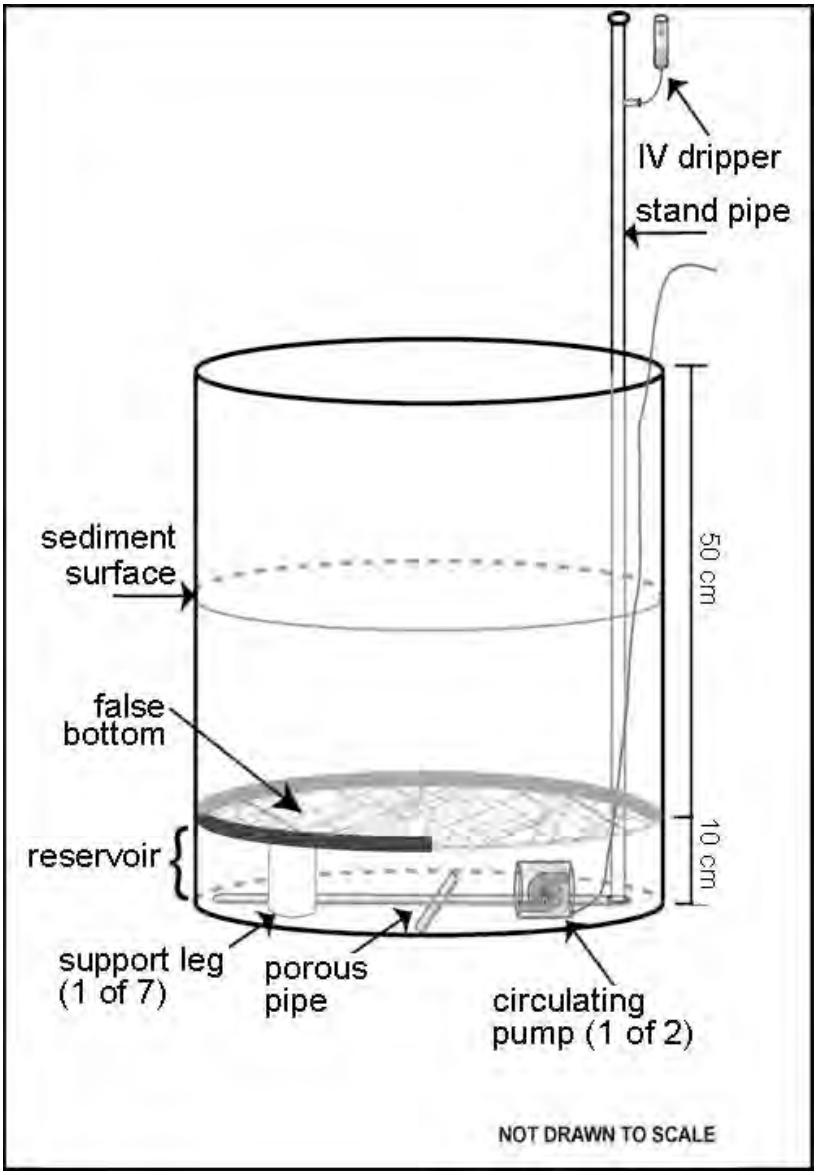
IV dripper
stand pipe
sediment surface
50 cm
false bottom
reservoir
10 cm
support leg (1 of 7)
porous pipe
circulating pump (1 of 2)
NOT DRAWN TO SCALE

Figure 2-2. Plumbing schematic for field deployment.

a) Plan view and b) cross section of circulating porewater system. Porewater from the porewater well located in the subtidal zone (dotted lines), was pumped to the shore where it was amended with isotopic and SF_6 tracers in a mixing chamber. Porewater with tracers (solid lines) was pumped back to the subtidal zone and into each perfusionator through a PVC standpipe.

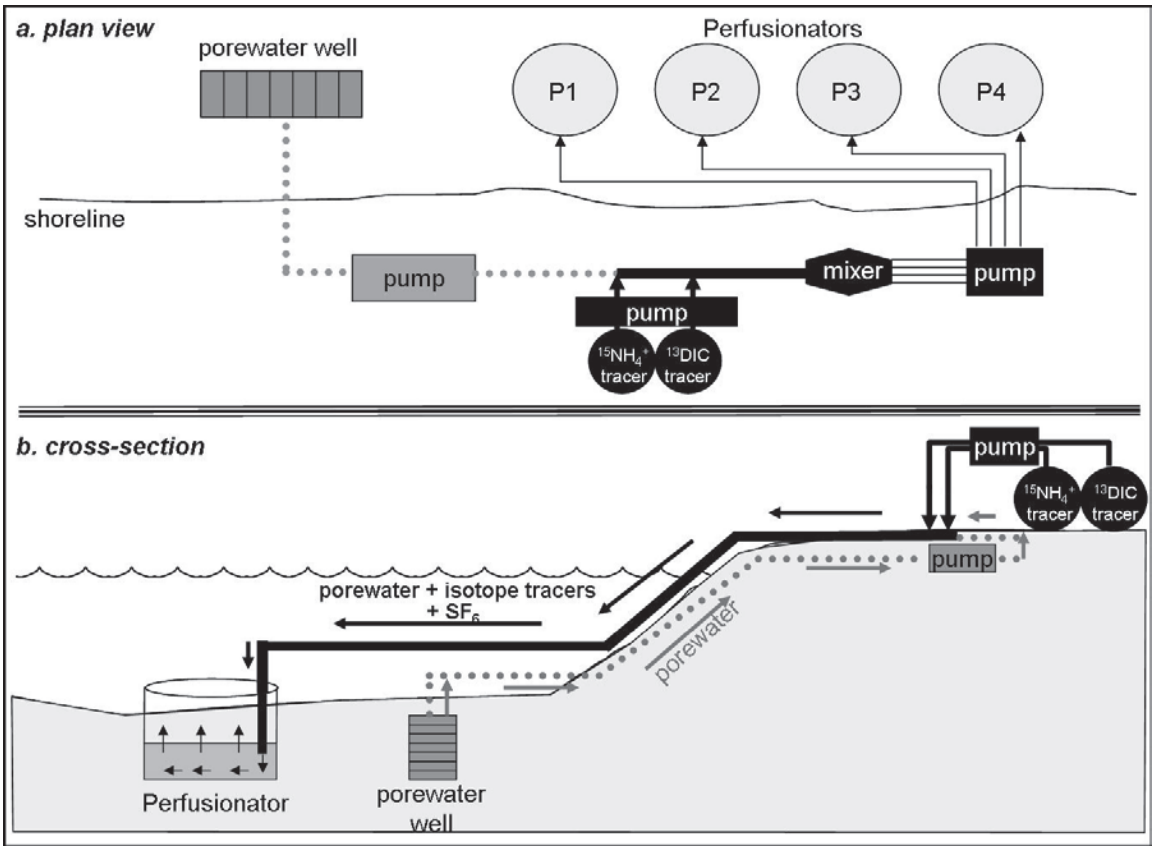
a. plan view
porewater well
Perfusionators
P1
P2
P3
P4
shoreline
pump
mixer
pump
pump
$^{15}NH_4^+$ tracer
^{13}DIC tracer
b. cross-section
pump
$^{15}NH_4^+$ tracer
^{13}DIC tracer
pump
porewater + isotope tracers + SF_6
porewater
Perfusionator
porewater well

Figure 2-3. Rhodamine WT concentrations for the laboratory test of the perfusionator.

The y-axis represents RWT concentrations as % of source solution, which was 100%. RWT concentrations were measured in the water column (dashed line, triangles; n =1), and in the sediments at 6 cm (squares, dotted lines) and 15 cm (circles, solid lines) depths. Sediments were sampled in both center (C) and edge (E) positions, according to inset in diagram. Open symbols correspond to center positions (mean ± SE; n = 5), closed symbols correspond to edge positions (mean ± SE; n = 4).

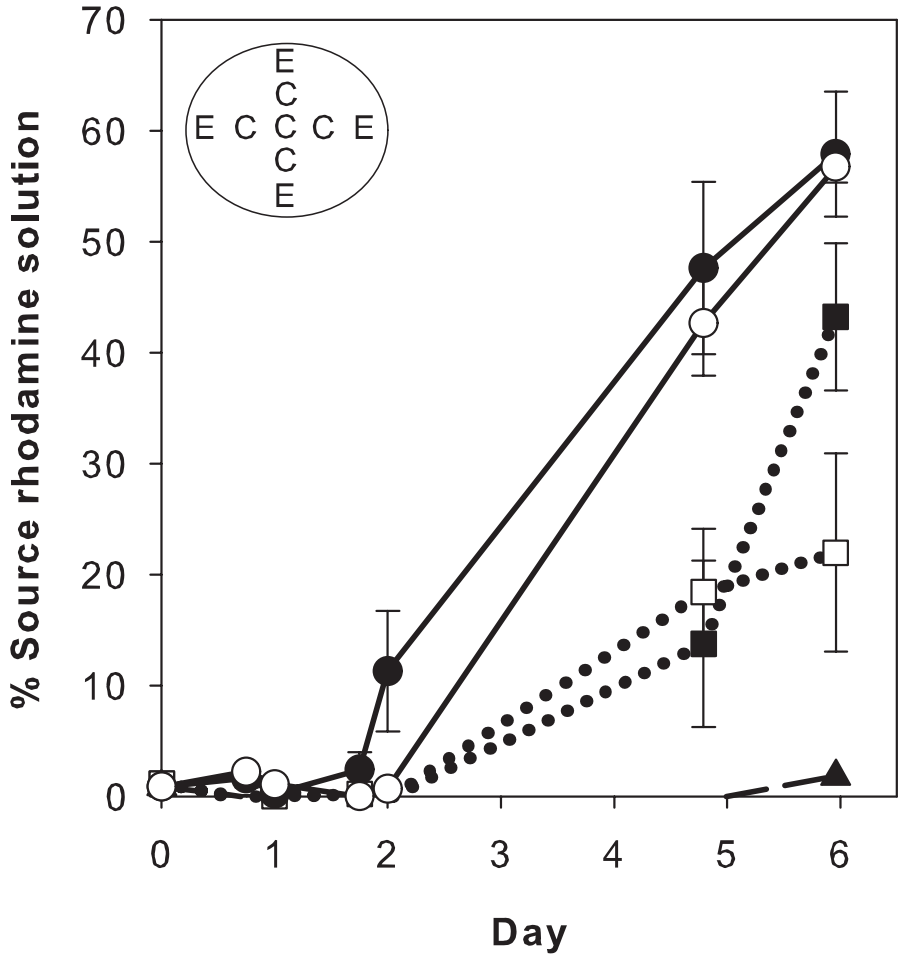
% Source rhodamine solution
Day
70
60
50
40
30
20
10
0
0
1
2
3
4
5
6
E
C
E C C C E
C
E

Figure 2-4. SF_6 concentrations during outdoor mesocosm array experiment.

Plan view of individual perfusionators (a-d). Contour plots show SF_6 concentrations (nM) at 5 cm sediment depth. Star denotes location of standpipe within each mesocosm. Square grid shows 10 sampling positions.

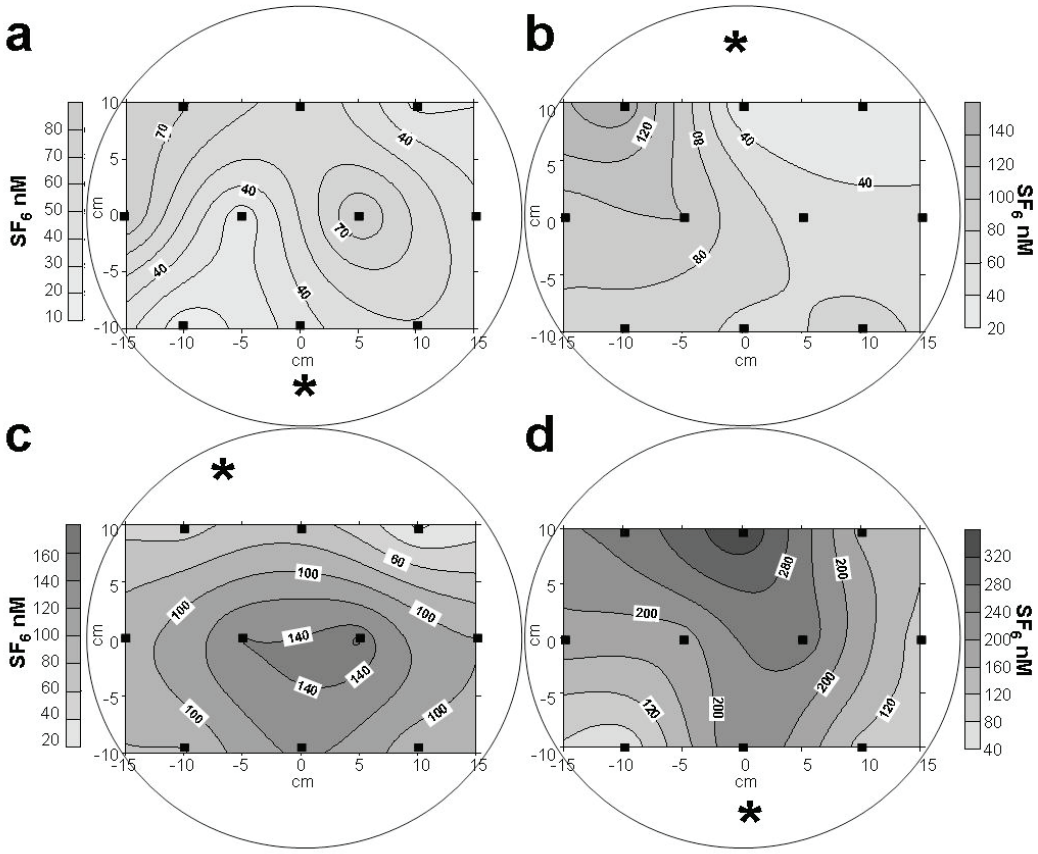
a
b
c
d
SF6 nM
cm
*

Figure 2-5. Bulk sediment isotopic enrichments for surface sediments (0-1 cm) during outdoor mesocosm array experiment.

Solid lines (closed symbols) indicate $\delta^{15}N$ and dotted lines (open symbols) indicate $\delta^{13}C$. Symbols represent average values ± 1 SE (n = 2). Vertical dotted grey line at Day 15 indicates the end of the isotope addition period. A $\delta^{15}N$ value of 10,000 ‰ is 3.89 atom% ^{15}N, and $\delta^{13}C$ of 1000 is 2.19 atom% ^{13}C.

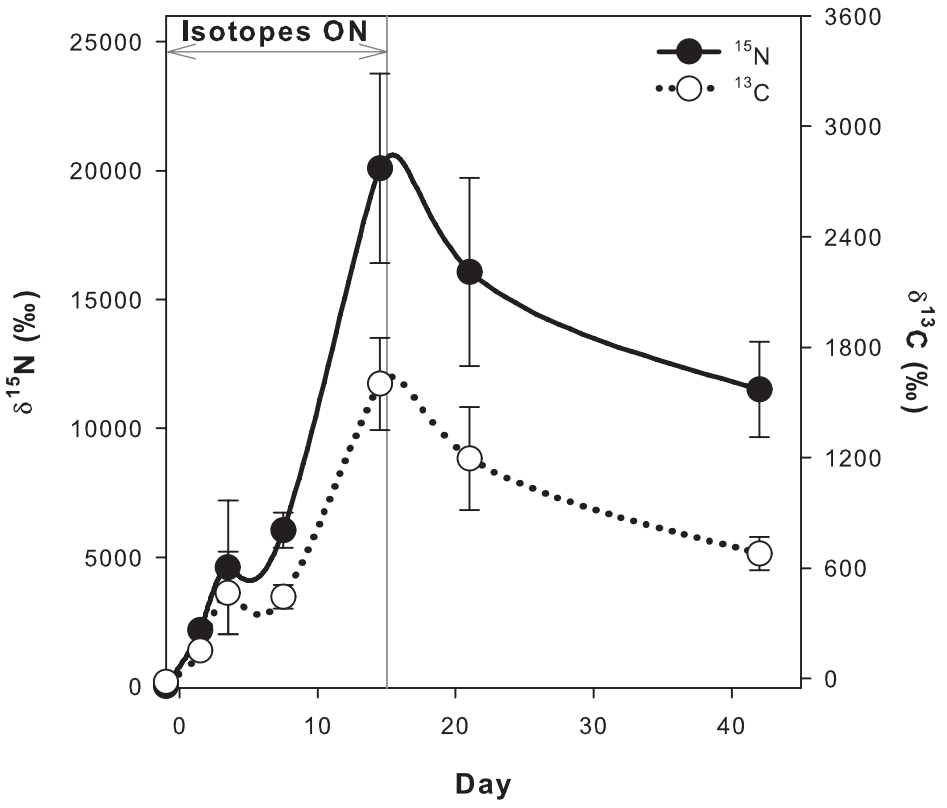
Isotopes ON
^{15}N
^{13}C
δ^{15}N (‰)
δ^{13}C (‰)
Day
25000
20000
15000
10000
5000
0
3600
3000
2400
1800
1200
600
0
0
10
20
30
40

Figure 2-6. SF_6 concentrations during field deployment of the perfusionator.

Plan view of 4 (a-d) individual perfusionators. Contour plots show SF_6 concentrations (nM) at 5 cm sediment depth. Star denotes location of standpipe within each mesocosm. Square grid shows 10 sampling positions.

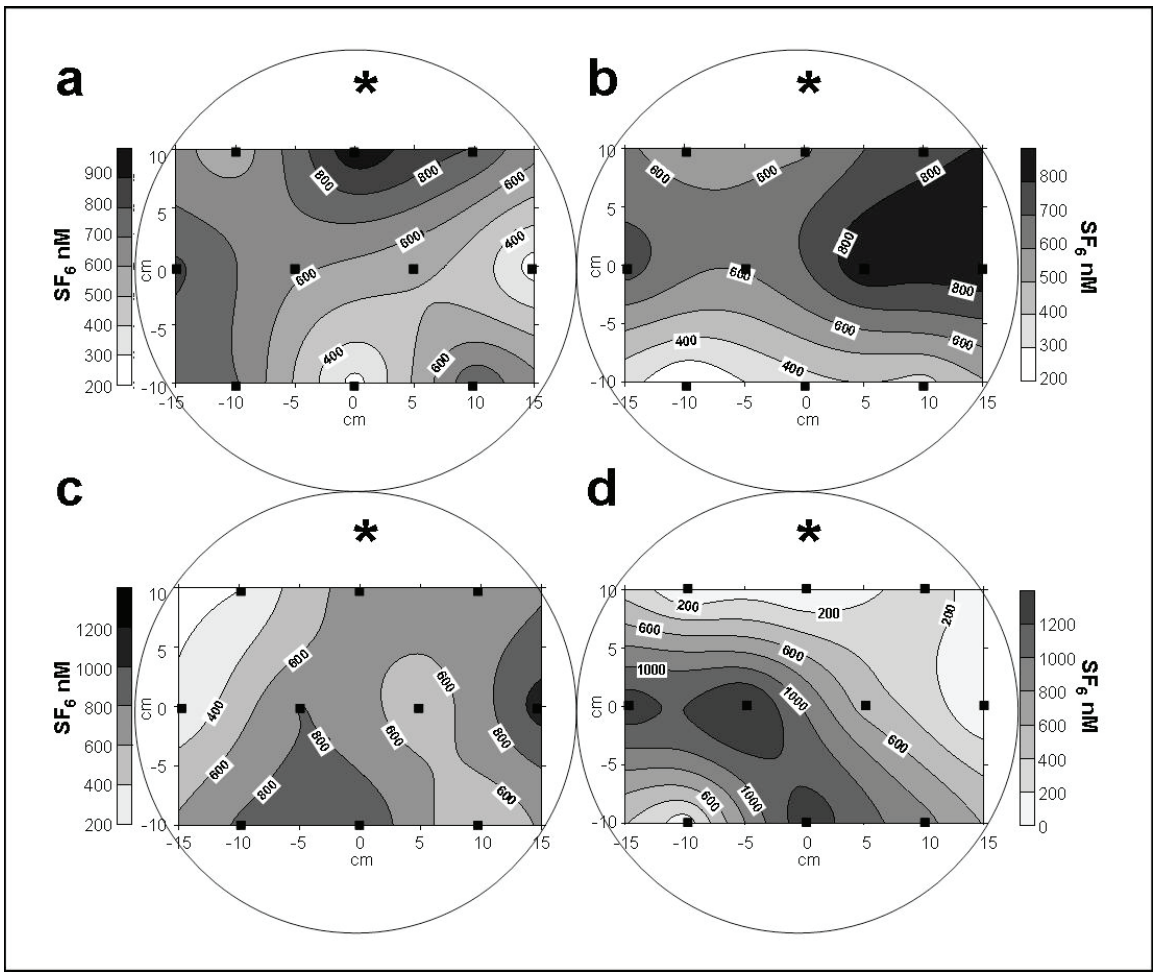
a
b
c
d
SF6 nM
cm

Figure 2-7. Bulk sediment isotopic enrichments for surface sediments (0-1 cm) during the field deployment of the perfusionator.

Solid lines (closed symbols) indicate $\delta^{15}N$ and dotted lines (open symbols) indicate $\delta^{13}C$. Symbols represent average values ± 1 SE (n = 4). Vertical dotted grey line at Day 12 indicates the end of the isotope addition period.

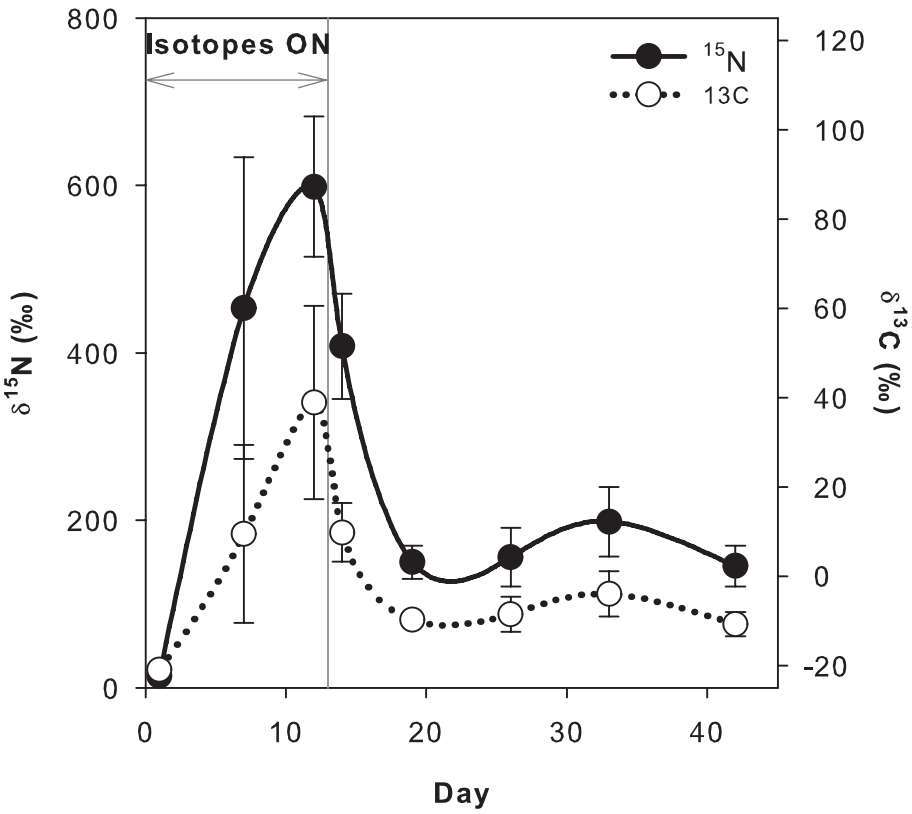
Isotopes ON
15N
13C
800
600
400
200
0
120
100
80
60
40
20
0
-20
0
10
20
30
40
Day
δ15N (‰)
δ13C (‰)

Figure 2-8. Isotopic enrichment ($\delta^{15}N$) for porewater NH_4^+ during the field deployment of the perfusionator.

Symbols represent average values ± 1 SE (n = 4). Vertical dotted grey line at Day 12 indicates the end of the isotope addition period.

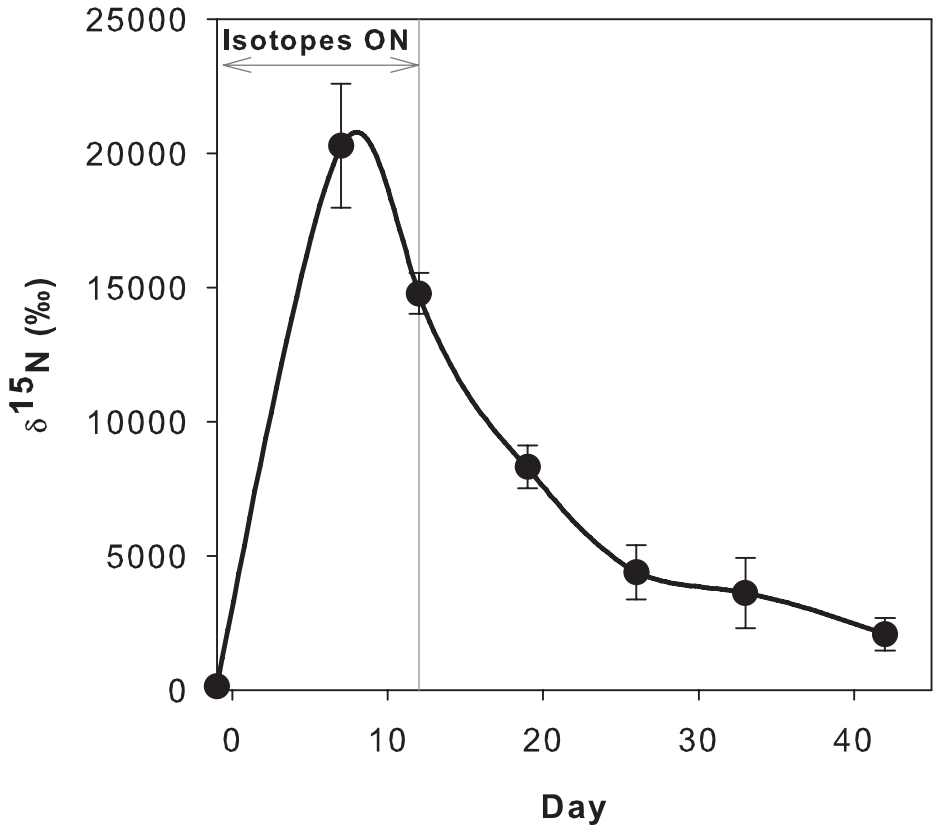
Isotopes ON
25000
20000
15000
10000
5000
0
δ15N (‰)
0
10
20
30
40
Day

CHAPTER 3: BENTHIC ALGAE DETERMINE SEDIMENT ORGANIC MATTER COMPOSITION IN SHALLOW PHOTIC SEDIMENTS

Hardison, A.K.

Canuel, E.A.

Anderson, I.C.

Tobias, C.R.

Veuger, B.

Abstract

Sediment organic matter in shallow coastal systems performs important ecosystem functions such as providing food for infauna and epifauna, aiding in sediment stability, and providing storage for carbon and nutrients. Sediment organic matter composition may be affected by the dominant primary producer, which has been shown to be sensitive to changes in nutrient loading to shallow systems. We investigated the influence of microphytobenthos (MPB) and benthic macroalgae on sediment organic matter quantity and quality in an experimental system using bulk and molecular level (total hydrolyzable amino acids, THAA; phospholipid linked fatty acids, PLFA) analyses. Over the course of the 42-day experiment, MPB activity in light treatment increased total organic carbon (TOC) and total nitrogen (TN) by 173 and 141%, respectively, compared to the dark treatment. THAA comprised a substantial fraction of sediment organic matter (~16% of TOC, 35% of TN) and followed bulk accumulation patterns. Mole percent composition of the THAA pool indicated that sediment in light treatments were composed of more labile organic material while dark sediment organic matter was more degraded, with higher proportions of Glycine and D-alanine. PLFA content, which made up ~1% of TOC and represented viable biomass, contained high levels of algal fatty acids in light treatments, particularly those derived from diatoms. MPB activity increased the lability of sediment organic matter, which likely resulted in the observed increases in bacterial PLFA concentrations in light treatments. Macroalgae were added to half of the light treatments and grew to 410 ± 102 gdw m^{-2} by Day 42. Macroalgae decreased sediment organic matter buildup, with TOC and TN increasing by only 130 and 94%, respectively,

compared to light treatments without macroalgae, likely as a result of shading, and thereby reducing production of benthic microalgae. The presence of macroalgae decreased sediment organic matter lability as well, which resulted in diminished buildup of bacterial biomass. By the final day of the experiment, PCA analyses suggested that sediment composition in treatments with macroalgae were more similar to dark treatments and less similar to light treatments without macroalgae. Overall benthic micro- and macroalgae fundamentally altered sediment organic matter quality and quantity, which has important ecological consequences in these systems.

Introduction

Shallow coastal bays make up approximately 13% of the world's coastline, are among the most highly productive ecosystems on earth, and are distinctly vulnerable to effects from the growing problem of nutrient over-enrichment due to increased human activities ("cultural eutrophication") (Nixon, 1995; NRC, 2000; Pedersen *et al.*, 2004). One consequence of nutrient loading to many of these systems has been a shift in primary producer community structure. Because much of the sediments exists within the euphotic zone, benthic autotrophs typically dominate production in these bays. Observations from a number of systems have shown that as nutrient loading increases, ephemeral macroalgae, phytoplankton, and epiphytes increase, while slow-growing perennial macrophytes such as seagrass decrease (Duarte, 1995; Hauxwell *et al.*, 2001; Sand-Jensen & Borum, 1991; Valiela *et al.*, 1992). For example, in Waquoit Bay, MA, ephemeral populations of green (*Cladophora*) and red (*Gracilaria*) macroalgae replaced *Zostera marina* seagrass when nutrient loadings increased six-fold (Hauxwell *et al.*, 2003). The mechanisms underlying this shift in community structure relate to differences among plant types in nutrient uptake and growth strategies (Nielsen *et al.*, 1996; Sand-Jensen & Borum, 1991). Microphytobenthos (MPB), including benthic microalgae and cyanobacteria, often contribute significantly to primary production within these shallow systems; however, their response as the autotrophic community structure shifts in the face of nutrient over-enrichment is not well understood.

Through structure, physiology, and growth, the dominant plants in a community greatly affect both the physical and biological conditions of a system,

including overall community structure (Heck *et al.*, 2003; Norkko, 1998; Orth *et al.*, 1984), ecosystem processes such as nutrient cycling (Risgaard-Petersen, 2003; Tyler *et al.*, 2001), and hydrologic conditions (Fonseca & Calahan, 1992; Jumars *et al.*, 2001; Paterson & Black, 1999). For example, the presence of ephemeral macroalgae often leads to episodic anoxia and increased sulfide concentrations (Krause-Jensen *et al.*, 1999; Sfriso *et al.*, 1992), which negatively affect fish and benthic fauna, as well as other autotrophs (Gray *et al.*, 2002; Hauxwell *et al.*, 2003; Norkko *et al.*, 2000; Raffaelli *et al.*, 1998; Sundback & McGlathery, 2005). Macroalgae also affect other primary producers directly through shading and/or competition for nutrients. Because of their location at the sediment surface or floating just above the sediments, macroalgae may decrease light availabile for MPB, thereby decreasing or possibly inhibiting MPB production (Sundback & McGlathery, 2005; Tyler *et al.*, 2003; Valiela *et al.* 1997), although, some MPB communities show evidence of photo-acclimation to low-light environments and are not affected by shading by overlying macroalgal mats (Sundback & McGlathery, 2005; Sundback *et al.*, 1996). In addition to light, macroalgae may out-compete MPB for water column nutrients, particularly when MPB are nutrient-limited, which often occurs in sandy sediments in warm months (Sundback & McGlathery, 2005; Nilsson *et al.*, 1991).

Shifts in plant community structure have also been linked to changes in sediment composition (Benoy & Kalff, 1999; Kenworthy *et al.*, 1982), which in turn could affect ecosystem services like nutrient cycling and secondary production. For example, macrophyte canopies enhance accumulation of fine, organic-rich particles compared with unvegetated sediments (Benoy & Kalff, 1999; Gacia *et al.*, 2002). Sediment organic matter consists of material from a variety of living and non-living sources and performs

important ecosystem functions such as providing food for infauna and epifauna, aiding in sediment stability (e.g. extrapolymeric substances produced by benthic microalgae (Wolfstein *et al.*, 2002)), and providing temporary or permanent storage for carbon (C) and nutrients. While sources contributing to sediment organic matter vary by system, microbial biomass often contributes a significant fraction of sediment organic matter in shallow systems (Bouillon & Boschker, 2006; Canuel & Martens, 1993; Volkman *et al.*, 2008). Specifically, MPB may be a particularly good source of labile organic matter, which may support bacterial production (Middelburg *et al.*, 2000; Volkman *et al.*, 2008).

The objectives of this study were to examine the influence of MPB on sediment organic matter quality and quantity, and to describe how the MPB contribution to sediment organic matter changes in the presence of a macroalgal bloom. Because gross measurements of sediment organic matter (e.g. total organic carbon, total nitrogen) do not provide information on source or availability, we combined bulk and molecular-level analyses to more accurately characterize the sediment organic matter of a shallow coastal bay. Specific organic compounds (biomarkers) were used to attribute organic matter to different sources (e.g. Boschker *et al.*, 1999; Canuel *et al.*, 1995; Volkman *et al.*, 2008).

Methods

Site description Sediments and macroalgae were collected from Hog Island Bay, Virginia (HIB; Fig. 1), which is located along the Delmarva Peninsula and part of the Virginia Coast Reserve, a Long-Term Ecological Research (LTER) site. HIB is a shallow coastal lagoon (< 2 m deep at mean low water), typical of temperate lagoons

along the U.S. East coast and is dominated by benthic autotrophs (McGlathery *et al.*, 2001; Thomsen *et al.*, 2006). Macroalgae are present throughout the lagoon in low to moderate densities (Thomsen *et al.*, 2006); however, we collected sediments and macroalgae from mid-lagoon shoal sites where localized blooms of macroalgae have previously developed and dominated benthic production during warmer months (McGlathery *et al.*, 2001; Thomsen *et al.*, 2006). Throughout the rest of the year when macroalgal biomass was low, MPB dominated (Anderson *et al.*, 2003; McGlathery *et al.*, 2001).

Experimental design A flow-through mesocosm array was set-up at the Virginia Institute of Marine Science (VIMS) Eastern Shore Laboratory (ESL) in Wachapreague, VA. In preparation for this experiment, we designed and tested an experimental apparatus that allowed for addition of nutrients simultaneously via surface water (SW) and porewater (PW). Nutrients in shallow coastal bays commonly enter through the SW (e.g. runoff and atmospheric deposition) and/or PW (e.g. groundwater and sediment remineralization), thus, it was important for our study, which focused on the community living at the sediment-water interface, to include nutrients from both sources. Discussion of the design and testing of the perfusionator can be found in Hardison et al. (Submitted). The "perfusionator" consisted of a 60 cm I.D. x 60 cm height translucent fiberglass cylinder that included a reservoir for PW at the base of the sediment column. Twelve mesocosms were filled to a depth of ~15 cm with intact sediments extruded from cores collected from the shoal field site in May 2007 (Fig. 1). At the ESL, the perfusionators were placed in shallow water baths under 30% shade cloth to control temperature and

light. The water column above the sediments was connected to a flow-through seawater system supplied with filtered seawater from the adjacent creek (1 μm) and was stirred continuously with a mini-jet pump to keep the water column well mixed. Once connected to the experimental system, the mesocosms equilibrated for two weeks before beginning the experiment.

Our experiment consisted of an incomplete factorial design made up of two factors, each with two levels: 1) Light (ambient vs. dark), and 2) Macroalgae (presence vs. absence of live macroalgae). All factors were crossed with the exception of the dark + macroalgae treatment, since, for logistical purposes, only light treatments received a macroalgal addition. Each treatment had $n = 4$.

For the nutrient additions, a peristaltic pump was used to add $(NH_4)_2SO_4$ and $NaHCO_3$ solutions to each mesocosm simultaneously via the SW and PW. NH_4^+ was added at a rate to achieve 25 μM above background levels (2-4 μM) in mesocosm SW and at approximate PW background levels (200-300 μM). HCO_3^- was added at a rate to achieve enrichment of 0.25 mM above dissolved inorganic C (DIC) background in SW (~2.5 mM) and at approximate PW background levels (~2.5 mM). Feed water was drawn from a creek adjacent to the ESL, pumped through a series of sand, bag (10 μm), cartridge (5 and 1 μm), and ultraviolet filters, and amended with HCO_3^- and NH_4^+ in a mixing chamber before delivery to each perfusionator. SW additions were delivered gravimetrically directly to the perfusionator water column at a rate of ~43 L day^{-1}, or a SW residence time of ~2 days. Fine-scale control of the SW flow rate at each mesocosm was achieved using IV drippers that were calibrated daily. PW additions were delivered gravimetrically through a standpipe into the perfusionator reservoir located below the

sediment column at a rate of ~15 L day^{-1}, or a porewater residence time of ~1.8 days. Fine scale control of the PW flow rate into each perfusionator was achieved using an IV dripper located at each standpipe, which was also calibrated daily.

Macroalgae (*Gracilaria vermiculophylla*) were collected live from HIB in May 2007 and returned to the laboratory. The algae were cleaned of epiphytes and epifauna, rinsed with 0.7 μm filtered seawater, and placed in aquaria inside a greenhouse. Filtered (0.7 μm) seawater was added to each tank and kept aerated while the algae were starved for 10 days before addition to the mesocosm. Macroalgae were "starved" to ensure depletion of internal stored nutrients and rapid uptake of the nutrients once in the mesocosms. Live macroalgae were added to half of the light treatments in densities observed naturally (124.8 ± 1.6 gdw m^{-2}; McGlathery *et al.*, 2001; Thomsen *et al.*, 2006).

Sampling Nutrient and macroalgal additions began on Day 0. The mesocosms were sampled prior to the additions to capture baseline conditions, and on Days 1, 3, 7, 14, 16, 21, 29 and 42. At each sampling, surface sediments (0-1 cm) were collected using two acrylic cores (5.7 cm I.D.) and reserved for bulk (total organic C (TOC), total nitrogen (TN)), amino acid, and fatty acid analyses. Sediments from both cores were combined in pre-combusted glass jars, immediately frozen at -4ºC, and frozen at -80ºC within 3 days. The remaining sediment in the cores was placed carefully back into the holes in the mesocosm sediments. Sediments were also collected for chlorophyll *a* concentrations using a cut-off syringe (1.1 cm I.D.). Samples were sectioned into 0-0.3 cm and 0.3-1.0 cm horizons, placed into 15 mL centrifuge tubes, immediately frozen at -4ºC, and

analyzed within 1 month. A different region of the sediment surface was sampled each day to avoid artifacts associated with re-sampling.

Macroalgae were removed from each mesocosm, patted dry, and weighed for a biomass estimate on Days 7, 14, 21, 29, and 42. Wet mass was converted to dry mass using percent water estimates (72%) from *G. vermiculophylla* collected in the field, and dry mass values were normalized to the mesocosm sediment surface area (0.29 m^2). The live macroalgae were kept in seawater from the respective mesocosms and returned as quickly as possible to avoid desiccation.

Bulk analyses Samples were analyzed for benthic chlorophyll *a* concentrations according to a modification of the method of Lorenzen (1967; Pinckney *et al.*, 1994). The sediment pellet was sonicated in 90% acetone, vortexed and extracted for 24 h at -4ºC. The supernatant was passed through a 0.45 μm filter and read on a Shimadzu UV-1601 UV Visible spectrophotometer (λ = 665, 750 nm). Chlorophyll *a* concentrations (mg m^{-2}) were calculated according to the equations in Lorenzen (1967). Chlorophyll *a* concentrations for the 0-0.3 and 0.3-1.0 cm sections were summed to obtain concentrations for 0-1 cm.

For bulk sediment TOC and TN measurements, sediments were freeze-dried, ground and homogenized, acidified to remove inorganic C (Hedges & Stern, 1984), and analyzed for TOC and TN using a Costech ECS 4010 elemental analyzer.

Total hydrolyzable amino acids Hydrolyzable amino acids (HAA) were analyzed on a subset of the sediment samples according to the method presented in Veuger et al. (2005).

Freeze dried sediment (1 g) was rinsed with 2N HCl and Milli-Q water to remove dissolved amino acids. The sediment pellet was then hydrolyzed with 6N HCl at 110ºC for 20 h. Following purification by cation exchange chromatography, amino acids were derivatized with isopropanol and pentafluoropropionic anhydride and further purified by solvent extraction. Concentrations of the derivatized D- and L-amino acids were measured by gas chromatography on a HP 6890 GC. The sum of concentrations of all amino acids analyzed will be referred to as total hydrolyzable amino acids (THAA).

Phospholipid linked fatty acids Total fatty acids were analyzed on a subset of the sediment samples according to a modified Bligh and Dyer (1959) method (Canuel *et al.*, 2007; Poerschmann & Carlson, 2006). Wet sediments (~12 g) were extracted using an accelerated solvent extractor system (Dionex ASE 200) adapted for in-cell silica gel chromatography. Each sample was extracted twice on the ASE: neutral lipids were collected following extraction with a 9:1 (v:v) hexane:acetone mixture at 50ºC, then polar lipids were collected following extraction with a 8:2 (v:v) methanol:chloroform solution at 80ºC. Neutral and polar lipid fractions were saponified using KOH-CH_3OH for 2h at 110ºC. Saponified samples were then extracted under basic and acidic conditions. The acid-extracted fractions were methylated with BF_3-CH_3OH to form fatty acid methyl esters (FAME). The neutral FAME included neutral and glycolipids while the polar FAME represented the phospholipid-linked fatty acids (PLFA). FAME concentrations were measured by gas chromatography with flame ionization detection (GC-FID, DB-5 column, HP 5890) and quantified using methyl heneicosanoate as an internal standard. Peak identities were verified using reference standards as well as coupled gas

chromatography mass spectrometry interfaced to a mass selective detector operated in electron impact mode (HP 6890, GC-MSD). Fatty acids are designated A:BωC, where A is the total number of carbon atoms, B is the number of double bonds, and C is the position of the first double bond from the aliphatic ‘‘ω’’ end of the molecule. The prefixes ‘‘i’’ and ‘‘a’’ refer to iso- and anteiso- methyl branched fatty acids (see Canuel *et al.*, 1997 and references therein).

Data analysis We applied repeated measures analysis of variance (ANOVA) to examine the effects of light (ambient vs. dark), macroalgae (presence vs. absence) and time (day) on the sediment parameters using the Mixed procedure in SAS 9.1 (SAS Institute Inc., Cary, NC). In all models, a compound symmetry error structure was used to model the within-subject covariance structure. Analysis of individual THAA and PLFA were conducted on mole percent abundance and concentration, respectively. Results presented use Type III sum of squares from the ANOVA model. Unless otherwise noted, values presented are means ± 1 SE for 4 replicates.

We performed principal components analysis (PCA; Minitab 15 software) to aid in evaluating relationships between treatments and response variables. PCA is used to simplify a dataset by identifying a small set of variables that accounts for a large portion of data variance. PCA were run with data from Days 1 and 42 to explore changes in PLFA (ng FA gdw^{-1}) and THAA (mole %) composition over the experiment. All THAA (11 compounds) and a sub-set of PLFA (9 compounds) representing all major fatty acid classes were used in the analyses. Prior to PCA, each dataset was normalized to total concentration to correct for differences in concentrations between samples (Yunker *et al.*,

2005). Any variables that were below detection were set to 1 prior to normalization. The centered logratio values (division by the geometric mean, followed by log transformation) were then autoscaled by dividing by the variable standard deviation. This data normalization procedure was performed to avoid artifacts of negative bias or closure associated with the dataset structure (Yunker *et al.*, 2005). PCA loadings describe the relationships between the PC and the response variables, while PCA scores describe the relationships between the treatments and the PC.

Results

Experimental conditions Temperature and salinity in the mesocosm water columns were similar among treatments and to the field site (Table 1). Macroalgae in the mesocosms grew steadily from 125 ± 1 to 410 ± 102 gdw m^{-2}, which was within the range observed at the Hog Island Bay field sites (Table 1; Fig. 2a). Concentrations of benthic chlorophyll *a* were higher for light treatments without macroalgae ("–Macro") and with macroalgae ("+Macro") than for the dark treatment ("Dark"; Fig. 2b). However, compared with the field value, all were within a factor of two. Mean TOC and TN concentrations for the light treatments were similar to the field values, but the Dark treatment values were lower.

Bulk sediments Surface sediment TN and TOC concentrations followed similar patterns throughout the experiment (Fig. 3a, b). TN for all samples began at ~14 μmol N gdw^{-1} and increased throughout the experiment, peaking on Day 42 at 35.2 ± 1.0, 28.4 ±

5.0, and 19.8 ± 3.1 μmol N gdw^{-1} for –Macro, +Macro, and Dark treatments, respectively. TOC increased from ~144 μmol C gdw^{-1} to 404.0 ± 20.6, 340.7 ± 67.0, and 248.6 ± 40.2 μmol C gdw^{-1} for –Macro, +Macro, and Dark treatments, respectively. Both TN and TOC showed significant Light, Macroalgae, and Time effects (Table 2). –Macro (light) treatment had highest TN and TOC concentrations, Dark was the lowest, and +Macro was intermediate. C:N ratios remained relatively constant over time and displayed no significant light or macroalgae effects (Fig. 3c; Table 2). C:N ratios across treatments over the experiment averaged 10.7 ± 0.2.

Benthic chlorophyll *a* content was highly variable over time, but generally showed the same patterns as sediment organic content (Fig. 2b). Between Day 0 and Day 42, concentrations for the –Macro treatment increased from 28.1 to 101.8 ± 34.2 mg Chl *a* m^{-2}, +Macro increased from 8.4 to 85.7 ± 60.4 mg m^{-2}, and the Dark treatment remained unchanged, with a mean across all samples of 11.9 ± 4.1 mg m^{-2}. –Macro was significantly higher than Dark (Table 2). Because of high variability between-mesocosms within a treatment, +Macro treatments were not significantly different than –Macro treatments.

Total Hydrolyzable Amino Acids (THAA) THAA concentrations showed similar patterns to sediment organic content (Fig. 4a). Concentrations for all treatments increased from ~4 μmol AA gdw^{-1} on Day 0 to 14.0 ± 1.3, 8.4 ± 1.1, and 6.8 ± 1.1 μmol AA gdw^{-1} on Day 21 for –Macro, +Macro, and Dark treatments, respectively. Concentrations remained steady through Day 42. –Macro had highest concentrations, Dark was lowest, and +Macro was intermediate (Fig. 4a, Table 2). THAA-C made up

approximately ~14% of TOC for both light treatments and 12% of TOC for Dark treatments, and THAA-N made up approximately 39 and 33% of TN for light and dark treatments, respectively.

Concentrations of four selected individual amino acids are presented as mole percentages in Figure 5; however, data for all 11 amino acids analyzed are presented in Table 3. Across all treatments, glycine (Gly) was the most abundant amino acid, making up approximately 25% of THAA, followed by L-alanine (L-Ala) and aspartine (Asp), L-glutamic acid (L-Glu), proline (Pro), threonine + valine (Thr + Val), leucine (Leu), lysine (Lys), isoleucine (Ile) and phenylalanine (Phe), and D-alanine (D-Ala). Most amino acids showed a significant light effect, with the exception of Pro, L-Glu, and Phe (Table 2). Mole percentages of Leu, L-Ala, Thr+Val, Ile, and Lys were higher for –Macro than Dark, while Gly, D-Ala and Asp were higher in the Dark treatment (Fig. 5a, b, c). The only amino acid to display a significant macroalgae effect was Lys, for which mole percentages were higher in –Macro treatments (Fig. 5d).

Phospholipid linked fatty acids (PLFA) PLFA concentrations followed patterns similar to those of sediment organic content (Fig. 4b). –Macro had highest concentrations, Dark was lowest, and +Macro was intermediate (Fig. 4b, Table 2.) PLFA-C made up a variable fraction of TOC over the course of the experiment. The Dark treatment was lowest, decreasing from 0.6 to 0.3 ± 0.03% of TOC from Days 0 to 42. Both light treatments began at 1.6% of TOC and generally decreased over time. By Day 42, –Macro was highest, at 1.2 ± 0.3% of TOC, while +Macro ended at 0.6 ± 0.002% of TOC.

Groups of PLFA showed the same concentration patterns over time as total PLFA (Fig. 6a, b; Table 2). Saturated fatty acids (SAT) were the most abundant group, making up ~ 50% of total PLFA, followed generally by monounsaturated (MUFA; ~30%), polyunsaturated (PUFA; 15%), and branched fatty acids (BrFA; ~5%). PUFA and BrFA are displayed (Fig. 6a, b); however SAT and MUFA followed similar patterns. All groups showed a significant light effect, with concentrations in -Macro exceeding Dark (Table 2). In addition, all groups except BrFA showed a significant macroalgae effect, with higher concentrations in the –Macro treatments.

Algal-specific fatty acids varied between treatments and over time as well (Fig. 6c-g)). Concentrations of 20:4ω6 and 20:5ω6 (diatoms; Fig. 6c, d; Volkman *et al.*, 1989), 18:2ω6 (diatoms, possibly green algae, cryptophytese; Fig. 6e; Volkman *et al.*, 1989), 18:4 (possibly cyanobacteria; Fig. 6f; Cook *et al.*, 2004a), and 22:6ω3 (diatoms, possibly dinoflagellates; Fig. 6g; Dijkman & Kromkamp, 2006) followed similar patterns. All were significantly higher in the -Macro treatment than Dark. Among light treatments, all except 18:2ω6 were higher in –Macro treatments (Table 2). 18:2ω6 showed no significant macroalgae effect. Generally, C_{20} PUFA were more abundant than C_{18} PUFA, although their relative abundances, as demonstrated by the ratios of 20:5w3/18:2w6, shifted over time (Fig. 6h). For light treatments, this ratio decreased from 5.7 to 1.9 ± 0.5 (–Macro) and 0.8 ± 0.3 (+Macro) from Day 0 to 42. BrFA, representing bacterial-specific fatty acids (sum of i14:0, i15:0, a15:0, i16:0, i17:0, a17:0; Boschker *et al.*, 2000; Kaneda, 1991), were also more concentrated in light treatments, but showed no significant macroalgae effect (Table 2; Fig. 6b).

Factor analysis PCA provided a summary of changes in sediment composition between treatments and over time. PC1 and PC2 explained 39.9 and 21.0% of the variance in PLFA composition, respectively (Fig. 7a, b). Both light treatments grouped closely on Day 1, with more positive scores on PC1 than the Dark treatment (Fig. 7a). Scores along PC2 were similar among treatments on Day 1. In contrast, the treatments were separated along both PC1 and PC2 on Day 42. On Day 42, both light treatments had lower scores on PC1 than Day 1; +Macro had lower scores on PC1 than –Macro, and Dark was most negative. The variables 14:0, 16:0, 20:5ω3, and 16:1ω7 had the most positive loadings on PC1 while BrFA and 18:2w6 had the most negative loadings (Fig. 7b). By Day 42, the treatments were also distributed along PC2. The Dark treatment had the lowest PC2 score, –Macro was the highest, and +Macro was intermediate. BrFA had negative PC1 and PC2 loadings, similar to Dark treatment scores on Day 42, while algal FA tended to have more positive loadings on PC2.

In a separate analysis of THAA, PC1 and PC2 explained 36.2 and 25.0% of the variance in THAA composition, respectively (Fig. 7c, d). Scores along both PC were similar among treatments on Day 1, grouping near zero, but diverged by Day 42 (Fig. 7c). By Day 42, the scores on both PC for the Dark treatment remained near Day 1 values, but both light treatments shifted towards more positive scores along PC1. The light treatments were also separated along PC2 on Day 42. –Macro had negative scores for PC2 while +Macro was positive. Mole percentages of Leu and Ile had the most positive loadings on PC1 while Gly and D-Ala were the most negative (Fig. 7d). Lys had positive PC1 and negative PC2 loadings, similar to scores for –Macro on Day 42.

Discussion

Benthic micro- and macroalgae play an important role in system metabolism within shallow coastal bays. However, their independent and interactive influences on sediment organic matter are not well understood. In this study, we demonstrated that changes in autotrophic community structure that often result from excess nutrient loading can strongly influence sediment organic matter quality and quantity, which will ultimately affect its lability and turnover in the system.

Role of microphytobenthos To isolate the influence of MPB on sediment organic matter, we compared –Macro (ambient light) with the Dark treatment in our experimental system. Almost every sediment parameter we measured showed a clear light-dark difference, demonstrating the significant influence of MPB on sediment organic matter (Table 2). The quantity of sediment organic matter increased in –Macro, as demonstrated by bulk and molecular-level analyses. On a bulk scale, more sediment organic matter (TOC, TN) accumulated in ambient –Macro treatments compared with Dark treatments. By Day 42, TOC and TN in –Macro increased from baseline values by 173 and 141%, respectively, compared to only 77 and 39% in the Dark. These light-dark differences were clearly related to the activity of MPB. Chlorophyll *a* concentrations, which can be considered a proxy for MPB biomass, were higher in the –Macro treatment than in the Dark, indicating that MPB were not present and/or active in the Dark treatments.

Similarly, light-dark differences in THAA and PLFA concentrations indicated that the presence of MPB altered sediment organic matter composition as well. By Day

42, THAA increased from background levels by 180% in –Macro treatments compared to 14% in the Dark. Similarly, PLFA increased by 200% from background values in –Macro treatments and actually decreased by 27% in the Dark. Across treatments, THAA made up a substantial fraction of sediment organic matter (~30-40% of TN and 12-20% of TOC), similar to the concentration range found during other studies in shallow marine systems (Cook *et al.*, 2007; Veuger *et al.*, 2006). Since HAA are common amino acids found in proteins, which are abundant in all organisms, THAA included living material. THAA also likely included non-living (detrital) material because HAA have been shown to remain in sediments after cell death (Dauwe & Middelburg, 1998; Pantoja & Lee, 2003; Veuger *et al.*, 2006). PLFA, on the other hand, made up a smaller fraction of TOC (~1%), but represent only viable microbial organic matter because PLFA turnover rapidly after cell death (Parkes, 1987). Therefore, build up of THAA represented living biomass and detrital buildup while PLFA represented living biomass buildup alone.

Analysis of the PLFA composition lent insight into the composition of the microbial community that developed in the –Macro and Dark treatments. Not only did PUFA, a general algal indicator, increase over time in the light, but PLFA specific to different microalgal communities also showed different patterns over time. For example, 20:5ω3, which is specific to diatoms (Volkman *et al.*, 1989), was the most abundant PUFA, suggesting that diatoms were the dominant algal class within the surface sediments, which is consistent with surveys of microalgal community composition in temperate systems (MacIntyre *et al.*, 1996; Welker *et al.*, 2002). 22:6ω3, which was present in lower concentrations than 20:5ω3, is also found in diatoms (Dijkman & Kromkamp, 2006), as well as dinoflagellates (Volkman *et al.*, 1989), which do not often

contribute significantly to sediment microalgal communities (Barranguet *et al.*, 1997). Other algae that may have been present according to PLFA were green algae (18:2w6; Volkman *et al.*, 1989) and possibly cyanobacteria (18:4; Cook *et al.*, 2004b), both of which have been shown to seasonally dominate MPB communities in intertidal sediments (Barranguet *et al.*, 1997; Pinckney *et al.*, 1995). However, both of these C_{18} PUFA can also be present in diatoms, cryptophytes, and dinoflagellates (at trace levels) (Caron *et al.*; Viso & Marty, 1993), so we cannot say for certain if green algae and cyanobacteria were present. Over the course of the experiment, there may have been shifts in the algal community structure, as demonstrated by changes in the ratio of 20:5ω3/18:2ω6. As this ratio decreased over time, green algae may have been contributing more to sediment organic matter relative to diatoms than on Day 1. Previous work has linked changes in algal community structure with changes in nutrient limitation (Pinckney *et al.*, 1995; Sommer, 1996) and temperature (Tilman *et al.*, 1986). Neither temperatures nor N availability varied over the experiment; however, changes in other nutrients (e.g. silica, phosphorus) may have resulted in the potential shifts in algal composition that we observed. Algal species compositions can also change in response to top-down forces such as the feeding preferences of grazers (Duffy & Harvilicz, 2001). These shifts were not drastic, however. At the end of the experiment, when C_{18} PUFA were most concentrated, C_{20} PUFA were still more abundant, suggesting that diatoms were the dominant algal class in this study. It is not unexpected that sediment organic matter in the –Macro light treatment increased relative to the Dark since dark systems would be dependent on chemautotrophy as a source of new organic matter (or advection of an external source in the field). The significance of our experiment is that we were able to

quantify the contribution of MPB to sediment organic matter and to characterize the changes in sediment organic matter that result from MPB production. Our results are consistent with previous studies, which have investigated the influence of the *amount* of light, rather than the presence or absence of light, on sediment organic matter. For example, Spivak and colleagues (2007) observed increased sediment TOC and TN concentrations in an experimental seagrass system in treatments that received 69% more light than their shaded treatments. They also observed increased contributions of fatty acids derived from plant and algal sources with increased light, consistent with our PLFA results.

Our work further demonstrates that the lability of sediment organic matter changed as a result of MPB activity in the light. On a bulk level, TN was higher for the –Macro treatment, which suggests that the sediment organic matter in the light was more labile (available for degradation) than in the dark because N is generally the limiting element in temperate marine systems. This may have been due to lower levels of THAA in the dark; THAA contributed a smaller proportion of N to TN compared with the –Macro treatments. On the molecular level, changes in THAA composition also indicated changes in organic matter lability. The mole percentages of Leu and Ile were higher while Gly was lower in -Macro. Dauwe and Middelburg (1998) developed a degradation index based on amino acid composition, and found that mole percentages of Gly increased and Leu and Ile decreased with increasing degradation. They suggested that selective preservation of structural compounds versus preferential breakdown of cell plasma material explained the contrasting behavior of the individual molecules. The fact that the Dark treatment followed the patterns predicted by this degradation index suggests

that detrital material rather than newly produced biomass (e.g. by bacteria) was the dominant source of sediment organic matter in the Dark treatment. Increases in total THAA and PLFA concentrations are also consistent with increased organic matter lability. High contributions of THAA to sediment organic matter and the general susceptibility of N-containing amino acids to microbial mineralization make THAA a potentially major source of inorganic N in sediments (Pantoja & Lee, 2003). Similarly, fatty acids, particularly PUFA, are considered labile and make up an important component of energy flow in benthic food webs (Canuel *et al.*, 1995; Canuel & Martens, 1996; Sun *et al.*, 1997).

These changes in sediment organic matter quantity and quality in turn further shaped the sediment microbial community. The presence of labile sediment organic matter increased bacterial production in the –Macro light treatment by providing more substrate for bacteria. Bacterial specific PLFA concentrations were higher in the light, suggesting build up of heterotrophic bacterial biomass within the sediments. Bacterial PLFA increased in the Dark treatments for the first two weeks of the experiment, but then decreased for the remainder of the experiment, ending on Day 42 below initial values. This suggested that bacteria used up available labile organic matter in the Dark treatments by Day 14. Previous studies have suggested that bacterial and MPB activities may be coupled in a number of ways. First, bacteria can directly decompose detrital MPB material, as has been observed in numerous studies (Cook *et al.*, 2007; Veuger *et al.*, 2007). Second, benthic microalgae, particularly diatoms, excrete exopolymeric substances (EPS) that aid in sediment stability and/or motility (Smith & Underwood, 1998; Taylor & Paterson, 1998; Welker *et al.*, 2002), which also may serve as a substrate

for bacteria (Goto *et al.*, 2001; Middelburg *et al.*, 2000). Lack of bacterial biomass buildup in the Dark treatments, in the absence of photosynthesizing-MPB, suggests that organic matter substrate became limiting after the pool of labile organic matter in the sediments was exhausted.

Overall, MPB fundamentally altered the sediments in this shallow photic system. They produced labile organic matter that supported an active heterotrophic bacterial community and increased C and N storage in the sediments. We likely observed higher MPB and bacterial abundances relative to the field because the mesocosm system removed some predation pressure and resuspension. However, our objectives were to compare treatments and assess the differences due to the presence of MPB. Thus, we present these changes as estimates of the potential influence of MPB on sediment organic matter.

Role of benthic macroalgae Our second objective was to observe the influence of a macroalgal bloom on sediment organic matter. MPB are limited by bottom-up forcings such as light and nutrients (Hillebrand & Sommer, 2000; Stutes *et al.*, 2006) as well as top-down control by grazers. However, light availability is thought to be the primary factor regulating MPB community growth (Heip *et al.*, 1995; Spivak *et al.*, 2007; Stutes *et al.*, 2006). Macroalgae have been shown to "self shade;" light is attenuated within the layers of an algal mat (Krause-Jensen *et al.*, 1996; Peckol & Rivers, 1996), affecting overall mat metabolism (Brush & Nixon, 2003; Krause-Jensen *et al.*, 1996). Self-shading has been suggested as a possible cause for mid-summer macroalgal mat crashes that have been observed in numerous systems (McGlathery *et al.*, 2001; Sfriso *et al.*, 1992). Thus,

light available to plants below macroalgal mats (e.g. seagrass) will also be reduced due to shading by macroalgae and is suggested as a mechanism by which macroalgal blooms have contributed to global seagrass declines (Hauxwell *et al.*, 2001). It is therefore likely that shading of the sediment surface by macroalgae may also reduce MPB activity (Sundback & McGlathery, 2005). Macroalgae were added to the mesocosms at densities observed in Hog Island Bay as well as other shallow coastal bays, and their final densities (4-fold increase) were within the range of more eutrophied lagoons (Hauxwell *et al.*, 2001; McGlathery *et al.*, 2001; Pregnall & Rudy, 1985; Sfriso *et al.*, 1992). Our intensive sampling throughout the experiment allowed us to track changes between the light treatments with and without macroalgae as the macroalgal bloom developed. We were able to not only detect changes in many of the sediment parameters that suggested that the presence of macroalgae influenced sediment organic matter, but we were also able to detect the timing of those changes relative to the increase in macroalgal density.

Numerous sediment parameters suggested that macroalgae affected sediment organic matter quantity. TOC, TN, THAA, and PLFA concentrations were all lower in +Macro treatments compared to –Macro treatments. By Day 42, organic matter accumulation in +Macro treatments was intermediate between the –Macro and Dark treatments. TOC, TN, and THAA increased from background values by 130, 94, and 97%, respectively. PLFA, on the other hand, increased until ~Day 14 and then decreased 15% from initial values by Day 42, similar to the Dark treatments.

Molecular-level analyses also indicated that the Macroalgae treatment affected the composition of sediment organic matter. Total PUFA, and individual algal PLFA concentrations were lower in +Macro treatments indicating that macroalgae limited MPB

production. Like total PLFA, not all individual algal PLFA showed a significant macroalgae treatment effect even though concentrations on Day 42 were lower in +Macro versus –Macro. This was likely due to the similar trajectories followed by both light treatments for the first ~14 days of the experiment, which was then followed by divergent trajectories for the treatments with and without macroalgae. After Day 14, concentrations of organic matter parameters in +Macro treatments were lower than –Macro treatments. These changes over time likely related to the macroalgal density within the mesocosms. By Day 14, macroalgal biomass was ~300 gdw m^{-2}. According to a study by Krause-Jensen and colleagues (1996), this is the estimated value above which macroalgae completely block light reaching MPB. After this critical density in our experiment, MPB production decreased and sediment organic matter built up more slowly in +Macro treatments. Even if macroalgal biomass had remained below 300 gdw m^{-2}, chronic shading by macroalgae would have likely decreased MPB metabolism, as has been observed in studies investigating the effects of shading on MPB metabolism (Stutes *et al.*, 2006; Sundback & McGlathery, 2005). In the field, unattached macroalgae may be more motile than in our study; however, the degree of motility will depend on system-specific factors such as the degree of eutrophication, how widespread the macroalgal bloom is, and the depth and fetch of the system. It is not uncommon in eutrophied systems for macroalgal blooms to reach densities above 300 gdw m^{-2} and persist for days to weeks (see Sundback & McGlathery, 2005 and references therein), which is sufficiently long, according to our results, to negatively affect MPB metabolism.

As with our light-dark comparison, the presence of macroalgae also changed the quality of sediment organic matter. Concentrations of PLFA in +Macro treatments

remained level after Day 14, and the fraction of TOC from PLFA-C actually decreased, suggesting that production of labile organic matter slowed down compared to the –Macro treatment. The mole fraction of Lys was also lower in +Macro treatments with values that were similar to the Dark treatment. Lys makes up a large fraction of THAA in macroalgae and bacteria (5-15%) (Cowie & Hedges, 1992), so a lower concentration in sediment THAA likely indicated decreased microbial activity. Additional studies suggest that Lys is selectively degraded due to its simple structure and high N content (Cowie & Hedges, 1992). As a result of changes in sediment organic matter quantity and composition, the heterotrophic bacterial community differed in treatments with macroalgae. Bacterial PLFA concentrations were lower in treatments with macroalgae by Day 42; however, there was not a significant macroalgae effect across treatments. Again, as with total PLFA, we attribute this to the similarity between light treatments at lower macroalgal densities.

Synthesis PCA results summarized the changes in the dominant controls on sediment organic matter on Day 1 versus Day 42. On Day 1, light influenced PLFA composition, promoting development of more algal fatty acids in both light treatments than in the Dark. Because the macroalgae had only been present for 1 day, there were no significant macroalgae differences. THAA composition did not yet differ between any treatments. By Day 42, after macroalgal biomass had increased by 4-fold, all treatments existed along a gradient of PLFA and THAA composition. Sediment composition in +Macro treatments shifted away from –Macro treatments towards the Dark treatments, with less influence from algal PLFA and the more labile amino acids (e.g. Leu, Ile) and more

influence from bacterial PLFA and less labile amino acids (e.g. Gly, D-Ala). In both light treatments, we also observed shifts in MPB community composition by Day 42. On Day 1, 20:5ω3 was the most prominent algal PUFA, and by Day 42, algae producing 18:2ω6 contributed relatively more to algal PLFA than on Day 1.

Overall, MPB fundamentally altered sediment organic matter quality and quantity; however, the role of MPB as a source of labile sediment organic matter was significantly diminished due to shading by macroalgae. The potential ecological consequences of decreased MPB production are numerous. For example, biogeochemical processes such as denitrification are affected by diel variations in oxygen related to MPB metabolism as well as competition with MPB for dissolved N (An & Joye, 2001; Rysgaard *et al.*, 1995). In addition, MPB are a nutrient-rich food source for numerous faunal grazers (Miller *et al.*, 1996) and to heterotrophic bacteria (Banta *et al.*, 2004). Sediment stability is also enhanced by the presence of benthic diatoms that produce EPS (Tolhurst *et al.*, 2002). Lastly, macroalgae likely decreased retention of C and N in MPB and bacterial biomass in surface sediments, which diminished a potentially important sink for C and N in these systems (McGlathery *et al.*, 2007). Our results demonstrate that shading by macroalgae significantly altered sediment organic matter properties that influence ecosystem processes, and chronic shading by dense macroalgal blooms will likely result in surface sediments that more closely resemble sediments outside of the euphotic zone.

Literature Cited

An, S., Joye, S.B., (2001) Enhancement of coupled nitrification-denitrification by benthic photosynthesis in shallow estuarine sediments. *Limnology and Oceanography*, 46(1), 62-74.

Anderson, I.C., McGlathery, K.J., Tyler, A.C., (2003) Microbial mediation of 'reactive' nitrogen transformations in a temperate lagoon. *Marine Ecology Progress Series*, 246, 73-84.

Banta, G.T., Pedersen, M.F., Nielsen, S.L., (2004) Decomposition of marine primary producers: Consequences for nutrient recycling and retention in coastal ecosystems. In: S.L. Nielsen, G.T. Banta, M.F. Pedersen (Eds.), *Estuarine Nutrient Cycling: The Influence of Primary Producers* (Ed. by S.L. Nielsen, G.T. Banta, M.F. Pedersen), pp. 187-216. Kluwer Academic Publishers, Netherlands.

Barranguet, C., Herman, P.M.J., Sinke, J.J., (1997) Microphytobenthos biomass and community somposition studied by pigment biomarkers: importance and fate in the carbon cycle of a tidal flat. *Journal of Sea Research*, 38, 59-70.

Benoy, G.A., Kalff, J., (1999) Sediment accumulation and Pb burdens in submerged macrophyte beds. *Limnology and Oceanography*, 44, 1081-1090.

Bligh, E.G., Dyer, W.J., (1959) A Rapid Method of Total Lipid Extraction and Purification. *Canadian Journal of Biochemistry and Physiology*, 37(8), 911-917.

Boschker, H.T.S., Brouwer, J.F.C.d., Cappenberg, T.E., (1999) The contribution of macrophyte-derived organic matter to microbial biomass in salt-marsh sediments: Stable carbon isotope analysis of microbial biomarkers. *Limnology and Oceanography*, 44(2), 309-319.

Boschker, H.T.S., Wielemaker, A., Schaub, B.E.M., Holmer, M., (2000) Limited coupling of macrophyte production and bacterial carbon cycling in the sediments of *Zostera* spp. meadows. *Marine Ecology Progress Series*, 203, 181-189.

Bouillon, S., Boschker, H.T.S., (2006) Bacterial carbon sources in coastal sediments: a cross-system analysis based on stable isotope data of biomarkers. *Biogeosciences*, 3, 175-185.

Brush, M.J., Nixon, S.W., (2003) Biomass layering and metabolism in mats of the macroalga Ulva lactuca L. *Estuaries*, 26(4A), 916-926.

Canuel, E.A., Cloern, J.E., Ringelberg, D.B., Guckert, J.B., Rau, G.H., (1995) Molecular and isotopic tracers used to examine sources of organic matter and its

incorporation into the food webs of San Francisco Bay. *Limnology and Oceanography*, 40(1), 67-81.

Canuel, E.A., Freeman, K.H., Wakeham, S.G., (1997) Isotopic compositions of lipid biomarker compounds in estuarine plants and surface sediments. *Limnology and Oceanography*, 42(7), 1570-1583.

Canuel, E.A., Martens, C.S., (1993) Seasonal-Variations in the Sources and Alteration of Organic-Matter Associated with Recently-Deposited Sediments. *Organic Geochemistry*, 20(5), 563-577.

Canuel, E.A., Martens, C.S., (1996) Reactivity of recently deposited organic matter: Degradation of lipid compounds near the sediment-water interface. *Geochimica et Cosmochimica Acta*, 60(10), 1793-1806.

Canuel, E.A., Spivak, A.C., Waterson, E.J., Duffy, J.E., (2007) Biodiversity and food web structure influence short-term accumulation of sediment organic matter in an experimental seagrass system. *Limnology and Oceanography*, 52(2), 590-602.

Caron, B., et al. (1996) Status of the VIRGO experiment. *Nuclear Physics B*, 107-109.

Cook, P.L.M., Butler, E.C.V., Eyre, B.D., (2004a) Carbon and nitrogen cycling on intertidal mudflats of a temperate Australian estuary. I. Benthic metabolism. *Marine Ecology-Progress Series*, 280, 25-38.

Cook, P.L.M., Revill, A.T., Clementson, L.A., Volkman, J.K., (2004b) Carbon and nitrogen cycling on intertidal mudflats of a temperate Australian estuary. III. Sources of organic matter. *Marine Ecology-Progress Series*, 280, 55-72.

Cook, P.L.M., Veuger, B., Boer, S., Middelburg, J.J., (2007) Effect of nutrient availability on carbon and nitrogen incorporation and flows through benthic algae and bacteria in near-shore sandy sediment. *Aquatic Microbial Ecology*, 49, 165-180.

Cowie, G.L., Hedges, J.I., (1992) Sources and Reactivities of Amino-Acids in a Coastal Marine-Environment. *Limnology and Oceanography*, 37(4), 703-724.

Dauwe, B., Middelburg, J.J., (1998) Amino acids and hexosamines as indicators of organic matter degradation state in North Sea sediments. *Limnology and Oceanography*, 43(5), 782-798.

Dijkman, N.A., Kromkamp, J.C., (2006) Phospholipid-derived fatty acids as chemotaxonomic markers for phytoplankton: application for inferring phytoplankton composition. *Marine Ecology-Progress Series*, 324, 113-125.

Duarte, C.M., (1995) Submerged Aquatic Vegetation in Relation to Different Nutrient Regimes. *Ophelia*, 41, 87-112.

Duffy, J.E., Harvilicz, A.M., (2001) Species-specific impacts of grazing, amphipods in an eelgrass-bed community. *Marine Ecology-Progress Series*, 223, 201-211.

Fonseca, M.S., Calahan, J.A., (1992) A preliminary evaluation of wave attenuation by four species of seagrass. *Estuarine Coastal and Shelf Science*, 25, 565-576.

Gacia, E., Duarte, C.M., Middelburg, J.J., (2002) Carbon and nutrient deposition in a Mediterranean seagrass (Posidonia oceanica) meadow. *Limnology and Oceanography*, 47(1), 23-32.

Goto, N., Mitamura, O., Terai, H., (2001) Biodegradation of photosynthetically produced extracellular organic carbon from intertidal benthic algae. *Journal of Experimental Marine Biology and Ecology*, 257(1), 73-86.

Gray, J.S., Wu, R.S., Or, Y.Y., (2002) Effects of hypoxia and organic enrichment on the coastal marine environment. *Marine Ecology Progress Series*, 238, 249-279.

Hardison, A.K., Tobias, C.R., Stanhope, J.W., Canuel, E.A., Anderson, I.C., (Submitted) An experimental apparatus for laboratory and field-based perfusion of sediment porewater with dissolved tracers. *Estuaries and Coasts*.

Hauxwell, J., Cebrian, J., Furlong, C., Valiela, I., (2001) Macroalgal canopies contribute to eelgrass (*Zostera marina*) decline in temperate estuarine ecosystems. *Ecology*, 82(4), 1007-1022.

Hauxwell, J., Cebrian, J., Valiela, I., (2003) Eelgrass *Zostera marina* loss in temperate estuaries: relationship to land-derived nitrogen loads and effect of light limiataion imposed by algae. *Marine Ecology Progress Series*, 247, 59-73.

Heck, K.L., Hays, G., Orth, R.J., (2003) Critical evaluation of the nursery role hypothesis for seagrass meadows. *Marine Ecology Progress Series*, 253, 123-136.

Hedges, J.I., Stern, J.H., (1984) Carbon and Nitrogen Determinations of Carbonate-Containing Solids. *Limnology and Oceanography*, 29(3), 657-663.

Heip, C., Goosen, N.K., Herman, P., Kromkamp, J.C., Middelburg, J.J., Soetaert, K., (1995) Production and consumption of biological particles in temperate tidal estuaries. *Oceanography and Marine Biology Annual Reviews*, 33(1-150).

Hillebrand, H., Sommer, U., (2000) Marine microbenthic community structure regulated by nitrogen loading and grazing pressure. *Marine Ecology Progress Series*, 204, 27-38.

Jumars, P.A., Eckman, J.E., Koch, E., (2001) Macroscopic animals and plants in benthic flows. In: B.P. Boudreau, B.B. Jorgensen (Eds.), *The benthic boundary layer* (Ed. by B.P. Boudreau, B.B. Jorgensen), pp. 320-347. Oxford University Press.

Kaneda, T., (1991) Iso-Fatty and Anteiso-Fatty Acids in Bacteria - Biosynthesis, Function, and Taxonomic Significance. *Microbiological Reviews*, 55(2), 288-302.

Kenworthy, W.J., Zieman, J.C., Thayer, G.W., (1982) Evidence for the influence of seagrasses on the benthic nitrogen cycle in a coastal plain estuary near Beaufort, North Carolina (USA). *Oecologia*, 54, 152-158.

Krause-Jensen, D., Christensen, P.B., Rysgaard, S., (1999) Oxygen and nutrient dynamics within mats of the filamentous macroalga *Chaetomorphalinum Estuaries*, 22, 31-38.

Krause-Jensen, D., McGlathery, K., Rysgaard, S., Christensen, P.B., (1996) Production within dense mats of the filamentous macroalga Chaetomorpha linum in relation to light and nutrient availability. *Marine Ecology-Progress Series*, 134(1-3), 207-216.

Lorenzen, C.J., (1967) Determination of Chlorophyll and Pheo-Pigments - Spectrophotometric Equations. *Limnology and Oceanography*, 12(2), 343-&.

MacIntyre, H.L., Geider, R.J., Miller, D.C., (1996) Microphytobenthos: The ecological role of the "secret garden" of unvegetated, shallow-water marine habitats .1. Distribution, abundance and primary production. *Estuaries*, 19(2A), 186-201.

McGlathery, K.J., Anderson, I.C., Tyler, A.C., (2001) Magnitude and variability of benthic and pelagic metabolism in a temperate coastal lagoon. *Marine Ecology-Progress Series*, 216, 1-15.

McGlathery, K.J., Sundback, K., Anderson, I.C., (2007) Eutrophication in shallow coastal bays and lagoons: the role of plants in the coastal filter. *Marine Ecology-Progress Series*, 348, 1-18.

Middelburg, J.J., Barranguet, C., Boschker, H.T.S., Herman, P.M.J., Moens, T., Heip, C.H.R., (2000) The fate of intertidal microphytobenthos carbon: An in situ C-13-labeling study. *Limnology and Oceanography*, 45(6), 1224-1234.

Miller, D.C., Geider, R.J., MacIntyre, H.L., (1996) Microphytobenthos: The ecological role of the "secret garden" of unvegetated, shallow-water marine habitats .2. Role in sediment stability and shallow-water food webs. *Estuaries*, 19(2A), 202-212.

Nielsen, S.L., Enriquez, S., Duarte, C.M., SandJensen, K., (1996) Scaling maximum growth rates across photosynthetic organisms. *Functional Ecology*, 10(2), 167-175.

Nilsson, P., Jonsson, B., Swanberg, I.L., Sundback, K., (1991) Response of a Marine Shallow-Water Sediment System to an Increased Load of Inorganic Nutrients. *Marine Ecology-Progress Series*, 71(3), 275-290.

Nixon, S.W., (1995) Coastal Marine Eutrophication - a Definition, Social Causes, and Future Concerns. *Ophelia*, 41, 199-219.

Norkko, A., (1998) The impact of loose-lying algal mats and predation by the brown shrimp Crangon crangon (L.) on infaunal prey dispersal and survival. *Journal of Experimental Marine Biology and Ecology*, 221, 99-116.

Norkko, J., Bonsdorff, E., Norkko, A., (2000) Drifting algal mats as an alternative habitat for benthic invertebrates: species-specific responses to a transient resource. *Journal of Experimental Marine Biology and Ecology*, 248, 79-104.

NRC, (2000) *National Research Council. Clean coastal waters: understanding and reducing the effects of nutrient pollution*. National Academy Press, Washington, DC.

Orth, R.J., Heck, K.L., van Montfrans, J., (1984) Faunal components in seagrass beds: a review of the influence of plant structure and prey characteristics on predator-prey relationships. *Estuaries*, 7, 339-250.

Pantoja, S., Lee, C., (2003) Amino acid remineralization and organic matter lability in Chilean coastal sediments. *Organic Geochemistry*, 34(8), 1047-1056.

Parkes, R.J., (1987) Analysis of microbial communities within sediments using biomarkers. In: M. Hetcher, R.T.G. Gray, J.G. Jones (Eds.), *Ecology of Microbial Communities* (Ed. by M. Hetcher, R.T.G. Gray, J.G. Jones), pp. 147-177. Cambridge University Press, Cambridge.

Paterson, D.M., Black, K.S., (1999) Water flow, sediment dynamics, and benthic biology. *Advances in Ecological Research*, 29, 155-193.

Peckol, P., Rivers, J.S., (1996) Contribution by macroalgal mats to primary production of a shallow embayment under high and low nitrogen-loading rates. *Estuarine Coastal and Shelf Science*, 43(3), 311-325.

Pedersen, M.F., Nielsen, S.L., Banta, G.T., (2004) Interactions between vegetation and nutrient dynamics in coastal marine ecosystems: An introduction. In: S.L. Nielsen, G.T. Banta, M.F. Pedersen (Eds.), *Estuarine Nutrient Cycling: The Influence of Primary Producers* (Ed. by S.L. Nielsen, G.T. Banta, M.F. Pedersen). Kluwer, Dordrecht.

Pinckney, J., Paerl, H.W., Fitzpatrick, M., (1995) Impacts of Seasonality and Nutrients on Microbial Mat Community Structure and Function. *Marine Ecology-Progress Series*, 123(1-3), 207-216.

Pinckney, J., Papa, R., Zingmark, R., (1994) Comparison of High-Performance Liquid-Chromatographic, Spectrophotometric, and Fluorometric Methods for

Determining Chlorophyll a Concentrations in Estuarine Sediments. *Journal of Microbiological Methods*, 19(1), 59-66.

Poerschmann, J., Carlson, R., (2006) New fractionation scheme for lipid classes based on "in-cell fractionation" using sequential pressurized liquid extraction. *Journal of Chromatography A*, 1127(1-2), 18-25.

Pregnall, A.M., Rudy, P.P., (1985) Contribution of green macroalgal mats (*Enteromorpha* spp.) to seasonal production in an estuary. *Marine Ecology Progress Series*, 24, 167-176.

Raffaelli, D.G., Raven, J.H., Poole, L.J., (1998) Ecological impact of green macroalgal blooms. *Oceanography and Marine Biology - an Annual Review*, 36(97-125).

Risgaard-Petersen, (2003) Coupled nitrification-denitrification in autotrophic and heterotrophic estuarine sediments: On the influence of benthic microalgae. *Limnol. Oceanogr.*, 48(1), 93-105.

Rysgaard, S., Christensen, P.B., Nielsen, L.P., (1995) Seasonal-Variation in Nitrification and Denitrification in Estuarine Sediment Colonized by Benthic Microalgae and Bioturbating Infauna. *Marine Ecology-Progress Series*, 126(1-3), 111-121.

Sand-Jensen, K., Borum, J., (1991) Interactions among phytoplankton, periphyton, and macrophytes in temperate freshwaters and estuaries. *Aquatic Botany*, 41, 137-175.

Sfriso, A., Pavoni, B., Marcomini, A., Raccanelli, S., Orio, A.A., (1992) Particulate Matter Deposition and Nutrient Fluxes onto the Sediments of the Venice Lagoon. *Environmental Technology*, 13(5), 473-483.

Smith, D.J., Underwood, G.J.C., (1998) Exopolymer production by intertidal epipelic diatoms. *Limnology and Oceanography*, 43(7), 1578-1591.

Sommer, U., (1996) Nutrient competition experiments with periphyton from the Baltic Sea. *Marine Ecology-Progress Series*, 140(1-3), 161-167.

Spivak, A.C., Canuel, E.A., Duffy, J.E., Richardson, J.P., (2007) Top-down and bottom-up controls on sediment organic matter composition in an experimental seagrass ecosystem. *Limnology and Oceanography*, 52(6), 2595-2607.

Stutes, A.L., Cebrian, J., Corcoran, A.A., (2006) Effects of nutrient enrichment and shading on sediment primary production and metabolism in eutrophic estuaries. *Marine Ecology-Progress Series*, 312, 29-43.

Sun, M.Y., Wakeham, S.G., Lee, C., (1997) Rates and mechanisms of fatty acid degradation in oxic and anoxic coastal marine sediments of Long Island Sound, New York, USA. *Geochimica et Cosmochimica Acta*, 61(2), 341-355.

Sundback, K., McGlathery, K.J., (2005) Interactions between benthic macro- and microalgae in the marine environment. In: E. Kristensen, J.E. Kostka, R.H. Haese (Eds.), *Interactions between macro- and microorganisms in marine sediments.* (Ed. by E. Kristensen, J.E. Kostka, R.H. Haese). American Geophysical Union.

Sundback, K., Nilsson, P., Nilsson, C., Jonsson, B., (1996) Balance between autotrophic and heterotrophic components and processes in microbenthic communities of sandy sediments: A field study. *Estuarine Coastal and Shelf Science*, 43(6), 689-706.

Taylor, I.S., Paterson, D.M., (1998) Microspatial variation in carbohydrate concentrations with depth in the upper millimetres of intertidal cohesive sediments. *Estuarine Coastal and Shelf Science*, 46, 359-370.

Thomsen, M.S., McGlathery, K.J., Tyler, A.C., (2006) Macroalgal distribution patterns in a shallow, soft-bottom lagoon, with emphasis on the nonnative Gracilaria vermiculophylla and Coldium fragile. *Estuaries and Coasts*, 29(3), 465-473.

Tilman, D., Kiesling, R., Sterner, R., Kilham, S.S., Johnson, F.A., (1986) Green, Bluegreen and Diatom Algae - Taxonomic Differences in Competitive Ability for Phosphorus, Silicon and Nitrogen. *Archiv Fur Hydrobiologie*, 106(4), 473-485.

Tolhurst, T.J., Gust, G., Paterson, D.M., (2002) The influence of an extracellular polymeric substance (EPS) on cohesive sediment stability. In: J.C. Winterwerp, C. Kranenburg (Eds.), *Fine Sediment Dynamics in the Marine Environment* (Ed. by J.C. Winterwerp, C. Kranenburg). Elsevier, San Diego.

Tyler, A.C., McGlathery, K.J., Anderson, I.C., (2001) Macroalgae mediation of dissolved organic nitrogen fluxes in a temperate coastal lagoon. *Estuarine Coastal and Shelf Science*, 53(2), 155-168.

Tyler, A.C., McGlathery, K.J., Anderson, I.C., (2003) Benthic algae control sediment-water column fluxes of organic and inorganic nitrogen compounds in a temperate lagoon. *Limnology and Oceanography*, 48(6), 2125-2137.

Valiela, I., Foreman, K., Lamontagne, M., Hersh, D., Costa, J., Peckol, P., Demeoandreson, B., Davanzo, C., Babione, M., Sham, C.H., Brawley, J., Lajtha, K., (1992) Couplings of Watersheds and Coastal Waters - Sources and Consequences of Nutrient Enrichment in Waquoit Bay, Massachusetts. *Estuaries*, 15(4), 443-457.

Valiela, I., McClelland, J., Hauxwell, J., Behr, P.J., Hersh, D., Foreman, K., (1997) Macroalgal blooms in shallow estuaries: Controls and ecophysiological and ecosystem consequences. *Limnology and Oceanography*, 42(5), 1105-1118.

Veuger, B., Eyre, B.D., Maher, D., Middelburg, J.J., (2007) Nitrogen incorporation and retention by bacteria, algae, and fauna in a subtropical intertidal sediment: An in situ N-15-labeling study. *Limnology and Oceanography*, 52(5), 1930-1942.

Veuger, B., Middelburg, J.J., Boschker, H.T.S., Houtekamer, M., (2005) Analysis of N-15 incorporation into D-alanine: A new method for tracing nitrogen uptake by bacteria. *Limnology and Oceanography-Methods*, 3, 230-240.

Veuger, B., van Oevelen, D., Boschker, H.T.S., Middelburg, J.J., (2006) Fate of peptidoglycan in an intertidal sediment: An in situ C-13-labeling study. *Limnology and Oceanography*, 51(4), 1572-1580.

Viso, A.C., Marty, J.-C., (1993) Fatty acids from 28 marine microalgae. *Phytochemistry*, 34, 1521-1533.

Volkman, J.K., Jeffrey, S.W., Nichols, P.D., Rogers, G.I., Garland, C.D., (1989) Fatty-Acid and Lipid-Composition of 10 Species of Microalgae Used in Mariculture. *Journal of Experimental Marine Biology and Ecology*, 128(3), 219-240.

Volkman, J.K., Revill, A.T., Holdsworth, D.G., Fredericks, D., (2008) Organic matter sources in an enclosed coastal inlet assessed using lipid biomarkers and stable isotopes. *Organic Geochemistry*, 39, 689-710.

Welker, C., Sdrigotti, E., Covelli, S., Fagan, J., (2002) Microphytobenthos in the Gulf of Trieste (Northern Adriatic Sea): Relationship with Labile Sedimentary Organic Matter and Nutrients. *Estuarine, Coastal and Shelf Science*, 55, 259-273.

Wolfstein, K., de Brouwer, J.F.C., Stal, L.J., (2002) Biochemical partitioning of photosynthetically fixed caarbon by benthic diatoms during short-term incubatiions at different irradiances. *Mar Ecol Prog Ser*, 245, 21-31.

Yunker, M.B., Belicka, L.L., Harvey, H.R., Macdonald, R.W., (2005) Tracing the inputs and fate of marine and terrigenous organic matter in Arctic Ocean sediments: A multivariate analysis of lipid biomarkers. *Deep-Sea Research II*, 52, 3478-3508.

Table 3-1: Parameters measured concurrently at Hog Island Bay field sites and in mesocosms.

Field samples were taken at shoal sites on three dates while mesocosm experiment was being conducted. Mesocosm values are means of daily means across all time steps. Values are mean (SE) for field (n = 5) and mesocosm treatments (n = 9).

Parameter	**Field**	**-Macro**	**+Macro**	**Dark**
Temperature (°C)	24.1 (1.6)	23.6 (2.9)	23.9 (2.9)	23.7 (2.8)
Salinity (psu)	31.4 (0.6)	31.6 (1.3)	31.5 (1.3)	31.0 (1.0)
Macroalgal density (gdw m^{-2})	59.2 (30.7)	n/a	278.6 (31.4)	n/a
range	0 - 355	n/a	124 - 513	n/a
Benthic chlorophyll *a* (mg m^{-2})	24.9 (7.1)	74.1 (9.7)	59.5 (7.2)	11.9 (1.6)
Sediment TOC (mmol C gdw^{-1})	185.4 (32.3)	302.9 (23.3)	232.6 (15.3)	208.6 (21.1)
Sediment TN (mmol N gdw^{-1})	22.3 (3.1)	28.2 (1.9)	22.8 (1.0)	18.1 (1.5)

Table 3-2: Results of two-factor repeated measures ANOVA.

ANOVA used to test for differences in Light, Macroalgae over time for various sediment organic matter variables. Significant p values (< 0.05) are indicated in bold.

	LIGHT			MACROALGAE			TIME		
	df	F	p	df	F	p	df	F	p
TN	9	31.97	**0.0003**	9	8.73	**0.0161**	61	9.24	**<0.0001**
TOC	9	13.5	**0.0051**	9	7.61	**0.0222**	61	12.39	**<0.0001**
C:N	9	2.35	0.1598	9	2.77	0.1302	61	6.02	**<0.0001**
BCHLA	9	27.65	**0.0005**	9	0.83	0.3849	61	0.43	0.8325
THAA	8	29.94	**0.0006**	8	6.25	**0.0369**	38	4.57	**0.0020**
%THAA/TN	8	21.59	**0.0017**	8	4.62	0.0638	38	20.45	**<0.0001**
%THAA/TOC	8	12.83	**0.0072**	8	0.71	0.4249	38	24.76	**<0.0001**
%GLY	8	13.31	**0.0065**	8	0.07	0.7947	38	2.19	0.0759
%LGLU	8	0.05	0.8316	8	0.04	0.8561	38	1.95	0.1093
%LEU	8	113.11	**<0.0001**	8	0.08	0.7868	38	4.48	**0.0026**
%DALA	8	41.44	**0.0002**	8	0.3	0.6000	38	2.45	0.0508
%LALA	8	6.45	**0.0347**	8	0.19	0.6736	38	5.03	**0.0012**
%THR+VAL	8	8.4	**0.0199**	8	0.33	0.579	38	2.55	**0.0438**
%ILE	8	36.36	**0.0003**	8	0.71	0.425	38	8.29	**<0.0001**
%PRO	8	0.37	0.5583	8	2.64	0.1428	38	2.02	0.0975
%ASP	8	7.94	**0.0226**	8	3.13	0.1148	38	5.67	**0.0005**
%PHE	8	0.01	0.9235	8	0.06	0.8177	38	0.58	0.7173
%LYS	8	12	**0.0085**	8	10.17	**0.0128**	38	1.83	0.1312
PLFA	9	209.95	**<0.0001**	9	54.28	**<0.0001**	34	1.85	0.1424
%PLFA/TOC		65.84	**<0.0001**	9	5.18	**0.0489**	34	3.98	**0.0094**
SatFA	9	98.43	**<0.0001**	9	23.01	**0.001**	34	1.15	0.3552
MUFA	9	202.87	**<0.0001**	9	46.09	**<0.0001**	34	1.72	0.1559
PUFA	9	59.19	**<0.0001**	9	19.17	**0.0018**	34	1.24	0.3121
BrFA	9	17.01	**0.0026**	9	3.75	0.0848	34	5.37	**0.0010**
16:1ω7	9	36.25	**0.0002**	9	6.07	**0.0359**	34	1.59	0.1882
18:2ω6	9	19.03	**0.0018**	9	3.02	0.1162	34	3.11	**0.0204**
18:4	9	23.47	**0.0009**	9	7.66	**0.0218**	34	0.73	0.6094
20:4ω6	9	14.34	**0.0043**	9	6.32	**0.0331**	34	1.33	0.2753
20:5ω3	9	109.42	**<0.0001**	9	27.53	**0.0005**	34	1.97	0.1088
22:6ω3	9	47.14	**<0.0001**	9	12.12	**0.0069**	34	2.25	0.072
20:5/18:2	9	27.52	**0.0005**	9	1.99	0.1916	34	7.35	**<0.0001**

Table 3-3 Composition as mole percent for individual amino acids of THAA.

Values represent mean (SE), $n = 4$.

Treatment	Day	D-Ala	L-Ala	Thr+Val	Gly	Ile	Leu	Pro	Asp	L-Glu	Phe	Lys
-Macro	-1	0.92 (0.01)	13.55 (0.36)	6.89 (0.01)	26.49 (0.97)	3.46 (0.06)	6.03 (0.03)	7.89 (0.03)	15.62 (0.04)	12.03 (0.06)	1.87 (1.29)	5.26 (0.10)
	1	0.84 (0.04)	14.49 (0.09)	6.71 (0.25)	26.51 (0.81)	3.44 (0.1)	6.35 (0.18)	7.53 (0.13)	14.13 (0.26)	11.87 (0.29)	2.69 (0.11)	5.44 (0.15)
	3	0.82 (0.09)	13.59 (0.74)	6.83 (0.26)	23.62 (1.46)	3.17 (0.11)	7.13 (0.38)	7.46 (0.43)	16.05 (1.43)	12.36 (0.62)	3.23 (0.28)	5.75 (0.74)
	7	0.69 (0.03)	14.76 (0.26)	7.38 (0.40)	24.57 (1.44)	3.74 (0.25)	7.06 (0.56)	8.44 (0.65)	13.40 (0.3)	11.38 (1.19)	2.77 (0.25)	5.80 (0.36)
	14	0.70 (0.03)	15.56 (0.39)	7.46 (0.34)	23.46 (0.61)	4.12 (0.12)	7.94 (0.24)	8.04 (0.36)	11.88 (1.22)	11.34 (0.44)	3.26 (0.14)	6.24 (0.42)
	21	0.58 (0.04)	14.01 (0.69)	7.40 (0.26)	22.15 (1.20)	3.88 (0.07)	7.49 (0.16)	8.24 (0.34)	13.38 (0.81)	13.29 (0.88)	3.13 (0.10)	6.44 (0.48)
	42	0.71 (0.04)	14.82 (0.35)	7.62 (0.17)	22.65 (0.46)	4.10 (0.08)	7.88 (0.18)	7.73 (0.23)	13.85 (0.56)	11.51 (0.42)	3.21 (0.11)	5.93 (0.47)
+Macro	-1	0.92 (0.01)	13.55 (0.36)	6.89 (0.01)	26.49 (0.97)	3.46 (0.06)	6.03 (0.03)	7.89 (0.03)	15.62 (0.04)	12.03 (0.06)	1.87 (1.29)	5.26 (0.10)
	1	0.80 (0.00)	14.18 (0.16)	6.53 (0.15)	24.66 (0.05)	3.54 (0.01)	6.65 (0.01)	7.49 (0.12)	15.21 (0.13)	12.57 (0.23)	2.92 (0.09)	5.46 (0.04)
	3	0.70 (0.06)	13.29 (0.27)	6.77 (0.18)	24.86 (0.79)	3.61 (0.15)	8.04 (0.14)	6.78 (1.67)	16.23 (2.34)	11.95 (0.57)	3.25 (0.32)	4.52 (1.26)
	7	0.75 (0.02)	15.63 (0.48)	6.50 (0.92)	24.65 (0.21)	3.55 (0.06)	7.15 (0.06)	8.10 (0.11)	13.43 (0.87)	11.91 (0.57)	3.00 (0.16)	5.34 (0.11)
	14	0.82 (0.05)	15.35 (0.12)	7.49 (0.23)	25.14 (1.25)	3.67 (0.03)	6.94 (0.31)	7.75 (0.04)	13.49 (0.15)	11.20 (0.50)	2.89 (0.11)	5.25 (0.15)
	21	0.60 (0.04)	14.23 (0.50)	7.93 (0.11)	21.46 (0.44)	4.20 (0.07)	8.29 (0.02)	7.75 (0.14)	14.20 (1.07)	12.41 (0.35)	3.33 (0.14)	5.60 (0.15)
	42	0.79 (0.09)	13.59 (0.13)	7.55 (0.03)	22.91 (0.54)	3.53 (0.08)	7.13 (0.30)	6.95 (0.15)	16.94 (0.30)	12.28 (0.30)	3.17 (0.16)	5.14 (0.43)
Dark	-1	0.90 (0.01)	13.19 (0.36)	6.90 (0.01)	25.52 (0.97)	3.52 (0.06)	6.00 (0.03)	7.91 (0.03)	15.58 (0.04)	11.97 (0.06)	3.16 (1.29)	5.36 (0.10)
	1	0.90 (0.01)	14.11 (0.09)	6.65 (0.20)	26.21 (0.74)	3.42 (0.11)	6.16 (0.06)	7.67 (0.19)	14.77 (0.49)	11.83 (0.32)	3.21 (0.11)	5.08 (0.15)
	3	0.74 (0.15)	11.45 (2.08)	5.77 (0.70)	22.21 (2.61)	2.91 (0.10)	6.39 (0.19)	7.34 (0.32)	21.22 (2.92)	14.61 (2.17)	3.24 (1.03)	4.11 (0.41)
	7	0.97 (0.03)	14.59 (0.24)	7.28 (0.14)	25.43 (0.41)	3.43 (0.11)	6.44 (0.18)	8.01 (0.21)	13.78 (0.55)	11.39 (0.81)	2.88 (0.07)	5.79 (0.28)
	14	1.00 (0.05)	15.04 (0.29)	6.36 (0.73)	27.48 (0.67)	3.37 (0.12)	6.21 (0.30)	7.90 (0.19)	13.64 (0.73)	10.64 (0.44)	2.78 (0.18)	5.60 (0.20)
	21	0.94 (0.06)	13.30 (0.37)	6.86 (0.27)	26.53 (0.39)	3.55 (0.21)	6.23 (0.10)	8.40 (0.48)	14.52 (0.75)	11.53 (0.32)	2.78 (0.13)	5.37 (0.16)
	42	1.03 (0.04)	13.40 (0.43)	7.20 (0.09)	26.10 (0.52)	3.47 (0.11)	6.88 (0.24)	7.23 (0.43)	14.77 (0.93)	11.17 (0.38)	3.30 (0.22)	5.45 (0.26)

Figure 3-1. Study site.

Sediments and macroalgae were collected from a mid-lagoon shoal site in Hog Island Bay, Virginia, located along the Delmarva Peninsula, USA. Hog Island Bay is part of the Virginia Coast Reserve, a Long-Term Ecological Research (LTER) site.

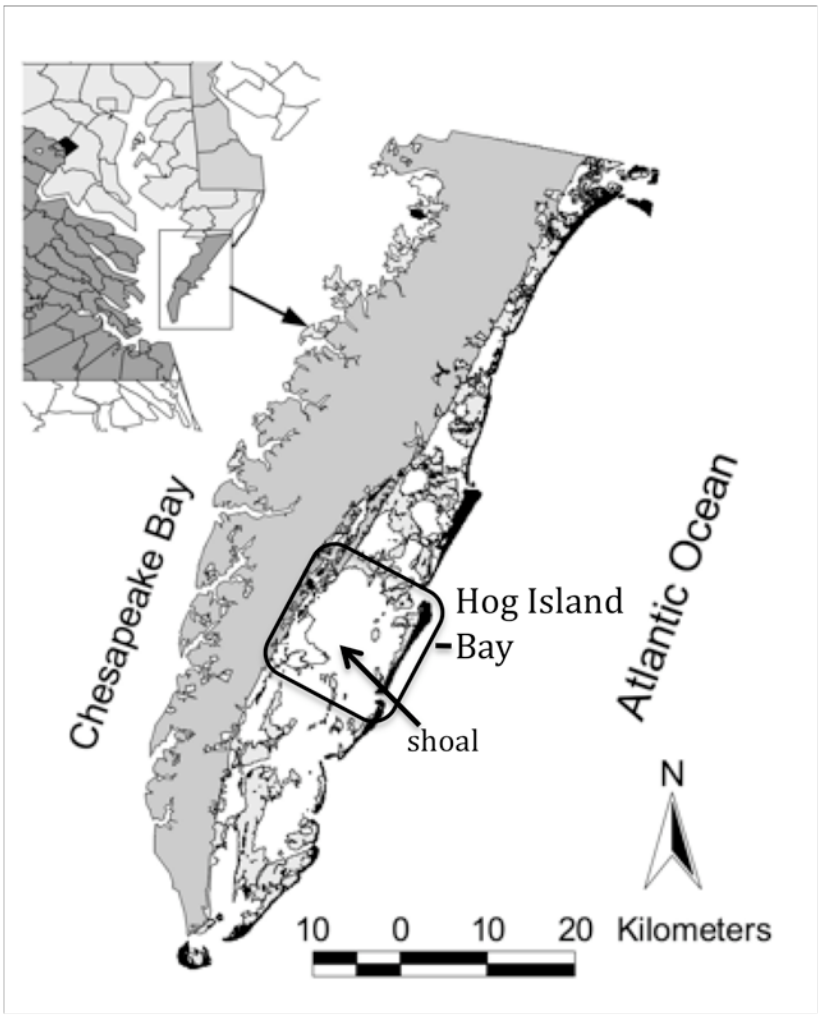
Chesapeake Bay
Atlantic Ocean
Hog Island
Bay
shoal
N
10 0 10 20 Kilometers

Figure 3-2. Macroalgal biomass (a) and benthic chlorophyll *a* concentrations for surface (0-1 cm) sediments (b).

Treatments shown are light with macroalgae ("+Macro"; solid lines, filled symbols), light without macroalgae ("-Macro"; solid lines, open symbols), and dark without macroalgae ("Dark"; dotted lines with filled symbols). Values are mean ± SE (n = 4).

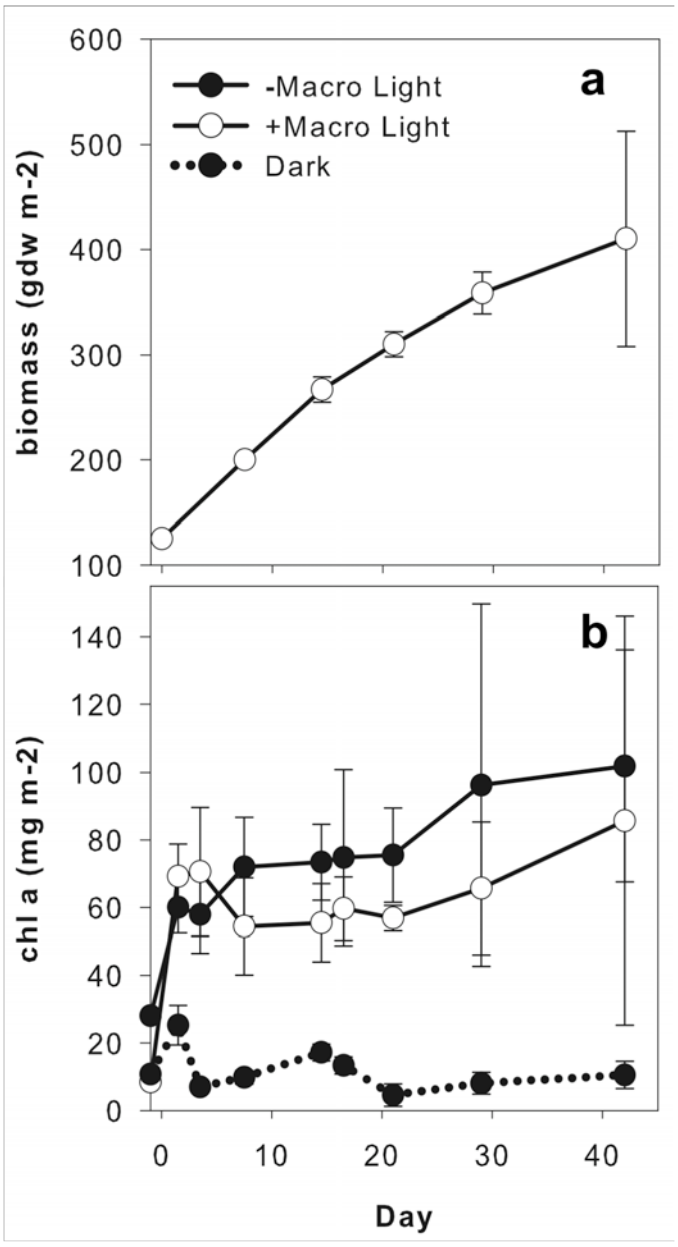
a
-Macro Light
+Macro Light
Dark
biomass (gdw m-2)
600
500
400
300
200
100
b
chl a (mg m-2)
140
120
100
80
60
40
20
0
0
10
20
30
40
Day

Figure 3-3. Total nitrogen (a) and total organic carbon (b) concentrations and C/N (c) in surface (0-1 cm) sediments.

Values are mean ± SE (n = 4).

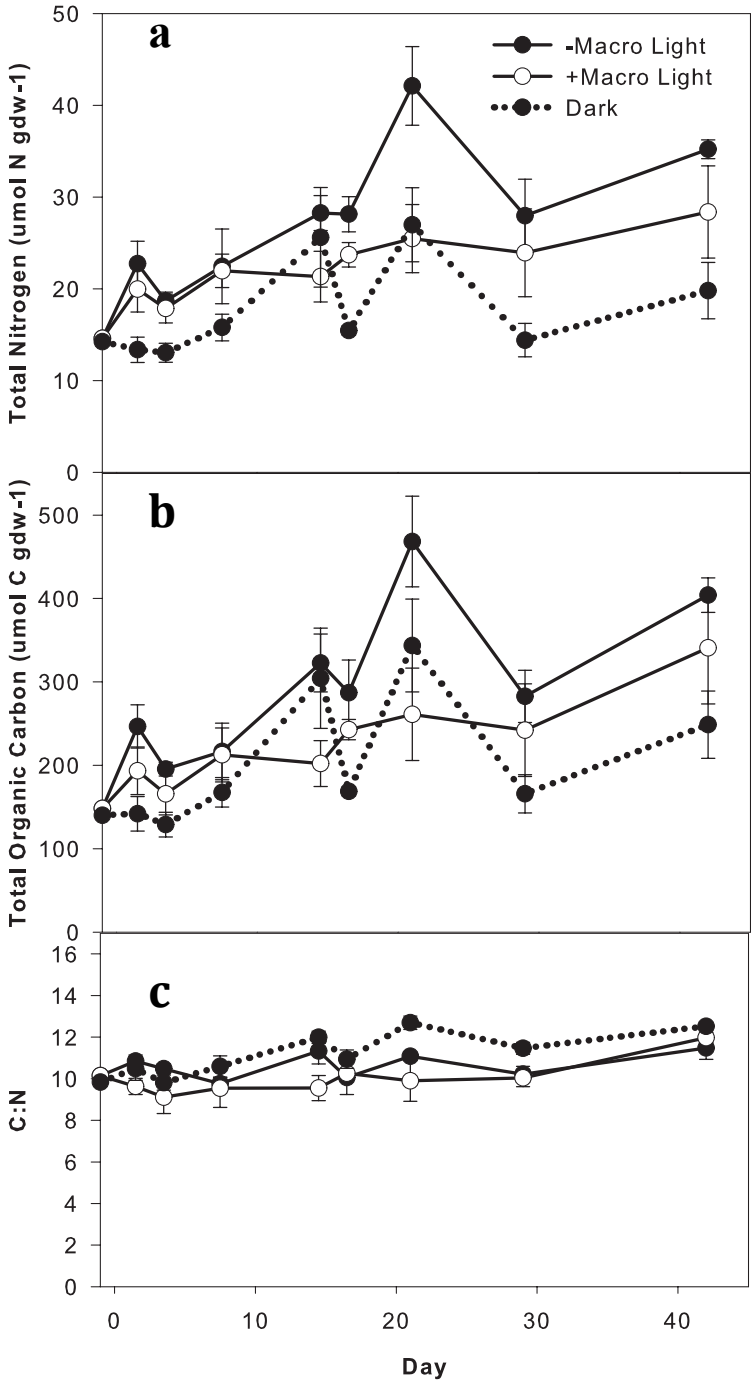
a
b
c
-Macro Light
+Macro Light
Dark
Total Nitrogen (umol N gdw-1)
Total Organic Carbon (umol C gdw-1)
C:N
Day
0
10
20
30
40
50
100
200
300
400
500
2
4
6
8
12
14
16

Figure 3-4. THAA (a) and total PLFA (b) concentrations in surface (0-1 cm) sediments.

Values are mean ± SE (n = 4).

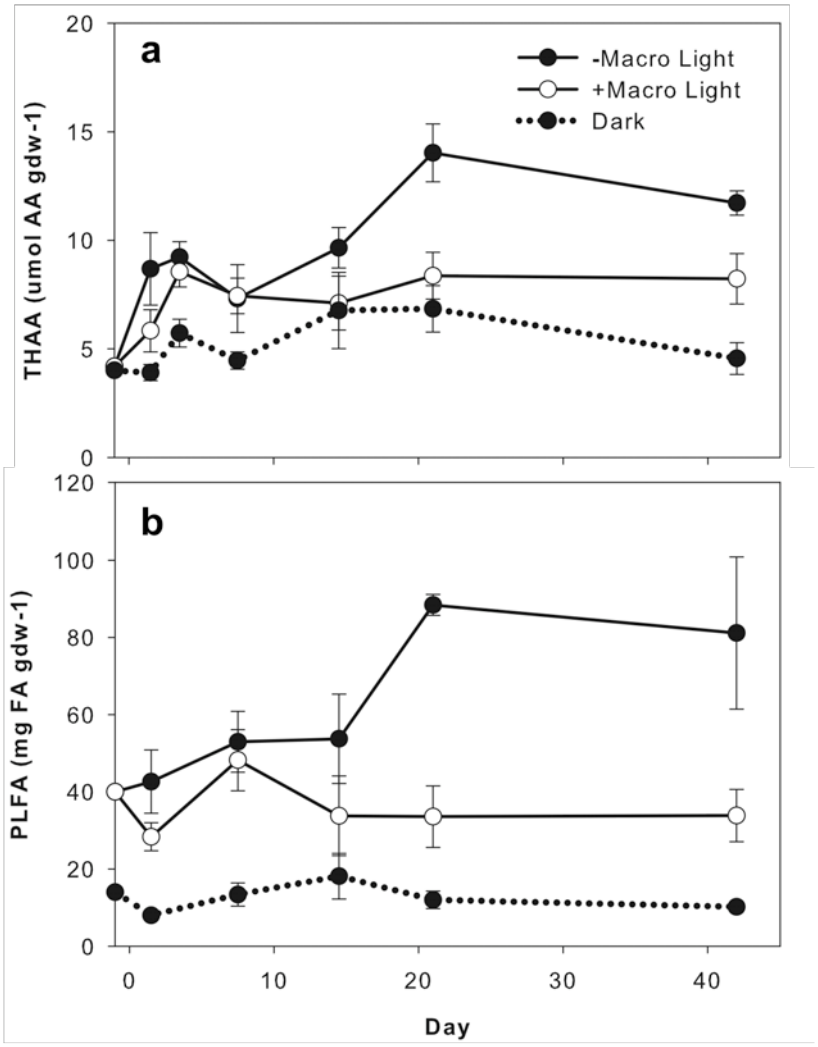
a
b
-Macro Light
+Macro Light
Dark
THAA (umol AA gdw-1)
PLFA (mg FA gdw-1)
Day
0
5
10
15
20
0
20
40
60
80
100
120
0
10
20
30
40

Figure 3-5. Composition as mole percent of THAA for select HAA.

a) Glycine, b) Lysine, c) Leucine, and d) D-alanine. Note scale differences between graphs. Values are mean ± SE (n = 4).

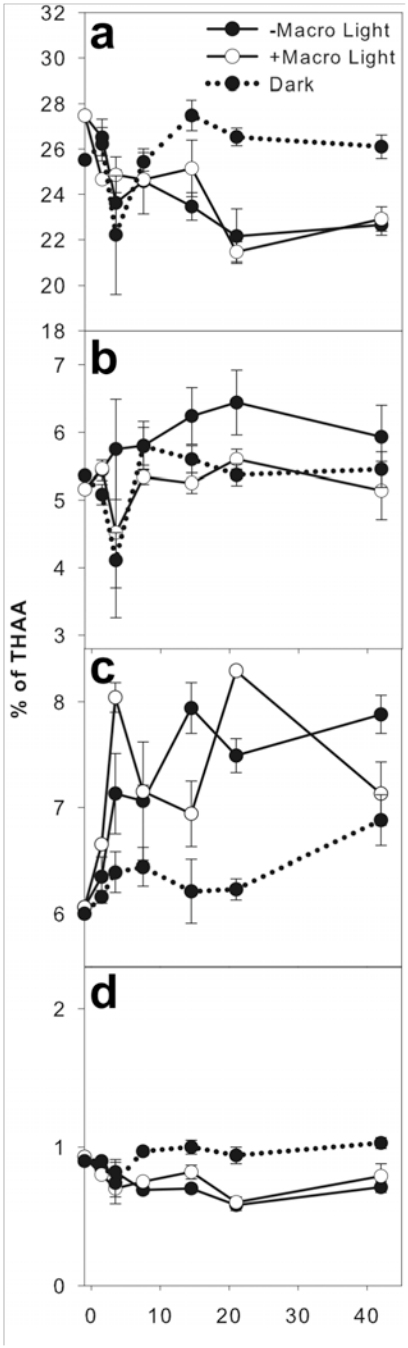
a
b
c
d
-Macro Light
+Macro Light
Dark
% of THAA
Day

Figure 3-6. Concentrations of select algal and bacterial PLFA.

Items (a) through (g) are in units of ng FA gdw^{-1}. Item (h) is unitless since it is a ratio of concentrations. Values are mean ± SE (n = 4).

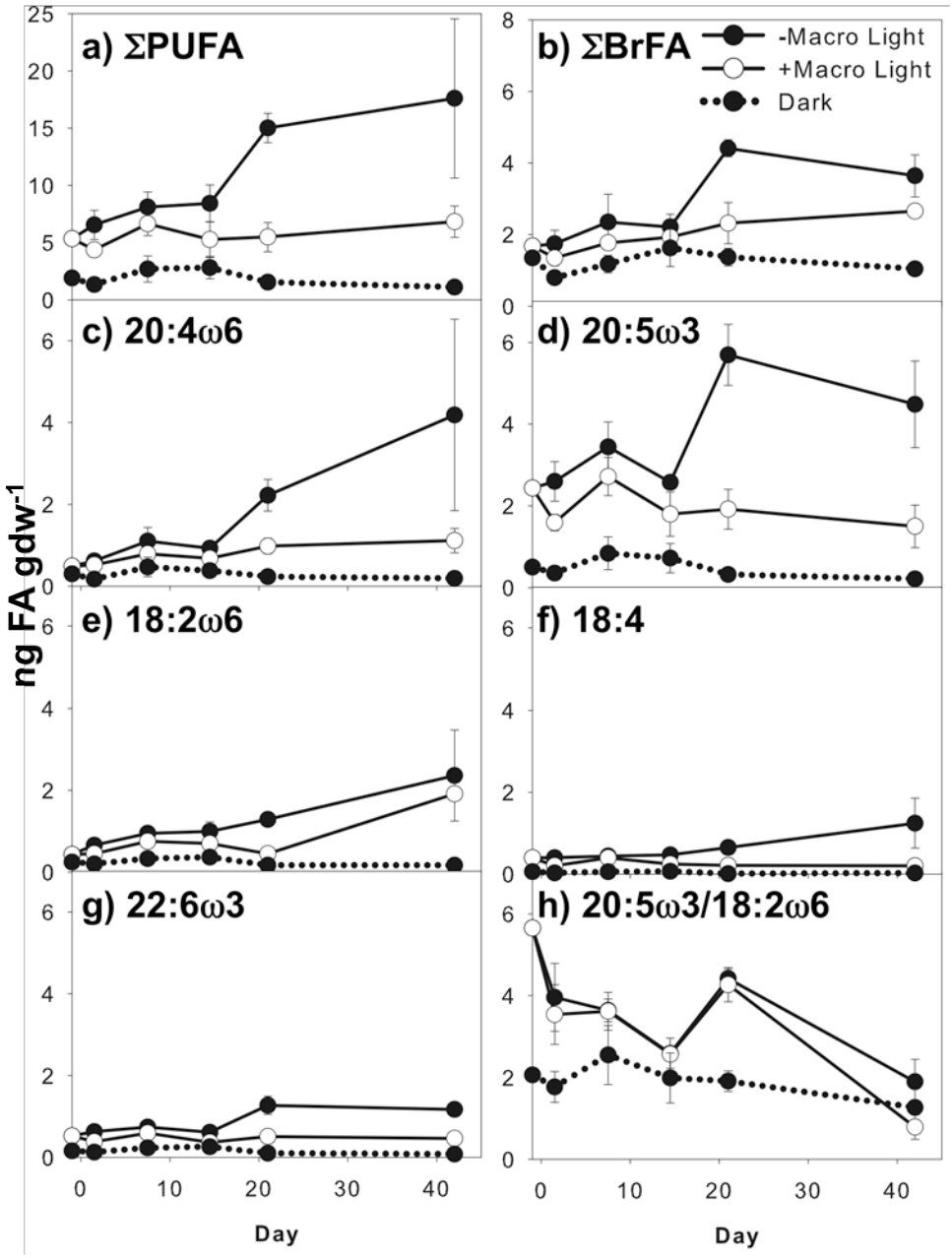
a) ΣPUFA
b) ΣBrFA
-Macro Light
+Macro Light
Dark
c) 20:4ω6
d) 20:5ω3
e) 18:2ω6
f) 18:4
g) 22:6ω3
h) 20:5ω3/18:2ω6
ng FA gdw-1
Day
Day

Figure 3-7. Score and loading results for PC1 and PC2 from PCA analyses. Scores (a) and loadings (b) for PLFA data and scores (c) and loadings (d) for THAA data are shown. Filled symbols in the score plots represent Day 1 observations and open symbols represent Day 42. Treatments are +Macro (triangles), -Macro (squares) and Dark (circles). Error bars represent standard error.

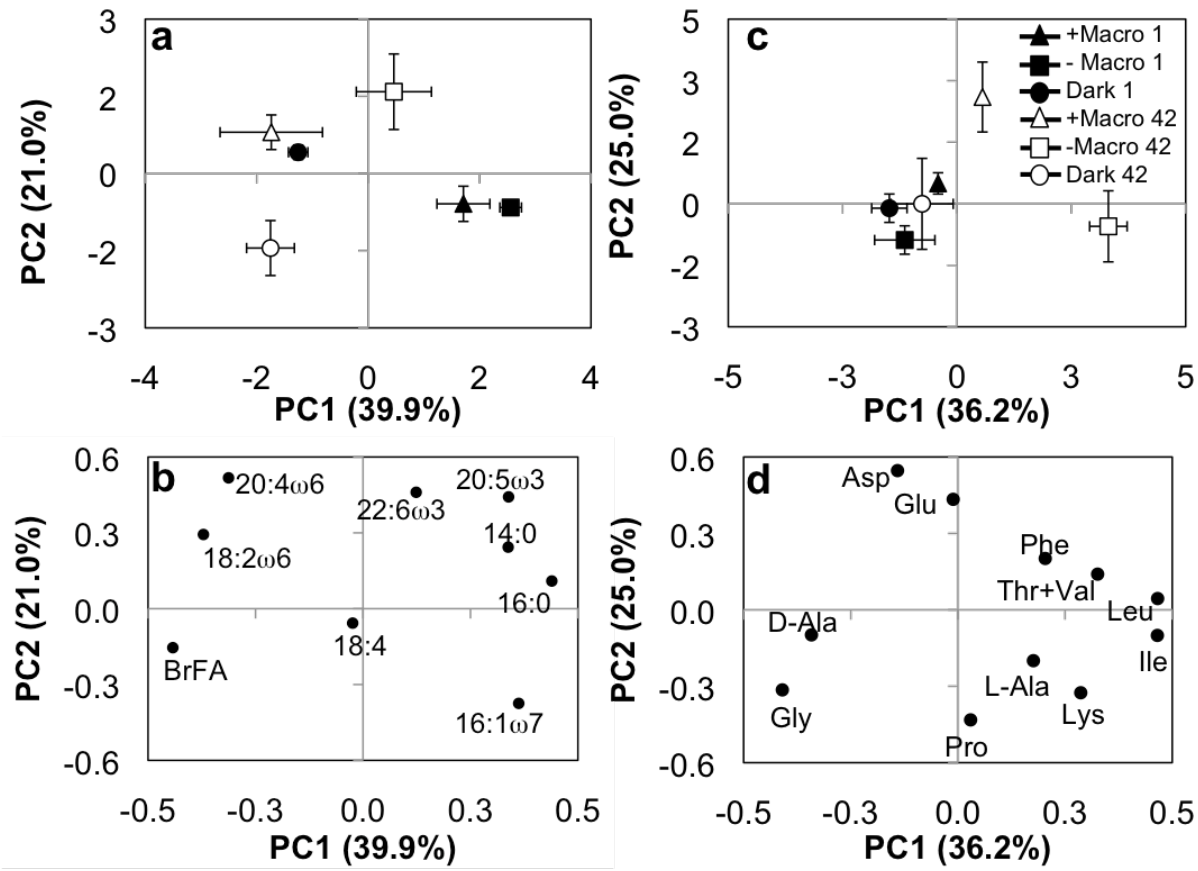
a
PC2 (21.0%)
PC1 (39.9%)
c
PC2 (25.0%)
PC1 (36.2%)
+Macro 1
- Macro 1
Dark 1
+Macro 42
-Macro 42
Dark 42
b
20:4ω6
20:5ω3
22:6ω3
14:0
18:2ω6
16:0
18:4
BrFA
16:1ω7
d
Asp
Glu
Phe
Thr+Val
Leu
D-Ala
Ile
L-Ala
Lys
Gly
Pro

CHAPTER 4: CARBON AND NITROGEN DYNAMICS IN SHALLOW PHOTIC SYSTEMS: INTERACTIONS BETWEEN MACRO- AND MICROALGAL COMMUNITIES

Hardison, A.K.

Canuel, E.A.

Anderson, I.C.

Tobias, C.R.

Veuger, B.

Formatted for submission to *Limnology and Oceanography.*

Acknowledgments

This research was supported by the National Science Foundation (VCR-LTER project DEB 0080381 and DEB 0621014; DEB Ecosystems 0542645 to VIMS and 0542635 to UNCW) and the Environmental Protection Agency (STAR FP916722010). The EPA has not officially endorsed this publication and the views expressed herein may not reflect the views of the EPA. This work would not have been possible without the help of M. Luckenbach, S. Fate, and R. Bonniwell at the VIMS ESL as well as H. Walker, D. Maxey, S. Salisbury, E. Lerberg, L. Palomo, C. Smith, and E. Ferer at VIMS. We are also grateful to K. Duernberger at UNCW and M. Houtekamer at NIOO for assistance in the lab.

Abstract

Sediments in shallow coastal bays are sites of intense biogeochemical cycling facilitated by a complex microbial consortium. Unlike deeper coastal environments, much of the benthos in shallow coastal bays is illuminated, and consequently, benthic autotrophs such as macroalgae and benthic microalgae play an integral role in nutrient cycling. These systems are prone to eutrophication due to nutrient loading from anthropogenic activities. Macroalgal blooms are considered a symptom of eutrophication, but their influence on sediment nutrient cycling dynamics is not fully understood. The objective of this study was to track carbon (C) and nitrogen (N) uptake into the sediments in the presence and absence of macroalgae. We used a dual stable isotope tracer approach in combination with compound-specific isotope analyses of hydrolzable amino acids (HAA) and phospholipid-linked fatty acids (PLFA) to quantify the uptake and retention of C and N within the bulk sediment, benthic microalgal, and bacterial pools. Stable isotope tracers ($^{15}NH_4^+$ and $H^{13}CO_3^-$) were added to the mesocosms via the surface water or pore water for the first 14 days of the 42-day experiment. Sediments exposed to ambient light/dark cycles rapidly took up label from both sources and retained the label for ~4 weeks after isotope additions ended. Benthic microalgae dominated sediment uptake of ^{13}C and ^{15}N, initially accounting for 100% of total uptake. Over time, heterotrophic bacterial uptake became relatively more important, increasing from 0% on Day 1 to 30-40% on Day 42, indicating a close coupling between benthic microalgal and bacterial production. In macroalgae treatments, macroalgae grew at a rate of ~5% day^{-1}, and reached final densities over 500 gdw m^{-2}. ^{13}C and ^{15}N were sequestered by macroalgae, but sediment

^{13}C and ^{15}N uptake decreased by ~40% compared to treatments without macroalgae. This was likely due to shading of the sediment surface by macroalgae, thereby decreasing benthic microalgal production, which in turn decreased bacterial production, as indicated by lower ^{13}C and ^{15}N labeling of bacterial biomarkers. Overall, the sediments serve as a sink for C and N through uptake and retention by the microbial community. This may play an important role in buffering the effects of increased nutrient loading; however, uptake of C and N by ephemeral macroalgae coupled with decreased uptake and retention of C and N by the sediments may ultimately accelerate nutrient cycling within the system, providing a positive feedback to eutrophication.

Introduction

In shallow coastal systems where the majority of the sediment surface exists within the euphotic zone, benthic primary producers such as seagrass, macroalgae, and benthic microalgae, often dominate nutrient cycling dynamics (McGlathery et al. 2004; Sand-Jensen and Borum 1991). Benthic plants serve as a sink for nutrients through uptake and immobilization and also indirectly affect nutrient cycles by changing the chemical and physical environment (Pedersen et al. 2004). Shallow bays are particularly vulnerable to nutrient enrichment because of their position along the coast, where human populations and associated anthropogenic nutrient loadings are rapidly increasing (NRC 2000). It has been hypothesized that increased nutrient loading may result in shifts in autotrophic community structure, but related shifts in biogeochemical cycles are less clear (McGlathery et al. 2007).

Macroalgal blooms represent a symptom of eutrophication in many shallow systems worldwide (Hauxwell et al. 2001; Lavery et al. 1991; McGlathery et al. 2007; Sfriso et al. 1992; Wazniak et al. 2007). The deleterious effects of macroalgae have been studied extensively, and include replacement of seagrass (Deegan et al. 2002; Hauxwell et al. 2001), as well as decreased diversity and biomass within the faunal and fish communities (Bowen and Valiela 2001; Holmquist 1997), which may translate to decreased food availability for upper trophic levels (Raffaelli 2000). However, the influence of these blooms on biogeochemical cycles is less clear. Macroalgae directly affect nutrient cycles by immobilizing nutrients, often in excess of their growth demands

(Peckol et al. 1994). Indeed, in eutrophied systems with large amounts of macroalgal biomass, water quality often appears good because macroalgae are so efficient at removing nutrients from the water column (Valiela et al. 1997). Since they reside at the sediment surface, macroalgae have the potential to influence nutrient cycling at the sediment-water interface, a zone of intense biogeochemical activity, mediated by autotrophic and heterotrophic microbes. However, to date, few studies have focused directly on the effect of macroalgae on the sediment microbial community. Benthic flux studies have revealed that macroalgae play a major role regulating nutrient cycling at the sediment surface. For example, McGlathery and colleagues (2001) used dissolved inorganic carbon (DIC) fluxes to document that benthic microalgal production increased following a macroalgal die-off, suggesting competition between macroalgae and benthic microalgae, possibly for light and/or nutrients. Tyler and colleagues (2003) found that macroalgal uptake resulted in an uncoupling of sediment-water column processes by controlling the exchange of dissolved inorganic nitrogen (DIN) as well as dissolved organic nitrogen (DON) between the sediments and water column. Dalsgaard (2003) measured lower denitrification rates in the presence of macroalgae, presumably because macroalgae out-competed sediment denitrifiers for water column nitrate. Conversely, Krause-Jensen and colleagues (1999) showed similar denitrification rates between bare and macroalgal-covered sediments, but that the oxic/anoxic interface (and hence the zone of nitrification-denitrification) was moved from the sediments up into the macroalgal mat. Thus, while benthic fluxes have been able to generate information about the net results of processes occurring at the sediment-water interface, it has been difficult to further describe the microbial "black box" within the sediments using flux data alone.

We conducted this study to explicitly track carbon (C) and nitrogen (N) uptake into sediment microbial pools in the presence and absence of macroalgae. At the sediment-water interface, nutrients in the water column (from e.g. from run-off, atmospheric deposition) as well as the sediment porewater (from e.g. groundwater, benthic remineralization of organic matter) are available for uptake by benthic autotrophs; thus, we designed an experimental apparatus that allowed us to introduce dissolved nutrients via surface water and porewater so that we could assess differences in uptake by the macroalgal and microbial communities (Hardison et al. Submitted-b). We used a dual stable isotope tracer approach in combination with compound-specific isotope analyses of microbial biomarkers (hydrolyzable amino acids and phospholipid-linked fatty acids) to track C and N into bulk sediments, sediment microbial pools and macroalgae.

Methods

Site description -- Sediments and macroalgae were collected from Hog Island Bay, Virginia (HIB) (Fig. 1), located along the Delmarva Peninsula, and part of the Virginia Coast Reserve, a Long-Term Ecological Research (LTER) site. HIB is a shallow coastal lagoon (< 2 m deep at mean low water), typical of temperate lagoons along the U.S. East coast and is dominated by benthic autotrophs (McGlathery et al. 2001; Thomsen et al. 2006). Macroalgae are present seasonally throughout the lagoon in low to moderate densities (Thomsen et al. 2006); however, we collected sediments and macroalgae from mid-lagoon shoal sites where localized blooms of macroalgae have

previously developed and dominated benthic production during the warmer months (McGlathery et al. 2001; Thomsen et al. 2006). Throughout the rest of the year when macroalgal biomass was low, benthic microalgae dominate (Anderson et al. 2003; McGlathery et al. 2001).

Experimental design -- A flow-through mesocosm array was assembled at the Virginia Institute of Marine Science (VIMS) Eastern Shore Laboratory (ESL) in Wachapreague, VA. In preparation for this experiment, we designed and tested an experimental apparatus that allowed for addition of nutrients simultaneously via surface water (SW) and porewater (PW). The "perfusionator" consisted of a 60 cm I.D. x 60 cm high translucent fiberglass cylinder that includes a reservoir for porewater at the base of the sediment column. Discussion of the design and performance of the perfusionator can be found in Hardison et al. (Submitted-b). Twelve perfusionators were filled to a depth of ~15 cm with intact sediments extruded from cores taken at a mid-lagoon field site (Shoal) in May 2007 (Fig. 1). Care was taken not to transfer any macroalgae or visible macrofauna to the mesocosms. At the ESL, the perfusionators were placed in shallow water baths under 30% shade cloth to control temperature and light. The water column above the sediments was connected to a flow-through seawater system, supplied with filtered seawater from the adjacent creek (1 μm) and was stirred continuously with a mini-jet pump to keep the water column well mixed. Once connected to the experimental system, the mesocosms were allowed to equilibrate for two weeks before beginning the experiment.

Our experiment consisted of an incomplete factorial design made up of three factors, each with two levels: 1) Light (ambient vs. dark), 2) Isotope delivery source (via the SW or PW), and 3) Macroalgae (presence vs. absence of live macroalgae). All factors were crossed with the exception of the dark + macroalgae treatment, since, for logistical purposes, only light treatments received a macroalgal addition. Each treatment was run in duplicate.

For the nutrient additions, nutrients were added to each mesocosm simultaneously via the SW and PW. However, for each treatment, *isotopically-labeled* nutrients were only delivered via one source (i.e. for the PW treatment, isotopically labeled nutrients were added through the PW and unlabeled nutrients were added through the SW). A peristaltic pump was used to add $(^{15}NH_4)_2SO_4$ (25% ^{15}N) and $NaH^{13}CO_3$ (99% ^{13}C) solutions to the SW treatments, with a target isotopic enrichment of the NH_4^+-N pool of 25 at% and DIC of 9 at%. For the PW treatments, $(^{15}NH_4)_2SO_4$ (50% ^{15}N) and $NaH^{13}CO_3$ (99% ^{13}C) were pumped to achieve 30% ^{15}N enrichment of NH_4^+-N and 9% ^{13}C enrichment of DIC in sediment PW. Unlabeled nutrients were added at the same rates as the isotopically labeled nutrients to the corresponding mesocosms. Isotopes were added for the first 14 days of the 42-day experiment. For the remainder of the experiment (i.e. the "post-labeling" period), unlabeled nutrients were added via the SW and PW for all treatments. Feed water was drawn from a creek adjacent to the ESL, pumped through a series of sand, bag (10 μm), and cartridge (5 and 1 μm) filters, exposed to ultraviolet light to kill bacteria, and amended either with $H^{13}CO_3^- + {}^{15}NH_4^+$ or unlabeled $HCO_3^- + NH_4^+$ in a mixing chamber before delivery to each perfusionator. SW additions were delivered directly to the perfusionator water column gravimetrically at a

rate of ~43 L day^{-1}, or a SW residence time of ~2 days. Fine-scale control of the SW flow rate at each mesocosm was achieved using IV drippers, which were calibrated daily. PW additions were delivered through a standpipe into the perfusionator reservoir located below the sediment column at a rate of ~15 L day^{-1}, or a porewater residence time of ~1.8 days. Fine scale control of the PW flow rate into each perfusionator was achieved using an IV dripper located at each standpipe, which was also calibrated daily.

Macroalgae (*Gracilaria vermiculophylla*), collected live from HIB in May 2007, were returned to the laboratory, cleaned of epiphytes and epifauna, rinsed with 0.7 μm filtered seawater, and placed in aquaria inside a greenhouse. Filtered (0.7 μm) seawater was added to each aquarium and kept aerated while the algae were starved for 10 days before addition to the mesocosms. Macroalgae were "starved" to ensure depletion of internal stored nutrients and rapid uptake of the nutrients once in the mesocosms. Live macroalgae were added to the light + macroalgae treatments in densities observed naturally (124.8 ± 1.6 gdw m^{-2}; McGlathery et al. 2001; Stanhope et al. 2009; Thomsen et al. 2006).

Sampling -- Nutrient and macroalgal additions began on Day 0, and isotopes were added through Day 14. The mesocosms were sampled prior to the additions to capture baseline conditions, on Days 1, 3, 7, and 14 during the isotope-labeling period, and on Days 16, 21, 29 and 42, during the post-labeling period. At each sampling, surface sediments (0-1 cm) were collected using two acrylic cores (5.7 cm I.D.) and reserved for bulk (total organic C (TOC), total N (TN)), amino acid, and fatty acid analyses. Sediments from both cores were combined in pre-combusted glass jars, immediately

frozen at -4ºC, and frozen at -80ºC within 3 days. The remaining sediment in the cores was placed carefully back into the holes in the mesocosm sediments. Sediments were also collected for chlorophyll *a* concentrations using a cut-off syringe (1.1 cm I.D.). Samples were sectioned into 0-0.3 cm and 0.3-1.0 cm horizons, placed into 15 mL centrifuge tubes, immediately frozen at -4ºC, and analyzed within 1 month. A different region of the sediment surface was sampled each day to avoid artifacts associated with re-sampling.

Macroalgae were removed from each mesocosm, patted dry, and weighed on Days 7, 14, 21, 29, and 42. Wet mass was converted to dry mass using percent water determined (72%) from *G. vermiculophylla* collected in the field, and dry mass values were normalized to the mesocosm sediment surface area (0.29 m^2). Before addition to the mesocosms and when weighed for determination of growth, a small piece of macroalgal biomass was removed and reserved at -4ºC for isotopic analysis. The live macroalgae were kept in seawater from the respective mesocosms and returned as quickly as possible to avoid desiccation.

Bulk analyses -- Samples were analyzed for benthic chlorophyll *a* concentrations according to a modification of the method of Lorenzen (1967; Pinckney et al. 1994). The sediment pellet was sonicated in 90% acetone, vortexed and extracted for 24 h at -4ºC. The supernatant was passed through a 0.45 μm filter and read on a Shimadzu UV-1601 UV Visible spectrophotometer (λ = 665, 750 nm). Chlorophyll *a* concentrations (mg m^{-2}) were calculated according to the equations in Lorenzen (1967). Chlorophyll *a*

concentrations for the 0-0.3 and 0.3-1.0 cm sections were summed to obtain concentrations for 0-1 cm.

For bulk sediment TOC, TN, and isotopic measurements, sediments were freeze-dried, ground and homogenized, acidified to remove inorganic C (Hedges and Stern 1984), and analyzed for ^{13}C and ^{15}N using elemental analyzer coupled to a Thermo Delta V Plus isotope ratio mass spectrometer (EA-IRMS). Samples of macroalgae were dried at 40ºC, homogenized, and analyzed for ^{13}C and ^{15}N using the same EA-IRMS. Stable isotope ratios for carbon ($R= {}^{13}C/{}^{12}C$) and nitrogen ($R={}^{15}N/{}^{14}N$) were used to calculate δ-values:

$$\delta X\ (‰) = [(R_{sample} / R_{standard}) -1] \times 1000 \quad (1)$$

where X = ^{13}C or ^{15}N. Standards were expressed relative to international standards Vienna Pee Dee Belemnite (VPDB) and atmospheric N_2 for ^{13}C- and ^{15}N analyses, respectively. δX was used to calculate atom% X, which was used to calculate excess X (absolute amount of incorporated ^{13}C or ^{15}N):

$$at\%X = [100 \times R_{standard} \times ((\delta X_{sample} / 1000) + 1)] / [1 + R_{standard} \times ((\delta X_{sample} / 1000) + 1)] \quad (2)$$

$$\text{excess X (nmol X gdw}^{-1}) = [(at\%X_{sample} - at\%X_{control})/ 100] \times [concentration_{sample}] \quad (3)$$

where concentrations were expressed in moles C or N relative to sediment or macroalgal dry weight. The control (unlabeled) samples were collected before the isotopic additions.

Total hydrolyzable amino acids -- Hydrolyzable amino acids (HAA) were analyzed on a subset of the sediment samples according to the method presented in Veuger et al. (2005). Freeze dried sediment (1 g) was rinsed with 2N HCl and Milli-Q water to remove dissolved amino acids. The sediment pellet was then hydrolyzed with 6N HCl at 110ºC for 20 h. Following purification by cation exchange chromatography, amino acids were derivatized with isopropanol and pentafluoropropionic anhydride and further purified by solvent extraction. Concentrations and stable isotope ratios for carbon ($R= {}^{13}C/{}^{12}C$) and nitrogen ($R={}^{15}N/{}^{14}N$) of the derivatized D- and L-amino acids were measured by gas chromatography combustion isotope ratio mass spectrometry (GC-c-IRMS), on a HP 6890 GC with a Thermo type III combustion interface and a Thermo Delta Plus IRMS. δ-and at%X values were calculated according to equations 1 and 2, and used to calculate excess X according to equation 3, where concentration is AA concentrations expressed in moles C or N relative to sediment dry weight. Carbon isotopic values of amino acids were corrected for the C atoms added during derivatization using a mass balance approach following Veuger et al. (2006). The sum of concentrations of, and/or excess label incorporated in, all amino acids analyzed will be referred to as total hydrolysable amino acids (THAA). The ratio of excess ^{13}C or ^{15}N incorporation into D-alanine (D-Ala), a bacterial specific amino acid, relative to L-alanine (L-Ala), an amino acid made by all organisms, was calculated as:

$$\text{D/L-Ala ratio (D/L-Ala)} = (\text{excess X in D-Ala}) / (\text{excess X in L-Ala}) \quad (4)$$

where X is ^{13}C or ^{15}N. During hydrolysis, some racemization of L-Ala to D-Ala takes place, resulting in a D/L-Ala value of ~0.017 (Veuger et al. 2007b). We corrected values of excess isotope in D-Ala for this racemization according to Veuger et al. (2007a), whereas values of D/L-Ala were left uncorrected. Instead, the D/L-Ala value of 0.017 will be indicated graphically in our results (Veuger et al. 2007b). We estimated the bacterial contribution to total ^{13}C or ^{15}N incorporation according to Veuger (2007a):

$$\text{Bacterial contribution (\%)} = [(\text{excess X D/L-Ala} - 0.017) / (\text{bacterial D/L-Ala} - 0.017)] \times 100\% \quad (5)$$

where X is ^{13}C or ^{15}N. Bacterial D/L-Ala represents the D/L-Ala abundance ratio for bacteria. The upper bound of the ratio ranges from 0.05 for Gram negative (G-) bacteria to 0.1 for Gram positive (G+) bacteria and cyanobacteria (Veuger et al. 2007b). Previous work suggests that G+ bacteria are more prominent in deeper (anaerobic) sediments (Moriarty and Hayward 1982). Since our study used sandy photic sediments, we assumed that the contribution from G+ bacteria was negligible. Additionally, photosynthetic pigment analyses conducted on sediments from the mesocosms suggested that cyanobacterial contributions to the microbial community were minimal (M. Waters, pers. comm.). As a result, we further assumed that contribution from cyanobacteria to the D/L-Ala ratio of the total microbial community was negligible and estimated the bacterial D/L-Ala ratio for our sediments to be 0.05. The lower bound of D/L-Ala, when

bacteria do not take up any label, is 0.017, which represents abiotic racemization of L-Ala (Veuger et al. 2007b). Thus, excess ^{13}C and ^{15}N D/L-Ala ratio values should fall between these upper (0.05) and lower (0.0017) limits, with higher values indicating a higher bacterial contribution to the total label uptake since only bacteria incorporate label into D-Ala.

Phospholipid linked fatty acids -- Total fatty acids were analyzed on a subset of the sediment samples according to a modified Bligh and Dyer (1959) method (Canuel et al. 2007; Poerschmann and Carlson 2006). Wet sediments (~12 g) were extracted using an accelerated solvent extractor system (Dionex ASE 200) adapted for in-cell silica gel chromatography. Each sample was extracted twice on the ASE: neutral lipids were collected following extraction with a 9:1 (v:v) hexane:acetone mixture at 50ºC, then polar lipids were collected following extraction with a 8:2 (v:v) methanol:chloroform solution at 80ºC. Neutral and polar lipid fractions were saponified using KOH-CH_3OH for 2h at 110ºC. Saponified samples were then extracted under basic and acidic conditions. The acid-extracted fractions were methylated with BF_3-CH_3OH to form fatty acid methyl esters (FAME). The neutral FAME included neutral and glycolipids while the polar FAME represented the phospholipid-linked fatty acids (PLFA). FAME concentrations were measured by gas chromatography with flame ionization detection (GC-FID, DB-5 column, HP 5890) and quantified using methyl heneicosanoate as an internal standard. Peak identities were verified using reference standards as well as coupled gas chromatography mass spectrometry (HP 6890 GC-MSD). Fatty acids are designated A:BωC, where A is the total number of C atoms, B is the number of double bonds, and C

is the position of the first double bond from the aliphatic ‘‘ω’’ end of the molecule. The prefixes ‘‘i’’ and ‘‘a’’ refer to iso- and anteiso- methyl branched fatty acids (see Canuel et al. 1997 and references therein). Stable C isotope ratios (R= $^{13}C/^{12}C$) for PLFA were measured at NIOO using a Thermo GC-c-IRMS system composed of a Trace GC Ultra gas chromatograph (BPX70 column) coupled to a Delta Plus Advantage IRMS through a GC/C-III interface. These isotope values were used to calculate $\delta^{13}C$ (Eq. 1) and at%^{13}C (Eq. 2). Excess ^{13}C was calculated according to equation 3, where concentrations were FAME concentrations expressed in moles C relative to dry weight sediment. Actual PLFA isotopic values were derived from the FAME isotopic compositions by correcting for the isotopic composition of the C added during derivatization using a mass balance approach.

We analyzed ^{13}C uptake into total PLFA as well as specific groups of PLFA. Excess ^{13}C in polyunsaturated fatty acids (PUFA: $C_{20:5\omega3}$, $C_{20:4\omega6}$, $C_{22:5\omega3}$, $C_{22:5\omega6}$) represented uptake into benthic microalgal biomass (Volkman et al. 1998) while excess ^{13}C in branched odd fatty acids (BrFA: iso- and anteiso- branched $C_{13:0}$, $C_{15:0}$, $C_{17:0}$, $C_{19:0}$) represented heterotrophic bacterial uptake (Boschker et al. 2000; Perry et al. 1979). The ratio of excess ^{13}C in BrFA relative to the sum of BrFA and PUFA (bacteria-to-algae ratio, BAR) was calculated as:

$$BAR = (\text{excess } ^{13}C \text{ in BrFA}) / (\text{excess } ^{13}C \text{ in BrFA} + \text{excess } ^{13}C \text{ in PUFA}) \quad (6)$$

This ratio ranges from 0 to 1, where 0 represents 100% benthic microalgal (0% bacterial) uptake and 1 represents 0% benthic microalgal (100% bacterial) uptake of label.

Data analysis -- We applied repeated measures analysis of variance (ANOVA) to examine the effects of isotope delivery source (PW vs. SW), light (ambient vs. dark), macroalgae (presence vs. absence) and time (day) on the sediment parameters using the Mixed procedure in SAS 9.1 (SAS Institute Inc., Cary, NC). In all models, a first-order ante-dependence error structure (Kenward 1987) was used to model the within-subject covariance structure. Unless otherwise noted, values presented are means ± 1 SE for 2 replicates.

Results

Macroalgae and Bulk Sediments -- Macroalgal growth was nearly linear throughout the experiment, increasing from ~125 gdw m^{-2} on Day 0 to 308 and 513 gdw m^{-2} on Day 42 for SW and PW, respectively (Fig. 2a). This represented an average growth rate of 5-6% day^{-1}. There were no differences in macroalgal biomass between SW and PW treatments throughout the experiment, except for a trend on Day 42 when SW was greater than PW (n = 1 for that day only; Table 1; Fig. 2a). For both SW and PW treatments, excess ^{13}C in macroalgae increased throughout the labeling period, peaked on Day 14 or 21, and decreased through Day 42 (Fig. 2b). There was not a significant isotope source difference, although there was a trend of SW values exceeding PW values. Excess ^{15}N in macroalgae also became enriched throughout the labeling period, peaked on Day 21, and decreased through Day 42 (Fig. 2c). Again, there was not

a significant isotope source difference, although there was a trend of PW values generally exceeding SW values.

Averaged across time steps, total organic carbon (TOC) and total nitrogen (TN) concentrations in sediment were 248 ± 13 μmol C gdw^{-1} and 23 ± 1 μmol N gdw^{-1}, respectively (SE; n = 36 treatment means). All treatments began with similar benthic chlorophyll *a* content (14.8 ± 4.5 mg chl*a* m^{-2}); however, throughout the experiment, benthic chlorophyll *a* concentrations in dark mesocosms became significantly lower than ambient light (Fig. 3, Table 1). There was no significant Macroalgae effect among light treatments. Overall, benthic chlorophyll *a* increased in the light treatments, although with high variability.

Excess ^{13}C and ^{15}N in bulk sediments are presented in Figure 4. In both SW and PW treatments, the ambient light treatments were more enriched than the dark treatments (Table 1), reaching levels well above natural abundance (max $\delta^{13}C$ ~2000‰ and $\delta^{15}N$ ~20000‰ vs. background $\delta^{13}C$ ~ -20‰ and $\delta^{15}N$ ~10‰). Excess ^{13}C in light treatments increased during the labeling period, peaked during the post-labeling period on Day 21, and then decreased through Day 42 (Fig. 4a,b). Among the light treatments, excess ^{13}C in treatments with macroalgae were significantly lower than treatments without macroalgae (Fig. 4a,b; Table 1). The same patterns were observed for excess ^{15}N in both SW and PW treatments: light treatments were more enriched than dark treatments, and treatments with macroalgae were less enriched than treatments without macroalgae (Fig. 4c,d; Table 1). For ^{13}C and ^{15}N, we calculated uptake rates (nmol X gdw^{-1} day^{-1}) during the labeling period as the slopes for changes in excess label (X = ^{13}C or ^{15}N) on Days 1 through Day 21, when the highest enrichments were measured. Similarly, we calculated

loss rates (nmol X gdw^{-1} day^{-1}) during the post-labeling period as the slopes for changes in excess label from Days 21 through 42. Uptake rates were higher for light treatments than dark (Table 2). Within a treatment, rates of ^{13}C and ^{15}N uptake into bulk sediments during the labeling period generally exceeded loss rates, which were often small or not significantly different from zero ($p > 0.05$). Uptake rates were highest for light treatments without macroalgae.

PLFA -- Across all sampling days, PLFA made up a constant fraction of TOC: 1.1 ± 0.3 and 0.3 ± 0.1% of TOC across light and dark treatments, respectively ($n = 20$ treatment means for light, $n = 10$ for dark). Excess ^{13}C in total PLFA followed patterns similar to bulk sediments (Fig. 5a,b). In both SW and PW treatments, ambient light treatments were more enriched than the dark (Fig. 5a,b; Table 1). Among the light treatments, excess ^{13}C in mesocosms with macroalgae were significantly lower than treatments without macroalgae (Fig. 5a,b, Table 1). As with the bulk sediments, we calculated uptake and loss rates of ^{13}C-PLFA. Most uptake and loss rates for PLFA were not significantly different from zero ($p > 0.05$), due to high variability between replicates.

Excess ^{13}C in specific groups of fatty acids provided insight into the microbial groups within the sediments responsible for the label incorporation. Excess ^{13}C in PUFA, which represented BMA uptake, showed patterns similar to total PLFA, displaying both light and macroalgae effects (Fig. 5c,d; Table 1). Excess ^{13}C in BrFA, which represented bacterial uptake, also showed patterns similar to total PLFA (Fig. 5e,f). In both SW and PW treatments, light treatments were more enriched than dark treatments (Fig. 5e,f; Table 1). There was no significant macroalgae difference; however, treatments without

macroalgae were generally higher than those with macroalgae, following the same trend as total PLFA and PUFA (Table 1). To compare the relative uptake between bacterial and BMA communities in the light treatments, we used the bacteria-to-algae ratio (BAR; Fig. 6a,b). For both SW and PW, BMR increased throughout the experiment. There were no significant differences in BAR between light treatments with and without macroalgae (Table 1).

THAA -- Across all sampling days, THAA made up 33 ± 6 and 26 ± 6% of TN and 14 ± 2 and 10 ± 1% of TOC in ambient light and dark treatments, respectively (SE; n = 20 treatment means for light, n = 10 for dark). Excess ^{13}C and ^{15}N in THAA showed the same general patterns as bulk sediment and PLFA, displaying both Light and Macroalgae effects (Fig. 7; Table 1). Uptake and loss rates were calculated for THAA as described above for bulk sediments. Uptake rates were higher for light treatments than dark, and within a treatment, rates of ^{13}C and ^{15}N uptake exceeded loss rates, which were often small or not significantly different from zero ($p > 0.05$) (Table 2). As with bulk sediments, uptake rates were highest for light treatments without macroalgae.

Excess ^{13}C and ^{15}N in D-Ala, a bacterial biomarker, showed the same general patterns as the THAA (Fig. 8). There was a significant light effect for both ^{13}C and ^{15}N (Fig. 8; Table 1), although, among the light treatments, there was a significant macroalgae effect for ^{15}N but not ^{13}C (Table 1). However, for both SW and PW, treatments without macroalgae were generally higher than those with macroalgae, following the same trend as bulk sediments, PLFA, and THAA. To compare the relative uptake between bacterial and BMA communities in the light treatments, we used the ratio

of excess ^{13}C or ^{15}N in D-Ala to L-Ala (D/L-Ala; Fig. 9). For ^{13}C and ^{15}N, in both SW and PW, D/L-Ala increased throughout the experiment. We estimated bacterial contribution to total label incorporation according to Equation 5. For ^{13}C, there was an increase over the course of the experiment from 0 to 15% bacterial uptake for SW and 0 to 30% bacterial uptake for PW (Fig. 9a,b, right axes). For ^{15}N, this represented an increase from 0 to 28% bacterial uptake for SW and 0 to 54% bacterial uptake for PW (Fig. 9c, d). There were no significant differences between light treatments with and without macroalgae (Table 1).

Discussion

Macroalgal nutrient uptake -- Macroalgal growth rates of ~5-6% day^{-1} in the mesocosms were within the range of rates reported for *Gracilaria* spp. in temperate systems similar to HIB (Marinho-Soriano et al. 2006; Navarro-Angulo and Robledo 1999; Raikar et al. 2001; Yokoya et al. 1999). Growth was constant throughout the labeling and post-labeling periods because nutrients were continuously added throughout the experiment. Addition of isotopically-labeled nutrients allowed us to track ^{13}C and ^{15}N into macroalgal biomass, which provided insight into macroalgal nutrient uptake patterns which we could not have learned by monitoring growth rates alone. For example, regardless of whether isotopes were delivered via SW or PW, macroalgae took up ^{13}C and ^{15}N, suggesting that macroalgae used C and N from both sources. This is consistent with previous studies showing that macroalgae can take up nutrients from the water column as well as those released from the sediments (McGlathery et al. 1997; Sundback

et al. 2003; Thybo-Christesen et al. 1993; Tyler et al. 2001). Continued isotopic enrichments of macroalgal tissue following the end of the isotope addition period provides additional insight into nutrient cycling dynamics within a macroalgal mat. ^{13}C and ^{15}N enrichments in macroalgae peaked on Day 21, one week after the isotopes were turned off. Since the flushing rates of the SW and PW were approximately 2 days, isotopes in the surface water or released from the sediments were available for macroalgal uptake for a couple of days before being flushed out. However, continued enrichment of macroalgal tissue for a week or more following the end of the isotope addition may also have reflected recycling of ^{13}C and ^{15}N within the mat, as observed in previous studies (Krause-Jensen et al. 1999; McGlathery et al. 1997; Thybo-Christesen et al. 1993). Thybo-Christesen and colleagues (1993) measured large and frequent changes in nutrients, oxygen, pH, and temperature within the layers of a mat, which, they suggested, behave almost as a closed system. Following Day 21, ^{13}C and ^{15}N content in macroalgal tissue decreased, likely reflecting dilution by unlabeled C and N as macroalgae continued to grow and take up nutrients. By Day 42, the isotopic content of the macroalgae had not yet returned to background levels, indicating storage of the label as biomass, and suggesting that macroalgae act as a temporary sink (at least 4 weeks) for C and N, which is in agreement with other studies (Thybo-Christesen et al. 1993, McGlathery et al. 1996, Pedersen et al. 2004).

Macroalgae served as a sink for C and N during our experiment, just as in field studies, where macroalgal blooms have grown to well over 500 gdw m^{-2} (Hauxwell et al. 2001; McGlathery et al. 2001; Sfriso et al. 1992). It is important to note that the experiment was conducted during the peak growing season for macroalgae in Hog Island

Bay (McGlathery et al. 2001; Tyler et al. 2001), where the macroalgal population often displays a precipitous decline in mid- to late-summer, similar to other coastal lagoons (Astill and Lavery 2001; Sfriso et al. 1992; Thornemiller et al. 1983; Valiela et al. 1992). Thus, in nature, macroalgae may only store C and N temporarily. Once the bloom begins to decline, dissolved organic matter and inorganic nutrients are released to the water column, fueling bacterial and phytoplankton production (Castaldelli et al. 2003; McGlathery et al. 2001; Nedergaard et al. 2002; Tyler et al. 2001). Our recent work also suggests that up to 50% of macroalgal biomass may be transferred to the sediments following die-off of a bloom, supporting sediment heterotrophic bacteria and benthic microalgal production (Hardison et al. *Submitted-a*). In systems that experience the most extreme macroalgal die-offs, hypoxic or anoxic conditions may develop in the water and sediments, further disrupting nutrient cycling and organic matter decomposition (Astill and Lavery 2001; Sfriso et al. 1992; Sundback et al. 1990).

Macroalgal-benthic microalgal interactions --In shallow systems where light reaches the sediment surface, benthic microalgae have been shown to play a central role in regulating nutrient cycling at the sediment-water interface (Anderson et al. In press; McGlathery et al. 2004; Pedersen et al. 2004); we measured multiple parameters that suggest that they were active in our mesocosms as well. Benthic chlorophyll *a* concentrations and label enrichments in bulk sediments in ambient light treatments were significantly higher than in the dark. This indicates that $H^{13}CO_3^-$ and $^{15}NH_4^+$ uptake into bulk sediments in the light was dominated by benthic microalgae. Further, excess ^{13}C and ^{15}N in THAA and excess ^{13}C in total PLFA also showed a strong dependence on light.

Label enrichment in these pools represents uptake by the microbial community, including both autotrophic and heterotrophic organisms. The strong light-dependence of ^{13}C and ^{15}N uptake into these pools indicates the importance of autotrophic (benthic microalgal) uptake and/or recycling by heterotrophic organisms of autotrophic production. Additionally, elevated excess ^{13}C in benthic microalgal fatty acids (C_{20}, C_{22} PUFA) provided the most direct evidence that benthic microalgae were fixing ^{13}C. Finally, the ratios of excess ^{13}C in branched fatty acids to algal fatty acids (BAR) and excess ^{13}C and ^{15}N in D-Ala to L-Ala (D/L-Ala) were low, suggesting that total label incorporation was dominated by benthic microalgae rather than bacteria in this study. We will discuss the change in these ratios over time and the role of bacterial label incorporation in the next section.

Excess ^{13}C and ^{15}N in bulk sediments, THAA, and total PLFA were lower in treatments with macroalgae, suggesting that macroalgae limited benthic microalgal C and N uptake. The most specific biomarkers for benthic microalgae were the PUFA, which showed less ^{13}C enrichment in the treatments with macroalgae. While there was no significant effect of macroalgae on benthic chlorophyll *a* concentrations in the surface sediments, benthic chlorophyll *a* concentrations are not necessarily a direct indication of benthic microalgal productivity, as pigment levels can vary depending on light availability, nutrient concentration, and algal species (Agusti et al. 1994). Macroalgae growing above the sediment surface have the capacity to compete with BMA for nutrients and/or reduce the amount of light available to microalgae (shading) (Sundback and McGlathery 2005 and references therein). Because we were supplying nutrients simultaneously via the SW and PW, neither C nor N was likely limiting in our treatments,

although benthic micro- and macroalgae may have competed for other nutrients such as phosphorus (Valiela et al. 1997). Further, in the treatments with macroalgae, we observed labeling of both macroalgae and benthic microalgae regardless of isotope source. Thus, macroalgae were not sequestering all of the label in the SW treatments thereby preventing benthic microalgal uptake of that label. Similarly, benthic microalgae did not intercept all of the labeled nutrients in the PW treatments thereby preventing uptake by macroalgae.

As a result, we believe the primary mechanism by which macroalgae limited benthic microalgal productivity was through shading. Indeed, macroalgal growth is often sufficiently dense to self-shade the layers of the mat nearest the sediment surface (Brush and Nixon 2003; McGlathery et al. 1997); thus they must limit the amount of light reaching benthic microalgae. Krause-Jensen and colleagues (1996) estimated complete shading of benthic microalgae to occur at macroalgal densities above 300 gdw m^{-2}. In our experiment, macroalgae attained biomasses of 300 gdw m^{-2} by Day 14, suggesting that benthic microalgal productivity may have been diminished during the first two weeks of the experiment and reduced, or possibly shut down, for the remainder of the experiment as macroalgae continued to grow through Day 42. Our results are consistent with those of Tyler and colleagues (2003) who found sediments underlying macroalgal mats to be net heterotrophic. On average, macroalgal densities in Hog Island Bay are less than 300 gdw m^{-2}; however, localized blooms greater than 300 gdw m^{-2} have been observed (McGlathery et al. 2001). Moreover, the densities attained during this experiment are within the range of those observed in more eutrophic coastal systems (Hauxwell et al. 2001; Sfriso et al. 1992; Wazniak et al. 2007). Whether through nutrient

or light competition, macroalgae clearly reduced benthic microalgal productivity, thereby diminishing retention of C and N as benthic microalgal biomass.

Algal-bacterial interactions -- Macroalgal and microalgal growth in coastal systems are closely linked, as discussed previously, due to shading by macroalgae. Our results further suggest that sediment bacteria and algal growth are closely coupled in these systems. The direct negative influence of macroalgae on benthic microalgal production likely translated to diminished bacterial production as well. As with benthic microalgal biomarkers, ^{13}C and ^{15}N label incorporation into bacterial biomarkers (D-Ala and BrFA) was strongly light-dependent and was diminished in the presence of macroalgae. Excess ^{13}C values in PUFA and bacterial biomarkers were linearly related (BrFA: $r^2 = 0.60$, $p < 0.0001$; D-Ala: $r^2 = 0.52$, $p < 0.0001$), suggesting that labeling of benthic microalgae and bacteria tracked one another, which supports the observation from numerous studies that bacteria rely on benthic microalgal production (Cook et al. 2007; Middelburg et al. 2000; Veuger et al. 2007a). Benthic microalgal and bacterial production are thought to be closely coupled in shallow photic systems and can be linked in at least three ways. First, because benthic microalgal turnover is on the order of days (Middelburg et al. 2000; Sundback et al. 1996), bacteria can directly recycle benthic microalgal biomass, resulting in transfer of benthic microalgal ^{13}C and ^{15}N to bacteria. Second, benthic microalgae have been shown to exude over 50% of C fixed as extrapolymeric substances (EPS), which can serve as a substrate for bacterial production (Evrard et al. 2008; Goto et al. 2001; Smith and Underwood 2000). Benthic microalgal EPS would be ^{13}C-labeled as long as benthic microalgae were fixing $H^{13}CO_3^-$. Since

EPS is N-poor, bacteria would likely have to take up $^{15}NH_4^+$ directly to meet their metabolic needs (Cook et al. 2007; Goldman and Dennett 2000; Williams 2000). This would also result in ^{13}C and ^{15}N labeling of bacterial biomass. Lastly, bacterial remineralization of ^{13}C- and ^{15}N-labeled BMA material results in release of inorganic ^{13}C and ^{15}N that can be subsequently taken-up by BMA (Anderson et al. 2003).

To further illustrate the coupling between bacteria and benthic microalgae in this system, we analyzed the ratios of excess ^{13}C in the BAR and excess ^{13}C and ^{15}N in D/L-Ala in the ambient light treatments. Changes in these ratios over time illustrated changes in the relative contributions of benthic microalgae and bacteria to total label uptake. The ratios were low throughout the labeling period, indicating dominance by benthic microalgae, began to increase around Day 21, and reached their highest levels on Day 42. This increase corresponded to relatively more label uptake into bacterial biomass, suggesting that ^{13}C and ^{15}N first passed through the benthic microbial community before being taken up by bacteria. This is corroborated by findings of Middelburg and colleagues (2000) and Evrard and colleagues (2008), suggesting rapid and direct transfer of ^{13}C from benthic microalgae to bacteria in intertidal and subtidal sediments, respectively. While macroalgae affected absolute label uptake into the various microbial pools, they did not affect either BAR or the D/L-Ala ratios, suggesting that the relative contribution to total uptake from bacteria and benthic microalgae remained unchanged in the presence of macroalgae. The shuttling of C and N back-and-forth between benthic microalgae and bacteria likely increased retention in the sediments and accounted for the slower rates of isotope loss in the bulk sediments, and THAA, compared with the rates of uptake during the labeling period (Table 2). These results further suggest that

macroalgae may reduce overall retention of C and N in sediments by reduction of benthic microalgal production, which, in turn, reduced bacterial production.

Nutrient retention and eutrophication -- Previous work corroborates the results of our experiment showing that benthic macroalgae are a sink for C and N in shallow coastal systems (McGlathery et al. 2004; Pedersen et al. 2004). In our experiment, isotopic labels persisted in the bulk sediments for at least four weeks after the isotope additions ended, suggesting that the sediments also serve as a sink for C and N. We suggest that this is facilitated by the sediment microbial community. To determine the size of the macroalgae sink relative to the sediments, we calculated the total label (either ^{13}C or ^{15}N) sequestered by the macroalgal blooms within each mesocosm, and compared that with the total label taken up into bulk sediments across the sediment surface (0-1cm; 0.29 m^{-2}) of each mesocosm (Table 3). In treatments with macroalgae, label "storage" in macroalgal biomass was always higher than in bulk sediments. Further, in most cases for treatments without macroalgae, total label stored in sediments was less than total label sequestered by macroalgae, so macroalgae represented a large, albeit temporary, C and N sink in these systems. As previously discussed, label uptake into sediments with macroalgae was diminished relative to treatments without macroalgae. This reduction in C and N uptake into sediments, averaged across all days and treatments, was ~ 40% (range 10-85%), which clearly has important ecological consequences.

The ephemeral nature of macroalgal blooms distinguishes them from other benthic autotrophs. Macroalgae are efficient at taking up nutrients diffusing from the sediments or the water column, are capable of luxury uptake, and can accumulate in large

blooms during warmer months (Hauxwell et al. 2003; McGlathery et al. 1997; McGlathery et al. 1996; Pavoni et al. 1992). However, once macroalgae decline or die, their nutrients are re-released to the water column, where they can support phytoplankton, including harmful algal blooms, and bacterial metabolism (McGlathery et al. 2001; Sfriso et al. 1992; Tyler et al. 2003). In contrast to macroalgae, retention within the sediment microbial pool would be expected to be a more stable sink. Sequestration of nutrients within sediment microbial biomass may remove nutrients from the water column, and the close coupling between benthic microalgae and bacteria may effectively retain those nutrients within the sediments during times of the year that are favorable for phytoplankton blooms. Thus, shunting nutrients through macroalgae rather than benthic microalgae will likely provide a positive feedback to eutrophication, whereas, the sediment microbial community may play an important role in buffering the effects of increased nutrient loading. This role is likely diminished in the presence of macroalgae.

Literature Cited

Agusti, S., S. Enriquez, H. Frostchristensen, K. Sand-Jensen, and C. M. Duarte. 1994. Light-Harvesting among Photosynthetic Organisms. Functional Ecology **8:** 273-279.

Anderson, I. C., K. J. McGlathery, and A. C. Tyler. 2003. Microbial mediation of 'reactive' nitrogen transformations in a temperate lagoon. Marine Ecology Progress Series **246:** 73-84.

Anderson, I. C., J. W. Stanhope, A. K. Hardison, and K. J. McGlathery. In press. Sources and fates of nitrogen in Virginia Coastal Bays. *In* M. J. Kennish and H. W. Paerl [eds.], Coastal Lagoons: Critical Habitats of Environmental Change. Taylor and Francis.

Astill, H., and P. S. Lavery. 2001. The dynamics of unattached benthic macroalgal accumulations in the Swan-Canning Estuary. Hydrological Processes **15:** 2387-2399.

Bligh, E. G., and W. J. Dyer. 1959. A Rapid Method of Total Lipid Extraction and Purification. Canadian Journal of Biochemistry and Physiology **37:** 911-917.

Boschker, H. T. S., A. Wielemaker, B. E. M. Schaub, and M. Holmer. 2000. Limited coupling of macrophyte production and bacterial carbon cycling in the sediments of *Zostera* spp. meadows. Marine Ecology Progress Series **203:** 181-189.

Bowen, J. L., and I. Valiela. 2001. The ecological effects of urbanization of coastal watersheds: historical increases in nitrogen loads and eutrophication of Waquoit Bay estuaries. Canadian Journal of Fish and Aquatic Science **58:** 1489-1500.

Brush, M. J., and S. W. Nixon. 2003. Biomass layering and metabolism in mats of the macroalga Ulva lactuca L. Estuaries **26:** 916-926.

Canuel, E. A., K. H. Freeman, and S. G. Wakeham. 1997. Isotopic compositions of lipid biomarker compounds in estuarine plants and surface sediments. Limnology and Oceanography **42:** 1570-1583.

Canuel, E. A., A. C. Spivak, E. J. Waterson, and J. E. Duffy. 2007. Biodiversity and food web structure influence short-term accumulation of sediment organic matter in an experimental seagrass system. Limnology and Oceanography **52:** 590-602.

Castaldelli, G. and others 2003. Decomposition dynamics of the bloom forming macroalga Ulva rigida C. Agardh determined using a C-14-carbon radio-tracer technique. Aquatic Botany **75:** 111-122.

Cook, P. L. M., B. Veuger, S. Boer, and J. J. Middelburg. 2007. Effect of nutrient availability on carbon and nitrogen incorporation and flows through benthic algae and bacteria in near-shore sandy sediment. Aquatic Microbial Ecology **49:** 165-180.

Dalsgaard, T. 2003. Benthic primary production and nutrient cycling in sediments with benthic microalgae and transient accumulation of macroalgae. Limnology and Oceanography **48:** 2138-2150.

Deegan, L. A. and others 2002. Nitrogen loading alters seagrass ecosystem structure and support of higher trophic levels. Aquatic Conservation: Marine and Freshwater Ecosystems **12:** 193-212.

Evrard, V., P. L. M. Cook, B. Veuger, M. Huettel, and J. J. Middelburg. 2008. Tracing carbon and nitrogen incorporation and pathways in the microbial community of a photic subtidal sand. Aquatic Microbial Ecology **53:** 257-269.

Goldman, J. C., and M. R. Dennett. 2000. Growth of marine bacteria in batch and continuous culture under carbon and nitrogen limitation. Limnology and Oceanography **45:** 789-800.

Goto, N., O. Mitamura, and H. Terai. 2001. Biodegradation of photosynthetically produced extracellular organic carbon from intertidal benthic algae. Journal of Experimental Marine Biology and Ecology **257:** 73-86.

Hardison, A. K., E. A. Canuel, I. C. Anderson, and B. Veuger. *Submitted-a*. Fate of macroalgae in benthic systems: Carbon and nitrogen cycling within the microbial community. Marine Ecology Progress Series.

Hardison, A. K., C. R. Tobias, J. W. Stanhope, E. A. Canuel, and I. C. Anderson. Submitted-b. An experimental apparatus for laboratory and field-based perfusion of sediment porewater with dissolved tracers. Estuaries and Coasts.

Hauxwell, J., J. Cebrian, C. Furlong, and I. Valiela. 2001. Macroalgal canopies contribute to eelgrass (*Zostera marina*) decline in temperate estuarine ecosystems. Ecology **82:** 1007-1022.

Hauxwell, J., J. Cebrian, and I. Valiela. 2003. Eelgrass *Zostera marina* loss in temperate estuaries: relationship to land-derived nitrogen loads and effect of light limiataion imposed by algae. Marine Ecology Progress Series **247:** 59-73.

Hedges, J. I., and J. H. Stern. 1984. Carbon and Nitrogen Determinations of Carbonate-Containing Solids. Limnology and Oceanography **29:** 657-663.

Holmquist, J. G. 1997. Disturbance and gap formation in a marine benthic mosaic: influence of shifting macroalgal patches on seagrass structure and mobile invertebrates. Marine Ecology-Progress Series **158:** 121-130.

Kenward, M. G. 1987. A Method for Comparing Profiles of Repeated Measurements. Applied Statistics-Journal of the Royal Statistical Society Series C **36:** 296-308.

Krause-Jensen, D., P. B. Christensen, and S. Rysgaard. 1999. Oxygen and nutrient dynamics within mats of the filamentous macroalga *Chaetomorphalinum* Estuaries **22:** 31-38.

Krause-Jensen, D., K. McGlathery, S. Rysgaard, and P. B. Christensen. 1996. Production within dense mats of the filamentous macroalga Chaetomorpha linum in relation to light and nutrient availability. Marine Ecology-Progress Series **134:** 207-216.

Lavery, P. S., R. J. Lukatelich, and A. J. McComb. 1991. Changes in the Biomass and Species Composition of Macroalgae in a Eutrophic Estuary. Estuarine Coastal and Shelf Science **33:** 1-22.

Lorenzen, C. J. 1967. Determination of Chlorophyll and Pheo-Pigments - Spectrophotometric Equations. Limnology and Oceanography **12:** 343-&.

Marinho-Soriano, E., W. S. C. Moreira, and M. A. A. Carneiro. 2006. Some aspects of the growth of Gracilaria birdiae (Gracilariales, Rhodophyta) in an estuary in northeast Brazil. Aquaculture International **14:** 327-336.

McGlathery, K., K. Sundback, and I. Anderson. 2004. The Importance of Primary Producers for Benthic Nitrogen and Phosphorus Cycling, p. 231-261. *In* S. L. Nielsen, G. T. Banta and M. Pedersen [eds.], Estuarine Nutrient Cycling: The Influence of Primary Producers. Kluwer Academic Publishers.

McGlathery, K. J., I. C. Anderson, and A. C. Tyler. 2001. Magnitude and variability of benthic and pelagic metabolism in a temperate coastal lagoon. Marine Ecology-Progress Series **216:** 1-15.

McGlathery, K. J., D. Krause-Jensen, S. Rysgaard, and P. B. Christensen. 1997. Patterns of ammonium uptake within dense mats of the filamentous macroalga Chaetomorpha linum. Aquatic Botany **59:** 99-115.

McGlathery, K. J., M. F. Pedersen, and J. Borum. 1996. Changes in intracellular nitrogen pools and feedback controls on nitrogen uptake in Chaetomorpha linum (chlorophyta). Journal of Phycology **32:** 393-401.

McGlathery, K. J., K. Sundback, and I. C. Anderson. 2007. Eutrophication in shallow coastal bays and lagoons: the role of plants in the coastal filter. Marine Ecology-Progress Series **348:** 1-18.

Middelburg, J. J., C. Barranguet, H. T. S. Boschker, P. M. J. Herman, T. Moens, and C. H. R. Heip. 2000. The fate of intertidal microphytobenthos carbon: An in situ C-13-labeling study. Limnology and Oceanography **45:** 1224-1234.

Moriarty, D. J. W., and A. C. Hayward. 1982. Ultrastructure of Bacteria and the Proportion of Gram-Negative Bacteria in Marine-Sediments. Microbial Ecology **8:** 1-14.

Navarro-Angulo, L., and D. Robledo. 1999. Effects of nitrogen source, N : P ratio and N-pulse concentration and frequency on the growth of Gracilaria cornea (Gracilariales, Rhodophyta) in culture. Hydrobiologia **399:** 315-320.

Nedergaard, R. I., N. Risgaard-Petersen, and K. Finster. 2002. The importance of sulfate reduction associated with *Ulva lactuca* thalli during decomposition: a mesocosm approach. Journal of Experimental Marine Biology and Ecology **275:** 15-29.

NRC. 2000. National Research Council. Clean coastal waters: understanding and reducing the effects of nutrient pollution. National Academy Press.

Pavoni, B., A. Marcomini, A. Sfriso, R. Donazzolo, and A. A. Orio. 1992. Changes in an Estuarine Ecosystem - the Lagoon of Venice as a Case-Study. Acs Symposium Series **483:** 287-305.

Peckol, P., B. Demeoanderson, J. Rivers, I. Valiela, M. Maldonado, and J. Yates. 1994. Growth, Nutrient-Uptake Capacities and Tissue Constituents of the Macroalgae Cladophora-Vagabunda and Gracilaria-Tikvahiae Related to Site-Specific Nitrogen Loading Rates. Marine Biology **121:** 175-185.

Pedersen, M. F., S. L. Nielsen, and G. T. Banta. 2004. Interactions between vegetation and nutrient dynamics in coastal marine ecosystems: An introduction. *In* S. L. Nielsen, G. T. Banta and M. F. Pedersen [eds.], Estuarine Nutrient Cycling: The Influence of Primary Producers. Kluwer.

Perry, G. J., J. K. Volkman, R. B. Johns, and H. J. Bavor. 1979. Fatty-Acids of Bacterial Origin in Contemporary Marine-Sediments. Geochimica et Cosmochimica Acta **43:** 1715-1725.

Pinckney, J., R. Papa, and R. Zingmark. 1994. Comparison of High-Performance Liquid-Chromatographic, Spectrophotometric, and Fluorometric Methods for Determining Chlorophyll a Concentrations in Estuarine Sediments. Journal of Microbiological Methods **19:** 59-66.

Poerschmann, J., and R. Carlson. 2006. New fractionation scheme for lipid classes based on "in-cell fractionation" using sequential pressurized liquid extraction. Journal of Chromatography A **1127:** 18-25.

Raffaelli, D. 2000. Interactions between macro-algal mats and invertebrates in the Ythan estuary, Aberdeenshire, Scotland. Helgoland Marine Research **54:** 71-79.

Raikar, S. V., M. Iima, and Y. Fujita. 2001. Effect of temperature, salinity and light intensity on the growth of Gracilaria spp. (Gracilariales, Rhodophyta) from Japan, Malaysia and India. Indian Journal of Marine Sciences **30:** 98-104.

Sand-Jensen, K., and J. Borum. 1991. Interactions among phytoplankton, periphyton, and macrophytes in temperate freshwaters and estuaries. Aquatic Botany **41:** 137-175.

Sfriso, A., B. Pavoni, A. Marcomini, S. Raccanelli, and A. A. Orio. 1992. Particulate Matter Deposition and Nutrient Fluxes onto the Sediments of the Venice Lagoon. Environmental Technology **13:** 473-483.

Smith, D. J., and G. J. C. Underwood. 2000. The production of extracellular carbohydrates by estuarine benthic diatoms: The effects of growth phase and light and dark treatment. Journal of Phycology **36:** 321-333.

Stanhope, J. W., I. C. Anderson, and W. G. Reay. 2009. Base flow nutrient discharges from lower Delmarva Peninsula watersheds of Virginia. Journal of Environmental Quality **38:** 2070-2083.

Sundback, K., B. Jonsson, P. Nilsson, and I. Lindstrom. 1990. Impact of Accumulating Drifting Macroalgae on a Shallow-Water Sediment System - an Experimental-Study. Marine Ecology-Progress Series **58:** 261-274.

Sundback, K., V. Enoksson, W. Graneli, and K. Pettersson. 1991. Influence of sublittoral microphytobenthos on the oxygen and nutrient flux between sediment and water: a laboratory continuous-flow study. Marine Ecology Progress Series **74:** 263-279.

Sundback, K. and others 2003. Importance of benthic nutrient regeneration during initiation of macroalgal blooms in shallow bays. Marine Ecology-Progress Series **246:** 115-126.

Sundback, K., P. Nilsson, C. Nilsson, and B. Jonsson. 1996. Balance between autotrophic and heterotrophic components and processes in microbenthic communities of sandy sediments: A field study. Estuarine Coastal and Shelf Science **43:** 689-706.

Thomsen, M. S., K. J. McGlathery, and A. C. Tyler. 2006. Macroalgal distribution patterns in a shallow, soft-bottom lagoon, with emphasis on the nonnative Gracilaria vermiculophylla and Coldium fragile. Estuaries and Coasts **29:** 465-473.

Thornemiller, B., M. M. Harlin, G. B. Thursby, M. M. Bradycampbell, and B. A. Dworetzky. 1983. Variations in the Distribution and Biomass of Submerged Macrophytes in 5 Coastal Lagoons in Rhode-Island, USA. Botanica Marina **26:** 231-242.

Thybo-Christesen, M., M. B. Rasmussen, and T. H. Blackburn. 1993. Nutrient Fluxes and Growth of Cladophora-Sericea in a Shallow Danish Bay. Marine Ecology-Progress Series **100:** 273-281.

Tyler, A. C., K. J. McGlathery, and I. C. Anderson. 2001. Macroalgae mediation of dissolved organic nitrogen fluxes in a temperate coastal lagoon. Estuarine Coastal and Shelf Science **53:** 155-168.

---. 2003. Benthic algae control sediment-water column fluxes of organic and inorganic nitrogen compounds in a temperate lagoon. Limnology and Oceanography **48:** 2125-2137.

Valiela, I. and others 1992. Couplings of Watersheds and Coastal Waters - Sources and Consequences of Nutrient Enrichment in Waquoit Bay, Massachusetts. Estuaries **15:** 443-457.

Valiela, I., J. McClelland, J. Hauxwell, P. J. Behr, D. Hersh, and K. Foreman. 1997. Macroalgal blooms in shallow estuaries: Controls and ecophysiological and ecosystem consequences. Limnology and Oceanography **42:** 1105-1118.

Veuger, B., B. D. Eyre, D. Maher, and J. J. Middelburg. 2007a. Nitrogen incorporation and retention by bacteria, algae, and fauna in a subtropical intertidal sediment: An in situ N-15-labeling study. Limnology and Oceanography **52:** 1930-1942.

Veuger, B., J. J. Middelburg, H. T. S. Boschker, and M. Houtekamer. 2005. Analysis of N-15 incorporation into D-alanine: A new method for tracing nitrogen uptake by bacteria. Limnology and Oceanography-Methods **3:** 230-240.

---. 2007b. Update of "Analysis of N-15 incorporation into D-alanine: A new method for tracing nitrogen uptake by bacteria" (Veuger et al. 2005, Limnol. Oceanogr. Methods 3: 230-240). Limnology and Oceanography-Methods **5:** 192-194.

Veuger, B., D. van Oevelen, H. T. S. Boschker, and J. J. Middelburg. 2006. Fate of peptidoglycan in an intertidal sediment: An in situ C-13-labeling study. Limnology and Oceanography **51:** 1572-1580.

Volkman, J. K., S. M. Barrett, S. I. Blackburn, M. P. Mansour, E. L. Sikes, and F. Gelin. 1998. Microalgal biomarkers: A review of recent research developments. Organic Geochemistry **29:** 1163-1179.

Wazniak, C. E., M. R. Hall, T. J. B. Carruthers, B. Sturgis, W. C. Dennison, and R. J. Orth. 2007. Linking water quality to living resources in a mid-Atlantic lagoon system, USA. Ecological Applications **17:** S64-S78.

Williams, P. J. l. B. 2000. Heterotrophic bacteria and the dynamics of dissolved organic material, p. 153-200. *In* D. L. Kirchman [ed.], Microbial Ecology of the Oceans. Wiley-Liss, Inc.

Yokoya, N. S., H. Kakita, H. Obika, and T. Kitamura. 1999. Effects of environmental factors and plant growth regulators on growth of the red alga Gracilaria vermiculophylla from Shikoku Island, Japan. Hydrobiologia **399:** 339-347.

Table 4-1: Results of two-factor repeated measures ANOVA.

Repeated measures ANOVA was used to test for differences in isotope delivery source, macroalgae, and light over time for isotopic enrichments (^{13}C or ^{15}N) of various sediment pools. Significant p values (< 0.05) are indicated in bold.

Parameter	Isotope	Isotope delivery			Macroalgae			Light			Day		
		df	F	p	df	F	p	df	F	p	df	F	p
BULK	^{15}N	6	23.9	**0.0027**	6	20.2	**0.0042**	6	63.6	**0.0002**	54	19.1	**< 0.0001**
	^{13}C	6	2.86	0.1416	6	14.8	**0.0085**	6	77.5	**0.0001**	54	22.6	**< 0.0001**
THAA	^{15}N	5	10.5	**0.0231**	5	14.3	**0.0128**	5	37.9	**0.0016**	32	29.3	**< 0.0001**
	^{13}C	5	2.03	0.2135	5	10.2	**0.0242**	5	52.3	**0.0008**	33	50.2	**< 0.0001**
DALA	^{15}N	5	9.98	**0.0251**	5	9.13	**0.0293**	5	25.1	**0.0041**	32	26.0	**< 0.0001**
	^{13}C	5	0.73	0.4331	5	5.36	0.0684	5	41.3	**0.0014**	33	46.0	**< 0.0001**
D/L-Ala	^{15}N	5	0.66	0.4543	5	0.47	0.5243	5	183.7	**< 0.0001**	31	25.7	**< 0.0001**
	^{13}C	5	14.6	**0.0124**	5	0.64	0.4593	--	--	--	27	28.1	**< 0.0001**
MACRO	^{15}N	2	3.63	0.1972							6	21.4	**0.0011**
	^{13}C	2	3.57	0.1993							6	0.97	0.4861
PLFA	^{13}C	6	2.45	0.1684	6	8.34	**0.0278**	6	15.1	**0.0081**	30	30.7	**< 0.0001**
BrFA	^{13}C	6	3.30	0.1190	6	4.50	0.0782	6	13.5	**0.0105**	30	19.1	**< 0.0001**
PLFA	^{13}C	6	0.95	0.3679	6	23.0	**0.0030**	6	54.7	**0.0003**	30	63.1	**< 0.0001**
BMR	^{13}C	6	0.16	0.7014	6	0.56	0.4829	6	67.0	**0.0002**	30	29.6	**< 0.0001**
Chl *a*	--	6	3.06	0.1306	6	2.00	0.2070	6	42.5	**0.0006**	55	5.74	**<0.0001**

Table 4-2: Uptake and loss rates for label into bulk, THAA, and PLFA.

Values are mean (SE), *n* = 2. Uptake rates (nmol X gdw^{-1} day^{-1}) were calculated as the slope of excess label (X = ^{13}C or ^{15}N) from Days 1 - 21. Loss rates (nmol X gdw^{-1} day^{-1}) were calculated as the slope of excess label from Days 21 – 42. Slopes with significant p values ($p < 0.05$) are represented in bold.

			BULK				THAA				PLFA	
			^{13}C		^{15}N		^{13}C		^{15}N		^{13}C	
	Treatment	Rate	slope	r^2	slope	r^2	slope	r^2	slope	r^2	slope	r^2
Pore Water	Dark	Uptake	**6.35 (1.41)**	0.67	**6.04 (1.92)**	0.50	**2.09 (0.58)**	0.62	**3.05 (0.90)**	0.59	0.033 (0.031)	0.17
		Loss	-0.23 (2.72)	0.00	-1.63 (2.23)	0.12	-0.405 (1.26)	0.05	-1.05 (1.48)	0.20	-0.0105 (0.023)	0.10
	Light +Macro	Uptake	**104 (32.4)**	0.51	**50.7 (13.2)**	0.60	28.4 (12.3)	0.64	22.2 (10.3)	0.61	1.40 (1.74)	0.25
		Loss	-10.1 (56.0)	0.01	-12.0 (22.9)	0.08	-14.0	--	-10.9	--	-1.56	--
	Light NoMacro	Uptake	**296 (60)**	0.71	**109 (21)**	0.74	**79.1 (15.5)**	0.77	**61.7 (11.9)**	0.77	**6.53 (1.96)**	0.65
		Loss	**-119 (32)**	0.78	**-37.1 (10.9)**	0.74	**-36.6 (6.9)**	0.93	**-24.8 (3.2)**	0.97	-7.01 (1.77)	0.89
Surface Water	Dark	Uptake	**6.74 (1.31)**	0.73	**3.66 (0.82)**	0.67	**2.65 (0.40)**	0.84	**2.13 (0.44)**	0.77	0.203 (0.280)	0.08
		Loss	-3.81 (2.16)	0.44	-2.66 (1.28)	0.52	-1.79 (0.50)	0.87	-1.52 (0.57)	0.78	-0.0712 (0.0334)	0.82
	Light +Macro	Uptake	**221 (43)**	0.73	**26.8 (7.56)**	0.56	**53.2 (17.8)**	0.56	**15.2 (3.8)**	0.70	2.02 (3.42)	0.06
		Loss	-138 (78)	0.52	-13.1 (11.8)	0.29	-27.2 (33.4)	0.40	-5.65 (10.2)	0.24	-1.29 (2.38)	0.23
	Light NoMacro	Uptake	**305 (36)**	0.88	**43.3 (3.5)**	0.94	**83.3 (7.2)**	0.94	**22.5 (1.9)**	0.94	6.40 (2.88)	0.45
		Loss	-143 (68)	0.52	-14.0 (13.2)	0.22	-39.1 (10.3)	0.88	-6.57 (4.89)	0.47	**-5.24 (1.18)**	0.91

Table 4-3: Isotope inventory in macroalgae and sediments.

Total label (^{15}N or ^{13}C) in macroalgal bloom and surface sediments (0-1 cm) of entire mesocosm (0.29 m^2) for surface water and porewater treatments across 4 days. % Red. refers to the percent reduction (decrease) in total label in surface sediments for treatments with macroalgae versus without macroalgae.

		^{15}N (mmol ^{15}N $mesocosm^{-1}$)				^{13}C (mmol ^{13}C $mesocosm^{-1}$)			
	Day	Macro	Sediment		% Red.	Macro	Sediment		% Red.
			No Macro	+Macro			No Macro	+Macro	
Surface Water	7	3.67 (0.21)	1.43 (0.14)	0.77 (0.34)	46	52.3 (5.2)	10.4 (1.4)	8.72 (4.4)	16
	14	2.75 (0.86)	2.99 (0.31)	1.82 (0.17)	39	73.0 (13.2)	24.0 (4.6)	15.9 (3.9)	29
	21	6.14 (0.25)	4.03 (0.52)	2.73 (1.02)	32	76.3 (19.4)	27.6 (2.0)	19.6 (6.23)	30
	42	3.37 (1.27)	2.72 (0.62)	1.56	43	42.0 (18.7)	13.7 (2.6)	7.51	45
Pore Water	7	1.68 (1.23)	2.22 (1.04)	1.98 (0.59)	11	12.2 (4.1)	4.82 (2.16)	4.36 (0.35)	10
	14	6.50 (2.86)	8.29 (2.60)	1.99 (1.25)	76	42.9 (19.0)	24.8 (7.3)	3.34 (1.62)	85
	21	17.8 (6.1)	9.12 (0.42)	4.33 (1.22)	53	65.2 (15.2)	24.1 (1.0)	8.76 (3.41)	65
	42	18.7 (2.1)	5.67 (0.74)	3.17	44	60.0 (5.4)	13.0 (2.1)	7.60	43

Figure 4-1. Map of study site.

Sediments and macroalgae were collected from a mid-lagoon shoal site in Hog Island Bay, Virginia, located along the Delmarva Peninsula, USA. Hog Island Bay is part of the Virginia Coast Reserve, a Long-Term Ecological Research (LTER) site.

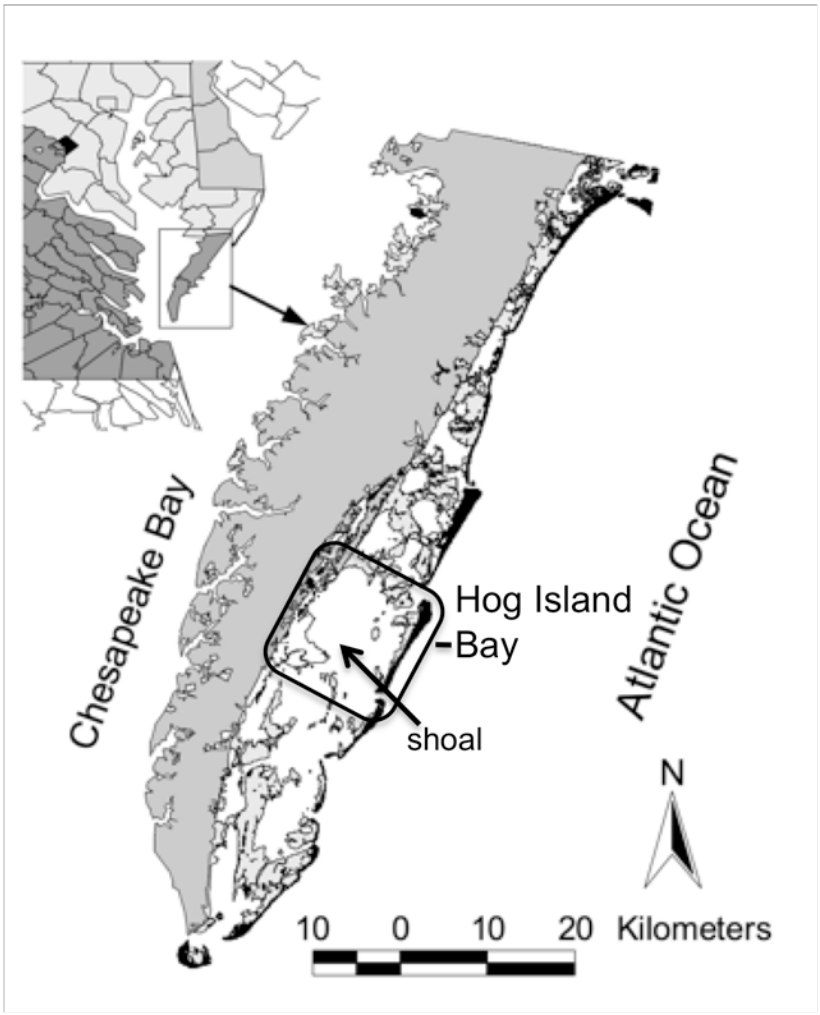
Chesapeake Bay
Atlantic Ocean
Hog Island
Bay
shoal
N
10 0 10 20 Kilometers

Figure 4-2. Macroalgal biomass and isotopic enrichment.

Biomass (a) and excess ^{13}C (b) and ^{15}N (c) in surface water (closed symbols) and pore water (open symbols) treatments. The grey shaded area indicates the isotope addition period. Values are mean ± SE (n = 2).

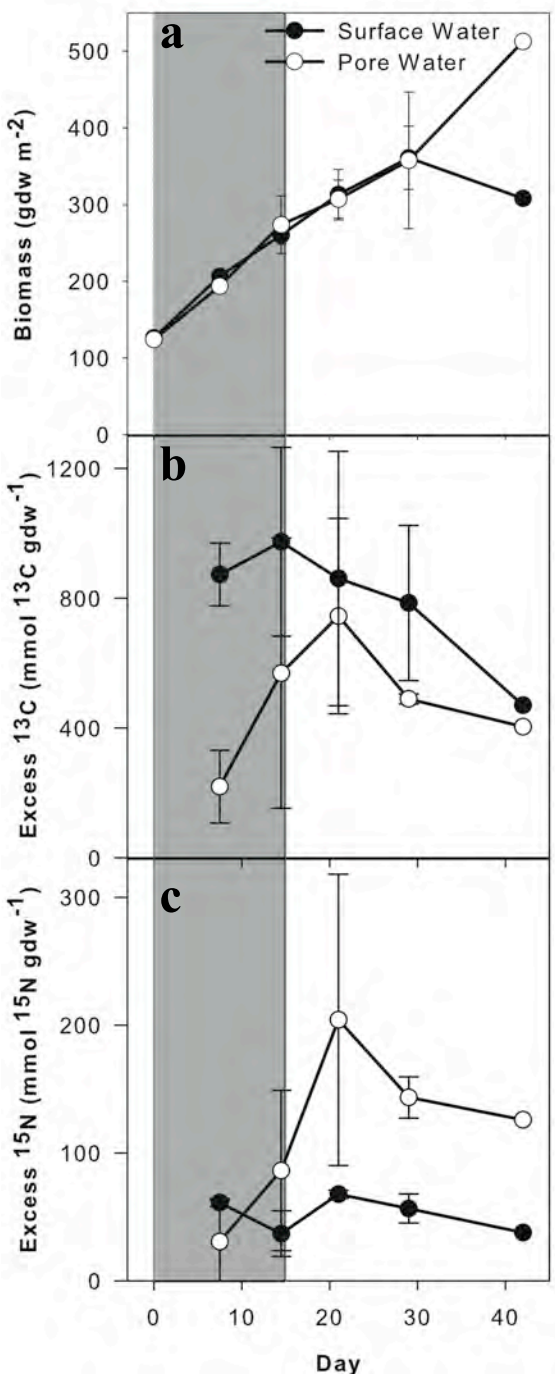
a
b
c
Surface Water
Pore Water
Biomass (gdw m-2)
Excess 13C (mmol 13C gdw-1)
Excess 15N (mmol 15N gdw-1)
Day
0
100
200
300
400
500
800
1200
10
20
30
40

Figure 4-3. Benthic chlorophyll *a* concentrations in a) Surface Water and b) Pore Water treatments.

Treatments shown are light with macroalgae (solid lines, filled symbols), light without macroalgae (solid lines, open symbols), and dark without macroalgae (dotted lines with filled symbols). Baseline samples were taken 4 days prior to adding the nutrients and macroalgae. Values are mean ± SE (n = 2).

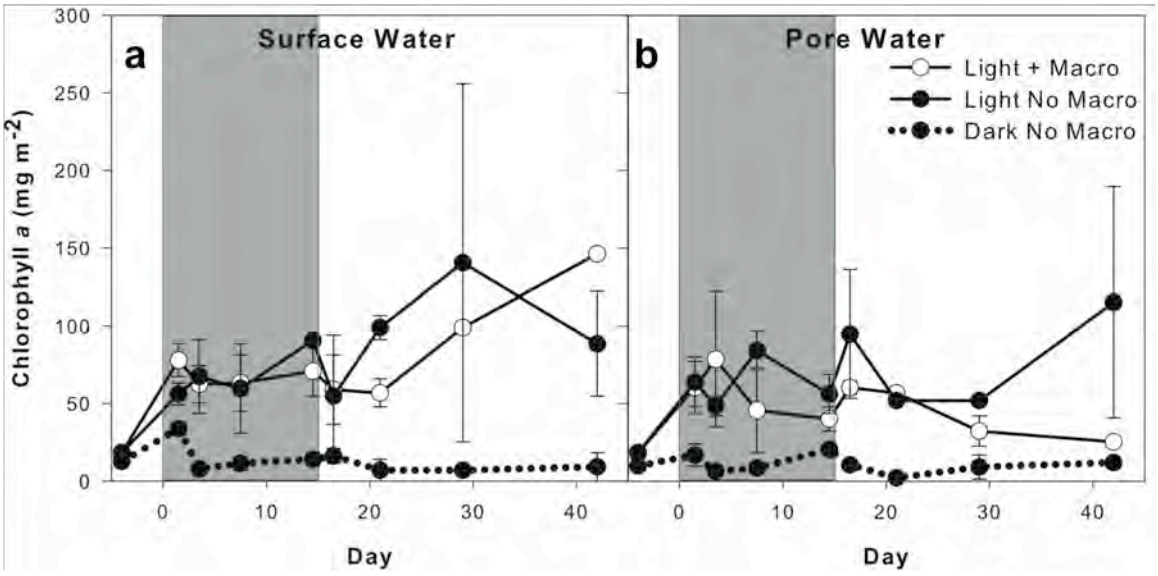
a
Surface Water
b
Pore Water
Light + Macro
Light No Macro
Dark No Macro
Chlorophyll a (mg m-2)
300
250
200
150
100
50
0
0
10
20
30
40
Day
Day

Figure 4-4. Bulk sediment isotopes.

Excess ^{13}C (a ,b) and ^{15}N (c, d) in bulk sediments in Surface Water (a, c) and Pore Water (b, d) treatments. Values are mean ± SE (n = 2).

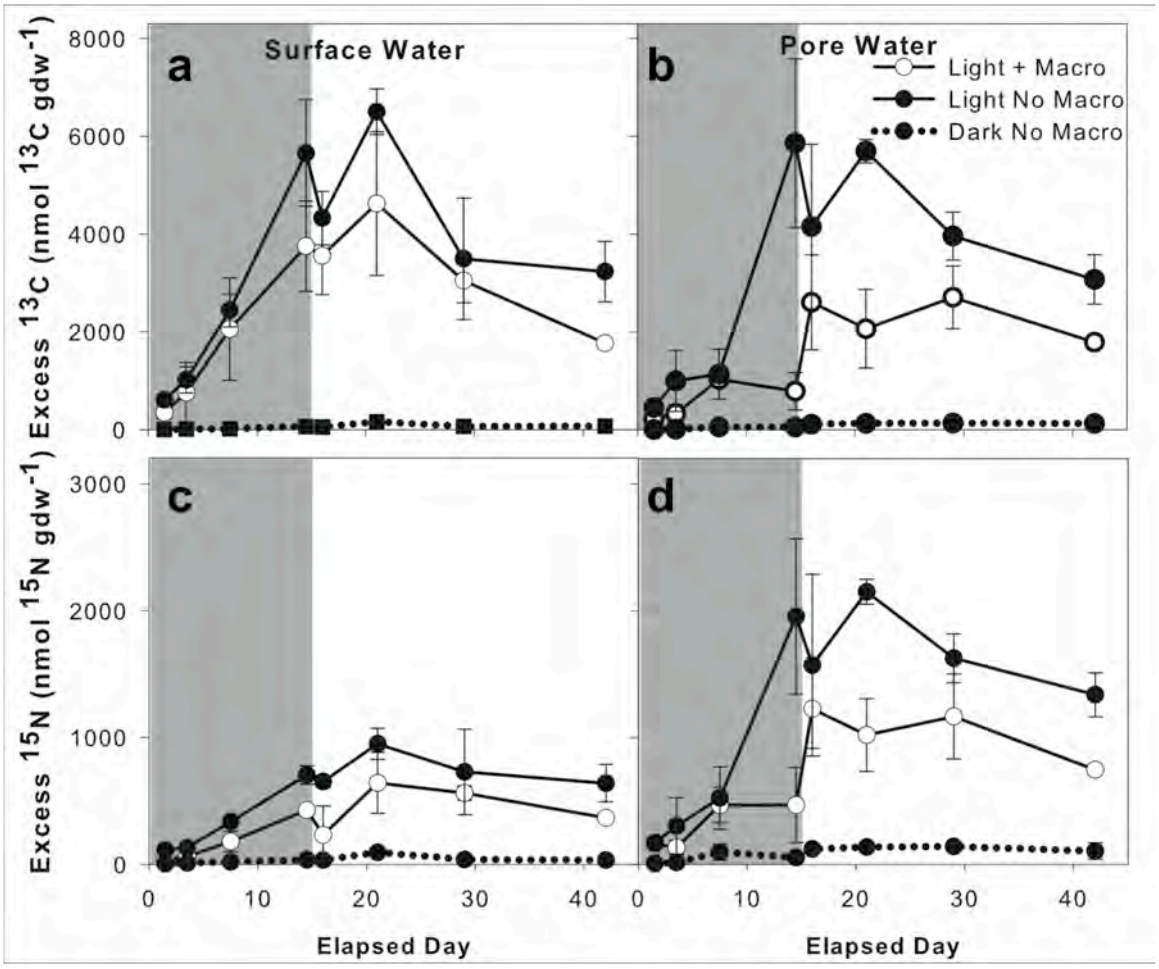
a
Surface Water
b
Pore Water
Light + Macro
Light No Macro
Dark No Macro
c
d
Excess ^{13}C (nmol ^{13}C gdw^{-1})
Excess ^{15}N (nmol ^{15}N gdw^{-1})
8000
6000
4000
2000
0
3000
2000
1000
0
0
10
20
30
40
Elapsed Day
Elapsed Day

Figure 4-5. PLFA isotopic enrichments.

Excess ^{13}C in total PLFA (a, b), C_{20} and C_{22} polyunsaturated fatty acids (PUFA; c, d), and branched odd fatty acids (BrFA; e, f) for Surface Water (a, c, e) and Pore Water (b, d, f) treatments. Values are mean ± SE (n = 2).

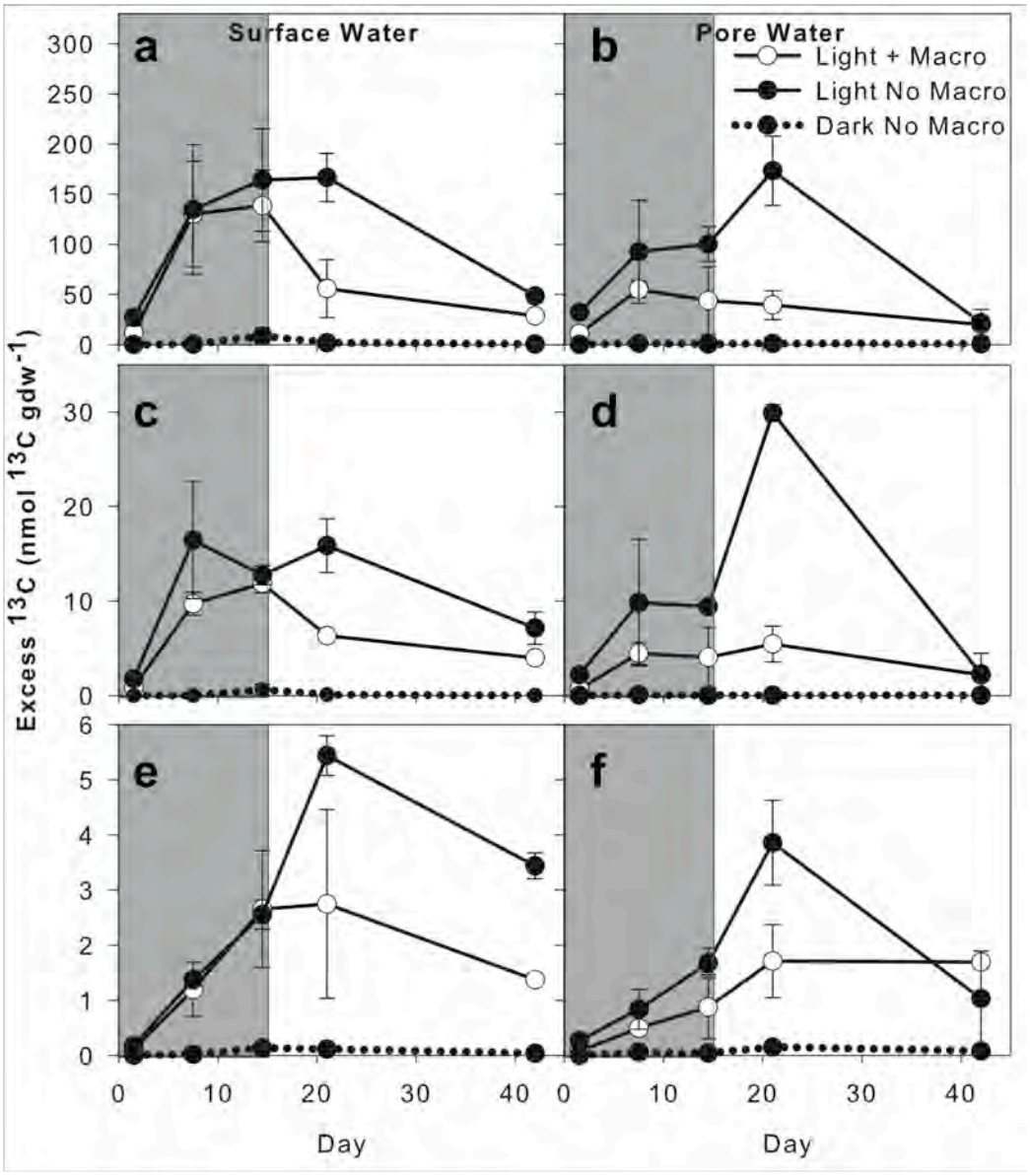
a
Surface Water
b
Pore Water
Light + Macro
Light No Macro
Dark No Macro
c
d
e
f
Excess ^{13}C (nmol ^{13}C gdw^{-1})
Day
Day

Figure 4-6. The PLFA bacteria-to-algae (BAR) and D/L-Ala ratios.

BAR is the ratio of excess ^{13}C in branched odd fatty acids (BrFA) to the sum of BrFA and polyunsaturated fatty acids (BrFA + PUFA) for light mesocosms in a) Surface Water and b) Pore Water treatments. The ratio of excess ^{13}C (c, d) and ^{15}N (e, f) in D-alanine/L-alanine (D/L-Ala) for light mesocosms in Pore Water (c, e) and Surface Water (d, f) treatments. The dashed horizontal lines in c-f represent the racemization background (0.017). Values on the right y-axes correspond to estimates of bacterial and algal contribution to total label incorporation. Values are mean ± SE (n = 2).

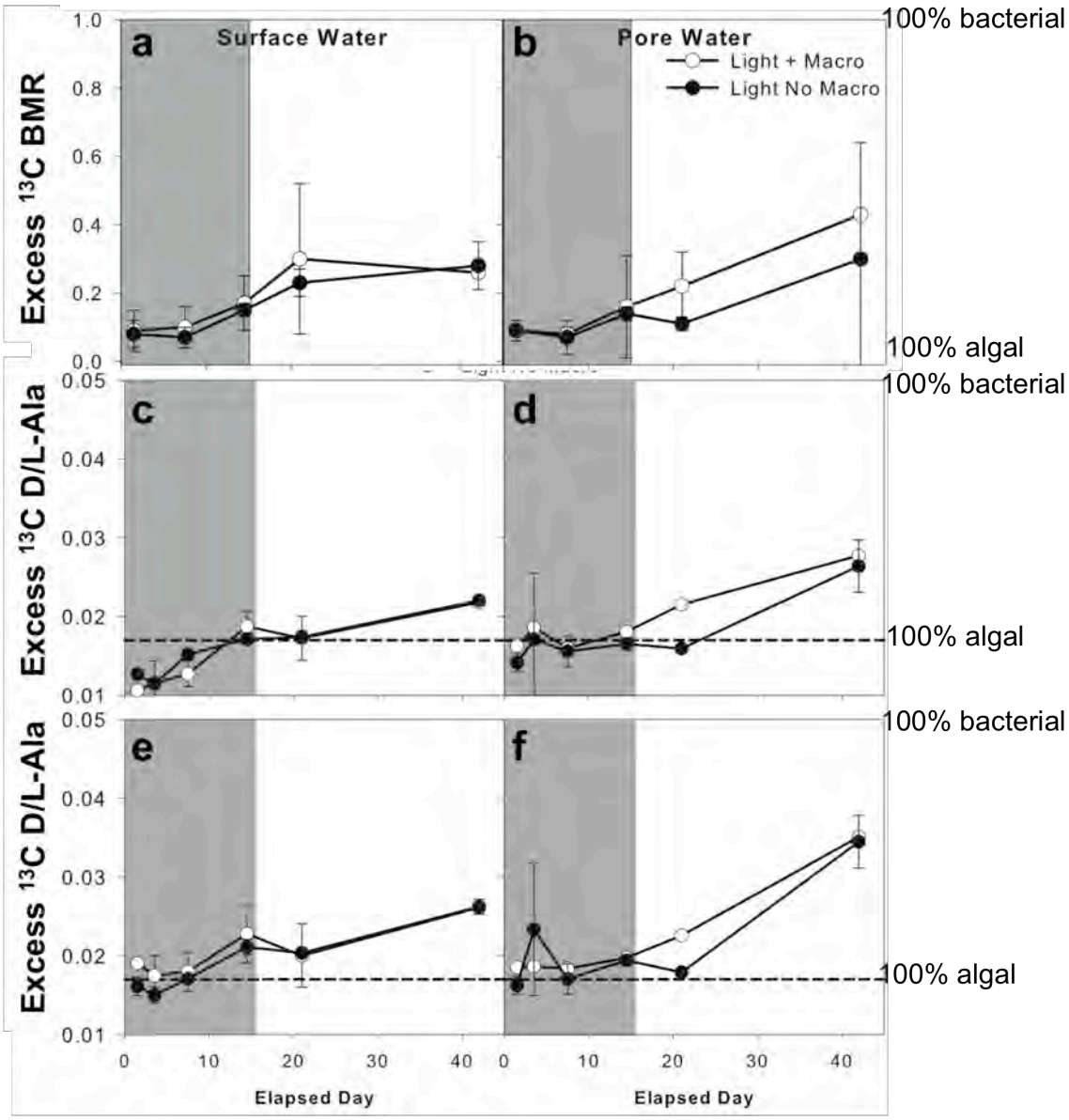
a
Surface Water
b
Pore Water
Light + Macro
Light No Macro
c
d
e
f
Excess ¹³C BMR
Excess ¹³C D/L-Ala
Excess ¹³C D/L-Ala
1.0
0.8
0.6
0.4
0.2
0.0
0.05
0.04
0.03
0.02
0.01
0
10
20
30
40
Elapsed Day
100% bacterial
100% algal
100% bacterial
100% algal
100% bacterial
100% algal

Figure 4-7. THAA isotopic enrichments.

Excess ^{13}C (a ,b) and ^{15}N (c, d) in total hydrolyzable amino acids (THAA) in Surface Water (a, c) and Pore Water (b, d) treatments. Values are mean ± SE (n = 2).

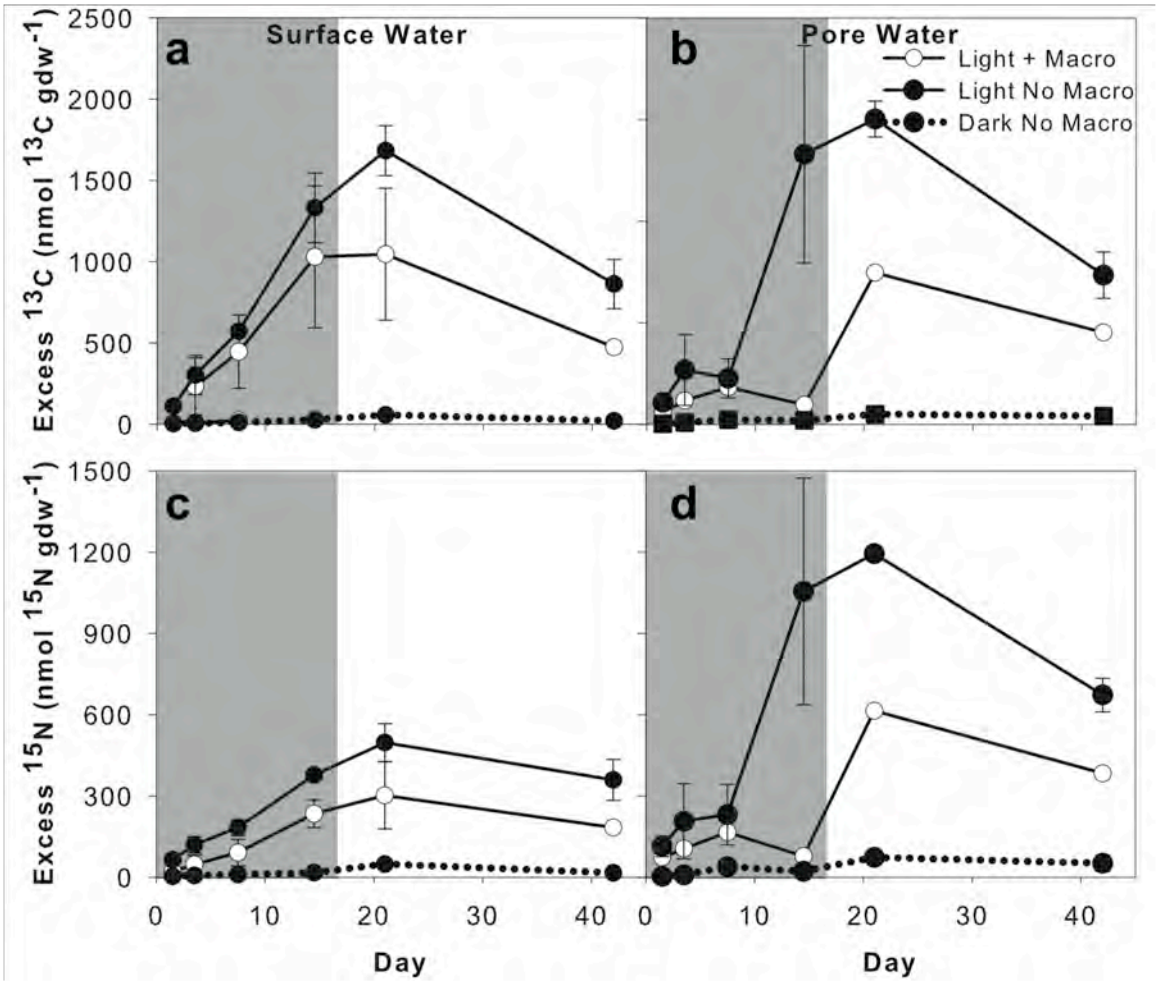
a
Surface Water
b
Pore Water
Light + Macro
Light No Macro
Dark No Macro
Excess ^{13}C (nmol ^{13}C gdw^{-1})
Excess ^{15}N (nmol ^{15}N gdw^{-1})
c
d
0
500
1000
1500
2000
2500
300
600
900
1200
10
20
30
40
Day

Figure 4-8. D-alanine isotopic enrichments.

Excess ^{13}C (a ,b) and ^{15}N (c, d) in D-alanine (D-Ala) in surface water (a, c) and pore water (b, d) treatments. Values are mean ± SE (n = 2).

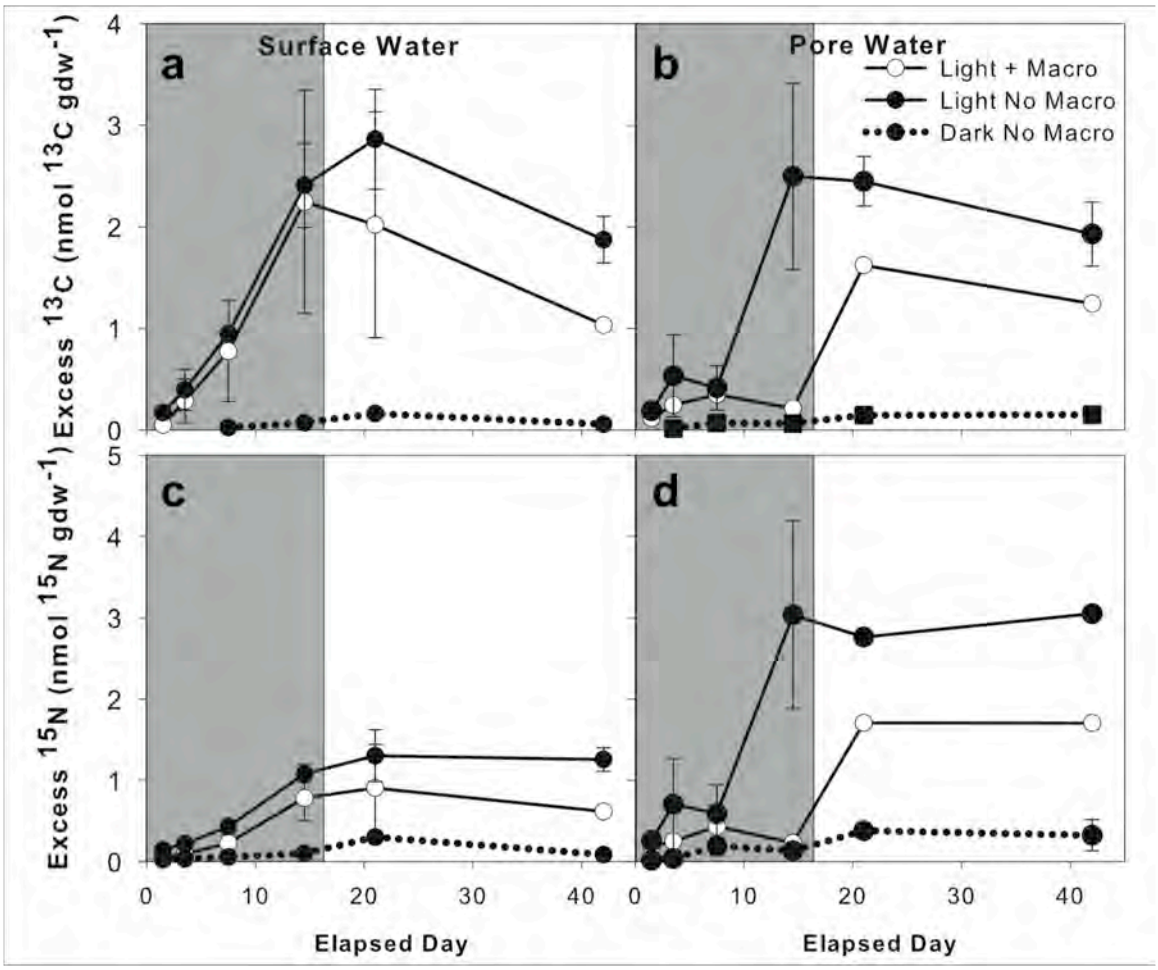
a
Surface Water
b
Pore Water
Light + Macro
Light No Macro
Dark No Macro
c
d
Excess 13C (nmol 13C gdw-1)
Excess 15N (nmol 15N gdw-1)
Elapsed Day
Elapsed Day

CHAPTER 5: FATE OF MACROALGAE IN BENTHIC SYSTEMS: CARBON AND NITROGEN CYCLING WITHIN THE MICROBIAL COMMUNITY

Amber K. Hardison[1*], Elizabeth A. Canuel[1], Iris C. Anderson[1], Bart Veuger[2]

1. Virginia Institute of Marine Science, College of William and Mary, P.O. Box 1346, Gloucester Point, VA 23062

2. Netherlands Institute of Ecology, Center for Estuarine and Marine Ecology, P.O. Box 140, 4400 AC Yerseke, The Netherlands

Submitted to *Marine Ecology Progress Series* in October, 2009.

[*] Corresponding author. Email: amber@vims.edu

ABSTRACT

High nutrient loading to coastal bays is often accompanied by the presence of bloom-forming macroalgae, which take-up and sequester large amounts of carbon (C) and nitrogen (N) while growing. This pool is temporary, however, as nuisance macroalgae exhibit a bloom and die-off cycle, influencing the biogeochemical functioning of these systems in unknown ways. The objective of this work was to trace the C and N from senescing macroalgae into relevant sediment pools. A macroalgal die-off event was simulated by the addition of freeze-dried macroalgae (*Gracilaria* spp.), pre-labeled with stable isotopes (^{13}C and ^{15}N), to sediment mesocosms. The isotopes were traced into bulk sediments and partitioned into benthic microalgal (BMA) and bacterial biomass using microbial biomarkers to quantify the uptake and retention of macroalgal C and N. Bulk sediments took up label immediately following the die-off, and macroalgal C and N were retained in the sediments for >2 weeks. Approximately 6 to 50% and 2 to 9% of macroalgal N and C, respectively, were incorporated into the sediments. Label from the macroalgae appeared in both bacterial and BMA biomarkers, suggesting that efficient shuttling of macroalgal C and N between these communities may serve as a mechanism for retention of macroalgal nutrients within the sediments.

Keywords: stable isotopes, macroalgae, benthic microalgae, bacteria, biomarker, coastal eutrophication.

INTRODUCTION

Macroalgal blooms are increasingly recognized as a symptom of eutrophication in shallow coastal systems worldwide (Duarte 1995, Valiela et al. 1997). Their proliferation has been linked to increased nutrient loadings (Hauxwell et al. 2001, Bintz et al. 2003), and in many systems macroalgae have replaced slower-growing seagrasses and perennial macrophytes (Duarte 1995, Valiela et al. 1997, Hauxwell et al. 2001, Bintz et al. 2003, McGlathery et al. 2007). In temperate systems blooms usually develop in spring and collapse in mid- to late-summer, when high temperatures and self-shading negatively affect algal productivity (Peckol & Rivers 1995, McGlathery et al. 1997, Brush & Nixon 2003, Higgins et al. 2008). The deleterious effects these blooms have on the surrounding system while alive and following die-off have been studied extensively (e.g. Sfriso et al. 1992, Raffaelli 2000, Hauxwell et al. 2001, Cummins et al. 2004, Nuzzi & Waters 2004).

Blooms can attain biomasses up to 10 kg wet weight m^{-2} (Gordon & Mccomb 1989, Pavoni et al. 1992, Valiela et al. 1992, Morand & Briand 1996, Astill & Lavery 2001). While growing, macroalgae take-up and sequester significant quantities of nutrients, often at similar magnitudes to nutrient loading, thereby serving effectively as a nutrient "filter" (Thybo-Christesen et al. 1993, 1996, Valiela et al. 1997, McGlathery et al. 2001, Pedersen et al. 2004). However, these blooms are not long-lived and, therefore, do not serve as a permanent nutrient reservoir. Although the fate of senescent macroalgal biomass is not fully known, it likely greatly impacts nutrient cycling dynamics within these systems.

Studies of macroalgal bloom decay have demonstrated rapid breakdown of biomass, resulting in release of both inorganic and organic nutrients to the water column (Buchsbaum et al. 1991, Tyler et al. 2001, Castaldelli et al. 2003, Garcia-Robledo et al. 2008), supporting phytoplankton and bacterial metabolism (Sfriso et al. 1992, Nedergaard et al. 2002). Fewer studies have focused on macroalgal decay within the sediments (Nedergaard et al. 2002, Lomstein et al. 2006, Rossi 2007, Garcia-Robledo et al. 2008), where heterotrophic bacterial densities are significantly higher than in the water column (Deming & Baross 1993, Schmidt et al. 1998, Ducklow 2000). In addition, most of the sediment studies have been conducted in low or no light environments even though light is typically available to shallow sediments where macroalgal die-offs occur and sediment biogeochemistry is largely affected by benthic microalgal (BMA) activity (Underwood & Kromkamp 1999). While nutrients associated with senescent macroalgal blooms are recycled and can have a positive feedback on phytoplankton production in the water column, nutrients released during macroalgal decay in the sediments may support benthic microalgal (BMA) and bacterial production, which could intercept the return of nutrients to the overlying water column. If shallow-water sediments, thus, behave as a nutrient "filter" the response by phytoplankton may be reduced, and benthic production could effectively buffer the system from further eutrophication. In order to better constrain the input and retention of macroalgae-associated nutrients in the sediments, we used a dual stable isotope labeling approach to track macroalgal carbon (C) and nitrogen (N) into bulk sediments and the sediment microbial community after a simulated macroalgal die-off.

METHODS

Site description Sediments and macroalgae were collected from two lagoons along the Delmarva Peninsula, USA: Hog Island Bay, Virginia (HIB) and Isle of Wight Bay, Maryland (IWB; Fig. 1). These bays are typical of temperate lagoons along the U.S. East Coast. Both are shallow, on average less than 2 m deep at mean low water, and are characterized by ephemeral macroalgal blooms (Goshorn et al. 2001, McGlathery et al. 2001, Thomsen et al. 2006); however, there are important differences between the lagoons. External loading of nutrients (N) to HIB (14 kg N ha^{-1} y^{-1}; Anderson et al. In press) is lower than for IWB (65 kg N ha^{-1} y^{-1}; Boynton et al. 1996), and as a result, macroalgal densities in HIB are lower and only dominant at select sites during brief portions of the year (this study, Boynton et al. 1996, Goshorn et al. 2001, McGlathery et al. 2001, Stanhope et al. 2009).

Experimental design A flow-through mesocosm array was set-up at the Virginia Institute of Marine Science (VIMS) Eastern Shore Laboratory (ESL) in Wachapreague, VA. Each mesocosm (0.61 m diameter x 0.61 m height) was constructed of translucent fiberglass to allow maximum light penetration (87% visual light transmission; Solar Components Corp.). Three mesocosms were filled with sediments from each lagoon in June 2006 to a depth of ~20 cm using intact sediments extruded from cores taken at the field sites. Care was taken not to include any macroalgae or visible macrofauna in the collected cores. At the ESL, the mesocosms were placed in shallow water baths under 30% shade cloth to control temperature and light. Ambient, filtered (10 μm) seawater,

pumped from the creek adjacent to the ESL, was delivered gravimetrically to each mesocosm at a rate that achieved a water column flushing time of ~2 days, similar to the flushing time observed at the study sites (Oertel 2001). The water column was circulated using mini-jet pumps (Aquatic Ecosystems, Inc.) secured on the inner tank wall ~18 cm above the sediment surface to avoid sediment resuspension. The mesocosms were equilibrated for two weeks before beginning the experiment. Water column temperature and salinity were measured in each mesocosm throughout the experiment using a YSI datasonde.

Macroalgae (*Gracilaria* spp.) were collected from both lagoons in May 2006 and returned to the laboratory for isotopic labeling. The macroalgae were cleaned of epiphytes and epifauna, rinsed with 0.7 μm filtered seawater, and placed in separate aquaria inside a greenhouse. Filtered (0.7 μm) seawater was added to each tank and aerated during labeling. The algae were starved for 10 days and then fertilized daily for 14 days with a solution containing 50 at% ^{15}N-NH_4^+ (as NH_4Cl) and 98 at% ^{13}C-HCO_3^- (as $NaHCO_3$). Rates of N and C addition were estimated to sustain tissue N at 3% and C at 25% of dry weight with a growth rate of 5% day^{-1} following the procedure of Tyler and McGlathery (2006). To insure that phosphorus (P) was not limiting, P was added to provide a 10:1 ratio of N:P. At the end of the labeling period, the algae were rinsed with filtered (0.7 μm) seawater, patted dry, and freeze-dried intact. The final isotopic enrichments of the dead macroalgae were approximately 30 at% ^{15}N and 9 at% ^{13}C. After the mesocosm equilibration period, the intact, isotopically-labeled, freeze-dried algae were added to the surface of sediments in corresponding mesocosms from HIB or IWB, at ambient densities observed in each system (HIB: 84 gdw m^{-2}; IWB: 184 gdw m^{-}

^{2}; Table 1). The intact macroalgae settled to the sediment surface, but retained some buoyancy for the first few days due to the gentle water circulation; after the second day, macroalgae were no longer visible.

Sediment sampling The mesocosms were sampled one day prior to the macroalgal additions to capture baseline conditions (Day 0) and on Days 1, 2, 7, and 14 after the additions. At each sampling, surface sediments (0-1 cm), collected using two acrylic cores (5.7 cm I.D.), were reserved for bulk (total organic C (TOC), total N (TN)), amino acid, and fatty acid analyses. Sediments from both cores were combined in pre-combusted glass jars, immediately frozen at -4ºC, and frozen at -80ºC within 3 days. The remaining sediment in the cores was placed carefully back into the holes in the mesocosm sediments. Surface sediments (0-1 cm) from a third acrylic core were collected and processed immediately for determination of bulk density and organic and water contents. Sediments were also collected for chlorophyll *a* concentrations using a cut-off syringe (1.1 cm I.D.). Samples were sectioned into 0-0.3 cm and 0.3-1.0 cm horizons, placed into 15 mL centrifuge tubes, immediately frozen at -4ºC, and analyzed within 1 month. A different region of the sediment surface was sampled each time to avoid re-sampling any sediments.

Bulk sediment analyses Sediments for percent water and organic matter (OM) were processed immediately. A known volume of sediment was weighed, dried at 40ºC and re-weighed for water content and bulk density. The dried sediments were combusted for 4 h at 500ºC to obtain ash-free dry weight (AFDW). Samples were analyzed for

benthic chlorophyll *a* concentrations according to a modification of the method of Lorenzen (1967, Pinckney et al. 1994). The sediment pellet was sonicated in 90% acetone, vortexed and extracted for 24 h at -4ºC. The supernatant was passed through a 0.45 μm filter and read on a Shimadzu UV-1601 UV Visible spectrophotometer (λ = 665, 750 nm). Chlorophyll *a* concentrations (mg m^{-2}) for the 0-0.3 and 0.3-1.0 cm sections were calculated according to the equations in Lorenzen (1967) and added to obtain concentration for 0-1 cm.

For bulk sediment TOC, TN, and isotopic measurements, sediments were freeze-dried, ground and homogenized, acidified with 10% HCl to remove inorganic C (Hedges & Stern 1984), and analyzed for $^{13}C/^{12}C$ and $^{15}N/^{14}N$ using a PDZ Europa ANCA-GSL elemental analyzer interfaced to a PDZ Europa 20-20 isotope ratio mass spectrometer (Sercon Ltd., Cheshire, UK; EA-IRMS) at the University of California at Davis Stable Isotope Facility. Stable isotope ratios for C ($R= {}^{13}C/{}^{12}C$) and N ($R={}^{15}N/{}^{14}N$) were used to calculate δ-values in units of per mil (‰):

$$\delta X\ (‰) = [(R_{sample} / R_{standard}) - 1] \times 1000 \qquad (1)$$

where X = ^{13}C or ^{15}N. Samples were expressed relative to international standards Pee Dee Belemnite (PDB, C) and atmospheric N. δX was used to calculate atom% X, which was used to calculate excess X (absolute amount of incorporated ^{13}C or ^{15}N):

$$at\%X = [100 \times R_{standard} \times ((\delta X_{sample} / 1000) + 1)] / [1 + R_{standard} \times ((\delta X_{sample} / 1000) + 1)] \qquad (2)$$

$$\text{excess X (nmol X gdw}^{-1}) = [(\text{at\%X}_{\text{sample}} - \text{at\%X}_{\text{control}})/ 100] \times [\text{concentration}_{\text{sample}}] \quad (3)$$

where, concentrations were expressed in moles C or N relative to sediment dry weight. The control (unlabeled) samples were collected on Day 0, before macroalgae were added to the mesocosms.

Hydrolyzable amino acids Hydrolyzable amino acids (HAAs) were extracted and analyzed according to the method presented in Veuger et al. (2005). Freeze dried sediment (1 g) was rinsed with 2N HCl and Milli-Q water to remove dissolved amino acids. The sediment pellet was then hydrolyzed with 6N HCl at 110ºC for 20 h. Following purification by cation exchange chromatography, amino acids were derivatized with isopropanol and pentafluoropropionic anhydride and further purified by solvent extraction. Concentrations and stable isotope ratios for C ($R= {}^{13}C/{}^{12}C$) and N ($R={}^{15}N/{}^{14}N$) of the derivatized D- and L-amino acids were measured at the Netherlands Institute of Ecology (NIOO) by gas chromatography combustion isotope ratio mass spectrometry (GC-c-IRMS), on a HP 6890 GC (Chirasil L-Val column) with a Thermo type III combustion interface and a Thermo Delta Plus IRMS. δ-and at% X values were calculated according to equations 1 and 2 and used to calculate excess X according to equation 3, where concentrations were AA concentrations expressed in moles C or N relative to sediment dry weight. Carbon isotopic values of amino acids were corrected for the C atoms added during derivatization using a mass balance approach following

(Veuger et al. 2006). The sum of concentrations of, and/or excess label incorporated in, all amino acids analyzed will be referred to as total hydrolyzable amino acids (THAA).

The ratio of excess ^{13}C or ^{15}N incorporation into D-alanine (D-Ala), a bacterial-specific amino acid, relative to L-alanine (L-Ala), an amino acid made by all organisms, was calculated as:

$$\text{D/L-Ala ratio (D/L-Ala)} = (\text{excess X in D-Ala}) / (\text{excess X in L-Ala}) \quad (4)$$

where X was ^{13}C or ^{15}N. During hydrolysis some racemization of L-Ala to D-Ala takes place, resulting in a D/L-Ala value of ~0.017 (Veuger et al. 2007b). We corrected values of excess isotope in D-Ala for this racemization according to Veuger et al. (2007a), whereas values of D/L-Ala have been left uncorrected. Instead, the D/L-Ala value of 0.017 will be indicated graphically in our results (Veuger et al. 2007b). We estimated the bacterial contribution to total ^{13}C or ^{15}N incorporation according to Veuger (2007a):

$$\text{Bacterial contribution (\%)} = [(\text{excess X D/L-Ala} - 0.017) / (\text{bacterial D/L-Ala} - 0.017)] \times 100\% \quad (5)$$

where X was ^{13}C or ^{15}N. Bacterial D/L-Ala represents the D/L-Ala abundance ratio for bacteria. The upper bound of the ratio ranges from 0.05 for Gram negative (G-) bacteria to 0.1 for Gram positive (G+) bacteria and cyanobacteria (Veuger et al. 2007b). Previous work suggests that G+ bacteria are more prominent in deeper (anaerobic) sediments

(Moriarty & Hayward 1982). Since our study used sandy photic sediments, we assumed that the contribution from G+ bacteria was negligible. Additionally, photosynthetic pigment analyses conducted on sediments from the HIB field sites suggested that cyanobacterial contribution to the microbial community was negligible (M. Waters, pers. comm.). As a result, we further assumed that their contribution to the D/L-Ala ratio of the total microbial community was negligible, and we estimated the bacterial D/L-Ala ratio for our sediments to be 0.05. This will also be indicated graphically in our results. The lower bound of D/L-Ala, when bacteria do not take up any label, is 0.017, which represents abiotic racemization of L-Ala (Veuger et al. 2007b). Thus, excess ^{13}C and ^{15}N D/L-Ala ratio values should fall between these upper and lower limits, with higher values indicating a higher bacterial contribution to the total label uptake since only bacteria incorporate label into D-Ala.

Phospholipid linked fatty acids Total fatty acids were analyzed according to a modified Bligh and Dyer (1959) method (Poerschmann & Carlson 2006, Canuel et al. 2007). Wet sediments (~12 g) were extracted using an accelerated solvent extractor system (Dionex ASE 200) adapted for in-cell silica gel chromatography. Each sample was extracted twice on the ASE: neutral lipids were collected following extraction with a 9:1 (v:v) hexane:acetone mixture at 50ºC; then polar lipids were collected following extraction with a 8:2 (v:v) methanol:chloroform solution at 80ºC. Neutral and polar lipid fractions were saponified using KOH-CH_3OH for 2h at 110ºC. Saponified samples were then extracted under basic and acidic conditions. The acid-extracted fractions were methylated with BF_3-CH_3OH to form fatty acid methyl esters (FAME). The neutral

FAME included neutral and glycolipids while the polar FAME represented the phospholipid-linked fatty acids (PLFA). FAME concentrations were measured by gas chromatography with flame ionization detection (GC-FID, DB-5 column, HP 5890) and quantified using methyl heneicosanoate as an internal standard. Peak identities were verified using reference standards as well as coupled gas chromatography mass spectrometry (GC-MSD, HP 6890). Fatty acids are designated A:BωC, where A is the total number of carbon atoms, B is the number of double bonds, and C is the position of the first double bond from the aliphatic ‘‘ω’’ end of the molecule. The prefixes ‘‘i’’ and ‘‘a’’ refer to iso- and anteiso- methyl branched fatty acids (see Canuel et al. 1995 and references therein). Stable C isotope ratios (R= $^{13}C/^{12}C$) for PLFA were measured at NIOO by Thermo GC/C-IRMS system composed of a Trace GC Ultra gas chromatograph (BPX70 column) coupled to a Delta Plus Advantage IRMS through a GC/C-III interface and were used to calculate $\delta^{13}C$ (Eq. 1) and at%^{13}C (Eq. 2). Excess ^{13}C was calculated according to equation 3, where concentrations were FAME concentrations expressed in moles C relative to dry weight. Actual PLFA isotopic values were derived from the FAME isotopic compositions by correcting for the isotopic composition of the C added during derivatization using a mass balance approach.

Field monitoring Concurrent with the mesocosm experiment, we conducted field measurements of various water column and sediment parameters at the sediment collection sites within each lagoon on two sampling dates. Triplicate measurements of water temperature and salinity were taken using a YSI datasonde during each sampling. Triplicate samples for sediment percent OM and benthic chlorophyll *a* concentrations

were also collected and measured as described above for the mesocosm experiment. We also monitored macroalgal biomass from May through October 2006. Macroalgae samples (n = 3) were collected at multiple sites across HIB (n = 9) and IWB (n = 5), by randomly tossing a cylinder (0.42 m I.D.) and collecting the total biomass contained within the cylinder. The algae was dried at 40ºC and normalized to the cylinder area for biomass (gdw m^{-2}). The triplicate biomass values for each site were averaged to obtain a site biomass estimate. Since this experiment was designed to simulate a die-off event following a bloom, we report the ranges over the growing season of maximum biomass estimates for each site as well as the mean ± SE for all sites within each lagoon (Table 1).

Data analysis We applied repeated measures analysis of variance (ANOVA) to examine the effects of lagoon (Hog Island Bay vs. Isle of Wight Bay) and time (Days 0, 1, 2, 7, 14) on the sediment parameters using the Mixed procedure in SAS 9.1 (SAS Institute Inc., Cary, NC). In all models, a first-order ante-dependence error structure (Kenward 1987) was used to model the within-subject covariance structure. We present results from the type III test of fixed effects from the ANOVA model. To further explain the effects of time, post-hoc contrasts were used to compare the isotopic enrichment parameters for Days 1 and 2 with Days 7 and 14. Unless otherwise noted, mesocosm values presented are means ± 1 SE for 3 replicates.

RESULTS

Field and experimental conditions

Temperatures and salinities in the mesocosms were similar to values measured at the field sites during June (Table 1). Between-lagoon differences in organic content and benthic chlorophyll *a* concentrations in mesocosm sediments were also similar to those observed at the field sites (Table 1). The surface (0-1 cm) sediment organic content within HIB mesocosms was approximately twice as high as in IWB. These values represent mean ± SE (n = 15) over five sampling days, since sediment OM did not accumulate in either treatment over the course of the experiment (Table 2). In addition, benthic chlorophyll *a* concentrations were lower at HIB in the surface (0-1 cm) sediments than at IWB (Table 1). Again, these values represent mean ± SE (n = 15) since benthic chlorophyll *a* did not accumulate in either treatment over the experiment (Table 2). Similarly, organic content at the field sites was higher in HIB while benthic chlorophyll *a* concentrations were higher in IWB (Table 1). Peak macroalgal biomass from May through October 2006 ranged across the field sites from 0 to 192 and 29 to 538 gdw m^{-2} for HIB (n = 9) and IWB (n = 5), respectively (Table 1). The biomass of dead macroalgae added to the mesocosms fell within these ranges; approximately twice as much algae was added to the IWB treatments to reflect the higher macroalgal densities there.

Bulk isotopes

All sediment pools displayed similar isotopic enrichment patterns. Excess ^{13}C and ^{15}N in bulk sediments (0-1 cm) are presented in Figure 2. ^{13}C appeared in

mesocosms from both lagoons immediately following the addition of macroalgae (Day 1; 22.03 ± 0.29 and 62.76 ± 21.91 nmol ^{13}C gdw^{-1} for HIB and IWB, respectively) and excess ^{13}C values were similar on Day 2. Individual replicates (not shown) peaked on either Day 7 or Day 14, which accounted for the large variance associated with the means for those days. Nevertheless, post-hoc contrasts indicated that excess ^{13}C values were significantly higher on Days 7 and 14 than on Days 1 and 2 (Table 3; Fig. 2a). Excess ^{15}N followed the same pattern as ^{13}C: label first appeared on Day 1 (28.94 ± 5.96 and 79.61 ± 36.27 nmol ^{15}N gdw^{-1} for HIB and IWB, respectively), and values peaked on either Day 7 or 14. Again, post-hoc contrasts showed higher excess ^{15}N on Days 7 and 14 than Days 1 and 2 (Table 3, Fig. 2b). There were no significant lagoon differences in either excess ^{13}C or ^{15}N for bulk sediments (Table 3). Maximum isotopic enrichments were well above natural abundance levels ($\delta^{13}C$ ~200‰, $\delta^{15}N$ > 4000‰ relative to -14 and ~40‰ for $\delta^{13}C$ and $\delta^{15}N$, respectively). Given the maximum isotopic enrichments for each mesocosm and the masses of ^{13}C and ^{15}N that were added to each mesocosm as macroalgal material, we estimated that 6.4 ± 1.4 and 35.1 ± 10.3% of the added macroalgal ^{13}C and ^{15}N were incorporated into the sediments (0-1 cm) for HIB. In IWB, 2.9 ± 0.9 and 8.8 ± 2.1% of the macroalgal ^{13}C and ^{15}N were incorporated into the sediments.

Hydrolyzable amino acids

All biomarker concentrations were normalized to sediment TOC to account for the differences in organic content between HIB and IWB. THAA concentrations were

3.22 and 3.74 μmol AA $mgOC^{-1}$ on Day 0 for HIB and IWB, respectively and decreased slightly over the course of the experiment; there were no significant lagoon differences (Table 2). THAA represented a stable fraction of the sediment organic content, comprising ~13% of the TOC and ~30% of the TN. Excess ^{13}C and ^{15}N in the THAA pool (summed excess ^{13}C and ^{15}N in the individual amino acids) were lower than in the bulk pool, but displayed similar patterns, showing enrichments well above natural abundance; for THAA, maximum values of $\delta^{13}C > 500‰$ and $\delta^{15}N > 6000‰$, whereas background values were ~ -15 and 20‰ for $\delta^{13}C$ and $\delta^{15}N$, respectively. Excess ^{13}C appeared in both lagoons immediately following the macroalgal addition (Day 1; 10.34 ± 1.43 and 26.10 ± 13.46 nmol ^{13}C gdw^{-1} for HIB and IWB, respectively) and peaked on either Day 7 or 14 (Fig. 3a). Excess ^{15}N followed the same pattern as ^{13}C: label first appeared on Day 1 (13.80 ± 2.87 and 35.73 ± 12.02 nmol ^{15}N gdw^{-1} for HIB and IWB, respectively), and values peaked on either Day 7 or 14 (Fig. 3b). There were no significant lagoon differences for excess ^{13}C or ^{15}N in THAA; however there were significant time effects. Post-hoc contrasts indicated that excess ^{13}C and ^{15}N on Days 7 and 14 were significantly higher than on Days 1 and 2 (Table 3; Fig. 3a,b). Across all sampling days, excess ^{13}C and ^{15}N in THAA accounted for approximately 40% of excess ^{13}C and ^{15}N in bulk sediments, although, the ^{13}C and ^{15}N accounted for a greater fraction of the ^{13}C and ^{15}N in bulk sediment on Days 1 and 2 than on Days 7 and 14 (Tables 3, 4).

Excess ^{13}C and ^{15}N in individual amino acids provided additional information about the fate of macroalgal C and N within the sediment microbial pool. Excess ^{13}C (corrected for hydrolysis-induced racemization) appeared in D-Ala, a bacterial-specific amino acid, on Day 1 for both bays (HIB: 0.05 ± 0.01; IWB: 0.05 ± 0.02 nmol ^{13}C gdw^{-}

^{1}) and peaked on Day 7 or 14 (Fig. 3c; Table 3). Similarly, ^{15}N appeared on Day 1 (HIB: 0.06 ± 0.03; IWB: 0.08 ± 0.04 nmol ^{15}N gdw^{-1}) and peaked on Day 7 or 14 (Fig. 3d; Table 3). While the absolute values for excess ^{13}C and ^{15}N were low on Days 1 and 2 and increased throughout the experiment, the proportion of excess ^{13}C and ^{15}N in the bulk sediment pool that appeared in D-Ala was highest on Days 1 and 2 and then decreased through Day 14 (Tables 3, 4).

Additionally, the ratio of excess isotope (either ^{13}C or ^{15}N) in D-Ala to L-Ala (D/L-Ala, not corrected for hydrolysis-induced racemization), a common amino acid found in all organisms, indicated the relative importance of bacterial uptake to total label uptake (Veuger 2005; Fig. 4). The values for excess ^{13}C and ^{15}N in D/L-Ala showed similar patterns (Fig. 4a,b). Excess ^{13}C in D/L-Ala peaked in mesocosms for both bays on Day 1 (HIB: 0.053 $\pm$ 0.006; IWB: 0.042 $\pm$ 0.007) and decreased by Day 14 (HIB: 0.031 ± 0.005; IWB: 0.029 ± 0.002; Fig 4a). This represented a decrease from Day 1 to Day 14 from ~100 to 41% bacterial ^{13}C incorporation for HIB and 77 to 36% for IWB (Fig. 4a, right axis). Excess ^{15}N in D/L-Ala peaked on Day 1 (HIB: 0.044 ± 0.008; IWB: 0.033 ± 0.005) and decreased by Day 14 (0.028 ± 0.003 for HIB; 0.027 ± 0.0004)). This represented a decrease from Day 1 to Day 14 from ~100 to 33% bacterial ^{15}N incorporation for HIB and 49 to 32% for IWB (Fig. 4b, right axis). Even though excess ^{13}C D/L-Ala in HIB showed a trend of being higher than IWB, the treatments were not significantly different; however, excess ^{15}N in D/L-Ala was significantly higher for sediments from HIB than IWB (Table 3, Fig. 4).

Phospholipid linked fatty acids

Total PLFA concentrations, normalized to sediment TOC, remained steady throughout the experiment, and sediments from both lagoons had similar concentrations (~15 mg PLFA mg OC^{-1}; Table 2). PLFA represented ~1% of the sediment TOC for HIB and IWB. Excess ^{13}C in total PLFA were lower than in bulk and THAA pools, but followed a similar pattern. Label first appeared on Day 1 (HIB: 0.77 ± 0.03; IWB: 2.14 ± 1.34 nmol ^{13}C gdw^{-1}) and peaked on Day 7 or 14 (Fig. 5a). There were no lagoon effects, but excess ^{13}C values were significantly lower on Days 1 and 2 than on Days 7 and 14 (Table 3; Fig. 5a). Over the course of the experiment, excess ^{13}C in PLFA consistently accounted for ~3% of excess ^{13}C in bulk sediments for both lagoons (Tables 3, 4). Linear regressions of excess ^{13}C in PLFA with excess ^{13}C in THAA showed good agreement (r^2 = 0.72, p = 0.001 HIB; r^2 = 0.96, p < 0.001 IWB) suggesting that microbial biomarkers in each compound class tracked one another.

Excess ^{13}C in groups of individual PLFA provided additional information about the importance of specific sediment microbial pools in the cycling of macroalgal C and N. Excess ^{13}C appeared in branched odd fatty acids (BrFA: summed excess ^{13}C in iso- and anteiso- $C_{13:0}$, $C_{15:0}$, $C_{17:0}$, and $C_{19:0}$), representative of heterotrophic bacterial biomass (Perry et al. 1979), on Day 1 for both bays (HIB: 0.03 ± 0.02; IWB: 0.12 ± 0.04 nmol ^{13}C gdw^{-1}) and peaked on Day 7 or 14 (Fig. 5b; Table 3). Values of excess ^{13}C in BrFA were linearly related to excess ^{13}C in D-ala, another bacterial-specific biomarker (r^2 = 0.95, p < 0.0001 HIB; r^2 = 0.93, p < 0.0001 IWB). Excess ^{13}C also appeared in polyunsaturated fatty acids (PUFA: summed excess ^{13}C in $C_{20:4}$, $C_{20:5}$, $C_{22:5}$, and $C_{22:6}$), representative of algal biomass (Volkman et al. 1998), on Day 1 (HIB: 0.03 ± 0.01;

IWB: 0.06 ± 0.04 nmol ^{13}C gdw^{-1}) and peaked on Day 7 or 14 (Fig. 5c; Table 3). Overall, ^{13}C enrichments in PUFA were lower than for BrFA. Linear regressions of excess ^{13}C in BrFA and PUFA suggested that this trend was consistent across all time points and the fatty acid groups showed good agreement ($r^2 = 0.92$, $p < 0.0001$ HIB; $r^2 = 0.86$, $p < 0.0001$ IWB).

DISCUSSION

We conducted this experiment to simulate the die-off of a macroalgal bloom, an annual event common to many coastal lagoons worldwide (Sfriso et al. 1992, Valiela et al. 1997). We selected field sites within two lagoons representative of coastal bays along the east coast of the United States for collecting sediment and macroalgae. Both sites had sandy sediments, were ~1 m deep at mean low water and were exposed to similar light levels. Although the organic content of the sediments differed significantly between the bays, the values still fell within a relatively narrow range of 0.6 – 3.8%, typical of many coastal bays. Differences in benthic chlorophyll *a* concentrations in the mesocosms, which were consistent with differences in the field, were more pronounced than organic content and likely influenced the processing of macroalgal ^{13}C and ^{15}N in the sediments.

Since this experiment investigated the fate of dead macroalgae, we freeze-dried the macroalgae prior to adding it to the mesocosms. Most macroalgal decomposition studies have used frozen macroalgae (Buchsbaum et al. 1991, Nedergaard et al. 2002, Castaldelli et al. 2003, Garcia-Robledo et al. 2008) or buried live macroalgae (Franke et al. 2006, Rossi 2007); however, we did not freeze the macroalgae for logistical purposes, and we did not feel that burial of the algae in the sediments adequately represented the natural die-off process. Numerous phytoplankton fate studies have used freeze-dried material (Moodley et al. 2000, Aberle & Witte 2003, Witte et al. 2003). After one week, macroalgae were no longer visible in our mesocosms, indicating that all of the macroalgae was degraded, remineralized, or respired (either in the water column or

sediments), so we are confident that freeze-drying was appropriate for the purposes of our study.

Label incorporation into bulk sediments

Previous studies have shown that some decomposition of macroalgae occurs in the water column, resulting in release of inorganic and organic nutrients, consumption of dissolved oxygen, and release of toxic sulfides. These processes have been associated with phytoplankton blooms, fish and other faunal kills as well as seagrass declines (Buchsbaum et al. 1991, Sfriso et al. 1992, Hauxwell et al. 2001, Nedergaard et al. 2002, Cummins et al. 2004). The fate of macroalgal biomass deposited to the sediments, however, is less clear. Our bulk sediment isotope data suggest that a fraction of macroalgal-derived ^{13}C and ^{15}N appeared in the sediments; however, less label appeared in IWB than in HIB sediments, and less ^{13}C appeared than ^{15}N for both lagoons. In HIB, maximum values of ~6 and 35% of macroalgal ^{13}C and ^{15}N were observed in the sediments. In IWB ~3 and 9% of macroalgal ^{13}C and ^{15}N were incorporated into the sediments. We were careful not to include visible macroalgal fragments in our samples, so labeling in the sediments should have represented either detrital (macroalgal) POM or DOM or transfer of ^{13}C and ^{15}N to other active pools within the sediments, rather than direct sampling of macroalgal fragments. This is further supported by the uncoupling of ^{13}C and ^{15}N transferred to the sediments, which suggests that macroalgal C and N were transferred disproportionately. We believe that these stoichiometric and lagoonal differences in C and N transfer were related to microbial processes, as discussed below.

Sediments showed immediate enrichment in macroalgal ^{13}C and ^{15}N (Day 1), which increased over the course of the experiment. While the general trends were similar, replicates were variable suggesting heterogeneity within and/or across mesocosms. Some showed highest enrichments on Day 7; others did not peak until Day 14. This variability likely resulted from patchiness associated with the bloom deposition in our mesocosms or heterogeneity in the sediment microbial communities. Similar patchiness has been observed in field studies (Holmquist 1997, Sfriso & Marcomini 1999, McGlathery et al. 2001). Despite the observed variability, our statistical analyses confirmed that bulk isotopic enrichments at the end of the experiment (Days 7, 14) were higher than at the beginning of the experiment (Days 1, 2) for both lagoons, demonstrating accumulation and retention of macroalgal ^{13}C and ^{15}N in the sediments following the simulated die-off.

Patterns of ^{13}C and ^{15}N enrichment in THAA and PLFA tracked the bulk sediment enrichments. These pools showed immediate isotopic enrichment on Day 1 and peak enrichments on Days 7 and 14. The labeled THAA and PLFA in sediments collected on Days 1 and 2 likely represented rapid uptake by microbes, although some microscopic macroalgal detritus may have remained after removal of all visible fragments. The isotopically-labeled PLFA observed in the sediments on Days 7 and 14 most likely represented living microbial biomass given rapid rates of PLFA turnover (Parkes 1987). THAA on Days 7 and 14 may have included macroalgal detritus, but we observed no visible fragments of macroalgae by then, suggesting that the biomass had been decomposed.

Bacterial incorporation of macroalgal label

Overall, a smaller fraction of macroalgal ^{13}C appeared in the bulk sediments than ^{15}N for both lagoons. This is consistent with expected preferential uptake of N by the microbial community since N is typically the element limiting microbial production and, therefore, likely to be taken up efficiently, while C is relatively easily lost by respiration. More directly, the isotopic enrichments of specific amino acids and fatty acids provided an explicit indication of the communities in the sediments that were taking up macroalgal ^{13}C and ^{15}N. Enrichment of D-Ala and BrFA clearly demonstrated transfer of macroalgal label to bacterial biomass through decomposition. The correlations between excess ^{13}C in D-Ala and BrFA provided strong evidence for bacterial ^{13}C uptake, corroborating their use as two independent proxies for bacterial biomass. Appearance of the labels on Day 1 showed an immediate response by bacteria to the addition of fresh OM. This rapid response has been shown in previous studies investigating decomposition of macroalgae (Buchsbaum et al. 1991, Nedergaard et al. 2002, Castaldelli et al. 2003, Franke et al. 2006). For example, just minutes after macroalgae were added to sediments, Franke and others (2006) measured oxygen consumption rates nearly 18 times higher in sediments with macroalgae than in nearby sediments without macroalgae. While others have investigated metabolic responses to the addition of macroalgae, our study is the first to demonstrate explicitly the incorporation of macroalgal C and N into sediment bacterial biomass following a simulated die-off event.

Not only did the bacteria in our study respond rapidly to the addition of macroalgal biomass, but the bacterial biomarkers also showed prolonged enrichment of

^{13}C and ^{15}N throughout the two-week experiment. The prolonged enrichment of bacterial biomarkers may reflect incorporation into a refractory pool after cell death, which accumulated in the sediments. However, the PLFA were not likely part of the detrital pool given the rapid turnover of PLFA after cell death (Parkes 1987, Veuger et al. 2006), and at the timescale of our experiment, we believe accumulation of labeled detrital (bacterial) amino acids was negligible (Veuger et al. 2006). Instead, we believe the continued enrichment of the bacterial biomarkers on Days 7 and 14 is consistent with microbially-mediated decomposition of macroalgae. The isotopic labels could persist even longer in the sediments if recycling of macroalgal detritus by bacteria was coupled with BMA metabolism (next section). Regardless of the mechanism(s) responsible for the high isotopic enrichments in the bacterial pool, macroalgal ^{13}C and ^{15}N clearly persisted in the sediments for >2 weeks following the simulated die-off.

Interestingly, there were no significant between-lagoon differences in excess isotope levels in bulk, THAA, or PLFA even though twice as much dead macroalgae was added to the IWB mesocosms. We believe that the lower relative enrichments in IWB may be explained by slower decomposition rates. The rates and extent of decomposition are influenced by a variety of environmental, biological, and physical factors (Wakeham & Canuel 2006). In addition to differences in the amount of macroalgal biomass added to the treatments, the distinguishing characteristic of the lagoon treatments was the sediments, and by default, perhaps the microbial communities within the sediments. It is possible that the IWB bacteria that processed the macroalgal biomass may have been limited in a way that the HIB bacteria were not. For example, some studies have determined hydrolysis to be the rate-limiting step in decomposition (Arnosti 2004 and

references therein), either because hydrolysis rates are slow or because the organism required to produce a specific enzyme to break down specific macromolecules are absent or in low abundance. Regardless of the mechanism responsible for limiting retention of macroalgal ^{13}C and ^{15}N in IWB sediments, this difference could profoundly affect system-wide nutrient cycling. Since macroalgae in both lagoon treatments had visibly disappeared within days following the additions, more macroalgal decomposition likely took place in the IWB water column, which could promote phytoplankton growth and further eutrophication of the system.

Bacterial-BMA coupling

The ratio of isotopic enrichments in D/L-Ala provides information on the relative contribution of bacteria and algae to total label incorporation. High values of D/L-Ala indicate a larger contribution from bacteria relative to algae, while the minimum value (0.017) corresponds to zero bacterial uptake, or 100% algal label. Excess ^{13}C and ^{15}N in D/L-Ala was highest for both lagoons on Days 1 and 2 and then decreased throughout the experiment (Fig. 4), suggesting that algae contributed relatively more to total label uptake over time. Because we cannot exclude the possibility that macroalgal detritus may have contributed to the labeled L-Ala pools on Day 14, we estimated maximum contributions from BMA by Day 14 of ~60% of microbial ^{13}C uptake and ~68% of microbial ^{15}N uptake (Fig. 4a,b, right axes). The D/L-Ala ratios for IWB were consistently lower than for HIB until they converged on Day 14, indicating a proportionately lower bacterial contribution to total microbial uptake in IWB. This difference was corroborated by

benthic chlorophyll *a* levels in IWB, which were 4- to 5-times the levels in HIB, indicating a larger BMA population in IWB. The fact that these differences were present on Day 1 suggested the likelihood that BMA directly took up remineralized nutrients resulting from bacterial decomposition from the water column and/or that label was rapidly transferred from sediment bacterial to BMA. Lastly, ^{13}C enrichment in C_{20} and C_{22} PUFA provided a direct indication of label incorporation by BMA. We observed an initial labeling of the PUFA pool followed by a peak on Day 7 or 14. All of the known BMA-specific fatty acids are also present in many genera of macroalgae, including *Gracilaria* (Dembitsky et al. 1991, Khotimchenko 2005). Therefore, the C_{20} PUFA that we used may have represented macroalgal detritus on Days 1 and 2. However, given the low excess ^{13}C in PUFA on days 1 and 2 (Fig. 5c) as well as rapid PLFA turnover rates, the PUFA on Days 7 and 14 most likely represented living BMA rather than macroalgae. Together, these biomarkers supported incorporation of macroalgal ^{13}C and ^{15}N into BMA biomass.

In figure 6, we propose the mechanisms underlying the relationship between BMA, sediment bacteria, and macroalgal detritus in our experimental system. Results from this experiment suggest that macroalgal biomass was decomposed and taken up by heterotrophic bacteria in the surface sediments as dissolved organic matter (DOM). Bacteria incorporated some of the ^{13}C and ^{15}N into biomass and mineralized the remainder into the sediment pore water as $DI^{13}C$ and $DI^{15}N$. Bacteria may have also re-incorporated $DI^{15}N$ if the N content of the DOM substrate was insufficient to meet the bacterial metabolic demands (Goldman & Dennett 2000, Veuger et al. 2007a). BMA incorporated $DI^{13}C$ and $DI^{15}N$ from the pore water as well as the overlying water column,

where macroalgal detritus was also decomposing. BMA have also been shown to take up dissolved organic N directly (Nilsson & Sundback 1996). To complete the cycle, bacteria then recycled labeled BMA detritus and/or extrapolymeric substances (EPS) exuded by the BMA (Smith & Underwood 1998, Middelburg et al. 2000, Veuger et al. 2007a, Evrard et al. 2008). Good agreement between bacterial and BMA fatty acids supports a tight coupling between these communities (r^2 = 0.93 and 0.92 for HIB and IWB), although, bacteria have also been shown to recycle nutrients independent of BMA by reincorporating their own degradation products (Veuger 2006, 2007a). Overall, once the macroalgal biomass is hydrolyzed to DOM, it is effectively shuttled back and forth between bacteria and BMA in organic and inorganic forms. This efficient recycling of ^{13}C and ^{15}N has been observed in other studies (Middelburg et al. 2000, Veuger et al. 2007a). Numerous studies have shown BMA production to be limited when live macroalgae are present in dense accumulations, presumably due to light limitation at the sediment surface (Astill & Lavery 2001, McGlathery et al. 2001, Hardison et al. *In Prep*). However, our results suggest that once the light limitation is relieved after macroalgae die, 5 to 9% of C and 6 to 50% of N originally present as macroalgal biomass is transferred to the sediments and "stored" (temporarily) as microbial biomass. Even though macroalgal distributions may be patchy, the work of Franke and colleagues (2006) has shown that the effects of a macroalgal die-off may be expansive in the sediments of some systems. In their study, macroalgal-DOM was distributed well beyond the deposition location in systems that experienced advective flow, fueling heterotrophic bacteria throughout the sediments.

Summary and implications for eutrophied systems

The extent to which sediments act as a sink for macroalgal C and N depends largely on the amount of biomass transferred to the sediments as well as recycling processes within the sediments. In our experiment, less than half of the macroalgae was incorporated into the sediments from HIB, and even less for sediments from IWB. The isolation of our mesocosms from the hydrodynamic regime typically found in the environment may have biased the amount of macroalgal biomass that was transferred to the sediments relative to what occurs in the environment. On the one hand, we may have overestimated transfer of macroalgal material to the sediments if wave and tidal action disperse the macroalgal detritus and decrease deposition onto the sediment surface. On the other hand, our estimate may have been conservative if hydrodynamic mixing of the sediment surface entrains macroalgae into the sediments. In either case, it is clear from other laboratory and field studies that some fraction of macroalgae associated with blooms is transferred to the sediments following die-off (Sfriso et al. 1992, Lomstein et al. 2006, Garcia-Robledo et al. 2008). We suggest that further research investigating the influence of hydrodynamic forcings and sediment resuspension on macroalgal decomposition in the sediments is warranted. Nevertheless, our study suggests that uptake and recycling of C and N by BMA and bacteria within the sediments may serve as a temporary reservoir for a fraction of the C and N that was previously stored as macroalgal biomass. While bacteria are the primary agents of decomposition of the macroalgae, BMA intercept the return of nutrients to the water column, thereby diminishing phytoplankton uptake and a positive feedback to further eutrophication.

ACKNOWLEDGEMENTS

This research was supported by the National Science Foundation (VCR-LTER project DEB 0080381 and DEB 0621014; DEB Ecosystems 0542645 to I.C.A. and E.A.C.), the European Association of Organic Geochemists (Shell Travel Award to A.K.H.) and the Environmental Protection Agency (STAR FP916722010 to A.K.H.). The EPA has not officially endorsed this publication and the views expressed herein may not reflect the views of the EPA. This work would not have been possible without the help of M. Luckenbach, S. Fate, and R. Bonniwell at the VIMS ESL, J. Stanhope, H. Walker, B. Neikirk, E. Lerberg, C. Funkey, P. Littreal, and R. Bushnell at VIMS, and M. Houtekamer and P. v. Rijswijk at NIOO.

LITERATURE CITED

Aberle N, Witte U (2003) Deep-sea macrofauna exposed to a simulated sedimentation event in the abyssal NE Atlantic: in situ pulse-chase experiments using C-13-labelled phytodetritus. Marine Ecology-Progress Series 251:37-47

Anderson IC, Stanhope JW, Hardison AK, McGlathery KJ (In press) Sources and fates of nitrogen in Virginia Coastal Bays. In: Kennish MJ, Paerl HW (eds) Coastal Lagoons: Critical Habitats of Environmental Change. Taylor and Francis

Arnosti C (2004) Speed bumps and barricades in the carbon cycle: substrate structural effects on carbon cycling. Marine Chemistry 92:263-273

Astill H, Lavery PS (2001) The dynamics of unattached benthic macroalgal accumulations in the Swan-Canning Estuary. Hydrological Processes 15:2387-2399

Bintz JC, Nixon SW, Buckley BA, Granger SL (2003) Impacts of temperature and nutrients on coastal lagoon plant communities. Estuaries 26:765-776

Bligh EG, Dyer WJ (1959) A Rapid Method of Total Lipid Extraction and Purification. Canadian Journal of Biochemistry and Physiology 37:911-917

Boynton WR, Hagy JD, Murray L, Stokes C, Kemp WM (1996) A comparative analysis of eutrophication patterns in a temperate coastal lagoon. Estuaries 19:408-421

Brush MJ, Nixon SW (2003) Biomass layering and metabolism in mats of the macroalga Ulva lactuca L. Estuaries 26:916-926

Buchsbaum R, Valiela I, Swain T, Dzierzeski M, Allen S (1991) Available and refractory nitrogen in detritus of coastal vascular plants and macroalgae. Marine Ecology Progress Series 72:131-143

Canuel EA, Freeman KH, Wakeham SG (1995) Seasonal-Changes in the Sources of Organic-Matter Delivered to a Coastal Sediment - a Gc-Irms Approach. Abstracts of Papers of the American Chemical Society 210:70-Geoc

Canuel EA, Spivak AC, Waterson EJ, Duffy JE (2007) Biodiversity and food web structure influence short-term accumulation of sediment organic matter in an experimental seagrass system. Limnology and Oceanography 52:590-602

Castaldelli G, Welsh DT, Flachi G, Zucchini G, Colombo G, Rossi R, Fano EA (2003) Decomposition dynamics of the bloom forming macroalga Ulva rigida C. Agardh determined using a C-14-carbon radio-tracer technique. Aquatic Botany 75:111-122

Cummins SP, Roberts DE, Zimmerman KD (2004) Effects of the green macroalga Enteromorpha intestinalis on macrobenthic and seagrass assemblages in a shallow coastal estuary. Marine Ecology-Progress Series 266:77-87

Dembitsky VM, Pechenkinashubina EE, Rozentsvet OA (1991) Glycolipids and Fatty-Acids of Some Seaweeds and Marine Grasses from the Black-Sea. Phytochemistry 30:2279-2283

Deming JW, Baross JA (1993) The Early Diagenesis of Organic Matter: Bacterial Activity. In: Engel MH, Macko SA (eds) Organic Geochemistry. Plenum Press, New York, p 119-144

Duarte CM (1995) Submerged Aquatic Vegetation in Relation to Different Nutrient Regimes. Ophelia 41:87-112

Ducklow H (2000) Bacterial Production and Biomass in the Oceans. In: Kirchman DL (ed) Microbial Ecology of the Oceans. Wiley-Liss, Inc., New York, p 85-120

Evrard V, Cook PL, Veuger B, Huetel M, Middelburg J (2008) Tracing carbon and nitrogen incorporation and pathways in the microbial community of a photic subtidal sand. Aquatic Microbial Ecology 53:257-269

Franke U, Polerecky L, Precht E, Huettel M (2006) Wave tank study of particulate organic matter degradation in permeable sediments. Limnology and Oceanography 51:1084-1096

Garcia-Robledo E, Corzo A, de Lomas JG, van Bergeijk SA (2008) Biogeochemical effects of macroalgal decomposition on intertidal microbenthos: a microcosm experiment. Marine Ecology-Progress Series 356:139-151

Goldman JC, Dennett MR (2000) Growth of marine bacteria in batch and continuous culture under carbon and nitrogen limitation. Limnology and Oceanography 45:789-800

Gordon DM, Mccomb AJ (1989) Growth and Production of the Green-Alga Cladophora-Montagneana in a Eutrophic Australian Estuary and Its Interpretation Using a Computer-Program. Water Research 23:633-645

Goshorn D, McGinty M, Kennedy C, Jordan C, Wazniak C, Schwenke K, Coyne K (2001) An examination of benthic macroalgae communities as indicators of nutrients in middle atlantic coastal estuaries -- Maryland component Final Report 1998-1999, Maryland Department of Natural Resources, Annapolis, MD

Hardison AK, Anderson IC, Canuel EA, Tobias C, Veuger B (In Prep) Carbon and nitrogen dynamics in shallow photic systems: Interactions between macro- and microalgal communities.

Hauxwell J, Cebrian J, Furlong C, Valiela I (2001) Macroalgal canopies contribute to eelgrass (Zostera marina) decline in temperate estuarine ecosystems. Ecology 82:1007-1022

Hedges JI, Stern JH (1984) Carbon and Nitrogen Determinations of Carbonate-Containing Solids. Limnology and Oceanography 29:657-663

Higgins SN, Hecky RE, Guildford SJ (2008) The collapse of benthic macroalgal blooms in response to self-shading. Freshwater Biology 53:2557-2572

Holmquist JG (1997) Disturbance and gap formation in a marine benthic mosaic: influence of shifting macroalgal patches on seagrass structure and mobile invertebrates. Marine Ecology-Progress Series 158:121-130

Kenward MG (1987) A Method for Comparing Profiles of Repeated Measurements. Applied Statistics-Journal of the Royal Statistical Society Series C 36:296-308

Khotimchenko SV (2005) Lipids from the marine alga Gracilaria verrucosa. Chemistry of Natural Compounds 41:285-288

Lomstein BA, Guldberg LB, Neubauer ATA, Hansen J, Donnelly A, Herbert RA, Viaroli P, Giordani G, Azzoni R, de Wit R, Finster K (2006) Benthic decomposition of Ulva lactuca: A controlled laboratory experiment. Aquatic Botany 85:273-283

Lorenzen CJ (1967) Determination of Chlorophyll and Pheo-Pigments - Spectrophotometric Equations. Limnology and Oceanography 12:343-&

McGlathery KJ, Anderson IC, Tyler AC (2001) Magnitude and variability of benthic and pelagic metabolism in a temperate coastal lagoon. Marine Ecology-Progress Series 216:1-15

McGlathery KJ, Krause-Jensen D, Rysgaard S, Christensen PB (1997) Patterns of ammonium uptake within dense mats of the filamentous macroalga Chaetomorpha linum. Aquatic Botany 59:99-115

McGlathery KJ, Pedersen MF, Borum J (1996) Changes in intracellular nitrogen pools and feedback controls on nitrogen uptake in Chaetomorpha linum (chlorophyta). Journal of Phycology 32:393-401

McGlathery KJ, Sundback K, Anderson IC (2007) Eutrophication in shallow coastal bays and lagoons: the role of plants in the coastal filter. Marine Ecology-Progress Series 348:1-18

Middelburg JJ, Barranguet C, Boschker HTS, Herman PMJ, Moens T, Heip CHR (2000) The fate of intertidal microphytobenthos carbon: An in situ C-13-labeling study. Limnology and Oceanography 45:1224-1234

Moodley L, Boschker HTS, Middelburg JJ, Pel R, Herman PMJ, de Deckere E, Heip CHR (2000) Ecological significance of benthic foraminifera: C-13 labelling experiments. Marine Ecology-Progress Series 202:289-295

Morand P, Briand X (1996) Excessive growth of macroalgae: A symptom of environmental disturbance. Botanica Marina 39:491-516

Moriarty DJW, Hayward AC (1982) Ultrastructure of Bacteria and the Proportion of Gram-Negative Bacteria in Marine-Sediments. Microbial Ecology 8:1-14

Nedergaard RI, Risgaard-Petersen N, Finster K (2002) The importance of sulfate reduction associated with Ulva lactuca thalli during decomposition: a mesocosm approach. Journal of Experimental Marine Biology and Ecology 275:15-29

Nilsson C, Sundback K (1996) Amino acid uptake in natural microphytobenthic assemblages studied by microautoradiography. Hydrobiologia 332:119-129

Nuzzi R, Waters RM (2004) Long-term perspective on the dynamics of brown tide blooms in Long Island coastal bays. Harmful Algae 3:279-293

Oertel GF (2001) Hypsographic, hydro-hypsographic and hydrological analysis of coastal bay environments, Great Machipongo Bay, Virginia. Journal of Coastal Research 17:775-783

Parkes RJ (1987) Analysis of microbial communities within sediments using biomarkers. In: Hetcher M, Gray RTG, Jones JG (eds) Ecology of Microbial Communities. Cambridge University Press, Cambridge, p 147-177

Pavoni B, Marcomini A, Sfriso A, Donazzolo R, Orio AA (1992) Changes in an Estuarine Ecosystem - the Lagoon of Venice as a Case-Study. Acs Symposium Series 483:287-305

Peckol P, Rivers JS (1995) Physiological-Responses of the Opportunistic Macroalgae Cladophora-Vagabunda (L) Vandenhoek and Gracilaria-Tikvahiae (Mclachlan) to Environmental Disturbances Associated with Eutrophication. Journal of Experimental Marine Biology and Ecology 190:1-16

Pedersen MF, Nielsen SL, Banta GT (2004) Interactions between vegetation and nutrient dynamics in coastal marine ecosystems: An introduction. In: Nielsen SL, Banta GT, Pedersen MF (eds) Estuarine nutrient cycling: The influence of primary producers. Kluwer Academic Publishers, p 1-16

Perry GJ, Volkman JK, Johns RB, Bavor HJ (1979) Fatty-Acids of Bacterial Origin in Contemporary Marine-Sediments. Geochimica et Cosmochimica Acta 43:1715-1725

Pinckney J, Papa R, Zingmark R (1994) Comparison of High-Performance Liquid-Chromatographic, Spectrophotometric, and Fluorometric Methods for Determining Chlorophyll a Concentrations in Estuarine Sediments. Journal of Microbiological Methods 19:59-66

Poerschmann J, Carlson R (2006) New fractionation scheme for lipid classes based on "in-cell fractionation" using sequential pressurized liquid extraction. Journal of Chromatography A 1127:18-25

Raffaelli D (2000) Interactions between macro-algal mats and invertebrates in the Ythan estuary, Aberdeenshire, Scotland. Helgoland Marine Research 54:71-79

Rossi F (2007) Recycle of buried macroalgal detritus in sediments: use of dual-labelling experiments in the field. Marine Biology 150:1073-1081

Schmidt JL, Deming JW, Jumars PA, Keil RG (1998) Constancy of bacterial abundance in surficial marine seciments. Limnology and Oceanography 43:976-982

Sfriso A, Marcomini A (1999) Macrophyte production in a shallow coastal lagoon. Part II: Coupling with sediment, SPM and tissue carbon, nitrogen and phosphorus concentrations. Marine Environmental Research 47:285-309

Sfriso A, Pavoni B, Marcomini A, Raccanelli S, Orio AA (1992) Particulate Matter Deposition and Nutrient Fluxes onto the Sediments of the Venice Lagoon. Environmental Technology 13:473-483

Smith DJ, Underwood GJC (1998) Exopolymer production by intertidal epipelic diatoms. Limnology and Oceanography 43:1578-1591

Stanhope JW, Anderson IC, Reay WG (2009) Base flow nutrient discharges from lower Delmarva Peninsula watersheds of Virginia. Journal of Environmental Quality 38:2070-2083

Thomsen MS, Gurgel CFD, Fredericq S, McGlathery KJ (2006) Gracilaria vermiculophylla (Rhodophyta, Gracilariales) in Hog Island Bay, Virginia: A cryptic alien and invasive macroalga and taxonomic correction. Journal of Phycology 42:139-141

Thybo-Christesen M, Rasmussen MB, Blackburn TH (1993) Nutrient Fluxes and Growth of Cladophora-Sericea in a Shallow Danish Bay. Marine Ecology-Progress Series 100:273-281

Tyler AC, McGlathery KJ (2006) Uptake and release of nitrogen by the macroalgae Gracilaria vermiculophylla (Rhodophyta). Journal of Phycology 42:515-525

Tyler AC, McGlathery KJ, Anderson IC (2001) Macroalgae mediation of dissolved organic nitrogen fluxes in a temperate coastal lagoon. Estuarine Coastal and Shelf Science 53:155-168

Underwood GJC, Kromkamp J (1999) Primary production by phytoplankton and microphytobenthos in estuaries. Advances in Ecological Research, Vol 29 29:93-153

Valiela I, Foreman K, Lamontagne M, Hersh D, Costa J, Peckol P, Demeoandreson B, Davanzo C, Babione M, Sham CH, Brawley J, Lajtha K (1992) Couplings of Watersheds and Coastal Waters - Sources and Consequences of Nutrient Enrichment in Waquoit Bay, Massachusetts. Estuaries 15:443-457

Valiela I, McClelland J, Hauxwell J, Behr PJ, Hersh D, Foreman K (1997) Macroalgal blooms in shallow estuaries: Controls and ecophysiological and ecosystem consequences. Limnology and Oceanography 42:1105-1118

Veuger B, Eyre BD, Maher D, Middelburg JJ (2007a) Nitrogen incorporation and retention by bacteria, algae, and fauna in a subtropical intertidal sediment: An in situ N-15-labeling study. Limnology and Oceanography 52:1930-1942

Veuger B, Middelburg JJ, Boschker HTS, Houtekamer M (2005) Analysis of N-15 incorporation into D-alanine: A new method for tracing nitrogen uptake by bacteria. Limnology and Oceanography-Methods 3:230-240

Veuger B, Middelburg JJ, Boschker HTS, Houtekamer M (2007b) Update of "Analysis of N-15 incorporation into D-alanine: A new method for tracing nitrogen uptake by bacteria" (Veuger et al. 2005, Limnol. Oceanogr. Methods 3: 230-240). Limnology and Oceanography-Methods 5:192-194

Veuger B, van Oevelen D, Boschker HTS, Middelburg JJ (2006) Fate of peptidoglycan in an intertidal sediment: An in situ C-13-labeling study. Limnology and Oceanography 51:1572-1580

Volkman JK, Barrett SM, Blackburn SI, Mansour MP, Sikes EL, Gelin F (1998) Microalgal biomarkers: A review of recent research developments. Organic Geochemistry 29:1163-1179

Wakeham SG, Canuel EA (2006) Degradation and preservation of organic matter in marine seciments. In: Volkman JK (ed) Handbook of Environmental Chemistry, Vol 2, Part N. Springer-Verlag, p 295-321

Witte U, Aberle N, Sand M, Wenzhofer F (2003) Rapid response of a deep-sea benthic community to POM enrichment: an in situ experimental study. Marine Ecology-Progress Series 251:27-36

Table 5-1: Environmental parameters measured in the field and in the mesocosms. Except for peak macroalgal biomass, field values were combined for 2 sampling dates in June 2006 at 3 sites in each lagoon (n = 6). Mesocosm values are presented as the mean (± SE) across all 5 sampling days during experiment (n = 15). Peak macroalgal biomass values for the field correspond to the maximum biomass measured from May through October 2006 at multiple sites across HIB (n = 9) and IWB (n = 5). Mesocosm values correspond to the mass of freeze-dried, labeled macroalgae added to each mesocosm (n = 3).

	Field		Mesocosm	
Parameter	**HIB**	**IWB**	**HIB**	**IWB**
Temperature (°C)	28.3 (0.1)	28.6 (0.2)	22.2 (1.2)	23.0 (1.2)
Salinity (psu)	31.3 (0.01)	29.3 (0.08)	30.1 (0.7)	29.9 (0.7)
Sediment organic matter (%)	2.59 (0.77)	0.77 (0.10)	2.01 (0.18)	1.04 (0.07)
Chlorophyll *a* (mg Chl *a* m^{-2})	56.2 (14.5)	89.5 (19.7)	267 (3)	109 (7)
Peak Macroalgal Biomass (gdw m^{-2})				
- Range	0 -192	29 - 538	n/a	n/a
- Mean (SE)	52 (24)	176 (98)	83 (2)	183 (2)

Table 5-2: Bulk sediment characterization parameters and statistical results from repeated measures ANOVA.

Values for bulk sediment parameters as mean (± SE), n=3. P values are indicated for repeated measures ANOVA used to test for differences in lagoons over time for various sediment pools. Significant p values are indicated in bold.

		Experimental Day					ANOVA		
Parameter	**Lagoon**	**0**	**1**	**2**	**7**	**14**	**lagoon**	**time**	**interaction**
Organic matter	HIB	1.82 (0.48)	2.52 (0.70)	1.84 (0.11)	1.75 (0.31)	2.12 (0.22)	**0.0008**	0.6708	0.6958
(%)	IWB	1.20 (0.26)	0.93 (0.21)	0.96 (0.04)	0.89 (0.12)	1.22 (0.14)			
Chlorophyll *a*	HIB	15.0 (2.5)	29.0 (3.4)	28.1 (8.6)	29.0 (6.8)	33.7 (8.6)	**0.0010**	0.3187	0.9870
(mg Chl *a* $m^{-2)}$	IWB	93.7 (7.7)	108 (24)	112 (21)	110 (4)	124 (16)			
THAA	HIB	3.44	3.95 (0.70)	2.29 (0.04)	1.91 (0.17)	2.24 (0.11)	0.7074	**0.0023**	0.3591
(mmol AA $mgOC^{-1}$)	IWB	3.74	3.28 (0.28)	2.90 (0.15)	2.16 (0.13)	2.35 (0.27)			
PLFA	HIB	14.5 (5.4)	13.9 (3.6)	9.13 (1.78)	19.7 (1.5)	14.9 (1.9)	0.7033	0.1893	0.4235
(mg PLFA $mgOC^{-1}$)	IWB	15.7 (2.3)	11.9 (0.7)	14.2 (3)	13.9 (1.2)	19.5 (5.0)			

Table 5-3: Statistical results for repeated measures ANOVA of isotopic enrichments.

Results of two-factor repeated measures ANOVA used to test for differences in lagoons over time for isotopic enrichments (^{13}C or ^{15}N) of various sediment pools and percent enrichment of select sediment pools out of the bulk sediment enrichment. Results for the post-hoc contrast for Days 1 and 2 versus Days 7 and 14 are shown to the right. One outlier has been removed from the IWB ^{15}N THAA analyses (Day 2) which accounts for the reduced degrees of freedom for that treatment. Significant p values are indicated in bold.

		lagoon			time			interaction			Post-hoc contrast: Days 1 & 2 vs. 7 & 14		
Parameter	**Isotope**	**df**	**F**	**p**	**df**	**F**	**p**	**df**	**F**	**p**	**df**	**F**	**p**
Bulk Sediments	^{13}C	4	0.01	0.9163	12	6.98	**0.0057**	12	3.29	0.0580	12	19.16	**0.0009**
	^{15}N	4	0.42	0.5532	12	5.76	**0.0112**	12	0.8	0.5168	12	15.61	**0.0019**
THAA	^{13}C	4	0.25	0.6460	12	3.68	**0.0434**	12	1.57	0.2487	12	10.37	**0.0074**
	^{15}N	4	0.92	0.3921	11	3.63	**0.0485**	11	1.56	0.2542	11	9.93	**0.0092**
D-Ala	^{13}C	4	1.14	0.3461	12	2.21	0.1399	12	1.03	0.4147	12	5.16	**0.0424**
	^{15}N	4	2.76	0.1721	11	1.98	0.1755	11	1.05	0.4086	11	4.89	**0.0492**
D/L-Ala	^{13}C	4	5.92	0.0718	12	5.49	**0.0132**	12	1.21	0.3473	12	15.7	**0.0019**
	^{15}N	4	7.72	**0.0499**	11	17.83	**0.0002**	11	5.25	**0.0171**	11	16.21	**0.0020**
PLFA	^{13}C	4	0.79	0.4247	11	3.32	0.0605	11	1.06	0.4037	11	6.93	**0.0233**
Bacterial FA	^{13}C	4	1.11	0.3507	11	3.39	0.0575	11	1.08	0.3961	11	5.83	**0.0344**
Algal FA	^{13}C	4	0.68	0.4566	11	6.84	**0.0072**	11	1.61	0.2426	11	17.11	**0.0017**
THAA/Bulk (%)	^{13}C	4	6.38	0.0649	12	2.86	0.0815	12	0.57	0.6474	12	5.62	**0.0353**
	^{15}N	4	1.35	0.3102	11	7.8	**0.0046**	11	0.3	0.8255	11	19.83	**0.0010**
D-Ala/Bulk (%)	^{13}C	4	13.48	**0.0214**	12	13.08	**0.0004**	12	3.03	0.0712	12	33.01	**<0.0001**
	^{15}N	4	6.29	0.0662	11	16.59	**0.0002**	11	3.64	**0.0483**	11	15.59	**0.0023**
PLFA/Bulk (%)	^{13}C	4	0.58	0.4905	11	1.65	0.2338	11	1.55	0.2569	11	0.96	0.3476

Table 5-4. Fraction (%) of excess isotope (^{13}C or ^{15}N) in THAA, D-Ala, and PLFA out of excess isotope in bulk sediment.

Values are presented as the mean (± SE), $n = 3$, for each lagoon on each experimental day.

			Experimental Day			
Parameter	**Lagoon**	**Isotope**	**1**	**2**	**7**	**14**
THAA/Bulk (%)	HIB	^{13}C	47.1 (7.1)	51.0 (4.5)	26.4 (7.6)	50.9 (12.5)
		^{15}N	47.7 (1.5)	56.1 (9.1)	33.8 (5.1)	39.1 (2.7)
	IWB	^{13}C	37.1 (6.5)	38.9 (10.3)	30.3 (5.4)	31.3 (5.5)
		^{15}N	49.3 (8.3)	42.1 (10.9)	30.7 (2.5)	33.2 (4.7)
D-Ala/Bulk (%)	HIB	^{13}C	0.21 (0.05)	0.14 (0.03)	0.04 (0.01)	0.06 (0.03)
		^{15}N	0.19 (0.07)	0.23 (0.03)	0.07 (0.01)	0.05 (0.01)
	IWB	^{13}C	0.08 (0.01)	0.06 (0.03)	0.02 (0.01)	0.04 (0.01)
		^{15}N	0.10 (0.02)	0.10 (0.04)	0.03 (0.01)	0.04 (0.01)
PLFA/BULK (%)	HIB	^{13}C	3.46 (0.17)	2.94 (0.57)	3.53 (0.97)	4.89 (3.79)
	IWB	^{13}C	2.85 (1.01)	3.43 (1.09)	3.05 (0.59)	0.22 (0.01))

Figure 5-1. Study sites.

Sediments and macroalgae were collected from two coastal lagoons: Hog Island Bay, VA and Isle of Wight Bay, MD. Dark grey shaded areas indicate the watersheds of each lagoon. Hog Island Bay is located within the LTER Virginia Coast Reserve.

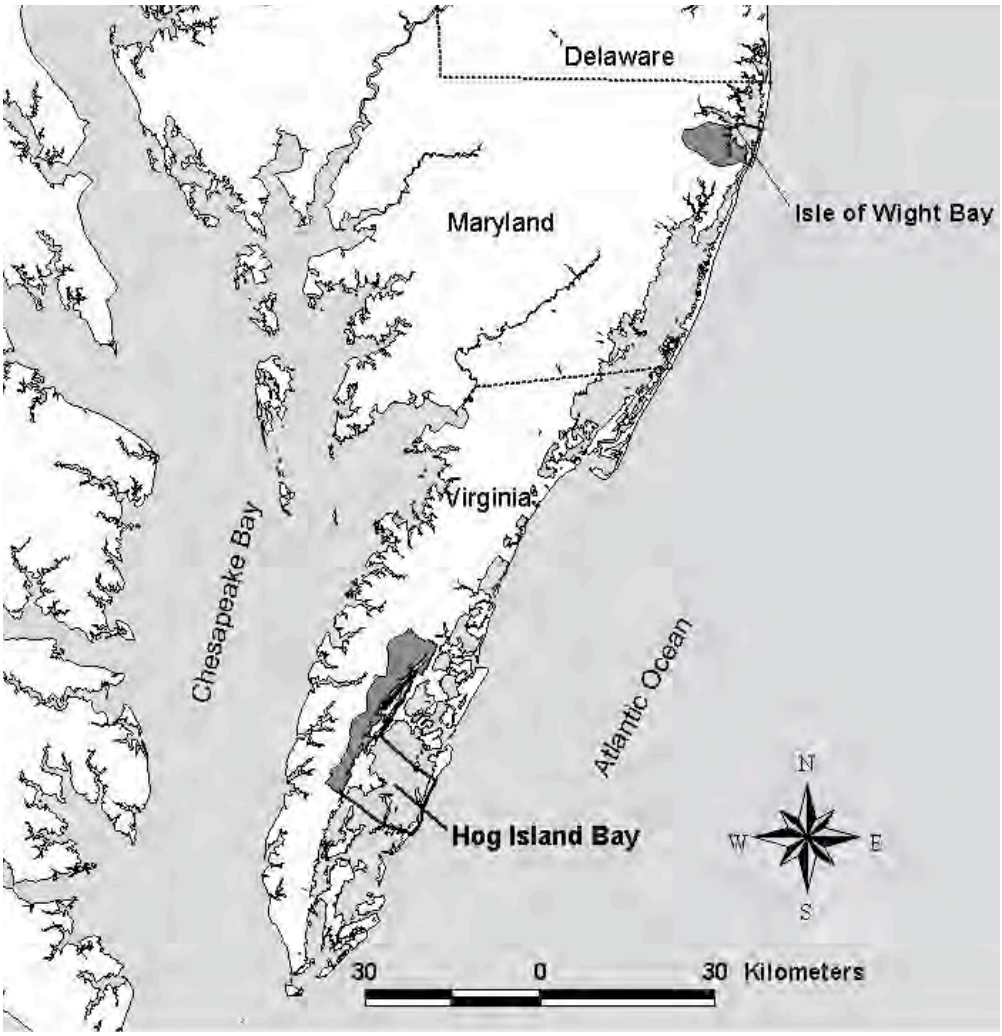
Delaware
Maryland
Isle of Wight Bay
Virginia
Chesapeake Bay
Atlantic Ocean
Hog Island Bay
N
W
E
S
30
0
30 Kilometers

Figure 5-2. Bulk sediment isotopic enrichments for HIB (solid lines) and IWB (dotted lines).

Values are reported as mean ± 1 SE (n = 3) for (a) excess ^{13}C and (b) excess ^{15}N.

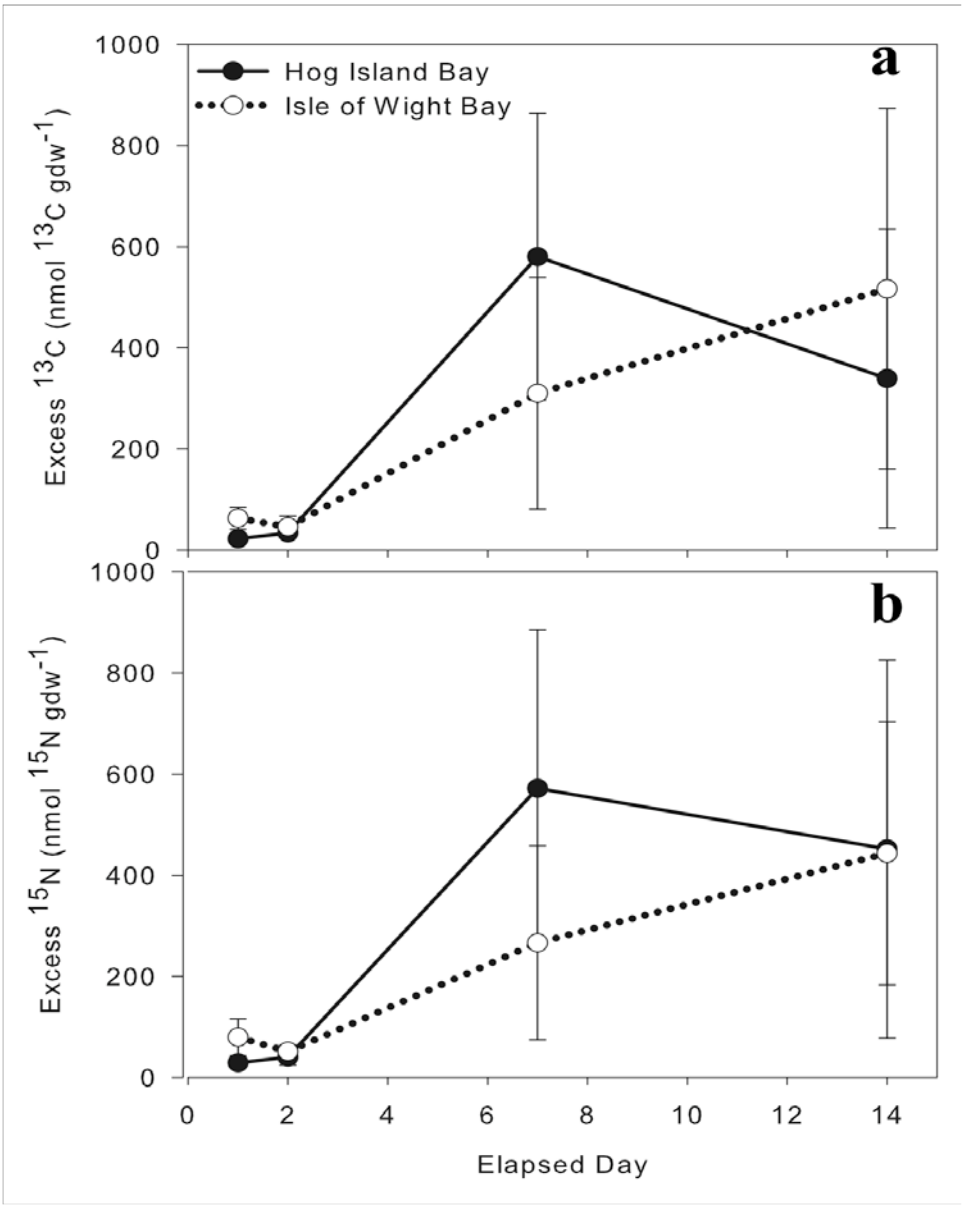
a
b
Hog Island Bay
Isle of Wight Bay
Excess ^{13}C (nmol ^{13}C gdw^{-1})
Excess ^{15}N (nmol ^{15}N gdw^{-1})
0
200
400
600
800
1000
0
2
4
6
8
10
12
14
Elapsed Day

Figure 5-3. Amino acid isotopic enrichments for HIB (solid line) and IWB (dotted line).

Values are mean ± 1 SE (n = 3) for excess (a) ^{13}C and (b) ^{15}N for THAA and (c) excess ^{13}C and (d) ^{15}N for D-Ala.

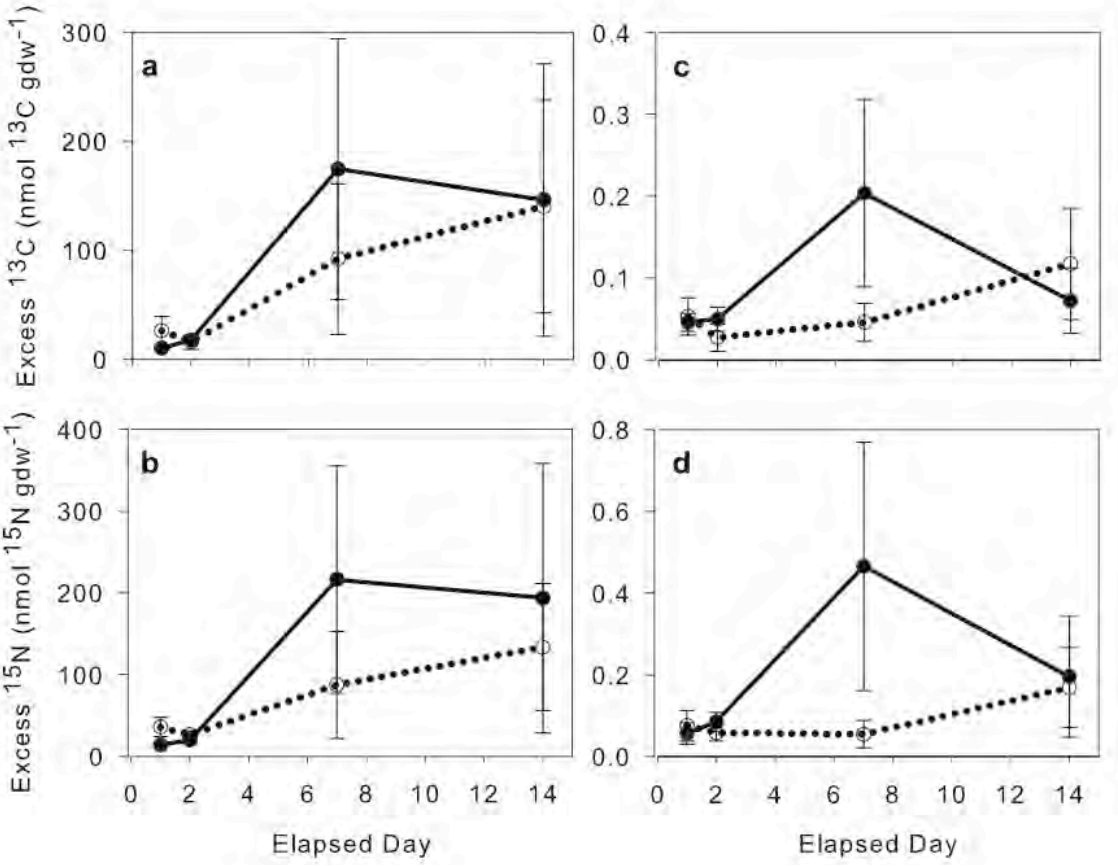
a
b
c
d
Excess ^{13}C (nmol ^{13}C gdw^{-1})
Excess ^{15}N (nmol ^{15}N gdw^{-1})
Elapsed Day
Elapsed Day

Figure 5-4. The ratio of excess ^{13}C (a) or ^{15}N (b) in D-Ala/L-Ala.

Values are mean ± 1 SE (n = 3) for HIB (solid lines) and IWB (dotted lines). The dashed horizontal gray lines represent the racemization background (0.017). The solid horizontal gray lines represent bacterial D/L-Ala abundance ratio (0.05). Values on the right y-axes correspond to estimates of bacterial contribution to total label incorporation.

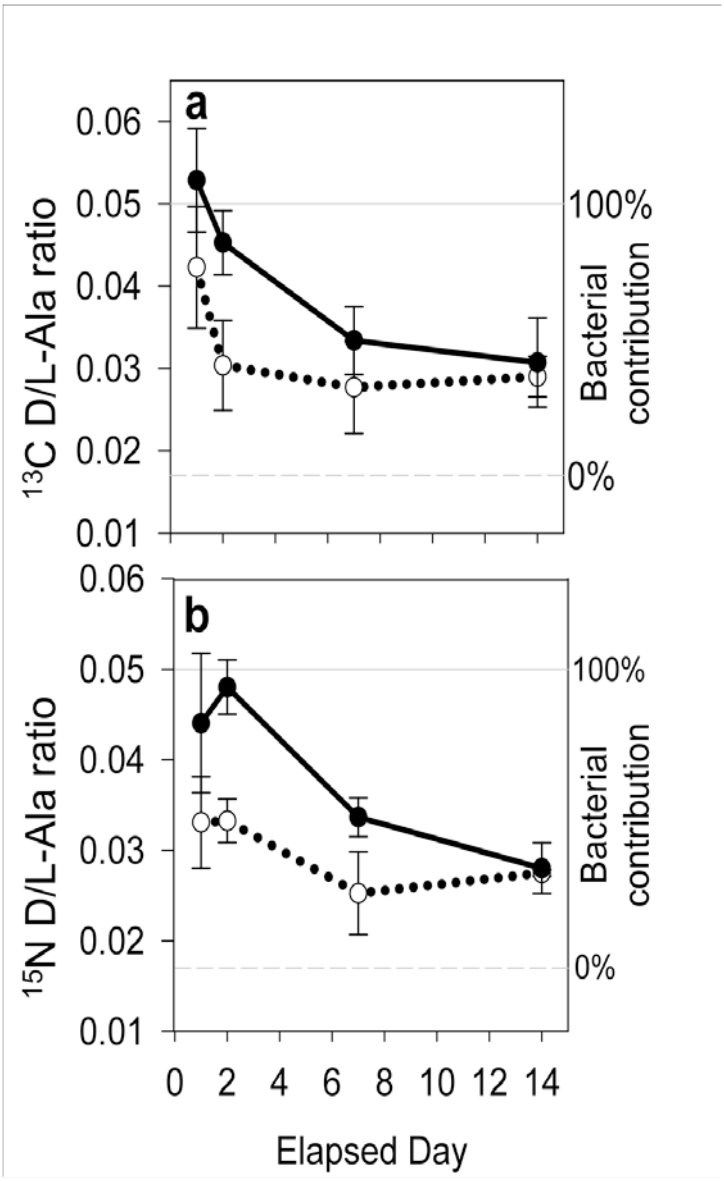
a
b
0.06
0.05
0.04
0.03
0.02
0.01
^{13}C D/L-Ala ratio
^{15}N D/L-Ala ratio
100%
0%
Bacterial contribution
0 2 4 6 8 10 12 14
Elapsed Day

Figure 5-5. PLFA isotopic enrichments.

Values are mean ±1 SE (n = 3) for excess ^{13}C in (a) total PLFA, (b) BrFA, which represent heterotrophic bacteria, and (c) PUFA, which represent algae for HIB (solid lines) and IWB (dotted lines).

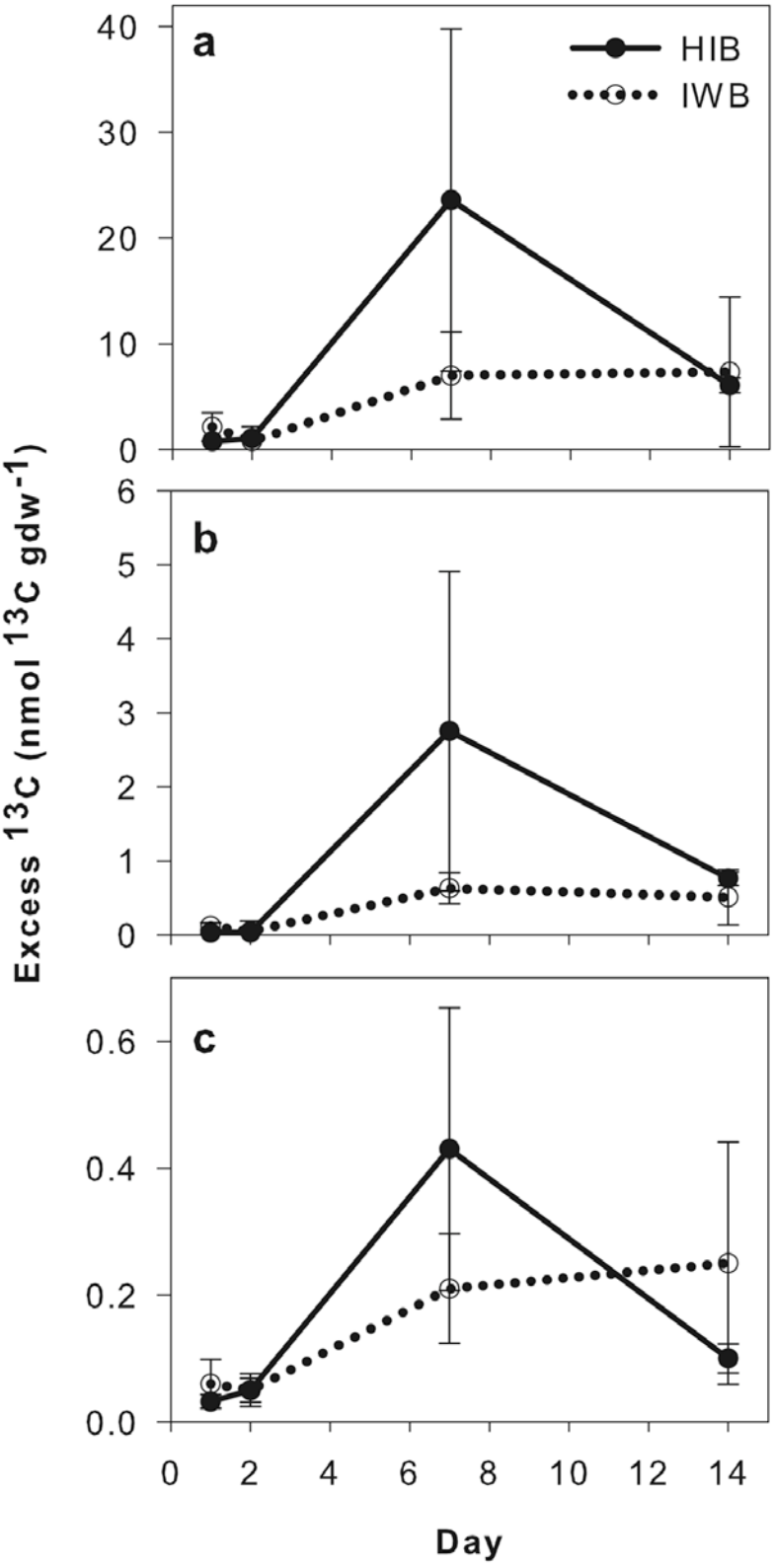
a
HIB
IWB
b
c
Excess ^{13}C (nmol ^{13}C gdw^{-1})
Day
0
2
4
6
8
10
12
14
0.0
0.2
0.4
0.6
1
3
5
20
30
40

Figure 5-6. Proposed mechanism for microbial processing of dead macroalgal biomass within the sediments.

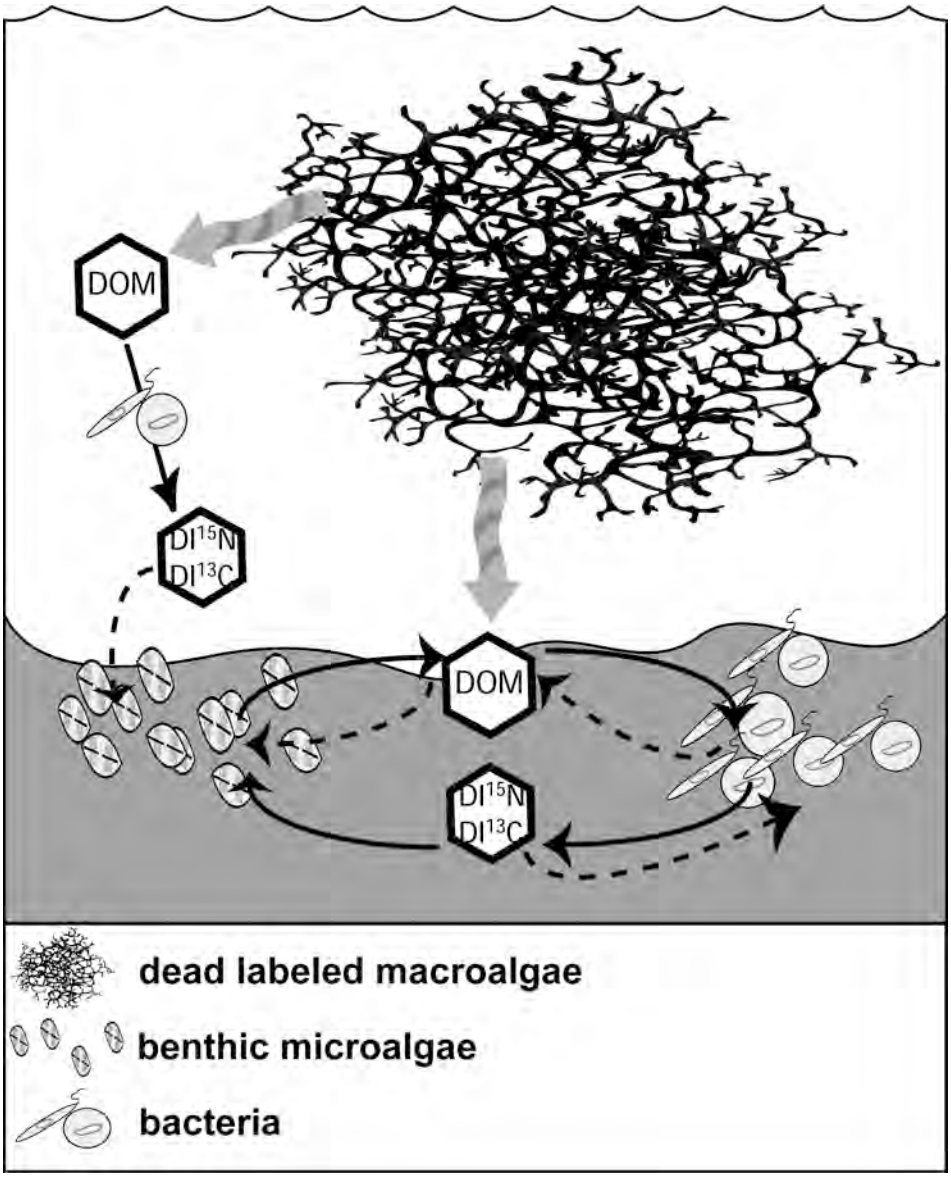
DOM
DI15N
DI13C
DOM
DI15N
DI13C
dead labeled macroalgae
benthic microalgae
bacteria

CHAPTER 6: SYNTHESIS

Ephemeral macroalgae are becoming more prevalent in coastal systems as a consequence of increased nutrient loading (Hauxwell et al. 2001; Sfriso et al. 1992; Wazniak et al. 2004), but their influence on sediment C and N cycling is not yet fully understood (McGlathery et al. 2007). In particular, their effect on C and N cycling within the sediment microbial community has not been studied directly, although flux studies indirectly suggest significant consequences result from the presence of macroalgae (Corzo et al. 2009; Dalsgaard 2003; McGlathery et al. 2001; Tyler et al. 2003). Thus, the objective of this work was to quantify the effects of living and dead macroalgae on sediment C and N cycling. Utilizing stable isotopic tracers and organic biomarkers, results from this work demonstrate that interactions between benthic macroalgae and the sediment microbial community fundamentally alter sediment nutrient cycling and its feedbacks to the overlying water column in shallow coastal systems. As a consequence, benthic autotrophs can act as a positive- or negative- feedback to eutrophication.

Figure 1 synthesizes the findings of this dissertation project by depicting the interactions between ephemeral macroalgae, benthic microalgae (BMA), and sediment bacteria over the typical bloom-and-die-off cycle of ephemeral macroalgae in shallow coastal systems. BMA play a particularly important role in regulating nutrient cycling in shallow coastal bays (Anderson et al. In press; McGlathery et al. 2004; Pedersen et al. 2004). Their location at the sediment-water interface allows them to intercept nutrients that would otherwise be released to the water column where they can potentially fuel phytoplankton blooms (Anderson et al. 2003). As a result, sediments where BMA are productive may serve as an important sink for nutrients, thereby buffering these systems from further eutrophication. This dissertation demonstrated that BMA used nutrients

from both the porewater and surface water to build biomass, thereby increasing the amount and lability of sediment organic matter, which in turn increased bacterial production. However, when macroalgal biomass was high, BMA production was substantially limited, likely as a result of shading, or possibly nutrient competition. Indeed, macroalgal growth is often sufficiently dense to self-shade the layers of the mat nearest the sediment surface (Brush and Nixon 2003; McGlathery et al. 1997); thus macroalgae likely limit the amount of light reaching BMA. Diminished BMA production resulted in lower sediment bacterial production as well. Although BMA were responsible for initial immobilization of the inorganic C and N that were added, heterotrophic bacteria became increasingly important over time. Incorporation of isotopic label into biomarkers for BMA initially and then into bacteria provided clear evidence for shuttling of C and N between BMA and bacteria, which corroborates findings of other studies that demonstrate coupling between these communities (Cook et al. 2007; Middelburg et al. 2000; Veuger et al. 2007). Although others have shown that BMA may act to retain nutrients in sediments (Anderson et al. 2003; Sundback and Miles 2000), demonstration of the shuttle between BMA and bacteria provides a mechanism that explains the prolonged retention (at least 4 weeks) of the isotopic tracers in the sediments after the isotope additions ended. Further, bacteria may act as a conduit for longer-term storage of C and N through production and accumulation of more recalcitrant forms of organic matter (e.g. peptidoglycan; (McCarthy et al. 1998; Veuger et al. 2006). Thus, by decreasing BMA production, macroalgae reduced overall retention of C and N in sediments by the microbial community thereby diminishing the role of the sediments in the 'coastal filter' (McGlathery et al. 2007).

Although macroalgae stored significant quantities of C and N while growing, thus serving as a nutrient sink, this retention was only temporary. Once macroalgae decline or die, macroalgae become a source of nutrients as their nutrients are re-released to the water column, where they can support phytoplankton, including harmful algal blooms, and bacterial metabolism (Castaldelli et al. 2003; McGlathery et al. 2001; Sfriso et al. 1992; Tyler et al. 2003). In contrast to macroalgae, retention within the sediment microbial pool would be expected to be a more stable sink. Sequestration of nutrients within sediment microbial biomass may remove nutrients from the water column, and the close coupling between BMA and bacteria may effectively retain and/or transform those nutrients within the sediments during times of the year that are favorable for phytoplankton blooms. Results from this dissertation also showed that following the simulated macroalgal die-off, 6 to 50% and 2 to 9% of macroalgal N and C, respectively, were incorporated into the surface sediments. Bacteria responded immediately to the pulse of organic matter and were the primary agents of decomposition of the macroalgae. However, BMA intercepted the return of nutrients to the water column. Once again, the close coupling between bacteria and BMA was demonstrated. In this experiment, some of the macroalgal-derived C and N was retained as microbial biomass within the sediments for at least 2 weeks following the macroalgal die-off. The importance of this potential sink will depend largely on the amount of biomass transferred to the sediments, which will depend on the hydrodynamics of the system as well as the influence of grazers (Duffy and Harvilicz 2001; Hauxwell et al. 1998).

Our mesocosm experiments allowed us to assess the mechanisms underlying nutrient cycling dynamics within the sediment microbial community in the presence and

absence of macroalgae and will contribute to our ability to predict the response of coastal bays to increased nutrient loading. This dissertation stresses the importance of coupling between BMA and sediment bacteria, which may serve to enhance nutrient retention within the sediments. Further, results from this dissertation provide new insights about sediment microbial community responses to ephemeral macroalgal blooms. Macroalgae diminish the role of BMA, which will in turn decrease retention of nutrients within the sediments. Once macroalgae die, some nutrients will be transferred to the sediments and stored within the microbial community, but this storage will be largely system-specific. These results indicate that macroalgae substantially influence nutrient cycling within these systems and should be incorporated into models predicting the effects of nutrient loading to shallow water ecosystems. Further work is needed to apply the findings from this work to the field. Preliminary work conducted during testing of the field-based perfusionator (Chapter 2) demonstrated C and N storage in surface sediments even when influenced by wave action and tidal pumping. More detailed field studies that include uptake by sediment microbes and the influence of macroalgae, as well as effects of hydrodynamic regime and upper trophic levels are warranted.

Literature Cited

Anderson, I. C., K. J. McGlathery, and A. C. Tyler. 2003. Microbial mediation of 'reactive' nitrogen transformations in a temperate lagoon. Marine Ecology Progress Series **246:** 73-84.

Anderson, I. C., J. W. Stanhope, A. K. Hardison, and K. J. McGlathery. In press. Sources and fates of nitrogen in Virginia Coastal Bays. *In* M. J. Kennish and H. W. Paerl [eds.], Coastal Lagoons: Critical Habitats of Environmental Change. Taylor and Francis.

Brush, M. J., and S. W. Nixon. 2003. Biomass layering and metabolism in mats of the macroalga Ulva lactuca L. Estuaries **26:** 916-926.

Castaldelli, G. and others 2003. Decomposition dynamics of the bloom forming macroalga Ulva rigida C. Agardh determined using a C-14-carbon radio-tracer technique. Aquatic Botany **75:** 111-122.

Cook, P. L. M., B. Veuger, S. Boer, and J. J. Middelburg. 2007. Effect of nutrient availability on carbon and nitrogen incorporation and flows through benthic algae and bacteria in near-shore sandy sediment. Aquatic Microbial Ecology **49:** 165-180.

Corzo, A., S. A. van Bergeijk, and E. Garcia-Robledo. 2009. Effects of green macroalgal blooms on intertidal sediments: net metabolism and carbon and nitrogen contents. Marine Ecology-Progress Series **380:** 81-93.

Dalsgaard, T. 2003. Benthic primary production and nutrient cycling in sediments with benthic microalgae and transient accumulation of macroalgae. Limnology and Oceanography **48:** 2138-2150.

Duffy, J. E., and A. M. Harvilicz. 2001. Species-specific impacts of grazing, amphipods in an eelgrass-bed community. Marine Ecology-Progress Series **223:** 201-211.

Hauxwell, J., J. Cebrian, C. Furlong, and I. Valiela. 2001. Macroalgal canopies contribute to eelgrass (*Zostera marina*) decline in temperate estuarine ecosystems. Ecology **82:** 1007-1022.

Hauxwell, J., J. McClelland, P. J. Behr, and I. Valiela. 1998. Relative importance of grazing and nutrient controls of macroalgal biomass in three temperate shallow estuaries. Estuaries **21:** 347-360.

McCarthy, M. D., J. I. Hedges, and R. Benner. 1998. Major bacterial contribution to marine dissolved organic nitrogen. Science **281:** 231-234.

McGlathery, K., K. Sundback, and I. Anderson. 2004. The Importance of Primary Producers for Benthic Nitrogen and Phosphorus Cycling, p. 231-261. *In* S. L. Nielsen, G. T. Banta and M. Pedersen [eds.], Estuarine Nutrient Cycling: The Influence of Primary Producers. Kluwer Academic Publishers.

McGlathery, K. J., I. C. Anderson, and A. C. Tyler. 2001. Magnitude and variability of benthic and pelagic metabolism in a temperate coastal lagoon. Marine Ecology-Progress Series **216:** 1-15.

McGlathery, K. J., D. Krause-Jensen, S. Rysgaard, and P. B. Christensen. 1997. Patterns of ammonium uptake within dense mats of the filamentous macroalga Chaetomorpha linum. Aquatic Botany **59:** 99-115.

McGlathery, K. J., K. Sundback, and I. C. Anderson. 2007. Eutrophication in shallow coastal bays and lagoons: the role of plants in the coastal filter. Marine Ecology-Progress Series **348:** 1-18.

Middelburg, J. J., C. Barranguet, H. T. S. Boschker, P. M. J. Herman, T. Moens, and C. H. R. Heip. 2000. The fate of intertidal microphytobenthos carbon: An in situ C-13-labeling study. Limnology and Oceanography **45:** 1224-1234.

Pedersen, M. F., S. L. Nielsen, and G. T. Banta. 2004. Interactions between vegetation and nutrient dynamics in coastal marine ecosystems: An introduction. *In* S. L. Nielsen, G. T. Banta and M. F. Pedersen [eds.], Estuarine Nutrient Cycling: The Influence of Primary Producers. Kluwer.

Sfriso, A., B. Pavoni, A. Marcomini, S. Raccanelli, and A. A. Orio. 1992. Particulate Matter Deposition and Nutrient Fluxes onto the Sediments of the Venice Lagoon. Environmental Technology **13:** 473-483.

Sundback, K., and A. Miles. 2000. Balance between denitrification and microalgal incorporation of nitrogen in microtidal sediments, NE Kattegat. Aquatic Microbial Ecology **22:** 291-300.

Tyler, A. C., K. J. McGlathery, and I. C. Anderson. 2003. Benthic algae control sediment-water column fluxes of organic and inorganic nitrogen compounds in a temperate lagoon. Limnology and Oceanography **48:** 2125-2137.

Veuger, B., B. D. Eyre, D. Maher, and J. J. Middelburg. 2007. Nitrogen incorporation and retention by bacteria, algae, and fauna in a subtropical intertidal sediment: An in situ N-15-labeling study. Limnology and Oceanography **52:** 1930-1942.

Veuger, B., D. van Oevelen, H. T. S. Boschker, and J. J. Middelburg. 2006. Fate of peptidoglycan in an intertidal sediment: An in situ C-13-labeling study. Limnology and Oceanography **51:** 1572-1580.

Wazniak, C. and others 2004. State of the Maryland Coastal Bays. Maryland Department of Natural Resources.

Figure 6-1. Conceptual diagram summarizing macroalgal and sediment microbial interactions in a shallow coastal system.

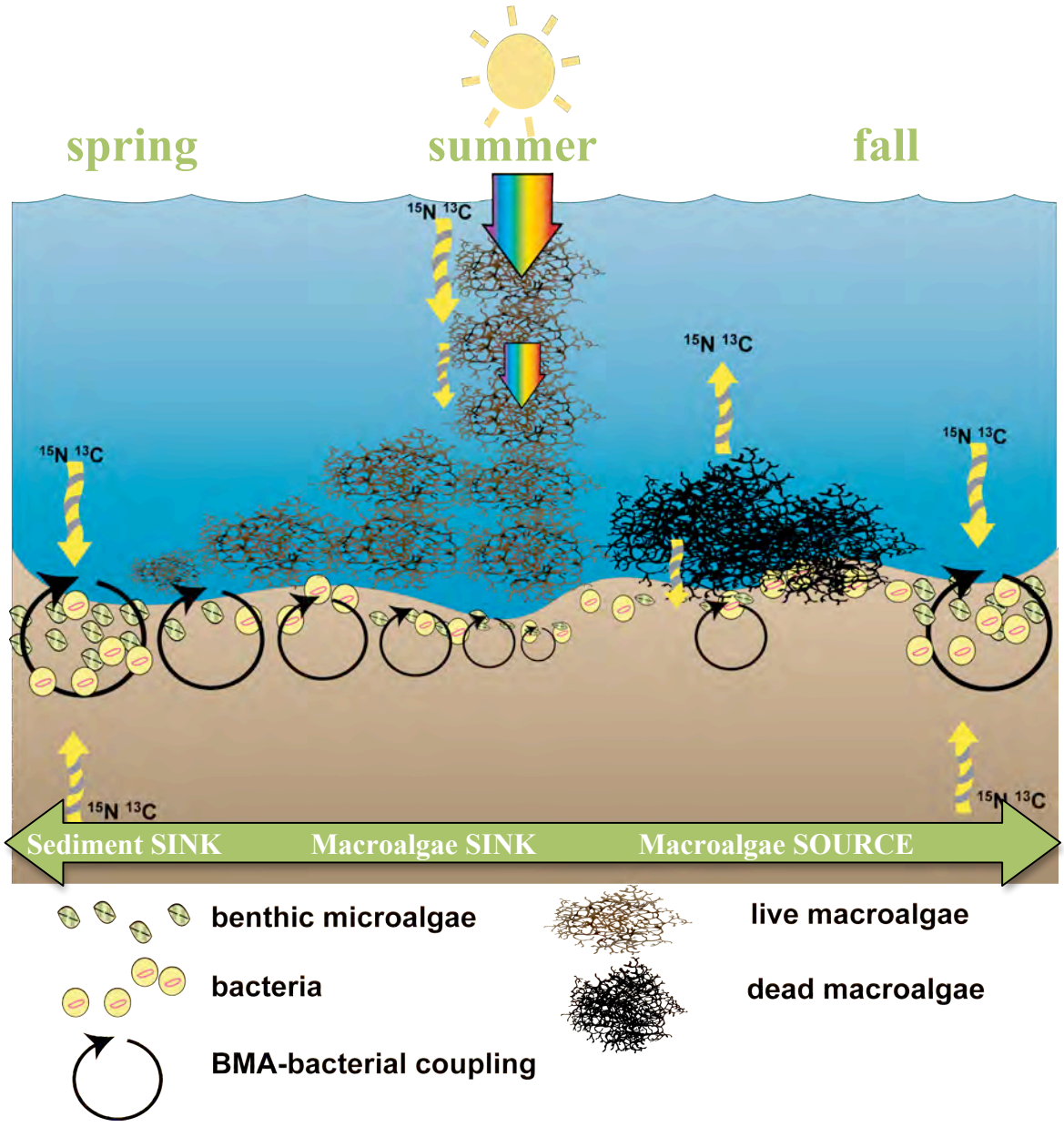
spring
summer
fall
15N 13C
15N 13C
15N 13C
15N 13C
15N 13C
Sediment SINK
Macroalgae SINK
Macroalgae SOURCE
benthic microalgae
bacteria
BMA-bacterial coupling
live macroalgae
dead macroalgae

APPENDIX A: CHAPTER 2 SF_6 DATA (nM)

		Mesocosm experiment				Field deployment			
x coord	y coord	M1	M4	M11	M13	M-A	M-B	M-C	M-D
-10	10	71	50	254	156	531	545	193	0
0	10	58	67	356	22	981	581	710	0
10	10	27	16	147	13	794	758	615	291
-15	0	81	93	185	84	821	761	416	1329
-5	0	24	141	182	101	622	612	806	1500
5	0	80	151	267	53	518	885	455	519
15	0	42	100	103	46	247	885	1104	0
-10	-10	13	78	49	73	708	200	830	63
0	-10	5	124	238	54	261	364	974	1324
10	-10	49	84	106	65	791	363	397	877

APPENDIX B: CHAPTER 2 STABLE ISOTOPE DATA
Mesocosm Experiment

Timestep	Day	Meso	Treatment	Macro	Light/Dark	Iso Source	δ15N (permil)	δ13C (permil)
T-1M	-1	2	MLS*NON-LABELED				10.225	-19.814
T-1M	-1	6	NDP*NON-LABELED				12.451	-19.504
1.5M	1.5	7	MLP	MAC	LIGHT	PW	2268.425	83.014
1.5M	1.5	16	NLP	NO MAC	LIGHT	PW	2188.79	152.117
1.5M	1.5	25	NLP	NO MAC	LIGHT	PW	2188.79	152.117
1.5M	1.5	26	MLP	MAC	LIGHT	PW	2450.853	102.455
T3.5M	3.5	7	MLP	MAC	LIGHT	PW	2957.216	226.151
T3.5M	3.5	16	NLP	NO MAC	LIGHT	PW	1452.233	191.738
T3.5M	3.5	25	NLP	NO MAC	LIGHT	PW	7786.91	739.438
T3.5M	3.5	26	MLP	MAC	LIGHT	PW	1688.009	134.33
T7.5M	7.5	7	MLP	MAC	LIGHT	PW	4448.689	349.586
T7.5M	7.5	16	NLP	NO MAC	LIGHT	PW	5211.722	363.389
T7.5M	7.5	25	NLP	NO MAC	LIGHT	PW	6896.931	522.921
T7.5M	7.5	26	MLP	MAC	LIGHT	PW	9984.583	814.252
T14.5M	14.5	7	MLP	MAC	LIGHT	PW	3603.332	237.644
T14.5M	14.5	16	NLP	NO MAC	LIGHT	PW	15597.53	1293.859
T14.5M	14.5	25	NLP	NO MAC	LIGHT	PW	24574.42	1907.376
T14.5M	14.5	26	MLP	MAC	LIGHT	PW	11448.23	650.046
T2P	16.5	7	MLP	MAC	LIGHT	PW	11064.41	636.396
T2P	16.5	16	NLP	NO MAC	LIGHT	PW	9749.595	847.266
T2P	16.5	25	NLP	NO MAC	LIGHT	PW	24703.92	1841.123
T2P	16.5	26	MLP	MAC	LIGHT	PW	19723.81	1339.425
T6.5P	21	7	MLP	MAC	LIGHT	PW	12589.04	772.029
T6.5P	21	16	NLP	NO MAC	LIGHT	PW	20545.93	1536.179
T6.5P	21	25	NLP	NO MAC	LIGHT	PW	11594.35	850.741
T6.5P	21	26	MLP	MAC	LIGHT	PW	13273.6	1044.088
T14.5P	29	7	MLP	MAC	LIGHT	PW	12571.79	815.316
T14.5P	29	16	NLP	NO MAC	LIGHT	PW	16769.88	1201.164
T14.5P	29	25	NLP	NO MAC	LIGHT	PW	23662.39	1655.104
T14.5P	29	26	MLP	MAC	LIGHT	PW	18535.12	1372.452
T27.5P	42	7	MLP	MAC	LIGHT	PW	9743.583	633.23
T27.5P	42	16	NLP	NO MAC	LIGHT	PW	9256.693	567.418
T27.5P	42	25	NLP	NO MAC	LIGHT	PW	13769.52	789.995

APPENDIX B: CHAPTER 2 STABLE ISOTOPE DATA

Field deployment

		bulk sediments		PW NH4+
Meso	Day	δ15N (permil)	δ13C (permil)	δ15N (permil)
M1	1	16.643	-24.583	139.506
M2	1	16.205	-19.814	204.171
M3	1	136.624	-14.92	n.s.
M4	1	12.347	-20.82	54.11
M1	7	901.641	60.456	26617.192
M2	7	196.172	-15.823	19498.311
M3	7	91.275	-17.762	19443.31
M4	7	413.093	-3.503	15532.915
M1	12	688.847	34.62	15386.636
M2	12	394.456	4.927	15671.179
M3	12	12.379	-18.831	13255.232
M4	12	713.491	92.126	n.s.
M1	14	462.868	14.149	n.s.
M2	14	535.022	23.822	n.s.
M3	14	303.019	-3.187	n.s.
M4	14	319.76	2.582	n.s.
M1	19	153.55	-8.737	9897.11
M2	19	166.954	-8.189	7271.462
M3	19	597.257	23.957	7785.117
M4	19	100.905	-13.491	125718
M1	26	240.003	1.496	5425.252
M2	26	125.72	-13.307	4354.915
M3	26	314.421	-1.377	1580.354
M4	26	100.37	-11.339	6181.5
M1	33	241.702	2.461	4884.275
M2	33	180.976	-8.413	3464.583
M3	33	178.504	-8.566	5.062
M4	33	266.247	4.178	6083.615
M1	42	148.777	-12.989	3324.244
M2	42	96.444	-13.837	1108.494
M3	42	157.627	-11.021	979.132
M4	42	198.619	-3.824	2924.228

APPENDIX C: CHAPTER 2 RHODAMINE DATA

Date	Time	Site	Depth (cm)	conc550 (%)
20-Apr	9:00	A	6	0.00
20-Apr	15:00	A	6	0.56
21-Apr	9:00	A	6	0.00
21-Apr	15:00	A	6	0.25
24-Apr	10:00	A	6	15.68
25-Apr	14:00	A	6	45.00
20-Apr	9:00	A	15	1.48
20-Apr	15:00	A	15	0.00
21-Apr	9:00	A	15	2.72
21-Apr	15:00	A	15	11.36
24-Apr	10:00	A	15	52.40
25-Apr	14:00	A	15	51.48
20-Apr	9:00	B	6	0.00
20-Apr	15:00	B	6	0.00
21-Apr	9:00	B	6	0.00
21-Apr	15:00	B	6	0.25
24-Apr	10:00	B	6	18.15
25-Apr	14:00	B	6	11.67
20-Apr	9:00	B	15	2.10
20-Apr	15:00	B	15	1.48
21-Apr	9:00	B	15	0.00
21-Apr	15:00	B	15	0.25
24-Apr	10:00	B	15	41.29
25-Apr	14:00	B	15	59.81
20-Apr	9:00	C	6	0.87
20-Apr	15:00	C	6	2.10
21-Apr	9:00	C	6	0.00
21-Apr	15:00	C	6	0.00
24-Apr	10:00	C	6	2.72
25-Apr	14:00	C	6	43.15
20-Apr	9:00	C	15	3.03
20-Apr	15:00	C	15	0.00
21-Apr	9:00	C	15	0.00
21-Apr	15:00	C	15	0.87
24-Apr	10:00	C	15	54.25
25-Apr	14:00	C	15	51.48
20-Apr	9:00	D	6	0.00
20-Apr	15:00	D	6	0.00
21-Apr	9:00	D	6	0.56
21-Apr	15:00	D	6	0.25
24-Apr	10:00	D	6	38.52
25-Apr	14:00	D	6	3.34
20-Apr	9:00	D	15	4.26

Plan view of mesocosm with RWT sampling locations

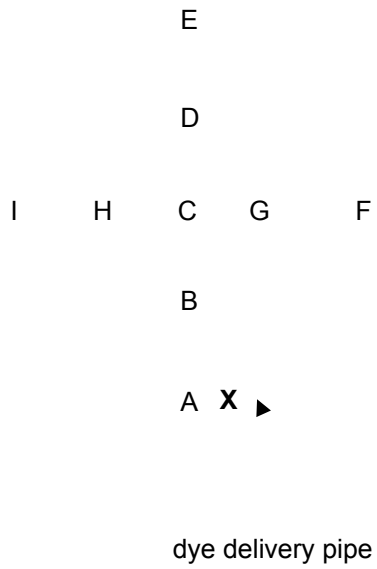

20-Apr	15:00	D	15	1.48
21-Apr	9:00	D	15	0.00
21-Apr	15:00	D	15	0.00
24-Apr	10:00	D	15	49.32
25-Apr	14:00	D	15	57.65
20-Apr	9:00	E	6	0.56
20-Apr	15:00	E	6	0.25
21-Apr	9:00	E	6	0.00
21-Apr	15:00	E	6	0.00
24-Apr	10:00	E	6	3.03
25-Apr	14:00	E	6	24.01
20-Apr	9:00	E	15	3.34
20-Apr	15:00	E	15	1.18
21-Apr	9:00	E	15	0.00
21-Apr	15:00	E	15	0.00
24-Apr	10:00	E	15	24.94
25-Apr	14:00	E	15	51.79
20-Apr	9:00	F	6	0.00
20-Apr	15:00	F	6	0.87
21-Apr	9:00	F	6	0.00
21-Apr	15:00	F	6	0.00
24-Apr	10:00	F	6	34.20
25-Apr	14:00	F	6	51.17
20-Apr	9:00	F	15	2.41
20-Apr	15:00	F	15	0.00
21-Apr	9:00	F	15	0.25
21-Apr	15:00	F	15	8.27
24-Apr	10:00	F	15	60.12
25-Apr	14:00	F	15	53.64
20-Apr	9:00	G	6	0.00
20-Apr	15:00	G	6	0.00
21-Apr	9:00	G	6	0.00
21-Apr	15:00	G	6	0.00
24-Apr	10:00	G	6	15.68
25-Apr	14:00	G	6	44.07
20-Apr	9:00	G	15	0.56
20-Apr	15:00	G	15	0.87
21-Apr	9:00	G	15	0.25
21-Apr	15:00	G	15	2.41
24-Apr	10:00	G	15	26.48
25-Apr	14:00	G	15	57.03
20-Apr	9:00	H	6	0.00
20-Apr	15:00	H	6	0.00
21-Apr	9:00	H	6	1.79
21-Apr	15:00	H	6	0.00
24-Apr	10:00	H	6	16.91
25-Apr	14:00	H	6	7.66
20-Apr	9:00	H	15	1.18

20-Apr	15:00	H	15	2.10
21-Apr	9:00	H	15	0.00
21-Apr	15:00	H	15	0.00
24-Apr	10:00	H	15	41.91
25-Apr	14:00	H	15	57.65
20-Apr	9:00	I	6	0.00
20-Apr	15:00	I	6	0.87
21-Apr	9:00	I	6	0.00
21-Apr	15:00	I	6	0.00
24-Apr	10:00	I	6	2.10
25-Apr	14:00	I	6	52.71
20-Apr	9:00	I	15	0.00
20-Apr	15:00	I	15	1.18
21-Apr	9:00	I	15	6.73
21-Apr	15:00	I	15	25.86
24-Apr	10:00	I	15	53.02
25-Apr	14:00	I	15	74.62
19-Apr	15:00	W	0	0.87
20-Apr	9:00	W	0	0.00
20-Apr	15:00	W	0	0.00
21-Apr	9:00	W	0	0.00
21-Apr	15:00	W	0	0.00
24-Apr	10:00	W	0	0.00
25-Apr	14:00	W	0	1.79
19-Apr	15:00		6	1.18
19-Apr	15:00		15	0.87

APPENDIX D: CHAPTER 3 BULK, THAA DATA

Timestep	Day	Meso	Treatment	TN (umol N gdw^{-1})	TOC (umol C gdw^{-1})	C:N	Benthic [Chla] (mg m^{-2})	Macro biomass (gdw m^{-2})	THAA (umol AA gdw^{-1})	THAA/TN (%)
T-1M	-1	2	MLS*NON-LAB	14.59	148.06	10.15	8.43	125.52	4.19	32.14
T-1M	-1	4	NLS*NON-LABELED				28.10			
T-1M	-1	6	NDP*NON-LAB	14.24	140.09	9.84	12.64		4.01	31.58
T-1M	-1	7	MLP					121.75		
T-1M	-1	10	MLS					127.17		
T-1M	-1	26	MLP					126.52		
1.5M	1.5	2	MLS	23.24	222.92	9.59	67.43			
1.5M	1.5	4	NLS	28.42	290.84	10.23	49.17		10.26	40.59
1.5M	1.5	6	NDP	14.32	143.13	10.00	9.83		3.97	31.08
1.5M	1.5	7	MLP	25.17	258.98	10.29	43.55		7.21	32.17
1.5M	1.5	10	MLS	14.96	150.91	10.08	88.50		4.47	33.35
1.5M	1.5	11	NLS	16.39	171.77	10.48	63.21		4.97	34.10
1.5M	1.5	12	NDS	15.85	191.95	12.11	37.93		4.67	32.92
1.5M	1.5	14	NDS	13.86	141.46	10.21	29.50		4.10	32.96
1.5M	1.5	16	NLP	23.07	261.74	11.35	47.76		7.05	34.01
1.5M	1.5	18	NDP	9.42	90.51	9.61	19.67		2.89	34.29
1.5M	1.5	25	NLP	23.07	261.74	11.35	80.07		12.47	60.75
1.5M	1.5	26	MLP	16.49	140.80	8.54	77.26			
T3.5M	3.5	2	MLS	20.28	185.82	9.16	74.45		9.99	55.46
T3.5M	3.5	4	NLS	20.19	203.32	10.07	91.31		11.26	63.59
T3.5M	3.5	6	NDP	15.37	167.10	10.87	7.02		7.23	52.42
T3.5M	3.5	7	MLP	19.42	206.49	10.63	35.12		8.51	47.65
T3.5M	3.5	10	MLS	18.43	178.70	9.69	50.57		7.18	43.84
T3.5M	3.5	11	NLS	17.00	189.44	11.15	43.55		8.05	53.38
T3.5M	3.5	12	NDS	12.39	117.82	9.51	9.83		6.24	56.07
T3.5M	3.5	14	NDS	13.86	133.67	9.64	5.62		4.30	33.13
T3.5M	3.5	16	NLP	17.10	175.63	10.27	42.14		8.48	55.47

T3.5M	3.5	18	NDP	10.50	96.98	9.23	5.62		5.17	54.05
T3.5M	3.5	25	NLP	20.44	213.53	10.45	54.79		9.12	49.88
T3.5M	3.5	26	MLP	13.27	92.00	6.93	122.22			
T7.5M	7.5	2	MLS	26.99	274.54	10.17	44.95	210.71	9.18	38.43
T7.5M	7.5	4	NLS	16.80	161.36	9.60	30.90		5.59	37.61
T7.5M	7.5	6	NDP	15.61	187.84	12.03	7.02		4.59	32.96
T7.5M	7.5	7	MLP	22.01	254.56	11.56	18.26	199.48	7.26	36.28
T7.5M	7.5	10	MLS	20.29	187.48	9.24	81.48	202.12	5.90	32.67
T7.5M	7.5	11	NLS	23.32	239.24	10.26	88.50		7.78	37.64
T7.5M	7.5	12	NDS	13.72	141.61	10.33	7.02		4.05	33.49
T7.5M	7.5	14	NDS	13.86	133.67	9.64	15.45		3.71	30.33
T7.5M	7.5	16	NLP	16.02	163.30	10.20	96.93		4.41	31.32
T7.5M	7.5	18	NDP	19.95	206.91	10.37	9.83		5.53	31.38
T7.5M	7.5	25	NLP	33.65	302.15	8.98	71.64		11.52	38.71
T7.5M	7.5	26	MLP	18.55	133.28	7.19	73.05	188.02		
T14.5M	14.5	2	MLS	22.93	196.37	8.56	54.79	268.70	8.89	43.89
T14.5M	14.5	4	NLS	24.48	231.92	9.47	89.91		9.85	45.54
T14.5M	14.5	6	NDP	37.83	433.79	11.47	21.07		10.74	31.07
T14.5M	14.5	7	MLP	14.31	156.64	10.94	32.31	300.28	4.28	33.56
T14.5M	14.5	10	MLS	27.61	281.30	10.19	87.10	251.90	8.15	33.32
T14.5M	14.5	11	NLS	28.36	343.85	12.12	91.31		8.57	34.75
T14.5M	14.5	12	NDS	31.67	378.26	11.94	18.26		8.70	30.99
T14.5M	14.5	14	NDS	16.05	188.89	11.77	9.83		4.00	28.03
T14.5M	14.5	16	NLP	26.75	316.63	11.84	68.83		8.02	34.07
T14.5M	14.5	18	NDP	16.89	216.15	12.80	19.67		3.64	24.39
T14.5M	14.5	25	NLP	33.46	397.90	11.89	43.55		12.20	41.19
T14.5M	14.5	26	MLP	20.45	174.15	8.52	47.76	247.08		
T2P	16.5	2	MLS	25.22	250.29	9.92	81.48			
T2P	16.5	4	NLS	32.53	365.56	11.24	15.45			
T2P	16.5	6	NDP	14.23	173.09	12.16	11.24			
T2P	16.5	7	MLP	25.27	248.48	9.83	64.62			

T2P	16.5	10	MLS	19.75	207.75	10.52	36.52			
T2P	16.5	11	NLS	23.63	180.25	7.63	94.12			
T2P	16.5	12	NDS	16.17	166.82	10.32	21.07			
T2P	16.5	14	NDS	15.00	154.52	10.30	11.24			
T2P	16.5	16	NLP	26.69	285.31	10.69	53.38			
T2P	16.5	18	NDP	16.39	180.18	10.99	9.83			
T2P	16.5	25	NLP	29.68	316.99	10.68	136.26			
T2P	16.5	26	MLP	24.59	264.41	10.75	56.19			
T6.5P	21	2	MLS	31.50	334.61	10.62	47.76	336.36	9.60	34.77
T6.5P	21	4	NLS	38.19	418.23	10.95	91.31		12.13	36.29
T6.5P	21	6	NDP	17.59	226.35	12.87	4.21		4.33	27.55
T6.5P	21	7	MLP	31.90	362.15	11.35	56.19	324.47	9.64	34.17
T6.5P	21	10	MLS	21.50	228.71	10.64	66.02	289.82	5.87	30.96
T6.5P	21	11	NLS	41.51	443.94	10.69	106.76		13.83	37.85
T6.5P	21	12	NDS	32.17	393.45	12.23	14.05		8.64	30.18
T6.5P	21	14	NDS	23.10	280.85	12.16	0.00		5.80	28.23
T6.5P	21	16	NLP	34.56	384.16	11.12	51.98		12.30	40.33
T6.5P	21	18	NDP	35.05	473.63	13.51	0.00		8.62	27.63
T6.5P	21	25	NLP	54.23	626.77	11.56	51.98		17.85	37.58
T6.5P	21	26	MLP	17.03	118.99	6.99	57.60	289.56		
T14.5P	29	2	MLS	24.74	232.81	9.41	98.33	384.76		
T15.5P	29	4	NLS	21.27	212.96	10.01	25.29			
T14.5P	29	6	NDP	18.34	206.18	11.24	1.40			
T15.5P	29	7	MLP	36.71	400.81	10.92	22.48	398.54		
T14.5P	29	10	MLS	20.14	185.74	9.22	99.74	313.15		
T15.5P	29	11	NLS	39.45	364.26	9.23	255.67			
T14.5P	29	12	NDS	12.27	138.78	11.31	7.02			
T15.5P	29	14	NDS	10.49	115.40	11.00	7.02			
T14.5P	29	16	NLP	26.63	285.22	10.71	51.98			
T15.5P	29	18	NDP	16.50	202.89	12.29	16.86			
T14.5P	29	25	NLP	24.54	268.01	10.92	51.98			

T15.5P	29	26	MLP	14.07	149.16	10.60	42.14	337.12		
T27.5P	42	4	NLS	34.71	380.49	10.96	54.79		12.19	39.81
T27.5P	42	6	NDP	26.06	332.22	12.75	15.45		5.87	25.35
T27.5P	42	7	MLP	23.35	273.71	11.72	25.29	512.59	7.07	33.99
T27.5P	42	10	MLS	33.40	407.75	12.21	146.10	307.95	9.39	31.78
T27.5P	42	11	NLS	34.02	358.00	10.52	122.22		12.22	40.79
T27.5P	42	12	NDS	13.90	169.73	12.21	18.26		3.15	25.50
T27.5P	42	14	NDS	15.14	190.53	12.59	0.00		3.44	25.79
T27.5P	42	16	NLP	38.22	436.02	11.41	189.64		12.43	36.68
T27.5P	42	18	NDP	24.09	302.00	12.54	8.43		5.78	26.88
T27.5P	42	25	NLP	33.87	441.64	13.04	40.74		10.05	33.93

	Mol%													
THAA/TOC (%)	D-Ala	L-Ala	Thr+Val	Gly	Ile	Leu	Pro	Asp	Glu	Phe	PLFA (ng FA gdw^{-1})	NEUT (ng FA gdw^{-1})	Total FA (ng FA gdw^{-1})	PLFA/TOC (%)
11.78	0.93	13.90	6.88	27.47	3.40	6.06	7.86	15.66	12.09	0.59	39943.98	30989.85	70933.83	1.62
12.43	0.90	13.19	6.90	25.52	3.52	6.00	7.91	15.58	11.97	3.16	14067.62	10320.58	24388.20	0.61
											29374.30	62873.19	92247.50	0.79
14.97	0.94	14.56	6.96	27.97	3.32	6.20	7.28	13.42	11.42	2.45	41827.97	46948.33	88776.30	0.87
12.04	0.88	14.11	7.20	26.10	3.63	6.15	7.78	14.41	11.59	3.32	6002.33	8031.38	14033.71	0.25
12.11	0.80	13.95	6.74	24.73	3.56	6.63	7.66	15.39	12.24	2.79	38156.70	62939.21	101095.91	0.89
12.84	0.80	14.40	6.32	24.59	3.52	6.66	7.32	15.03	12.89	3.06	23608.85	32728.68	56337.53	0.94
12.64	0.76	14.71	6.69	24.19	3.74	6.88	7.35	14.21	12.68	2.95	19809.03	62137.84	81946.87	0.69
10.38	0.91	14.03	6.26	27.35	3.54	6.15	8.10	13.83	11.27	3.06	9581.74	8630.91	18212.65	0.30
12.33	0.89	14.36	6.45	27.23	3.14	6.02	7.64	14.70	11.72	2.99	9545.91	8991.17	18537.09	0.41
11.41	0.79	14.41	6.01	27.10	3.35	6.15	7.68	14.67	11.82	2.79	53490.12	47883.47	101373.59	1.23
13.96	0.92	13.93	6.68	24.16	3.37	6.32	7.18	16.13	12.74	3.47	6882.99	7176.19	14059.18	0.46
20.42	0.86	14.27	7.16	26.80	3.37	6.17	7.81	14.23	11.54	2.57	55466.39	59806.80	115273.19	1.28
											22241.15	27553.16	49794.31	0.95
23.90	0.56	13.75	6.76	23.95	3.73	8.09	8.50	13.38	12.12	3.38				
24.85	0.59	11.98	6.18	22.48	2.91	6.50	7.76	16.32	13.55	3.91				
18.90	0.89	11.96	6.63	23.99	3.17	6.56	8.05	18.43	12.58	2.94				
17.42	0.81	12.68	7.12	26.68	3.26	7.74	2.93	21.62	13.00	2.55				
17.88	0.74	13.43	6.42	23.95	3.84	8.29	8.91	13.70	10.73	3.81				
18.33	0.81	14.80	6.99	26.58	3.20	6.94	8.33	12.84	11.05	2.81				
22.73	0.80	13.62	6.65	25.63	2.96	6.26	7.51	17.21	11.67	2.95				
15.02	0.30	5.47	3.71	14.43	2.72	6.82	6.50	29.88	21.06	6.03				
20.76	0.87	14.90	6.72	25.35	3.10	6.83	7.46	15.30	11.56	2.76				

22.15	0.96	14.76	6.10	24.79	2.79	5.93	7.31	19.36	13.13	1.05				
19.32	1.00	12.68	7.44	20.07	3.45	8.25	6.28	19.73	13.30	3.46				
14.63	0.72	16.71	7.83	24.65	3.40	7.28	8.23	11.65	11.57	2.73	67707.17	81161.27	148868.44	1.48
15.60	0.70	14.63	7.81	21.59	3.76	7.16	7.42	13.88	14.63	3.12	49133.94	47641.38	96775.31	1.82
10.60	0.94	13.87	7.12	25.15	3.27	5.99	7.65	14.58	13.69	2.70	10148.84	6167.45	16316.29	0.32
12.22	0.74	14.85	4.41	24.23	3.62	7.06	7.84	15.12	13.19	3.35	53680.61	66189.26	119869.87	1.26
13.70	0.79	15.35	7.24	25.09	3.62	7.09	8.23	13.51	10.97	2.92	39358.93	54344.99	93703.92	1.26
14.22	0.76	15.33	7.45	25.18	3.62	7.22	8.23	12.75	11.22	2.94	69399.08	123304.30	192703.38	1.74
12.44	0.97	14.78	7.38	25.17	3.20	6.34	7.83	14.48	11.01	2.82	9332.72	8429.29	17762.01	0.40
12.18	0.90	14.80	7.62	24.78	3.68	6.59	7.96	13.85	10.97	3.04	11901.57	9935.19	21836.76	0.53
12.13	0.71	14.10	8.02	23.23	4.41	8.29	7.80	13.94	10.75	2.99	32850.19	47620.72	80470.91	1.21
11.55	1.06	14.92	7.01	26.62	3.55	6.85	8.60	12.21	9.88	2.96	22188.30	12853.13	35041.43	0.66
15.99	0.60	14.96	6.23	28.30	3.18	5.59	10.32	13.03	8.94	2.01	60418.63	116853.42	177272.05	1.20
											32086.79	55724.45	87811.24	1.45
20.19	0.76	15.57	7.61	22.52	3.72	7.65	7.67	13.58	12.25	3.09	59319.62	100107.63	159427.25	1.81
18.95	0.73	14.81	7.57	22.53	3.83	7.51	7.56	14.38	12.46	3.01	43165.42	90948.66	134114.09	1.12
10.14	0.88	14.80	4.22	28.31	3.34	6.02	7.66	15.32	11.77	2.46	30370.62	13037.27	43407.89	0.41
11.68	0.94	15.10	6.98	27.52	3.69	6.45	7.77	13.15	10.27	2.94	10314.66	41359.44	51674.10	0.40
12.61	0.75	15.39	7.87	25.38	3.59	6.72	7.82	13.74	11.08	2.66	38628.42	62474.05	101102.48	0.83
11.27	0.64	14.98	8.19	22.32	4.13	7.57	7.30	13.46	11.47	3.11	88414.13	96989.79	185403.91	1.55
9.81	1.11	15.05	7.51	27.16	3.26	5.77	7.50	14.13	10.70	2.52	26095.28	11899.64	37994.92	0.42
8.92	1.03	15.82	6.68	28.70	3.17	5.96	8.30	11.90	9.64	2.91	7288.17	8599.50	15887.67	0.23
11.24	0.75	15.98	6.56	24.77	4.41	8.49	8.76	9.22	10.33	3.64	40464.84	90952.47	131417.31	0.77
7.36	0.98	14.48	7.03	25.74	3.71	7.10	8.13	13.19	10.42	3.23	8803.39	7296.95	16100.34	0.24
13.60	0.68	16.46	7.53	24.20	4.13	8.18	8.55	10.46	11.10	3.28	42932.38	85765.36	128697.74	0.65
											26920.78	53932.54	80853.32	0.93

13.01	0.66	15.34	8.17	22.41	4.32	8.26	8.04	11.92	11.67	3.34	43716.04	49472.86	93188.91	0.79
13.31	0.49	12.21	6.65	19.63	4.02	7.76	9.04	15.18	14.30	3.08	89825.93	70440.32	160266.25	1.29
8.30	0.84	12.65	6.09	26.51	4.19	6.42	9.76	12.90	11.87	3.04	5221.57	6745.44	11967.01	0.14
12.11	0.62	13.40	7.77	20.67	4.23	8.28	7.49	16.16	13.08	3.03	50643.77	49930.80	100574.57	0.84
11.71	0.51	13.95	7.86	21.31	4.06	8.32	7.72	14.53	12.48	3.61	19675.02	32641.49	52316.52	0.52
13.80	0.66	15.54	7.81	24.57	3.94	7.59	8.53	11.55	11.01	3.03	82794.77	83456.84	166251.61	1.12
9.36	1.05	14.22	6.95	27.43	3.26	6.14	8.38	13.97	10.62	2.58	14685.13	7681.27	22366.40	0.23
8.90	1.02	13.56	7.05	26.65	3.40	5.98	7.73	14.74	11.51	2.96	14260.08	9880.82	24140.91	0.31
14.62	0.54	13.99	7.74	20.63	3.88	7.60	7.45	14.18	15.01	3.42	95321.12	45284.10	140605.22	1.49
7.90	0.83	12.76	7.37	25.53	3.37	6.39	7.71	16.46	12.09	2.52	13855.04	37847.82	51702.86	0.17
12.68	0.63	14.32	7.41	23.78	3.68	7.01	7.96	12.61	12.82	2.97	85724.49	32379.63	118104.12	0.82
											20252.38	16675.67	36928.05	1.02

14.39	0.66	15.87	8.00	21.87	4.08	7.96	7.39	13.78	11.90	3.10	118239.07	77160.38	195399.45	1.89
7.57	1.03	14.68	7.01	27.37	3.37	6.43	6.88	14.17	10.16	3.30	12696.95	6354.02	19050.97	0.23
11.53	0.88	13.46	7.58	22.37	3.61	7.44	6.79	17.24	12.59	3.32	27109.65	20288.87	47398.52	0.60
10.18	0.70	13.72	7.53	23.45	3.45	6.83	7.10	16.64	11.98	3.01	40626.61	36036.15	76662.76	0.60
15.38	0.61	14.36	7.66	21.84	3.88	7.74	7.32	15.09	12.34	3.23	50556.01	58085.76	108641.77	0.85
8.20	0.92	13.03	7.28	24.86	3.56	7.07	6.24	16.07	11.93	3.87	10211.94	7309.17	17521.11	0.35
7.95	1.03	12.94	7.42	26.34	3.75	7.46	8.21	12.40	11.11	3.25	6610.98	7349.71	13960.69	0.21
12.67	0.79	14.48	7.65	23.43	4.20	7.49	8.30	14.11	11.41	3.00	112101.24	91597.75	203698.98	1.54
8.27	1.13	12.95	7.08	25.84	3.22	6.55	7.59	16.44	11.48	2.80	11304.29	9599.39	20903.69	0.23
10.22	0.76	14.57	7.15	23.46	4.22	8.33	7.92	12.40	10.40	3.52	43679.82	46511.32	90191.15	0.59

APPENDIX E: CHAPTER 3 PLFA DATA

Concentrations in ng FA gdw^{-1}

Timestep	MESO	12:0	i13	a13	13:0	i14	14:1w9	14:1w7	14:0	i15	a15	15:1	15:0	16:4*	16:3*	16:2*
T-1M	4	85.21	0.00	0.00	55.94	168.35	36.94	0.00	2123.36	357.61	373.46	602.94	4268.17	0.00	0.00	427.47
T-1M	12	58.85	19.07	23.98	34.20	161.99	0.00	0.00	561.29	322.12	376.06	43.30	397.34	0.00	0.00	235.04
T1.5M	2	88.28	19.20	21.31	56.31	142.09	33.01	0.00	1492.48	275.80	247.59	383.51	3157.88	0.00	69.59	276.63
T1.5M	4	212.50	56.52	25.64	61.03	206.03	46.90	0.00	2618.99	325.47	327.78	324.23	3166.71	0.00	0.00	482.83
T1.5M	6	0.00	0.00	25.05	0.00	77.25	0.00	0.00	226.73	146.97	180.30	19.41	188.11	0.00	0.00	99.86
T1.5M	7	130.69	32.73	30.53	82.61	197.91	71.45	0.00	1979.55	317.15	305.37	381.15	3441.56	0.00	0.00	318.35
T1.5M	10	167.36	30.12	20.14	38.73	138.23	27.11	0.00	1379.17	258.97	269.56	221.98	1782.18	0.00	0.00	238.28
T1.5M	11	35.49	0.00	0.00	0.00	0.00	0.00	0.00	1221.80	138.03	127.34	0.00	1937.88	0.00	0.00	191.25
T1.5M	12	78.02	35.42	15.72	24.71	125.89	0.00	0.00	366.47	237.17	261.17	70.74	258.12	0.00	16.69	154.79
T1.5M	14	46.48	17.71	0.00	19.70	95.94	13.09	0.00	342.12	196.11	213.86	21.24	216.91	0.00	12.41	141.23
T1.5M	16	201.20	53.82	25.58	68.31	188.03	47.41	0.00	3896.94	356.69	327.11	474.85	4143.52	0.00	0.00	536.29
T1.5M	18	49.13	16.66	0.00	14.22	67.18	0.00	0.00	264.08	157.02	170.99	35.97	164.63	0.00	0.00	86.79
T1.5M	25	44.05	27.90	0.00	59.75	193.49	35.90	0.00	2820.32	476.99	432.11	473.41	4783.50	0.00	0.00	487.53
T1.5M	26	46.74	0.00	0.00	28.61	85.86	0.00	0.00	1418.65	170.04	163.38	148.61	1356.84	0.00	0.00	157.77
T7.5M	2	129.50	0.00	37.45	66.13	187.13	56.83	0.00	5690.26	559.53	334.34	252.86	2267.82	0.00	0.00	407.65
T7.5M	4	96.94	0.00	0.00	88.58	0.00	0.00	0.00	2439.97	468.53	327.43	545.97	5071.99	0.00	233.24	0.00
T7.5M	6	57.61	18.55	30.00	25.47	128.44	18.20	0.00	406.54	260.97	267.88	25.47	251.66	0.00	0.00	171.93
T7.5M	7	103.45	0.00	28.46	73.17	165.19	59.25	0.00	4026.88	474.75	309.32	282.27	3054.53	0.00	0.00	305.40
T7.5M	10	79.10	0.00	0.00	39.05	130.99	34.84	0.00	3288.52	318.22	243.08	164.11	1255.48	0.00	51.01	253.57
T7.5M	11	94.34	21.83	0.00	62.24	103.29	39.29	23.43	6665.58	274.51	205.06	0.00	1134.81	0.00	0.00	0.00
T7.5M	12	97.27	29.30	15.77	25.13	102.69	0.00	0.00	329.81	231.99	218.95	54.04	242.35	0.00	15.16	144.73
T7.5M	14	74.03	23.62	23.91	30.64	103.74	26.72	19.46	483.05	227.28	221.30	21.50	297.75	0.00	0.00	212.02
T7.5M	16	93.47	31.87	0.00	51.57	166.33	52.66	0.00	1924.21	376.02	332.43	376.21	2376.35	0.00	0.00	300.93
T7.5M	18	138.95	66.77	0.00	35.88	213.08	0.00	0.00	563.19	452.10	412.80	107.55	323.80	0.00	45.03	283.70
T7.5M	25	65.76	25.04	0.00	36.99	108.77	47.56	19.20	6354.75	352.71	194.95	0.00	1545.87	0.00	0.00	0.00
T7.5M	26	46.32	0.00	0.00	36.40	111.06	0.00	0.00	2269.56	328.13	221.67	109.18	1042.02	0.00	37.56	294.07
T14.5M	2	154.80	43.41	0.00	70.47	164.29	59.86	17.34	4354.11	852.82	365.78	143.52	1818.42	0.00	231.44	505.45
T14.5M	4	103.39	30.43	0.00	55.74	192.41	50.14	0.00	2503.80	584.76	329.92	278.83	2484.06	0.00	393.29	557.68
T14.5M	6	163.44	45.03	32.16	34.63	330.21	0.00	0.00	1293.05	688.91	753.93	8.27	877.62	0.00	0.00	406.28
T14.5M	7	24.40	11.34	0.00	19.71	89.40	12.14	0.00	473.43	215.65	212.49	69.66	551.47	0.00	140.13	86.29

T14.5M	10	72.47	26.80	10.26	35.78	171.93	33.86	0.00	2621.75	485.92	340.02	85.84	760.16	0.00	164.97	401.63
T14.5M	11	107.67	29.43	57.33	80.25	225.72	86.11	30.05	5727.19	821.75	401.30	185.01	2345.44	0.00	93.20	445.97
T14.5M	12	127.08	41.41	28.64	40.43	198.55	24.62	0.00	1319.86	394.21	406.24	126.85	606.54	0.00	0.00	269.67
T14.5M	14	32.18	0.00	0.00	18.07	80.48	0.00	0.00	258.47	176.73	204.02	42.93	216.69	0.00	0.00	108.28
T14.5M	16	102.60	22.69	35.17	80.23	176.37	63.35	0.00	2266.47	441.88	298.86	361.48	3645.39	0.00	0.00	375.00
T14.5M	18	43.65	16.89	0.00	24.06	103.56	12.92	0.00	361.43	241.26	249.21	69.33	230.65	0.00	128.10	72.47
T14.5M	25	64.60	40.81	0.00	46.38	186.38	49.91	0.00	2706.73	619.88	339.15	173.22	1538.75	0.00	296.19	373.01
T14.5M	26	76.07	26.91	35.09	39.74	169.51	40.20	0.00	1954.18	535.59	299.48	33.91	904.18	0.00	0.00	346.53
T6.5P	2	172.00	62.39	0.00	65.54	289.93	57.67	0.00	2537.87	1059.12	492.12	416.86	2574.27	0.00	215.59	403.18
T6.5P	4	258.91	109.74	0.00	133.01	431.13	157.10	0.00	5551.78	1496.22	806.68	572.64	4501.42	0.00	262.05	837.72
T6.5P	6	42.80	16.04	0.00	16.43	78.16	12.75	0.00	225.42	183.69	166.55	9.00	116.08	0.00	0.00	94.80
T6.5P	7	185.84	85.75	0.00	108.59	394.16	86.33	0.00	2529.37	1113.49	658.30	422.86	3361.60	0.00	225.64	519.83
T6.5P	10	72.11	34.54	0.00	37.84	142.44	41.24	0.00	1195.96	405.43	275.95	117.29	925.69	0.00	0.00	259.94
T6.5P	11	188.62	79.19	0.00	100.77	356.78	121.19	0.00	5147.04	1144.88	606.10	356.24	3599.56	0.00	201.13	515.83
T6.5P	12	111.03	34.74	19.18	46.39	181.50	25.33	0.00	648.66	436.62	438.26	56.34	386.39	0.00	0.00	240.11
T6.5P	14	94.72	0.00	25.17	32.43	147.45	0.00	0.00	469.40	285.49	307.86	25.88	243.34	0.00	0.00	173.79
T6.5P	16	182.07	0.00	65.82	122.75	218.07	118.62	0.00	7090.37	879.32	579.75	0.00	6607.17	0.00	0.00	0.00
T6.5P	18	77.21	0.00	0.00	0.00	191.20	0.00	0.00	667.12	411.07	455.48	0.00	397.45	0.00	245.56	0.00
T6.5P	25	90.51	0.00	55.48	77.95	242.46	53.22	0.00	3590.75	964.88	700.22	0.00	5024.41	0.00	222.41	1225.93
T6.5P	26	84.67	0.00	69.75	42.78	123.55	31.19	0.00	956.91	394.41	220.42	140.27	988.70	0.00	99.59	226.29
T27.5P	4	963.51	129.71	34.97	115.88	528.14	104.32	41.59	7555.47	2092.58	882.38	393.18	1904.63	0.00	159.77	884.84
T27.5P	6	35.03	16.11	18.11	26.68	151.36	15.36	0.00	514.98	304.85	319.65	44.32	380.52	0.00	0.00	217.44
T27.5P	7	357.89	64.04	0.00	60.34	290.30	42.01	0.00	1151.31	809.38	524.50	147.99	910.01	0.00	0.00	369.65
T27.5P	10	384.69	48.59	0.00	63.87	274.90	49.33	0.00	1940.26	708.89	573.74	218.32	1558.99	0.00	0.00	377.35
T27.5P	11	205.42	86.97	0.00	137.53	345.56	63.26	0.00	2061.40	1015.17	631.41	241.07	3973.68	0.00	0.00	472.55
T27.5P	12	35.92	16.81	0.00	22.72	105.13	0.00	0.00	336.73	261.41	249.18	15.50	235.45	0.00	0.00	151.32
T27.5P	14	30.67	0.00	0.00	22.36	92.17	0.00	0.00	271.35	194.48	215.45	41.50	222.15	0.00	0.00	122.99
T27.5P	16	516.78	87.32	28.98	336.90	413.90	104.21	40.06	6259.75	1138.92	728.99	1332.89	18096.44	0.00	0.00	531.00
T27.5P	18	70.23	56.89	0.00	0.00	162.75	0.00	0.00	379.87	254.19	271.11	90.24	239.00	0.00	0.00	171.69
T27.5P	25	254.96	71.55	114.42	163.98	232.62	77.89	24.53	2822.48	744.84	463.57	75.41	1894.82	0.00	0.00	448.42

i16	16:1w9	16:1w7	16:1w5	16:0	10Me17br	i17	a17	17:1	17:0	18:3w6	18:4	18:2w6	18:3w3	18:1w9cis
301.82	151.02	7298.66	226.94	8918.80	112.03	137.94	109.49	2036.41	588.72	178.18	394.04	431.35	0.00	1061.58
68.90	113.25	1205.94	125.86	2195.09	130.08	101.60	117.72	337.34	205.63	16.83	56.90	243.32	0.00	478.85
323.07	0.00	4476.37	164.42	6334.72	139.31	169.78	77.81	1430.60	581.46	109.45	232.14	386.61	0.00	612.05
417.07	0.00	6918.31	209.42	10037.09	235.72	202.86	113.51	1359.93	493.70	191.98	410.22	704.82	0.00	1155.92
25.91	64.26	580.63	53.89	961.73	66.88	46.91	56.99	146.16	84.16	0.00	16.29	113.76	0.00	239.63
309.57	123.86	5179.63	176.24	8347.97	153.86	128.31	108.08	1520.55	549.87	160.09	242.01	447.47	0.00	1500.56
208.09	108.00	4153.91	132.76	5517.15	93.79	86.16	89.09	804.24	281.16	131.99	172.00	683.83	0.00	735.64
220.72	77.04	4095.39	101.31	4969.94	42.55	52.23	37.42	658.56	261.61	154.98	165.74	202.25	0.00	454.42
40.52	91.42	830.27	83.10	1428.13	95.00	87.49	85.21	231.99	161.43	13.26	21.25	304.64	0.00	401.17
60.66	75.28	892.41	76.89	1414.81	78.26	66.26	73.52	207.08	151.60	12.07	42.44	206.28	0.00	425.77
471.03	118.42	10624.65	281.41	14011.16	194.94	120.53	102.49	1834.08	547.63	267.69	621.72	966.83	0.00	1390.67
31.87	42.71	622.17	46.44	1062.95	90.46	61.47	56.42	129.12	82.41	36.14	27.35	181.74	0.00	320.71
352.68	156.44	8687.58	311.41	14273.81	190.83	304.41	194.72	2285.43	820.85	281.17	395.77	748.66	0.00	1448.05
167.93	45.82	4299.89	105.40	6818.05	53.31	58.24	50.56	591.10	211.11	156.67	161.11	279.12	0.00	653.41
469.12	451.20	15116.18	372.08	21456.82	176.15	158.75	105.72	1045.97	509.81	381.21	639.20	942.44	0.00	1246.68
1108.83	7296.78	357.55	0.00	10323.53	162.37	264.81	1873.28	521.02	808.32	161.32	409.74	868.78	0.00	1846.94
69.57	90.64	1144.70	88.37	1545.81	118.62	71.94	79.81	239.07	148.70	26.04	44.68	146.44	0.00	348.33
457.36	131.24	11173.08	284.80	17126.78	108.92	124.46	90.84	1315.62	507.31	237.17	419.81	687.74	0.00	1034.33
577.99	167.10	9978.33	242.59	11904.31	121.59	99.71	79.06	646.65	302.54	276.99	246.37	794.99	0.00	697.88
1243.69	0.00	21271.27	269.77	19864.86	77.35	98.04	74.81	536.04	300.51	1023.54	560.36	1326.32	0.00	1378.69
50.49	80.25	919.21	75.07	1405.00	87.19	84.22	79.44	240.76	150.57	0.00	33.20	436.90	0.00	428.50
52.13	106.94	1172.43	113.38	1760.57	83.50	75.43	78.20	305.88	168.49	17.64	47.59	238.50	0.00	878.72
317.52	235.34	5761.10	202.32	8589.17	138.44	116.76	112.70	1315.30	404.30	134.15	309.55	601.95	0.00	787.10
77.36	118.86	1552.76	123.16	2293.65	152.14	207.22	195.89	405.34	411.12	0.00	89.79	500.57	0.00	724.17
0.00	1134.20	16793.68	158.68	17368.97	24.96	89.96	53.70	478.93	280.14	758.84	481.03	985.06	0.00	1202.59
512.77	103.53	7117.98	195.80	9337.36	81.85	79.01	65.49	544.62	261.25	296.73	278.25	581.80	0.00	669.90
713.96	0.00	13065.81	323.40	16882.78	152.56	220.98	726.13	159.75	453.43	424.71	410.24	1176.16	0.00	1570.23
308.31	253.35	7793.72	266.51	10654.35	129.26	163.83	94.06	1351.86	527.45	169.93	387.42	840.42	0.00	1148.52
153.35	183.08	2517.13	240.53	5428.87	365.30	258.39	281.52	760.63	524.25	50.72	97.99	619.62	0.00	1657.41
58.71	0.00	1330.87	81.20	2110.29	106.77	94.75	65.94	385.88	146.85	0.00	117.41	216.25	0.00	288.58

211.19	0.00	8371.26	230.56	11995.93	142.31	157.96	97.02	429.93	251.80	267.24	261.29	744.53	0.00	781.64
500.62	460.77	19697.35	564.58	26815.66	252.73	214.00	167.10	284.89	733.61	742.78	925.58	1682.76	0.00	2156.26
210.13	108.79	3232.84	167.67	4759.51	192.16	211.29	142.72	433.42	390.68	86.37	120.26	644.96	0.00	873.52
22.29	0.00	697.48	56.14	1032.42	85.63	56.95	69.44	174.10	106.08	20.66	23.85	96.54	0.00	302.24
311.25	129.76	6232.19	233.69	10281.04	130.25	172.05	86.45	1900.56	664.22	216.15	263.26	698.19	0.00	1042.73
0.00	0.00	883.02	105.08	1373.91	113.89	75.81	29.06	185.77	148.75	0.00	22.42	93.77	0.00	393.85
468.38	201.41	8754.11	286.31	12263.06	124.74	166.39	102.39	974.46	422.35	215.87	299.41	752.90	0.00	1096.80
487.33	131.25	5554.92	213.56	6019.77	149.88	145.45	85.43	595.58	249.82	183.00	176.27	660.29	0.00	650.65
562.97	450.86	5939.77	414.49	9522.69	183.80	345.21	113.62	1446.06	643.26	126.57	317.86	573.22	0.00	1047.23
1054.51	979.20	14149.48	963.84	23959.28	320.46	568.74	228.02	2447.13	1303.80	261.58	700.56	1184.95	0.00	2279.38
26.90	0.00	610.62	48.98	896.40	88.98	55.73	46.25	87.27	97.48	0.00	0.00	73.73	0.00	178.24
695.33	391.13	7104.61	517.05	10747.43	193.83	358.33	143.20	1939.15	918.61	176.97	316.27	591.08	0.00	1268.23
277.39	164.52	2802.38	142.32	4928.11	104.98	153.53	75.08	476.02	263.55	70.08	119.17	321.31	0.00	519.99
1235.33	188.42	16591.51	1120.82	23081.46	271.30	370.41	177.99	1888.77	789.78	350.80	671.77	990.24	0.00	1496.22
93.68	69.38	1568.83	163.00	2406.72	217.63	135.30	117.57	352.50	255.40	0.00	0.00	179.98	0.00	523.35
49.57	70.38	1092.18	78.12	1793.53	155.28	153.34	107.28	191.26	252.95	381.81	32.90	172.82	0.00	471.65
1712.06	0.00	18665.52	632.97	22368.86	195.06	388.12	0.00	4027.45	1105.94	729.73	578.20	1622.88	0.00	3700.51
0.00	1804.69	191.46	0.00	2480.64	175.42	126.27	243.49	111.26	243.99	0.00	0.00	248.36	0.00	767.99
691.28	0.00	12310.54	603.09	18262.88	376.39	440.95	238.07	3396.36	1311.65	332.56	643.58	1353.04	0.00	4076.69
190.50	189.02	2396.22	168.00	4052.12	105.40	113.51	67.07	718.92	359.35	69.74	80.49	314.26	0.00	1244.51
205.78	997.38	6128.07	731.51	27407.06	299.42	605.51	279.88	1235.77	926.24	2810.94	3053.40	5545.24	0.00	7695.39
61.56	94.23	1076.49	104.64	2001.13	147.22	129.67	102.74	312.96	209.70	23.01	50.01	211.03	0.00	380.31
277.55	208.04	2568.22	246.69	4559.48	162.45	247.18	157.61	629.70	453.04	74.28	193.41	1983.67	0.00	1418.08
437.37	338.36	4669.05	288.02	7979.77	159.76	264.22	192.96	1170.87	583.22	88.99	207.23	1836.37	0.00	1559.16
321.35	190.95	7417.69	361.73	10858.72	208.33	322.03	163.84	2387.33	765.32	206.92	357.29	1089.18	0.00	1664.64
31.37	0.00	831.73	69.04	1439.41	162.58	86.23	83.40	169.23	174.42	41.13	0.00	145.52	0.00	417.70
31.48	48.04	676.57	67.61	1092.94	81.99	58.56	67.82	173.45	105.24	0.00	19.33	108.89	0.00	234.31
579.04	555.50	15313.64	601.34	23336.39	280.54	486.81	0.00	9777.81	2031.87	461.11	770.31	2192.00	0.00	2495.18
37.92	61.46	803.51	73.53	1685.71	140.77	87.63	91.66	170.92	185.00	0.00	28.61	214.77	0.00	395.68
228.20	249.30	3847.45	331.18	9158.62	166.05	257.24	138.44	1184.84	790.60	108.00	791.11	624.89	0.00	3439.05

18:2w3	18:1w9t	18:1w7	18:1w5	18:0	10Me19br	i19*	a19*	19:1*	19:0 i.s.	20:5w6	20:4w6	20:5w3	20:3w6	20:4w3	20:2*
0.00	961.46	79.45	0.00	1139.40	42.92	34.61	39.29	30.31	146.74	0.00	488.82	2438.12	52.74	41.15	89.35
0.00	698.27	68.13	0.00	1054.45	27.14	25.82	16.91	26.42	129.01	0.00	302.29	501.71	0.00	0.00	132.55
0.00	795.11	60.57	23.76	899.19	48.96	33.76	28.72	29.44	362.19	0.00	546.22	1932.35	78.86	80.57	112.43
0.00	1045.92	111.47	36.76	1213.01	98.55	75.45	73.06	52.64	404.30	0.00	480.76	2239.98	78.46	116.53	242.56
0.00	332.87	32.68	0.00	464.84	0.00	0.00	24.98	16.18	58.97	0.00	122.88	223.66	0.00	0.00	81.45
0.00	1291.14	138.72	65.92	1476.34	103.96	100.02	105.15	34.06	346.14	0.00	523.72	1944.80	85.52	86.77	328.95
0.00	725.41	86.17	32.63	917.05	31.50	40.83	21.03	22.52	128.74	0.00	344.35	1216.42	43.65	25.76	67.61
0.00	449.58	0.00	0.00	455.76	34.70	0.00	0.00	16.00	86.08	0.00	294.86	1396.46	49.53	48.12	49.39
0.00	556.53	49.11	24.08	589.89	12.13	34.75	19.43	21.20	122.56	0.00	195.83	307.48	0.00	0.00	59.06
0.00	606.98	55.37	20.85	770.38	35.28	20.37	23.97	19.71	103.20	0.00	241.25	587.41	19.71	14.68	110.70
0.00	1133.41	86.68	32.41	1068.29	81.63	39.10	30.31	39.73	205.87	0.00	776.39	3522.13	82.27	109.22	45.19
0.00	472.55	69.95	58.51	462.44	0.00	26.82	31.71	15.62	96.64	0.00	130.15	307.13	0.00	0.00	72.70
0.00	1633.22	144.23	55.29	1585.20	77.25	37.24	77.68	57.27	273.04	0.00	914.55	3238.48	135.49	238.44	627.50
0.00	576.44	38.19	0.00	510.91	30.58	0.00	46.87	0.00	69.38	0.00	659.96	1276.30	215.88	30.95	30.65
0.00	1796.52	98.55	38.19	1614.12	70.61	31.36	41.29	47.13	264.95	0.00	1075.70	3995.26	169.69	162.86	184.55
0.00	2108.17	0.00	245.97	1733.05	125.74	90.06	104.29	0.00	248.81	0.00	593.89	3001.28	0.00	49.23	296.46
0.00	613.16	48.32	15.16	535.33	23.71	0.00	22.00	39.42	168.25	0.00	247.56	469.03	20.53	13.26	69.30
0.00	1472.69	102.31	37.48	1220.33	46.72	32.30	42.63	39.08	247.94	0.00	776.17	2757.05	99.03	92.32	97.30
0.00	958.73	52.51	0.00	805.58	0.00	0.00	25.70	29.60	152.09	0.00	595.06	1788.16	95.31	56.22	67.89
0.00	1303.32	100.89	92.53	1365.42	186.95	0.00	23.93	19.22	135.15	0.00	1712.04	4485.43	269.16	161.13	46.92
0.00	574.13	47.07	15.92	571.96	14.17	34.94	15.65	23.19	212.02	0.00	185.54	308.80	0.00	0.00	31.30
0.00	746.30	21.26	0.00	787.84	0.00	0.00	0.00	28.02	254.18	0.00	269.56	547.58	0.00	0.00	26.20
0.00	963.51	73.74	31.53	853.24	61.23	0.00	54.63	0.00	235.41	0.00	462.33	1922.36	52.75	58.80	37.13
0.00	1138.61	97.83	46.87	1280.47	58.02	57.94	75.44	56.47	413.82	0.00	1172.93	2040.47	83.76	65.28	141.03
0.00	1414.70	79.57	40.56	890.04	80.16	0.00	0.00	22.59	65.22	0.00	1638.61	4363.88	256.50	178.50	35.25
0.00	1055.26	58.42	0.00	680.37	41.26	0.00	41.56	24.30	173.79	0.00	729.94	2338.96	99.31	55.40	106.60
0.00	2528.73	46.72	17.87	2255.98	0.00	40.31	26.56	67.24	152.71	0.00	1088.29	3092.19	185.18	173.42	248.50
0.00	1772.33	27.60	0.00	1214.55	0.00	32.11	23.31	49.47	131.65	0.00	784.41	2690.28	118.21	121.78	65.84
0.00	1610.86	279.26	164.51	2204.17	154.98	0.00	0.00	0.00	301.94	0.00	438.72	543.77	44.06	69.20	335.58
0.00	428.41	16.11	0.00	420.98	0.00	10.01	11.55	15.23	62.72	0.00	183.71	451.76	19.76	17.30	30.43

0.00	1333.02	23.57	0.00	1042.04	0.00	27.70	19.91	33.08	162.40	0.00	708.70	1915.29	132.13	92.41	86.93
0.00	2691.94	90.24	596.56	2295.65	0.00	642.88	29.81	41.79	497.13	0.00	1206.60	2943.14	307.60	150.79	1189.29
0.00	1369.24	85.57	28.84	1467.21	64.36	58.39	47.38	51.41	192.46	0.00	751.11	1779.26	54.78	77.61	35.84
0.00	403.99	41.09	197.98	476.82	0.00	17.35	44.09	14.60	131.81	0.00	134.90	213.30	0.00	0.00	105.95
0.00	1611.99	87.74	24.00	1229.86	0.00	26.67	17.24	40.22	245.92	0.00	880.27	2343.39	163.44	140.71	130.30
0.00	505.08	0.00	0.00	542.59	0.00	14.97	15.62	27.77	105.78	195.57	194.20	355.73	0.00	0.00	108.63
0.00	2146.37	35.14	0.00	1248.73	0.00	44.13	27.94	85.78	172.78	0.00	840.27	2329.53	145.08	106.57	95.98
0.00	1397.96	13.22	13.37	699.59	0.00	26.56	27.23	55.55	306.93	0.00	734.52	1738.13	97.00	60.97	138.58
0.00	2556.30	51.29	0.00	1767.36	0.00	0.00	0.00	123.02	218.05	0.00	1142.41	2276.39	87.89	0.00	370.19
0.00	5211.78	0.00	0.00	3305.92	0.00	0.00	113.76	117.81	442.17	0.00	1652.21	4415.58	114.61	154.45	546.96
0.00	341.95	0.00	0.00	456.65	0.00	0.00	0.00	20.55	96.71	0.00	84.56	136.18	0.00	0.00	54.63
0.00	2954.58	0.00	0.00	2191.22	0.00	0.00	0.00	159.99	250.09	0.00	1427.64	3135.34	90.84	72.00	457.89
0.00	957.91	0.00	0.00	940.75	0.00	0.00	0.00	37.84	126.51	0.00	602.12	1086.45	47.56	0.00	136.57
0.00	3659.60	0.00	0.00	2856.84	110.80	0.00	0.00	0.00	278.68	0.00	1494.33	4463.13	228.91	181.41	2692.24
0.00	989.63	0.00	0.00	881.31	55.78	37.72	24.52	58.71	145.46	0.00	359.46	476.46	0.00	0.00	167.25
0.00	626.10	67.99	179.35	980.18	24.93	38.75	225.51	38.28	239.90	0.00	185.64	260.64	0.00	0.00	464.07
0.00	3540.89	78.43	0.00	2362.02	493.09	0.00	0.00	98.46	105.18	0.00	3096.60	7386.32	373.54	114.07	184.65
0.00	863.07	0.00	0.00	876.77	0.00	0.00	0.00	46.38	238.49	0.00	301.01	413.39	0.00	0.00	0.00
0.00	4789.15	159.18	0.00	3145.60	234.03	0.00	0.00	184.26	440.41	0.00	2641.19	6501.71	277.27	374.82	222.64
0.00	1192.47	0.00	0.00	912.71	21.63	0.00	0.00	68.01	128.64	0.00	746.82	1181.73	98.69	27.55	101.01
0.00	5069.43	400.64	128.95	5399.33	0.00	76.40	75.68	175.04	340.32	0.00	11111.77	6554.13	1043.00	367.89	941.40
0.00	550.24	70.03	32.36	724.77	27.85	22.47	6.77	34.34	172.31	0.00	251.95	266.64	16.49	36.01	71.82
0.00	1520.96	156.49	56.75	1278.05	0.00	32.47	37.45	77.23	197.10	0.00	815.02	980.68	58.46	31.23	136.69
0.00	2010.51	238.85	96.84	2021.29	0.00	85.46	73.29	62.68	221.20	0.00	1410.58	2022.66	116.13	110.53	368.89
0.00	2356.82	202.75	78.78	1768.54	0.00	33.22	105.89	77.52	158.24	0.00	1498.90	2948.86	160.24	108.65	303.69
0.00	516.43	0.00	0.00	563.89	21.34	0.00	21.84	39.56	258.17	0.00	163.90	181.11	0.00	0.00	116.82
0.00	363.87	37.22	0.00	511.54	0.00	0.00	0.00	17.31	113.09	0.00	148.92	180.89	0.00	0.00	51.63
0.00	3038.28	212.78	66.97	2268.99	0.00	90.43	348.58	96.61	342.25	0.00	2930.84	6038.93	313.18	242.01	201.69
0.00	595.97	80.83	27.07	1062.92	25.84	26.17	33.42	39.17	245.83	0.00	199.08	232.04	0.00	0.00	106.68
0.00	2356.95	79.84	40.16	1910.99	77.73	0.00	0.00	140.13	186.48	0.00	1197.14	2390.85	137.69	105.88	117.03

20:3w3	20:1w9	20:1w7	20:1w5	20:0 i.s.	21:0 i.s.	22:6w6*	22:6w3	22:5w6*	22:5w3*	22:2*	22:1w9	22:1w7*	22:0	23:0 i.s.	24:1
67.05	167.58	142.72	0.00	1132.49	3086.58	62.14	523.43	0.00	105.63	47.78	32.17	24.39	517.79	1269.59	52.85
60.02	83.10	0.00	0.00	1090.05	1880.87	35.48	160.26	56.93	70.35	47.30	0.00	18.25	475.56	1327.48	72.94
80.23	235.41	44.74	0.00	983.02	2197.17	57.14	448.24	62.44	139.00	64.83	63.59	40.94	397.54	1379.09	107.96
55.84	218.68	94.18	0.00	1395.08	1409.38	64.58	534.46	154.93	194.93	400.96	55.18	28.71	660.64	1662.70	579.44
23.76	45.96	0.00	0.00	380.93	2852.35	0.00	61.72	0.00	0.00	91.23	0.00	0.00	146.26	610.01	0.00
53.00	213.77	118.27	0.00	1161.19	1814.39	54.79	568.77	369.30	220.40	531.57	54.93	25.58	514.90	1734.56	642.82
41.29	114.15	61.23	0.00	619.55	1560.17	36.36	267.07	70.00	87.80	46.59	29.24	0.00	315.00	1125.91	100.40
0.00	95.95	0.00	0.00	294.74	1909.79	0.00	342.01	27.62	83.70	28.66	87.58	19.19	193.22	517.90	0.00
32.42	74.70	0.00	0.00	766.86	1326.22	25.47	110.61	47.18	59.78	29.64	0.00	0.00	311.00	941.38	53.61
52.66	147.73	0.00	0.00	513.18	1885.08	41.73	258.32	46.76	77.21	107.22	0.00	0.00	224.62	695.90	175.97
70.78	193.18	203.38	0.00	1055.08	2527.61	90.62	714.07	93.49	196.30	69.47	59.71	21.92	499.51	980.33	156.06
16.36	37.81	0.00	0.00	265.01	2164.90	17.58	83.79	70.05	75.40	89.89	0.00	0.00	125.90	913.60	137.12
0.00	338.34	123.61	0.00	1682.04	2730.84	139.12	919.50	137.18	332.91	78.17	42.19	40.00	776.52	1860.76	73.97
36.24	200.35	73.26	0.00	380.77	2059.15	34.36	249.85	38.65	75.37	19.62	20.19	0.00	199.29	708.82	51.48
82.98	311.17	166.06	0.00	997.00	2615.95	106.89	935.32	137.54	247.80	66.52	65.60	40.05	600.31	1020.89	69.91
0.00	349.07	0.00	0.00	656.69	5629.94	0.00	1096.10	177.64	307.03	242.54	240.73	0.00	514.12	1657.09	337.58
33.94	77.43	0.00	0.00	773.58	1715.92	0.00	160.65	28.12	44.33	41.08	0.00	13.75	316.13	877.35	0.00
73.60	294.84	0.00	0.00	877.52	3013.76	71.30	668.21	103.46	207.03	60.99	66.39	52.11	500.80	1148.00	63.07
48.99	231.03	154.03	0.00	702.40	2809.67	50.36	274.19	55.33	103.37	0.00	0.00	0.00	368.85	1023.31	80.91
0.00	343.56	0.00	272.21	387.76	1293.22	0.00	673.27	90.60	210.91	36.69	55.57	35.91	239.23	381.02	0.00
31.66	66.53	0.00	0.00	594.75	1316.84	25.72	99.31	30.72	38.57	16.62	0.00	0.00	257.43	933.42	38.43
51.90	78.61	0.00	0.00	790.85	2216.60	39.06	159.46	42.43	78.20	41.78	0.00	15.37	315.21	1198.24	0.00
67.19	240.39	84.72	0.00	851.01	3172.49	52.70	527.51	61.06	149.17	29.79	50.89	29.66	405.77	1259.02	40.72
607.80	263.63	0.00	0.00	1739.57	3380.72	161.76	507.63	91.17	138.17	220.16	0.00	218.60	687.87	1402.99	405.73
0.00	464.66	0.00	263.64	363.49	1419.21	0.00	664.87	62.28	210.66	48.65	0.00	27.89	220.93	321.96	0.00
48.51	268.99	0.00	0.00	422.94	2422.67	73.79	495.76	64.34	131.73	34.43	40.67	22.24	209.66	872.18	63.31
109.64	415.92	87.74	0.00	481.64	1424.65	102.58	647.78	82.45	381.11	209.63	125.15	97.90	405.38	979.49	70.77
178.27	0.00	283.28	0.00	662.72	1645.24	105.15	715.72	107.65	293.96	69.44	119.70	85.00	523.61	980.83	109.72
83.26	160.12	0.00	0.00	2473.28	2231.22	0.00	61.59	254.63	172.22	408.21	0.00	22.11	928.31	1081.15	0.00
22.63	0.00	52.41	0.00	517.30	1250.44	21.53	111.06	21.50	55.36	20.25	59.70	14.81	239.65	933.20	0.00

56.16	150.16	0.00	0.00	991.40	1244.01	86.45	421.52	79.19	164.25	46.27	27.80	35.65	488.85	1129.65	74.27
68.60	363.54	133.13	0.00	1025.69	2310.32	127.39	655.39	334.47	481.61	1842.46	46.92	70.13	2976.58	1210.03	105.13
74.64	172.82	76.52	0.00	1806.78	1302.54	105.51	772.27	118.01	134.14	207.18	0.00	121.53	617.27	1076.22	249.44
19.46	60.34	0.00	0.00	484.80	1359.11	16.99	70.67	38.52	35.22	161.77	0.00	0.00	189.58	914.14	259.16
123.76	231.06	0.00	0.00	852.70	1151.96	84.26	563.97	89.62	248.43	36.56	61.98	34.35	444.13	871.10	76.27
0.00	83.45	0.00	0.00	568.03	4165.98	43.24	137.98	27.92	39.76	28.70	10.53	0.00	261.64	1095.54	61.15
137.13	302.57	71.59	0.00	722.33	2395.62	86.73	511.23	89.03	269.09	58.26	51.65	54.12	424.67	602.67	55.91
50.24	144.28	0.00	0.00	707.55	1717.80	76.46	302.80	85.02	172.46	40.75	26.05	29.24	261.17	801.35	51.59
0.00	382.10	114.68	0.00	887.02	4312.99	124.68	578.98	124.73	204.38	89.48	30.42	42.73	600.65	942.91	220.08
0.00	864.47	252.06	0.00	1851.92	10118.63	184.04	1114.82	206.46	400.08	215.87	0.00	132.08	1744.74	1752.12	314.08
0.00	45.81	0.00	0.00	486.16	1238.58	14.08	48.26	13.27	18.85	22.82	0.00	0.00	204.56	699.42	0.00
0.00	313.87	0.00	0.00	1213.16	5811.89	170.11	841.67	161.92	308.61	54.23	0.00	47.72	717.80	1609.88	58.77
0.00	204.62	0.00	0.00	508.52	4253.95	49.22	227.61	43.41	100.99	0.00	0.00	29.70	322.36	1301.55	80.41
0.00	0.00	507.00	0.00	1320.45	8895.78	171.83	796.72	144.78	502.58	66.64	0.00	59.67	814.52	1218.89	0.00
0.00	174.06	0.00	0.00	1320.60	1586.04	46.80	155.78	58.07	74.86	33.61	0.00	16.36	605.32	1260.42	0.00
33.76	90.05	0.00	0.00	1096.07	1645.09	25.63	88.64	73.98	77.97	558.49	0.00	0.00	597.91	1329.04	572.66
428.02	583.61	0.00	128.59	515.08	3341.97	200.56	1332.41	192.27	554.16	52.42	97.38	43.57	442.39	958.46	0.00
0.00	257.96	0.00	0.00	1293.30	6221.35	0.00	121.03	0.00	0.00	0.00	42.71	0.00	506.58	1387.61	94.30
420.96	864.28	0.00	123.13	2174.04	3838.69	289.01	1847.49	234.36	790.08	119.96	106.34	116.70	1100.02	853.75	0.00
67.69	131.11	0.00	0.00	410.74	2919.35	79.29	405.73	64.06	127.78	35.33	0.00	24.22	257.78	1025.95	0.00
1152.78	0.00	473.95	691.67	1715.13	2682.50	1599.59	1496.93	283.00	434.18	249.90	213.96	76.91	1545.54	1943.69	1360.54
36.21	49.29	0.00	0.00	1349.32	2303.30	31.15	95.66	39.78	38.72	38.49	29.18	20.92	549.55	1521.01	0.00
83.33	144.01	0.00	0.00	1200.42	3900.29	101.93	322.96	81.86	109.86	119.02	32.16	0.00	660.16	1634.48	120.65
117.33	236.59	0.00	0.00	1648.68	3356.77	159.22	604.29	208.31	262.32	315.58	183.18	40.81	736.27	1514.67	84.29
132.42	267.66	0.00	0.00	1157.21	4289.96	190.78	826.42	144.94	242.00	143.75	55.43	0.00	658.25	1691.83	112.68
0.00	104.05	0.00	0.00	812.46	2032.05	20.95	69.63	29.86	0.00	46.00	0.00	15.86	314.79	1581.99	0.00
19.05	50.37	0.00	0.00	522.06	1579.78	18.59	66.02	0.00	0.00	73.29	0.00	0.00	210.86	1040.84	84.14
259.35	419.60	192.55	0.00	1553.14	3563.54	320.14	1287.31	187.57	387.38	69.21	209.93	64.37	901.15	1596.17	209.54
25.99	80.72	0.00	0.00	1150.73	2632.51	25.81	93.26	52.47	55.92	86.58	0.00	0.00	426.11	1094.55	151.60
220.40	213.44	0.00	0.00	1379.30	2408.94	126.44	1081.95	108.73	215.85	45.84	25.32	31.93	842.05	777.23	0.00

24:0	25:0	26:0	27:0	28:0	29:0	30:0	31:0	32:0	Total	Sat FA's	Mono Unsat	Polyunsat	Br FA's	% Sat FA's
865.14	123.19	514.87	76.92	365.47	66.23	304.59	0.00	0.00	39943.98	20013.78	12905.43	5347.23	1677.54	50.10
793.01	129.14	547.86	93.50	450.25	89.74	399.70	0.00	0.00	14067.62	7485.62	3314.70	1918.98	1348.33	53.21
617.92	86.35	355.75	59.87	262.72	51.92	226.29	0.00	0.00	29374.30	14668.70	8541.99	4676.72	1486.90	49.94
895.46	118.41	543.02	95.82	415.03	197.88	349.50	0.00	0.00	41827.97	21078.80	12319.84	6353.82	2075.51	50.39
190.46	26.53	235.58	28.35	139.85	31.90	134.43	0.00	125.88	6002.33	2984.82	1556.72	834.59	626.19	49.73
778.62	102.79	447.95	73.56	307.79	293.60	262.11	0.00	0.00	38156.70	18789.90	11601.92	5935.50	1829.38	49.24
490.33	69.10	285.59	44.21	172.96	32.97	0.00	0.00	0.00	23608.85	11492.97	7405.64	3473.00	1237.24	48.68
262.97	35.15	195.12	37.54	170.72	24.15	141.29	0.00	123.80	19809.03	10066.45	6055.02	3034.56	653.00	50.82
483.19	77.34	330.44	58.40	225.49	76.15	197.01	0.00	0.00	9581.74	4665.79	2539.09	1378.11	998.74	48.69
297.57	42.32	176.68	27.48	111.00	22.01	89.90	0.00	0.00	9545.91	3953.55	2756.07	1972.06	864.22	41.42
759.10	86.29	398.84	72.68	311.51	288.70	284.74	0.00	0.00	53490.12	26638.43	16777.37	8162.45	1911.87	49.80
203.24	35.06	210.38	35.74	131.18	31.01	116.28	0.00	0.00	6882.99	2988.63	2005.34	1195.07	693.95	43.42
1244.28	176.37	730.60	113.32	537.49	102.52	451.69	0.00	0.00	55466.39	28520.28	15934.23	8674.46	2337.41	51.42
296.40	35.96	155.81	22.51	86.82	0.00	0.00	0.00	0.00	22241.15	11187.70	6804.17	3422.51	826.77	50.30
1074.39	106.87	488.70	75.00	361.47	70.63	313.30	0.00	0.00	67707.17	34825.15	21212.44	9535.60	2133.99	51.43
666.05	0.00	495.04	327.93	319.35	160.20	0.00	276.48	0.00	49133.94	23321.54	13849.79	7437.26	4525.35	47.47
30.03	73.97	348.16	64.81	302.65	65.85	271.64	59.95	274.12	10148.84	4778.42	2810.59	1516.89	1042.94	47.08
912.51	99.50	424.81	65.25	303.42	57.67	258.08	0.00	0.00	53680.61	28734.50	16437.03	6656.59	1852.49	53.53
646.18	76.36	335.47	53.68	209.35	40.36	161.67	0.00	0.00	39358.93	19566.48	13438.31	4757.79	1596.35	49.71
366.08	40.11	192.74	29.82	124.84	27.29	109.57	23.61	110.50	69399.08	30751.55	25763.55	10596.34	2287.63	44.31
401.31	72.47	296.71	58.88	237.96	53.19	206.55	0.00	0.00	9332.72	4406.59	2608.16	1398.24	919.73	47.22
486.20	77.68	333.33	60.88	267.51	56.05	247.36	0.00	259.35	11901.57	5705.95	3582.13	1771.92	841.57	47.94
565.31	75.65	315.29	52.34	213.54	41.40	168.08	0.00	0.00	32850.19	16129.69	10277.05	4767.38	1676.07	49.10
878.19	140.48	697.73	123.75	600.65	118.21	516.81	0.00	0.00	22188.30	8810.74	5326.33	6149.24	1901.98	39.71
316.77	30.25	167.17	29.33	127.39	12.04	110.56	0.00	98.82	60418.63	27655.78	22173.47	9684.16	905.21	45.77
360.23	35.43	174.74	24.74	102.61	0.00	81.93	0.00	0.00	32086.79	14662.61	10274.20	5667.18	1482.80	45.70
837.29	66.29	330.90	61.43	214.53	46.59	193.72	0.00	0.00	59319.62	28146.12	18841.35	9068.76	3263.39	47.45
786.73	78.67	401.99	58.65	259.68	50.21	192.33	192.33	0.00	43165.42	20087.54	13620.49	7599.43	1857.96	46.54
1167.50	151.88	812.31	24.55	778.81	248.99	641.97	137.64	699.04	30370.62	16117.06	7681.09	3585.87	2986.60	53.07
419.15	64.90	277.96	46.46	192.47	38.98	141.01	0.00	0.00	10314.66	5167.72	2766.31	1515.37	865.26	50.10

994.94	116.44	537.20	19.53	394.93	74.85	291.10	0.00	0.00	38628.42	19697.76	11647.71	5628.98	1653.98	50.99
1225.13	134.48	669.09	147.84	511.94	107.04	391.86	0.00	0.00	88414.13	44269.43	27691.14	13197.65	3255.92	50.07
810.80	122.79	533.04	89.29	391.76	158.22	310.65	0.00	0.00	26095.28	11745.14	7193.14	5231.59	1925.42	45.01
258.60	41.78	247.81	36.70	148.34	28.96	108.40	0.00	34.13	7288.17	3235.06	2250.05	1046.10	756.97	44.39
787.81	79.20	355.91	48.97	229.90	41.55	0.00	0.00	0.00	40464.84	20257.28	12189.23	6357.31	1661.02	50.06
389.92	47.74	150.40	60.45	234.86	24.58	0.00	212.76	49.27	8803.39	4156.66	2354.86	1448.49	843.38	47.22
575.82	55.05	269.75	42.51	174.42	33.73	0.00	0.00	0.00	42932.38	19866.55	14380.17	6606.27	2079.39	46.27
444.83	51.61	224.38	30.06	134.72	27.88	0.00	0.00	0.00	26920.78	11118.00	9013.33	4863.00	1926.45	41.30
1269.52	100.58	506.94	92.82	357.86	82.37	322.58	61.46	0.00	43716.04	20677.77	13355.96	6635.54	3046.77	47.30
2142.93	189.26	912.63	0.00	0.00	0.00	0.00	0.00	0.00	89825.93	44003.69	28550.81	12251.93	5019.51	48.99
311.17	51.32	206.11	0.00	18.50	0.00	0.00	0.00	0.00	5221.57	2642.93	1371.19	561.18	646.27	50.62
1549.71	140.79	736.11	0.00	0.00	0.00	0.00	0.00	0.00	50643.77	23187.06	15350.03	8550.04	3556.64	45.78
557.74	63.69	259.23	0.00	0.00	0.00	0.00	0.00	0.00	19675.02	9567.00	5608.78	3064.44	1434.80	48.63
1489.13	142.85	769.65	0.00	0.00	0.00	0.00	0.00	0.00	82794.77	38980.22	26068.63	13472.34	4273.59	47.08
946.82	146.64	556.12	0.00	41.29	70.66	0.00	0.00	0.00	14685.13	7102.76	4051.41	1792.37	1738.59	48.37
720.70	112.45	528.19	79.33	386.14	84.81	329.29	0.00	0.00	14260.08	6705.38	3529.08	2530.15	1495.47	47.02
767.45	90.21	327.77	52.89	249.17	49.25	214.54	0.00	195.17	95321.12	42228.03	31781.79	16845.82	4465.48	44.30
722.66	56.80	0.00	64.24	325.39	46.30	0.00	277.80	0.00	13855.04	6742.96	4179.80	1329.35	1602.93	48.67
1376.76	155.40	785.85	144.27	743.84	149.76	707.86	151.60	681.65	85724.49	37500.76	26838.43	17497.02	3888.28	43.75
46.28	59.06	340.25	54.73	279.24	54.35	233.93	0.00	193.30	20252.38	8916.15	6373.68	3726.06	1236.49	44.03
1321.39	154.70	830.99	92.01	720.83	88.92	395.08	0.00	0.00	118239.07	49421.59	26082.97	37688.76	5045.75	41.80
898.06	147.93	597.07	93.72	439.16	83.13	371.01	0.00	77.09	12696.95	7149.53	2848.88	1424.41	1274.13	56.31
1099.86	124.29	518.26	77.42	354.53	71.03	0.00	0.00	0.00	27109.65	11675.67	7433.01	5462.07	2538.91	43.07
1289.03	165.56	713.55	146.13	420.64	74.81	276.70	0.00	0.00	40626.61	18354.78	11295.46	8205.79	2770.59	45.18
1050.72	125.28	581.25	77.18	352.31	54.26	347.43	0.00	0.00	50556.01	23017.31	15565.28	8826.61	3146.81	45.53
578.35	107.23	583.86	111.00	520.24	109.64	433.47	88.05	372.15	10211.94	6027.32	2195.91	966.23	1022.48	59.02
287.08	43.11	182.51	31.36	127.24	20.25	106.37	0.00	0.00	6610.98	3265.04	1794.38	809.60	741.96	49.39
1516.93	171.29	670.56	96.84	416.43	76.44	297.66	0.00	0.00	112101.24	56994.44	34847.56	16192.02	4067.22	50.84
631.56	95.47	444.51	80.92	340.79	308.56	301.70	0.00	0.00	11304.29	6252.34	2627.60	1292.90	1131.46	55.31
1157.61	116.53	617.69	149.24	439.40	95.93	424.29	96.67	411.65	43679.82	21347.52	12303.40	7720.22	2308.69	48.87

% Mono Unsat	% Polyunsat	% Br FA's	BrOdd FA	PUFA (3+)	%BrOdd FA	%PUFA (3+)	SCFA	LCFA	TARFA	18PUFA	BoshkerBact
32.31	13.39	4.20	1207.36	4351.27	3.02	10.89	11127.37	2834.19	0.25	1003.57	1280.70
23.56	13.64	9.58	1160.48	1260.76	8.25	8.96	2815.23	2978.77	1.06	317.05	997.20
29.08	15.92	5.06	1062.25	3836.22	3.62	13.06	7915.48	2058.36	0.26	728.19	1049.12
29.45	15.19	4.96	1534.57	4522.66	3.67	10.81	12868.58	3275.76	0.25	1307.01	1387.82
25.94	13.90	10.43	548.09	448.30	9.13	7.47	1188.47	1059.24	0.89	130.04	463.10
30.41	15.56	4.79	1385.16	4309.16	3.63	11.29	10458.21	2781.31	0.27	849.56	1268.72
31.37	14.71	5.24	941.18	2436.69	3.99	10.32	7063.69	1410.16	0.20	987.83	961.02
30.57	15.32	3.30	432.28	2563.02	2.18	12.94	6227.24	1183.96	0.19	522.97	486.09
26.50	14.38	10.42	883.48	829.97	9.22	8.66	1872.63	1759.02	0.94	339.15	713.85
28.87	20.66	9.05	725.33	1406.64	7.60	14.74	1803.41	991.56	0.55	260.79	621.94
31.37	15.26	3.57	1332.20	6544.68	2.49	12.24	18109.30	2701.37	0.15	1856.23	1429.54
29.13	17.36	10.08	611.56	763.96	8.89	11.10	1376.16	888.77	0.65	245.23	497.02
28.73	15.64	4.21	1819.13	6732.61	3.28	12.14	17138.18	4132.80	0.24	1425.61	1599.50
30.59	15.39	3.72	572.98	2935.35	2.58	13.20	8283.43	796.80	0.10	596.90	625.41
31.33	14.08	3.15	1515.19	7934.45	2.24	11.72	27276.59	3090.68	0.11	1962.85	1648.66
28.19	15.14	9.21	3416.51	6029.47	6.95	12.27	12860.43	2759.17	0.21	1439.85	1904.80
27.69	14.95	10.28	893.49	1088.14	8.80	10.72	2009.95	1807.31	0.90	217.16	775.17
30.62	12.40	3.45	1258.40	5505.16	2.34	10.26	21257.12	2622.04	0.12	1344.73	1508.93
34.14	12.09	4.06	887.37	3641.35	2.25	9.25	15271.93	1891.91	0.12	1318.35	1322.79
37.12	15.27	3.30	962.48	9186.41	1.39	13.24	26624.79	1263.79	0.05	2910.21	1927.44
27.95	14.98	9.85	811.63	768.69	8.70	8.24	1832.09	1584.49	0.86	470.10	651.18
30.10	14.89	7.07	733.24	1253.43	6.16	10.53	2317.66	2103.57	0.91	303.73	625.70
31.28	14.51	5.10	1224.09	3797.58	3.73	11.56	10606.85	1837.37	0.17	1045.65	1266.05
24.01	27.71	8.57	1678.32	5003.77	7.56	22.55	2995.79	3763.69	1.26	590.36	1253.17
36.70	16.03	1.50	821.48	8615.19	1.36	14.26	23789.48	1113.27	0.05	2224.94	735.99
32.02	17.66	4.62	858.98	4650.27	2.68	14.49	11653.24	989.34	0.08	1156.78	1232.05
31.76	15.29	5.50	2428.55	6929.02	4.09	11.68	21391.69	2156.13	0.10	2011.11	2143.57
31.55	17.61	4.30	1387.68	6066.05	3.21	14.05	13261.54	2544.20	0.19	1397.76	1443.00
25.29	11.81	9.83	2580.22	1816.17	8.50	5.98	6885.37	5591.01	0.81	768.33	2205.67
26.82	14.69	8.39	728.49	1162.15	7.06	11.27	2608.12	1420.58	0.54	333.66	592.36

30.15	14.57	4.28	1307.91	4349.61	3.39	11.26	14690.15	2917.83	0.20	1273.06	1232.64
31.32	14.93	3.68	2616.33	8037.15	2.96	9.09	32650.52	6163.96	0.19	3351.13	2039.64
27.56	20.05	7.38	1586.79	4073.95	6.08	15.61	6206.46	3033.82	0.49	851.59	1294.69
30.87	14.35	10.39	654.20	573.56	8.98	7.87	1323.08	1094.32	0.83	141.05	524.61
30.12	15.71	4.10	1231.26	5117.27	3.04	12.65	12650.11	1987.47	0.16	1177.60	1316.11
26.75	16.45	9.58	756.71	1144.92	8.60	13.01	1778.99	1431.63	0.80	116.20	594.03
33.49	15.39	4.84	1465.44	5326.11	3.41	12.41	15034.39	1575.96	0.10	1268.18	1648.93
33.48	18.06	7.16	1331.62	3676.86	4.95	13.66	8050.02	1174.66	0.15	1019.56	1505.12
30.55	15.18	6.97	2256.27	5199.48	5.16	11.89	12232.56	3394.78	0.28	1017.65	2455.44
31.78	13.64	5.59	3643.62	9466.44	4.06	10.54	29769.98	4989.56	0.17	2147.09	3788.53
26.26	10.75	12.38	557.25	315.20	10.67	6.04	1164.62	791.67	0.68	73.73	455.31
30.31	16.88	7.02	2552.90	6927.01	5.04	13.68	13462.63	3144.41	0.23	1084.32	2861.27
28.51	15.58	7.29	1049.51	2346.61	5.33	11.93	6196.18	1203.01	0.19	510.56	1101.21
31.49	16.27	5.16	2760.67	9207.39	3.33	11.12	28417.12	3216.15	0.11	2012.81	3343.08
27.59	12.21	11.84	1517.34	1171.42	10.33	7.98	3166.42	2366.85	0.75	179.98	1150.07
24.75	17.74	10.49	1323.62	1160.98	9.28	8.14	2357.65	2838.83	1.20	587.53	858.36
33.34	17.67	4.68	2601.16	14985.87	2.73	15.72	29641.30	2388.85	0.08	2930.81	3467.63
30.17	9.59	11.57	1411.73	1080.99	10.19	7.80	3224.97	1999.78	0.62	248.36	1057.75
31.31	20.41	4.54	3010.02	14575.45	3.51	17.00	21944.14	5997.01	0.27	2329.18	2758.02
31.47	18.40	6.11	992.19	3049.17	4.90	15.06	5093.70	1518.91	0.30	464.49	928.87
22.06	31.88	4.27	4476.52	30067.38	3.79	25.43	35926.04	5149.46	0.14	11409.57	4109.51
22.44	11.22	10.03	1095.43	885.62	8.63	6.98	2551.14	3256.73	1.28	284.04	907.45
27.42	20.15	9.37	2035.09	2853.03	7.51	10.52	6068.67	2905.56	0.48	2251.36	2058.23
27.80	20.20	6.82	2106.91	5307.59	5.19	13.06	10304.72	3822.68	0.37	2132.59	2233.75
30.79	17.46	6.22	2566.88	6817.43	5.08	13.48	13125.55	3246.69	0.25	1653.39	2516.24
21.50	9.46	10.01	902.80	506.57	8.84	4.96	1812.06	3218.77	1.78	186.65	647.08
27.14	12.25	11.22	618.31	452.81	9.35	6.85	1394.97	1008.78	0.72	128.22	570.79
31.09	14.44	3.63	3190.58	13198.12	2.85	11.77	30112.92	4147.31	0.14	3423.41	3073.63
23.24	11.44	10.01	987.68	713.18	8.74	6.31	2135.81	2629.61	1.23	243.38	806.80
28.17	17.67	5.29	2033.84	6484.04	4.66	14.84	12236.06	4351.06	0.36	1524.00	1749.07

%SCFA	%LCFA	%18PUFA	%BoshkerBact
27.86	7.10	2.51	3.21
20.01	21.17	2.25	7.09
26.95	7.01	2.48	3.57
30.77	7.83	3.12	3.32
19.80	17.65	2.17	7.72
27.41	7.29	2.23	3.33
29.92	5.97	4.18	4.07
31.44	5.98	2.64	2.45
19.54	18.36	3.54	7.45
18.89	10.39	2.73	6.52
33.86	5.05	3.47	2.67
19.99	12.91	3.56	7.22
30.90	7.45	2.57	2.88
37.24	3.58	2.68	2.81
40.29	4.56	2.90	2.43
26.17	5.62	2.93	3.88
19.80	17.81	2.14	7.64
39.60	4.88	2.51	2.81
38.80	4.81	3.35	3.36
38.36	1.82	4.19	2.78
19.63	16.98	5.04	6.98
19.47	17.67	2.55	5.26
32.29	5.59	3.18	3.85
13.50	16.96	2.66	5.65
39.37	1.84	3.68	1.22
36.32	3.08	3.61	3.84
36.06	3.63	3.39	3.61
30.72	5.89	3.24	3.34
22.67	18.41	2.53	7.26
25.29	13.77	3.23	5.74

38.03	7.55	3.30	3.19
36.93	6.97	3.79	2.31
23.78	11.63	3.26	4.96
18.15	15.01	1.94	7.20
31.26	4.91	2.91	3.25
20.21	16.26	1.32	6.75
35.02	3.67	2.95	3.84
29.90	4.36	3.79	5.59
27.98	7.77	2.33	5.62
33.14	5.55	2.39	4.22
22.30	15.16	1.41	8.72
26.58	6.21	2.14	5.65
31.49	6.11	2.59	5.60
34.32	3.88	2.43	4.04
21.56	16.12	1.23	7.83
16.53	19.91	4.12	6.02
31.10	2.51	3.07	3.64
23.28	14.43	1.79	7.63
25.60	7.00	2.72	3.22
25.15	7.50	2.29	4.59
30.38	4.36	9.65	3.48
20.09	25.65	2.24	7.15
22.39	10.72	8.30	7.59
25.36	9.41	5.25	5.50
25.96	6.42	3.27	4.98
17.74	31.52	1.83	6.34
21.10	15.26	1.94	8.63
26.86	3.70	3.05	2.74
18.89	23.26	2.15	7.14
28.01	9.96	3.49	4.00

APPENDIX F: CHAPTER 4 BULK, THAA ISOTOPE DATA

Units are nmol ^{13}C (or ^{15}N) gdw^{-1}.

Day	Meso	Treatm	Bulk15N	Bulk13C	Dala15N	THAA15N	DLala15N	Dala13C	THAA13C	DLala13C	Macro15N	Macro13C
1.5	2	MLS	52.87	467.64								
1.5	4	NLS	112.05	580.43	0.16	66.44	0.02	0.21	140.51	0.01		
1.5	6	NDP	3.31	1.10	0.03	1.40		0.01	2.07			
1.5	7	MLP	191.95	268.19	0.18	73.80	0.02	0.12	59.41	0.02		
1.5	10	MLS	37.61	225.73	0.06	21.45	0.02	0.05	37.43	0.01		
1.5	11	NLS	117.13	645.80	0.13	62.75	0.01	0.13	80.50	0.01		
1.5	12	NDS	7.28	4.28	0.03	4.05	0.06	0.01	5.72			
1.5	14	NDS	4.67	3.60	0.02	2.49	0.05	0.01	4.22			
1.5	16	NLP	169.72	453.13	0.16	76.26	0.02	0.13	72.55	0.01		
1.5	18	NDP	12.31	6.36	0.02	2.61	0.05	0.01	3.61			
1.5	25	NLP	169.72	453.13	0.36	151.82	0.02	0.25	145.65	0.01		
1.5	26	MLP	135.81	173.37								
3.5	2	MLS	108.77	1374.16	0.15	80.74	0.01	0.50	408.20	0.01		
3.5	4	NLS	161.74	1285.87	0.27	149.57	0.02	0.60	423.84	0.01		
3.5	6	NDP	11.14	3.88	0.03	6.62	0.05	0.03	7.15			
3.5	7	MLP	192.80	511.12	0.25	105.32	0.02	0.25	117.55	0.02		
3.5	10	MLS	19.14	149.67	0.03	13.30	0.02	0.07	58.38	0.01		
3.5	11	NLS	104.18	753.38	0.17	89.53	0.01	0.19	182.37	0.01		
3.5	12	NDS	7.75	8.32	0.03	6.23	0.04	0.01	7.62			
3.5	14	NDS	15.73	16.25				0.00	2.55			
3.5	16	NLP	83.47	374.01	0.14	67.99	0.01	0.13	94.59	0.01		
3.5	18	NDP	18.78	14.18	0.04	9.98	0.03	0.02	10.90	0.01		
3.5	25	NLP	526.37	1623.08	1.27	345.29	0.03	0.94	442.29	0.02		
3.5	26	MLP	75.29	142.80								
7.5	2	MLS	261.94	3102.10	0.34	139.41	0.02	1.27	671.75	0.01	63427.91	941348.79
7.5	4	NLS	305.63	2103.25	0.37	153.40	0.02	0.96	572.67	0.02		
7.5	6	NDP	34.21	19.06	0.07	15.79	0.03	0.02	9.28	0.02		
7.5	7	MLP	327.38	945.27	0.43	165.81	0.02	0.35	182.83	0.02	7946.91	139798.36
7.5	10	MLS	101.99	1010.09	0.12	41.66	0.02	0.28	220.84	0.01	59021.16	804618.39
7.5	11	NLS	370.12	2783.08	0.49	213.33	0.02	0.94	571.53	0.01		

7.5	12	NDS	26.23	27.55	0.07	13.36	0.04	0.04	13.33	0.03		
7.5	14	NDS	15.73	16.25	0.04	6.61	0.04	0.01	8.16	0.02		
7.5	16	NLP	278.38	628.95	0.23	119.33	0.02	0.20	131.28	0.01		
7.5	18	NDP	160.00	86.91	0.30	61.65	0.03	0.11	36.32	0.02		
7.5	25	NLP	769.65	1645.49	0.94	342.63	0.02	0.63	323.68	0.02		
7.5	26	MLP	607.76	1111.99							53373.02	298756.10
14.5	2	MLS	468.14	4678.03	1.06	285.27	0.03	3.34	1466.55	0.02	24293.50	768348.79
14.5	4	NLS	633.46	4573.14	1.19	397.25	0.02	2.82	1545.72	0.02		
14.5	6	NDP	17.19	6.51	0.07	7.91	0.06	0.03	10.34	0.02		
14.5	7	MLP	172.85	405.80	0.23	77.98	0.02	0.21	96.76	0.02	41838.01	274370.23
14.5	10	MLS	389.11	2832.87	0.50	183.06	0.02	1.15	593.11	0.02	49489.16	1179768.83
14.5	11	NLS	777.41	6740.35	0.97	357.42	0.02	1.99	1116.15	0.02		
14.5	12	NDS	49.95	89.54	0.15	24.58	0.04	0.11	38.01	0.02		
14.5	14	NDS	22.80	43.05	0.05	9.37	0.04	0.04	14.88	0.02		
14.5	16	NLP	1343.30	4139.42	1.88	636.86	0.02	1.58	795.79	0.02		
14.5	18	NDP	92.95	99.03	0.20	35.68	0.04	0.10	28.94	0.03		
14.5	25	NLP	2568.09	7580.88	4.19	1472.53	0.02	3.41	1864.19	0.02		
14.5	26	MLP	764.43	1169.01							130585.15	863112.55
16.5	2	MLS	0.29	4356.34								
16.5	4	NLS	702.74	4874.47								
16.5	6	NDP	82.34	85.56								
16.5	7	MLP	914.18	1634.19								
16.5	10	MLS	462.87	2762.49								
16.5	11	NLS	604.83	3780.11								
16.5	12	NDS	53.79	83.17								
16.5	14	NDS	15.01	24.14								
16.5	16	NLP	854.73	2473.83								
16.5	18	NDP	161.11	136.21								
16.5	25	NLP	2288.79	5835.80								
16.5	26	MLP	1540.04	3574.88								
21.0	2	MLS	883.78	6092.53	1.44	425.52	0.02	3.13	1451.36	0.02	65478.64	583667.96
21.0	4	NLS	828.65	6036.13	0.98	427.18	0.02	2.37	1528.84	0.02		
21.0	6	NDP	127.32	107.88	0.31	63.41	0.04	0.11	35.57	0.03		
21.0	7	MLP	1306.55	2869.92	1.71	614.34	0.02	1.62	747.06	0.02	123597.66	531693.29
21.0	10	MLS	402.62	3154.43	0.37	178.73	0.02	0.91	640.53	0.01	70025.59	1138165.83

21.0	11	NLS	1074.08	6968.70	1.62	567.02	0.02	3.35	1836.48	0.02		
21.0	12	NDS	110.92	175.34	0.35	57.22	0.04	0.16	63.56	0.02		
21.0	14	NDS	79.36	150.25	0.25	39.24	0.05	0.17	50.92	0.03		
21.0	16	NLP	2248.24	5933.13	2.73	1220.81	0.02	2.20	1591.34	0.01		
21.0	18	NDP	147.04	155.01	0.45	83.41	0.04	0.18	65.03	0.03		
21.0	25	NLP	2052.36	5456.09	2.80	1167.20	0.02	2.69	1415.19	0.02		
21.0	26	MLP	733.50	1263.19							284715.95	957420.82
29.0	2	MLS	619.87	3504.55							63894.02	772371.75
29.0	4	NLS	393.04	2254.89								
29.0	6	NDP	133.62	104.75								
29.0	7	MLP	1501.42	3348.37							124170.21	475762.66
29.0	10	MLS	506.46	2596.09							43427.36	552941.14
29.0	11	NLS	1066.57	4735.59								
29.0	12	NDS	56.10	98.26								
29.0	14	NDS	22.03	39.56								
29.0	16	NLP	1432.14	3469.09								
29.0	18	NDP	149.26	165.59								
29.0	25	NLP	1819.43	4449.82								
29.0	26	MLP	831.39	2064.89							151089.19	502715.87
42.0	4	NLS	493.59	2615.43	1.11	283.95	0.03	1.64	711.32	0.02		
42.0	6	NDP	41.17	55.77	0.13	21.90	0.05	0.07	19.68	0.03		
42.0	7	MLP	747.31	1791.52	1.71	383.35	0.04	1.24	452.13	0.03	131355.10	459299.15
42.0	10	MLS	366.97	1770.19	0.62	183.49	0.03	1.03	474.12	0.02	38096.71	542439.71
42.0	11	NLS	788.27	3851.86	1.40	434.46	0.03	2.10	1013.88	0.02		
42.0	12	NDS	48.89	102.25	0.12	24.16	0.04	0.08	27.71	0.03		
42.0	14	NDS	19.41	44.50	0.05	8.37	0.05	0.03	12.42	0.03		
42.0	16	NLP	1164.18	2568.05	3.09	610.44	0.04	1.61	620.72	0.03		
42.0	18	NDP	170.01	198.92	0.52	80.76	0.05	0.23	63.71	0.04		
42.0	25	NLP	1511.23	3578.52	3.02	734.83	0.03	2.25	848.91	0.03		

APPENDIX G: CHAPTER 4 PLFA ISOTOPE DATA

Units are nmol ^{13}C gdw^{-1}

	T-1M							T1.5M	
	4	12	2	4	6	7	10	11	12
12:0		0.00	0.01	0.03	0.00	0.02	0.01		0.00
i13									
a13			0.00	0.00		0.00	0.00		0.00
13:0			0.01	0.01	0.00	0.01	0.00		0.00
i14			0.01	0.02	0.00	0.02	0.01		0.00
14:1w9		0.00	0.00					0.00	
14:1w7		0.00	0.00		0.00			0.00	
14:0	0.00	0.00	1.35	3.67	0.01	0.59	0.56	1.70	0.01
i15	0.00	0.00	0.03	0.04	0.00	0.02	0.02	0.02	0.00
a15	0.00	0.00	0.01	0.03	0.00	0.01	0.01	0.01	0.00
15:1		0.00	0.04	0.03	0.00	0.02	0.01	0.00	0.00
15:0	0.00	0.00	0.42	1.12	0.00	0.83	0.13	0.69	0.00
16:4*									
16:3*			0.02	0.00					
16:2*									
i16	0.00	0.00	0.19	0.24	0.00	0.04	0.04	0.15	0.00
16:1w9									
16:1w7	-0.02	0.00	4.59	10.49	0.02	2.04	1.97	5.99	0.03
16:1w5	0.00	0.00	0.10	0.19	0.00	0.04	0.04	0.09	0.00
16:0	-0.01	0.00	6.47	14.00	0.03	3.31	3.00	7.59	0.03
10Me17br			0.04	0.08	0.00	0.02	0.02		0.00
i17	0.00	0.00	0.05	0.07	0.00	0.01	0.01	0.02	0.00
a17									
17:1	0.00	0.00	0.18	0.36	0.00	0.25	0.07	0.19	0.00
17:0		0.00	0.08	0.09	0.00	0.05	0.03	0.06	0.00
18:3w6		0.00	0.05	0.06	0.00	0.02	0.02	0.13	0.00
18:4	0.00	0.00	0.15		0.00		0.08	0.19	
18:2w6			0.15	0.24		0.06	0.10	0.13	0.00
18:3w3									
18:1w9cis	0.00	0.00	0.21	0.44	0.00	0.13	0.12	0.26	0.00
18:2w3									
18:1w9t	0.00	0.00	0.24	0.32	0.00	0.11	0.08	0.17	0.01
18:1w7									
18:1w5									
18:0	0.00	0.00	0.19	0.32	0.00	0.08	0.08	0.16	0.00
10Me19br		0.00	0.01	0.01	0.00		0.00	0.01	0.00
i19*		0.00	0.01		0.00			0.00	
a19*									
19:1*		0.00	0.00	0.01	0.00	0.00	0.00	0.00	0.00
19:0 i.s.	0.00	0.00	0.02	0.02	0.00	0.01	0.01	0.02	0.00
20:5w6									
20:4w6	0.00	0.00	0.16	0.13	0.00	0.06	0.07	0.19	0.00
20:5w3	-0.01	0.00	0.97	1.69	0.00	0.33	0.30	1.10	0.00
20:3w6			0.03			0.01		0.03	
20:4w3	0.00	0.00	0.03	0.05			0.01	0.03	
20:2*									
20:3w3									
20:1w9	0.00	0.00	0.04	0.04	0.00	0.01	0.01	0.03	0.00

20:1w7		0.00	0.02	0.03	0.00	0.01	0.01	0.00	0.00
20:1w5									
20:0 i.s.	0.00	0.00	0.06	0.15	0.00	0.03	0.03	0.06	0.00
21:0 i.s.	0.00	0.00	0.03	0.04	0.00	0.01	0.02	0.03	0.00
22:6w6*									
22:6w3	0.00	0.00	0.10	0.14	0.00	0.03	0.02	0.10	0.00
22:5w6*									
22:5w3*	0.00	0.00	0.02	0.04	0.00	0.01	0.01	0.02	0.00
22:2*		0.00	0.01	0.04	0.00	0.01	0.00	0.01	0.00
22:1w9									
22:1w7*									
22:0	0.00	0.00	0.07	0.12	0.00	0.02	0.02	0.03	0.00
23:0 i.s.	0.00	0.00	0.02	0.04	0.00	0.01	0.02	0.03	0.00
24:1		0.00	0.02	0.04	0.00	0.03	0.00		0.00
24:0	0.00	0.00	0.13	0.10	0.00	0.05	0.03	0.05	0.00
25:0									
26:0	0.00	0.00	0.02	0.03	0.00	0.01	0.01	0.02	0.00
Total	-0.04	0.01	16.25	34.28	0.07	8.26	6.88	19.17	0.10
Sat FA's	-0.01	0.00	8.74	19.47	0.04	4.98	3.86	10.31	0.05
Mono Unsat	-0.02	0.00	5.45	11.93	0.03	2.64	2.31	6.74	0.04
Polyunsat	-0.01	0.00	1.71	2.39	0.00	0.53	0.60	1.92	0.00
Br FA's	0.00	0.00	0.35	0.48	0.00	0.12	0.11	0.20	0.01
% Sat FA's	26.05	38.82	53.80	56.81	53.82	60.23	56.12	53.78	52.59
% Mono Unsat	55.37	38.49	33.57	34.81	39.22	31.94	33.65	35.16	39.90
% Polyunsat	17.79	19.32	10.49	6.96	4.88	6.42	8.69	10.03	0.48
% Br FA's	0.79	3.38	2.14	1.41	2.08	1.40	1.54	1.04	7.03
BrOdd FA	0.00	0.00	0.15	0.22	0.00	0.06	0.06	0.05	0.00
PUFA (3+)	-0.01	0.00	1.55	2.11	0.00	0.46	0.50	1.78	0.00
%BrOdd FA	0.71	3.29	0.94	0.66	1.21	0.75	0.83	0.28	4.55
%PUFA (3+)	17.79	19.32	9.52	6.15	5.18	5.52	7.25	9.30	1.38
SCFA	-0.01	0.00	7.83	17.69	0.04	3.91	3.56	9.29	0.04
LCFA	0.00	0.00	0.22	0.25	0.00	0.08	0.07	0.10	0.00
TARFA	0.07	0.28	0.03	0.01	-0.01	0.02	0.02	0.01	0.04
18PUFA	0.00	0.00	0.35	0.29	0.00	0.08	0.19	0.45	0.00
BoshkerBact	0.00	0.00	0.23	0.32	0.00	0.08	0.07	0.17	0.01
%SCFA	31.00	34.49	48.21	51.61	49.89	47.35	51.78	48.47	42.48
%LCFA	2.12	9.51	1.34	0.73	-0.45	1.02	0.96	0.54	1.89
%18PUFA	1.32	0.85	2.16	0.86	0.22	0.98	2.81	2.34	-0.82
%BoshkerBact	0.92	3.80	1.43	0.94	1.79	0.97	1.05	0.91	5.99
C20 PUFA			1.13	1.81	0.00	0.39	0.37	1.29	0.00
c20+c22pufa 3+	-0.01	0.00	1.32	2.05	0.00	0.44	0.40	1.47	0.00
%c20+c22pufa3	16.46	18.47	8.12	5.98	4.96	5.27	5.82	7.65	1.31
BAR			0.09	0.10	0.19	0.12	0.10	0.03	0.77

14	16	18	25	26	2	4	6	7	10	11
0.00	0.01	0.00				0.06	0.00		0.03	
0.00	0.00					0.00	0.00			
0.00	0.01	0.00				0.07	0.00		0.01	
0.00	0.01	0.00				0.00	0.00		0.03	
0.00					0.00		0.00	0.00		0.03
0.01	2.85	0.01	2.60	1.08	18.67	6.23	0.07	4.16	8.04	20.67
0.00	0.03	0.00	0.05	0.03	0.84	0.58	0.01	0.25	0.22	0.45
0.00	0.02	0.00	0.03	0.02	0.25	0.20	0.00	0.11	0.08	0.26
0.00	0.06		0.08				0.00			
0.00	1.92	0.00	1.32	0.42	2.75	6.26	0.01	2.09	0.58	2.26
	0.00									0.00
0.00	0.14	0.00	0.15	0.06	0.89	2.30	0.00	0.31	0.69	3.45
0.02	8.39	0.02	8.74	4.03	50.42	1.06	0.29	11.80	25.09	66.46
0.00	0.16	0.00	0.23	0.08		0.00	0.01	0.26	0.45	
0.01	11.61	0.02	14.81	5.37	73.81	29.04	0.26	18.85	30.40	59.52
0.00	0.09	0.00				0.11	0.00		0.15	
0.00	0.04	0.00	0.14	0.03	0.35	0.27	0.00	0.09	0.12	0.24
0.00	0.67	0.00	0.67	0.23	1.66	0.58	0.01	0.88	0.40	1.22
0.00	0.15	0.00	0.24		0.81	0.71	0.00	0.32	0.17	0.64
0.00	0.09	0.00			0.80	0.18	0.00		0.36	2.72
0.00	0.32		0.30	0.11	1.73		0.01	0.36	0.44	1.63
0.00	0.28			0.15	2.50			0.57	1.37	3.78
0.00	0.44	0.00	0.63	0.26	2.75	2.10	0.02	0.71	0.91	2.97
0.00	0.27	0.01	0.44	0.21	3.65	3.79	0.04	1.07	1.17	2.80
0.00	0.21	0.00	0.34	0.15	2.57	1.77	0.01	0.60	0.79	2.38
0.00	0.02	0.00	0.02		0.12	0.09	0.00			0.41
0.00	0.01						0.00			
0.00	0.01	0.00	0.01		0.08		0.00		0.03	0.04
0.00	0.02	0.00	0.05	0.02	0.32	0.15	0.00	0.09	0.08	0.23
0.00	0.25	0.00	0.34	0.20	2.39	0.72	0.02	0.58	0.84	5.37
0.00	1.59	0.00	1.56	0.58	10.52	7.21	0.05	2.23	3.14	13.83
	0.03			0.08	0.39			0.07	0.14	0.78
0.00	0.04		0.10			0.08	0.00		0.07	0.45
		0.00								
0.00	0.05		0.07	0.06	0.54	0.34	0.00	0.17	0.21	0.83

0.00	0.05	0.00				0.00	0.00		0.19	
0.00	0.09	0.00	0.22	0.07	1.30	0.48	0.00	0.30	0.29	0.65
0.00	0.05	0.00	0.12	0.05	0.92	0.36	0.00	0.17	0.23	0.98
0.00	0.17	0.00	0.19	0.04	1.30	1.54	0.01	0.30	0.17	1.38
0.00	0.04	0.00	0.07		0.34	0.32	0.00	0.10	0.07	0.42
0.00	0.01	0.00	0.02			0.23	0.00	0.03		0.06
0.00	0.07	0.00	0.12	0.03	0.72	0.61	0.00	0.15	0.20	0.33
0.00	0.05	0.00	0.11	0.04	0.55	0.30	0.00	0.14	0.34	0.43
	0.01	0.00		0.01		0.11	0.00	0.03		0.00
0.00	0.09	0.00	0.20	0.05	1.19	0.51	0.00	0.35	0.39	0.52
0.00	0.03	0.00	0.11	0.02	0.30	0.14	0.00	0.10	0.11	0.21
0.05	30.21	0.07	33.58	13.29	182.34	67.21	0.82	46.52	77.05	196.11
0.02	16.94	0.04	19.75	7.12	100.82	45.39	0.36	26.63	40.72	86.53
0.03	10.11	0.03	10.87	4.87	59.10	7.97	0.36	14.91	28.45	74.36
0.00	2.81	0.00	2.57	1.16	19.97	10.28	0.08	4.23	6.60	30.41
0.00	0.35	0.01	0.39	0.13	2.45	3.57	0.02	0.75	1.29	4.81
45.95	56.08	54.46	58.81	53.59	55.29	67.53	43.39	57.24	52.84	44.12
51.82	33.45	37.91	32.38	36.65	32.41	11.86	44.35	32.05	36.92	37.92
-4.99	9.31	-0.23	7.66	8.75	10.95	15.30	9.79	9.09	8.56	15.51
7.22	1.15	7.86	1.16	1.01	1.34	5.31	2.46	1.62	1.67	2.45
0.00	0.20	0.00	0.24	0.07	1.55	1.26	0.01	0.45	0.57	1.37
0.00	2.52	0.00	2.55	1.02	17.47	10.05	0.08	3.63	5.22	26.57
5.73	0.67	5.33	0.71	0.54	0.85	1.88	1.81	0.96	0.74	0.70
-2.55	8.35	0.50	7.61	7.64	9.58	14.95	9.73	7.81	6.78	13.55
0.02	14.47	0.03	17.42	6.45	92.48	35.33	0.33	23.01	38.46	80.19
0.00	0.19	0.00	0.44	0.10	2.21	1.26	0.00	0.61	0.70	1.06
-0.01	0.01	0.04	0.03	0.02	0.02	0.04	0.00	0.03	0.02	0.01
0.00	0.69	0.00	0.30	0.26	5.03	0.18	0.01	0.93	2.17	8.13
0.00	0.20	0.01	0.23	0.11	1.97	3.09	0.01	0.66	1.03	4.16
38.25	47.90	43.82	51.87	48.53	50.72	52.57	40.07	49.46	49.92	40.89
-0.23	0.62	1.90	1.30	0.75	1.21	1.87	0.12	1.30	0.91	0.54
-1.53	2.27	0.09	0.89	1.95	2.76	0.27	0.82	2.00	2.82	4.14
6.21	0.65	7.60	0.69	0.80	1.08	4.60	1.76	1.42	1.33	2.12
0.00	1.84	0.00	1.90	0.78	12.91	7.93	0.06	2.80	3.98	19.19
0.00	2.12	0.00	2.25	0.90	14.94	9.86	0.07	3.27	4.43	22.22
-2.42	7.00	0.41	6.72	6.80	8.19	14.68	8.91	7.04	5.75	11.33
1.80	0.07	0.91	0.08	0.07	0.08	0.11	0.16	0.11	0.10	0.05

T7.5M										
11 rerun	12	14	16	18	25	25 rerun	26	2	4	6
	0.01	0.00	0.02	0.01				0.14	0.10	0.00
								0.00	0.00	0.00
	0.00	0.00	0.02	0.00				0.08	0.07	0.00
	0.01	0.00	0.04	0.01				0.21	0.29	0.00
				0.00						
0.04		0.00			0.02	0.03				0.00
21.17	0.04	0.02	2.79	0.08	16.02	16.59	5.02	15.00	7.80	0.02
0.39	0.01	0.00	0.15	0.03	0.55	0.48	0.26	2.29	1.39	0.00
0.19	0.01	0.00	0.08	0.03	0.23	0.16	0.14	0.59	0.45	0.00
		0.00		0.01						0.00
2.27	0.02	0.01	2.16	0.03	2.02	1.95	0.83	4.33	4.66	0.00
0.00					0.00	0.00				
3.63	0.00	0.00	0.20	0.00	0.00	0.00	0.71	1.46	0.74	0.00
67.82	0.14	0.13	10.93	0.57	44.23	46.90	17.68	47.23	25.43	0.04
	0.01	0.00	0.23	0.03		0.38	0.43	0.96	0.75	0.01
59.99	0.11	0.09	16.66	0.42	47.38	49.22	24.26	59.03	34.27	0.04
	0.00	0.00	0.09	0.01				0.32	0.23	0.00
0.22	0.00	0.00	0.08	0.01	0.21	0.16	0.14	0.52	0.36	0.00
				0.01						
1.09	0.01	0.00	0.98	0.04	0.88	0.64	0.75	0.33	2.43	0.00
0.54	0.00	0.00	0.25	0.04	0.52	0.32	0.36	0.93	0.95	0.00
2.63	0.00	0.00	0.09	0.00	1.76	1.57	0.59	0.95	0.46	0.00
1.66		0.00			1.20	1.17	0.56	1.09	1.00	0.00
3.92	0.01	0.00	0.35		2.47	2.50	1.28	3.25	2.04	
2.98	0.01	0.01	0.53	0.03	2.62	2.61	1.13	3.37	2.77	0.00
2.73	0.03	0.03	0.69	0.17	2.79	2.50	1.46	6.92	5.23	0.01
2.22	0.01	0.01	0.41	0.07	1.68	1.46	0.91	4.21	2.78	0.01
0.37	0.00	0.00	0.03		0.16			0.00	0.00	0.00
									0.06	
	0.00	0.00		0.00	0.04		0.04	0.12	0.11	0.00
0.18	0.00	0.00	0.05	0.01	0.12	0.04	0.20	0.20	0.19	0.00
5.56	0.00	0.00	0.28	0.03	3.83	3.56	1.20	3.09	2.10	0.00
14.26	0.01	0.01	2.16	0.08	10.06	10.20	3.59	10.30	8.58	0.00
0.79					0.60	0.61	0.17	0.48	0.31	
0.44			0.04		0.40	0.39	0.09		0.33	
				0.00						
0.74	0.00	0.00	0.13		0.94	0.69	0.36	0.91	0.00	0.00

0.00	0.00	0.00	0.06	0.00		0.00		0.23	0.81	0.00
0.46	0.00	0.00	0.18	0.02	0.58	0.40	0.43	0.64	0.80	0.00
0.24	0.00	0.00	0.20	0.01	0.57	0.16	0.39	0.52	0.48	0.00
1.42	0.00	0.00	0.28	0.02	1.04	1.03	0.41	1.26	1.62	0.00
0.18										
-0.15		0.00	0.06	0.00	0.33	0.32	0.12	0.83	0.66	
0.06	0.00	0.00	0.01	0.00	0.07	0.07	0.03	0.31	0.11	0.00
0.28	0.00	0.00	0.14	0.01	0.26	0.20	0.16	0.71	0.99	0.00
0.15	0.01	0.00	0.24	0.01	0.25	0.09	0.30	0.36	0.69	0.00
0.00	0.00	0.00		0.01	0.00	0.00		0.08	0.16	0.00
0.41	0.01	0.00	0.14	0.01	0.37	0.29	0.32	1.42	1.14	0.00
0.14	0.01	0.00	0.05	0.01	0.15	0.09	0.13	0.27	0.40	0.00
197.97	0.47	0.35	40.14	1.80	142.86	146.12	63.15	173.20	111.58	0.16
87.01	0.21	0.14	22.65	0.69	68.40	70.14	31.99	86.11	53.15	0.08
75.39	0.19	0.18	13.56	0.86	51.53	53.75	21.85	60.15	37.70	0.07
30.77	0.02	0.02	3.27	0.13	21.77	21.43	8.05	21.55	17.21	0.00
4.80	0.04	0.01	0.67	0.11	1.15	0.81	1.26	5.39	3.52	0.01
43.95	44.67	39.86	56.41	38.37	47.88	48.00	50.66	49.72	47.63	48.81
38.08	41.05	52.20	33.78	47.89	36.07	36.79	34.61	34.73	33.79	42.92
15.54	5.02	5.34	8.15	7.49	15.24	14.66	12.74	12.44	15.43	1.40
2.42	9.27	2.59	1.66	6.25	0.81	0.55	1.99	3.11	3.16	6.88
1.17	0.03	0.01	0.43	0.09	1.15	0.81	0.54	3.71	2.49	0.01
26.79	0.02	0.02	2.91	0.13	19.23	18.85	6.73	17.99	15.06	0.00
0.59	6.71	2.09	1.07	5.28	0.81	0.55	0.86	2.14	2.23	5.04
13.53	3.66	4.73	7.25	7.08	13.46	12.90	10.66	10.39	13.50	2.36
81.15	0.16	0.12	19.48	0.51	63.39	65.81	29.28	74.16	42.17	0.07
0.82	0.01	0.00	0.34	0.03	0.78	0.58	0.62	2.40	2.52	0.00
0.01	0.08	0.01	0.02	0.06	0.01	0.01	0.02	0.03	0.06	-0.02
8.21	0.01	0.00	0.43	0.00	5.43	5.25	2.43	5.28	3.50	0.00
4.20	0.04	0.01	0.46	0.08	0.78	0.65	1.12	4.55	2.87	0.01
40.99	34.43	33.79	48.51	28.48	44.37	45.04	46.36	42.82	37.79	42.90
0.42	2.85	0.30	0.85	1.76	0.55	0.40	0.97	1.38	2.26	-0.70
4.15	1.29	0.99	1.08	0.00	3.80	3.59	3.84	3.05	3.14	0.18
2.12	8.15	2.20	1.15	4.44	0.55	0.44	1.77	2.63	2.57	6.05
19.82	0.02	0.01	2.44	0.11	13.89	13.76	4.80	13.39	10.68	0.00
22.50	0.02	0.02	2.82	0.13	16.27	16.11	5.59	15.95	13.60	0.00
11.37	3.66	4.36	7.04	7.08	11.39	11.02	8.85	9.21	12.19	2.18
0.04	0.65	0.31	0.13	0.43	0.06	0.04	0.07	0.17	0.14	0.68

T14.5M										
7	10	11	12	14	16	18	25	26	2	4
			0.02		0.09	0.01		0.05	0.19	0.27
			0.01		0.03	0.00			0.00	0.00
			0.01		0.08	0.00		0.02	0.05	0.14
0.03	0.11		0.02		0.13	0.01		0.12	0.47	0.63
			0.00	0.00						
		0.03						0.00	0.00	
0.56	7.88	16.58	1.74	0.01	5.29	0.06	8.35	6.72	6.90	9.84
0.10	0.77	1.45	0.07	0.01	0.58	0.02	1.16	0.99	2.88	3.19
0.06	0.30	0.51	0.03	0.00	0.25	0.02	0.38	0.23	0.78	1.16
			0.02	0.00				0.02		
0.34	0.83	3.63	0.12	0.00	7.19	0.03	2.54	0.93	1.28	5.50
0.02	0.25	0.74	0.08	0.00	0.40	0.00	1.03	1.22	1.27	1.50
1.79	28.65	65.50	5.38	0.14	15.73	0.28	30.97	24.10	16.76	23.06
0.07	0.58		0.14	0.00	0.47	0.04	0.76	0.57	0.90	1.50
3.33	42.69	86.76	5.86	0.09	27.42	0.25	42.82	22.29	24.94	41.30
0.05	0.23		0.07	0.00	0.18	0.01			0.25	0.37
0.05	0.29		0.06	0.00	0.28	0.01	0.30	0.17	0.55	0.77
						0.00				
0.17	0.57	0.43	0.08	0.00	3.31		1.44	0.48	1.19	2.85
0.07	0.35	0.97	0.07	0.00	1.08	0.02	0.67	0.24	0.71	1.84
	0.48	1.11	0.03		0.38	0.00	0.55	0.25	0.27	0.56
	0.59	1.55			0.52		0.74	0.39		
	1.70	3.81	0.31		1.48		2.00	2.31		
0.16	1.56	4.15	0.21	0.01	2.00	0.03	2.74	1.41	2.05	3.59
0.33	3.06	5.23	0.33	0.03	3.23	0.08	6.00	4.02	6.66	10.78
0.26	2.03	4.02	0.20	0.01	1.96	0.04	2.73	1.08	2.42	4.48
			0.01	0.00	0.00	0.00		0.00		
								0.03	0.00	0.00
0.01	0.06	0.05	0.02	0.00	0.06	0.00	0.17	0.07	0.17	0.14
0.02	0.16	0.47	0.03	0.00	0.17	0.01	0.21	0.23	0.23	0.43
0.13	1.46	2.56	0.22	0.00	1.73	0.01	2.06	1.83	2.45	3.05
0.48	5.02	6.98	0.83	0.01	5.10	0.03	6.46	4.32	5.71	7.81
		0.53			0.32			0.22	0.15	
			0.03		0.26			0.12		
		0.40	0.04	0.00	0.36	0.01	0.59	0.21	0.66	1.27

0.04	0.00		0.02	0.00	0.00	0.00		0.00	0.21	0.46
0.10	0.56	1.09	0.10	0.00	0.55	0.01	0.88	0.30	0.77	1.60
0.08	0.34	1.41	0.05	0.00	0.27	0.01	0.55	0.18	1.20	1.27
0.05	0.63	0.87	0.09	0.00	0.78	0.01	0.77	0.36	0.86	1.23
0.02	0.22	0.62	0.03	0.00	0.39		0.40	0.23	0.29	0.45
0.01		1.16	0.03	0.00	0.05	0.00		0.03	0.11	0.20
0.07	0.41	2.06	0.05	0.00	0.43	0.01	0.48	0.15	0.76	2.58
0.08	0.36	0.62	0.04	0.00	0.29	0.01	0.17	0.11	0.53	0.52
			0.03		0.08	0.00		0.03	0.25	0.25
0.12	0.91	1.37	0.08	0.00	0.80	0.01	0.57	0.45	2.06	2.45
0.07	0.26	0.49	0.07	0.00	0.20	0.01	0.15	0.09	0.34	0.55
8.40	101.89	213.57	16.42	0.33	82.61	1.00	116.84	75.75	84.55	133.76
4.82	55.36	115.87	8.21	0.13	44.53	0.43	58.31	32.02	39.66	68.95
2.58	34.48	75.80	6.28	0.18	25.25	0.43	42.67	30.91	28.85	43.89
0.69	10.09	19.21	1.57	0.01	11.00	0.05	12.98	10.05	9.85	13.29
0.31	1.96	2.70	0.35	0.01	1.83	0.08	2.87	2.76	6.19	7.62
57.39	54.33	54.25	50.03	37.63	53.90	42.73	49.91	42.27	46.90	51.55
30.72	33.84	35.49	38.23	54.31	30.56	43.51	36.52	40.81	34.13	32.81
8.16	9.90	8.99	9.59	4.23	13.32	5.48	11.11	13.27	11.65	9.94
3.72	1.92	1.26	2.14	3.84	2.22	8.29	2.46	3.64	7.33	5.70
0.26	1.59	1.96	0.25	0.01	1.31	0.07	1.84	1.42	4.46	5.50
0.68	8.39	14.23	1.24	0.01	9.47	0.05	10.99	7.71	9.74	13.09
3.09	1.56	0.92	1.53	3.71	1.58	7.26	1.57	1.88	5.28	4.11
8.09	8.23	6.66	7.55	4.06	11.46	5.37	9.40	10.18	11.51	9.79
3.89	50.58	103.34	7.62	0.10	32.80	0.32	51.17	29.07	32.04	51.42
0.25	1.58	3.91	0.19	0.00	1.43	0.03	1.19	0.68	3.17	5.58
0.07	0.03	0.04	0.02	0.03	0.04	0.08	0.02	0.02	0.10	0.11
0.00	2.77	6.47	0.34	0.00	2.39	0.00	3.29	2.95	0.27	0.56
0.22	1.44	2.70	0.20	0.01	1.36	0.06	2.58	2.56	5.39	6.48
46.37	49.64	48.39	46.44	31.30	39.70	31.65	43.80	38.37	37.89	38.44
3.02	1.55	1.83	1.16	0.80	1.73	2.59	1.02	0.90	3.75	4.17
0.00	2.72	3.03	2.08	0.00	2.89	0.00	2.81	3.89	0.32	0.42
2.59	1.41	1.26	1.22	2.99	1.64	5.93	2.21	3.38	6.38	4.84
0.61	6.47	9.55	1.06	0.01	6.83	0.05	8.52	6.15	8.16	10.86
0.68	7.32	11.58	1.21	0.01	8.57	0.05	9.70	7.07	9.46	12.54
8.09	7.19	5.42	7.35	4.06	10.37	5.37	8.30	9.34	11.19	9.37
0.28	0.16	0.12	0.17	0.48	0.12	0.58	0.14	0.16	0.31	0.30

T6.5P										
6	7	10	11	12	14	16	18	25	26	4
	0.11	0.04		0.02	0.01	0.23		0.05	0.05	0.27
	0.00	0.00		0.00					0.06	0.03
	0.07	0.02		0.01						0.08
	0.33	0.13		0.02		0.31	0.03	0.23		0.42
0.00				0.00	0.00				0.03	
			0.00		0.00	0.00		0.00	0.00	
0.04	3.11	2.12	12.19	0.12	0.07	16.80	0.14	6.18	1.43	3.36
0.02	1.24	0.56	2.77	0.05	0.03	1.67	0.07	1.52	0.62	2.09
0.01	0.55	0.21	1.00	0.03	0.02	0.84	0.07	0.64	0.17	0.78
						0.00		0.00		
0.01	2.73	0.42	4.88	0.03	0.01	11.85	0.05	5.01	0.48	1.47
						0.00			0.17	
0.00	0.77	0.33	2.90	0.01	0.00	4.20	0.00	1.14	0.25	0.16
0.30	9.12	5.52	41.19	0.69	0.58	44.81	0.06	23.23	3.98	4.81
0.01	0.75	0.19	2.97	0.04	0.01	1.40	0.00	0.90	0.22	0.60
0.18	13.92	8.56	54.71	0.52	0.35	53.92	0.42	34.03	6.09	12.18
	0.15	0.09		0.03			0.03			0.19
0.01	0.35	0.18	0.79	0.02	0.01	0.85	0.02	0.60	0.12	0.49
				0.01	0.00		0.03			
0.01	1.52	0.28	2.90			7.35		3.57	0.38	0.89
0.01	0.80	0.22	1.38	0.02	0.01	2.00	0.03	1.64	0.29	0.72
0.00	0.23	0.09	0.97	0.00		1.78		0.72	0.16	2.20
			1.57		0.00	1.28		1.14	0.10	1.00
			2.40			3.79		2.30	0.37	1.32
0.01	1.23	0.66	3.14	0.04	0.03	7.29	0.06	6.61	1.60	2.47
0.08	4.15	1.62	9.76	0.21	0.11	8.04	0.16	10.05	2.28	3.50
0.03	1.82	1.42	5.86	0.07	0.05	4.29	0.07	5.46	1.25	1.94
0.00	0.00		0.23	0.00	0.00	1.27		0.33	0.01	
	0.00							0.00	0.00	
0.00	0.15	0.04	0.00	0.01	0.00	0.15	0.01	0.20	0.07	0.10
0.00	0.14	0.08	0.40	0.01	0.01	0.14	0.01	0.31	0.09	0.16
0.01	1.62	0.90	3.92	0.04	0.01	6.89	0.03	5.75	0.95	3.97
0.01	4.46	1.93	11.29	0.09	0.02	19.46	0.05	15.48	1.90	3.38
	0.10	0.06	0.52			0.84		0.51	0.10	0.45
			0.41			0.26		0.72		0.18
	0.51		8.90	0.02						0.44
0.00		0.24			0.00	1.25	0.03	1.71	0.15	0.00

0.00	0.00	0.00		0.00	0.00	0.00		0.00	0.00	0.26
0.00	0.43	0.26	1.57	0.03	0.02	0.57	0.03	1.03	0.19	0.58
0.00	0.56	0.20	1.26	0.02	0.01	0.45	0.03	0.48	0.15	0.30
0.00	0.90	0.24	1.24	0.02	0.00	2.53	0.01	4.19	0.51	0.67
0.00	0.27	0.09	0.86	0.01	0.00			1.57	0.12	0.21
0.00	0.04			0.00	0.00	0.08	0.00	0.15	0.02	0.09
0.00	0.41	0.25	0.93	0.02	0.01	0.55	0.02	1.03	0.18	1.12
0.00	0.55	0.43	0.60	0.03	0.00	0.28	0.04	0.26	0.21	0.35
0.00	0.03			0.00		0.00	0.01	0.00		0.48
0.00	1.12	0.42	1.79	0.03	0.01	0.96	0.04	0.95	0.04	0.70
0.00	0.25	0.09	0.55	0.03	0.00	0.16	0.00	0.23	0.10	0.29
0.73	52.79	26.93	181.99	2.19	1.38	207.11	1.42	137.85	24.23	53.31
0.26	24.33	13.58	82.27	0.86	0.53	90.76	0.77	54.58	9.91	22.13
0.41	16.94	8.55	59.96	0.99	0.74	70.31	0.32	46.26	8.71	13.10
0.02	8.13	3.31	32.09	0.18	0.04	36.91	0.09	32.53	4.39	13.92
0.04	3.40	1.50	7.68	0.16	0.07	9.14	0.24	4.47	1.23	4.15
36.12	46.08	50.42	45.21	39.57	38.18	43.82	54.13	39.60	40.88	41.52
55.65	32.09	31.73	32.94	45.24	53.60	33.95	22.57	33.56	35.93	24.58
2.45	15.39	12.28	17.63	8.07	3.11	17.82	6.02	23.60	18.12	26.11
5.78	6.43	5.57	4.22	7.12	5.11	4.41	17.28	3.24	5.06	7.79
0.04	2.30	1.04	4.78	0.13	0.07	4.63	0.21	3.09	0.97	3.58
0.02	7.58	3.31	20.79	0.16	0.04	33.03	0.09	30.08	4.00	12.07
5.55	4.35	3.84	2.63	6.07	4.89	2.23	14.95	2.24	4.01	6.71
2.41	14.36	12.28	11.42	7.11	2.93	15.95	6.02	21.82	16.51	22.64
0.22	17.13	10.73	66.89	0.66	0.43	70.94	0.56	40.26	7.57	15.80
0.01	1.77	0.77	3.27	0.08	0.02	1.67	0.06	2.21	0.32	2.12
0.03	0.10	0.07	0.05	0.13	0.04	0.02	0.11	0.05	0.04	0.13
0.00	0.23	0.09	4.94	0.00	0.00	6.86	0.00	4.16	0.63	4.53
0.04	2.89	1.23	6.66	0.10	0.05	7.02	0.18	3.54	1.04	3.45
29.43	32.45	39.83	36.76	29.99	31.44	34.25	39.31	29.21	31.23	29.65
1.00	3.36	2.87	1.79	3.88	1.22	0.81	4.24	1.60	1.31	3.97
0.00	0.44	0.35	2.71	0.00	0.14	3.31	0.00	3.02	2.59	8.49
5.02	5.47	4.58	3.66	4.40	3.93	3.39	12.35	2.56	4.28	6.47
0.02	6.08	2.83	15.21	0.13	0.03	26.34	0.08	21.23	2.85	7.35
0.02	7.35	3.21	18.25	0.16	0.04	29.97	0.09	28.22	3.58	8.86
2.41	13.92	11.93	10.03	7.11	2.79	14.47	6.02	20.47	14.76	16.63
0.70	0.23	0.24	0.19	0.46	0.63	0.12	0.71	0.09	0.20	0.23

T27.5P								
6	7	10	11	12	14	16	18	25
0.00	0.07	0.09	0.15		0.00		0.01	0.13
0.00	0.00	0.00	0.00					0.11
0.00	0.03	0.03			0.00			0.08
0.00	0.17	0.18		0.02	0.00	0.06	0.01	0.16
			0.08					
0.00			0.00		0.00			0.01
0.03	1.01	1.75	2.29		0.02		0.06	2.25
0.02	0.89	0.71	1.94	0.03	0.01	0.13	0.04	1.08
0.01	0.44	0.38	0.87	0.02	0.01	0.05	0.03	0.45
0.00					0.00			
0.01	0.72	0.70	2.46		0.00		0.02	1.37
0.00	0.25	0.35	0.40	0.00	0.00	0.05	0.00	0.24
0.15	2.85	5.76	6.75	0.28	0.09	5.18	0.32	4.67
0.02	0.25	0.26	0.43	0.01	0.01	0.12	0.02	0.34
0.12	4.93	8.12	9.49	0.23	0.07	3.79	0.30	9.51
0.01	0.13	0.09			0.00		0.02	
0.01	0.24	0.19	0.31	0.01	0.00	0.04	0.01	0.26
							0.01	
0.01	0.49	0.61	1.70	0.01	0.00	0.67		0.89
0.01	0.39	0.34	0.72		0.00		0.02	0.65
0.00	0.06		0.21	0.01	0.00	0.07		0.20
0.00			0.32		0.00			0.57
	0.61	0.60	0.82					0.64
0.01	0.69	0.76	1.39	0.03	0.01	0.20	0.03	2.75
0.07	1.46	1.50	3.08	0.08	0.03	0.49	0.11	3.33
0.02	0.81	0.92	1.83	0.04	0.01	0.17	0.06	1.61
0.00		0.00	0.00	0.00	0.00	0.00		0.05
0.00								0.00
0.00	0.05	0.03	0.07	0.00	0.00	0.01	0.00	0.13
0.00	0.10	0.07	0.11	0.01	0.00	0.01	0.01	0.11
0.01	0.98	1.53	1.64		0.01		0.02	1.51
0.01	1.05	1.99	2.79	0.02	0.01	0.63	0.02	2.65
			0.14					
0.00			0.10					0.10
				0.01		0.01	0.01	
0.00	0.12	0.15	0.27	0.01	0.00	0.03		0.23

0.00	0.00	0.00	0.00	0.00	0.00	0.02		0.00
0.01	0.35	0.43	0.50	0.01	0.00	0.02	0.04	0.53
0.01	0.21	0.17	0.54	0.01	0.00	0.01	0.02	0.23
0.00	0.16	0.36	0.59	0.01	0.00	0.09	0.00	0.71
0.00		0.12	0.18					0.15
0.00	0.04	0.08	0.08	0.00	0.00	0.00	0.00	0.03
0.00	0.28	0.27	0.36	0.01	0.00	0.02	0.01	0.65
0.00	0.18	0.21	0.23	0.01	0.00	0.01	0.02	0.24
0.00	0.05	0.03	0.05	0.00		0.00	0.01	0.00
0.00	0.57	0.65	0.78	0.01	0.00	0.02	0.02	1.00
0.00	0.16	0.18	0.19	0.00	0.00	0.00	0.02	0.23
0.52	19.98	28.70	42.46	0.84	0.29	11.87	1.19	38.71
0.19	9.00	13.05	18.28	0.29	0.11	4.00	0.52	17.48
0.26	5.96	9.10	13.82	0.43	0.15	6.72	0.49	12.35
0.02	2.91	4.66	6.85	0.04	0.02	0.81	0.06	6.54
0.05	2.12	1.89	3.51	0.07	0.02	0.33	0.12	2.34
36.36	45.02	45.46	43.05	34.92	36.55	33.74	43.92	45.14
50.13	29.81	31.69	32.54	51.72	50.19	56.63	41.11	31.90
4.05	14.57	16.25	16.14	4.58	5.88	6.82	4.73	16.90
9.45	10.60	6.60	8.27	8.77	7.38	2.82	10.24	6.06
0.04	1.70	1.37	3.11	0.06	0.02	0.22	0.11	1.95
0.02	2.26	3.99	5.96	0.03	0.02	0.80	0.05	5.88
8.39	8.49	4.78	7.33	6.62	6.45	1.86	8.93	5.03
3.96	11.29	13.90	14.04	3.60	5.68	6.70	3.79	15.18
0.15	6.02	9.97	11.93	0.23	0.08	3.79	0.36	11.89
0.00	1.02	1.09	1.33	0.02	0.00	0.04	0.06	1.88
0.02	0.17	0.11	0.11	0.08	0.06	0.01	0.15	0.16
0.00	0.68	0.60	1.34	0.01	0.00	0.07	0.00	1.41
0.03	1.75	1.61	3.20	0.07	0.02	0.29	0.08	1.92
28.60	30.14	34.73	28.09	27.82	28.23	31.94	30.66	30.71
0.61	5.09	3.81	3.14	2.14	1.68	0.38	4.63	4.85
0.46	3.39	2.07	3.15	0.75	0.19	0.60	0.00	3.64
6.62	8.76	5.62	7.54	7.76	5.97	2.48	6.73	4.97
0.01	2.03	3.51	4.44	0.02	0.01	0.63	0.04	4.15
0.02	2.19	3.99	5.44	0.02	0.02	0.72	0.05	5.11
3.50	10.97	13.90	12.81	2.85	5.50	6.10	3.79	13.19
0.68	0.43	0.26	0.34	0.65	0.53	0.22	0.70	0.25

APPENDIX H: CHAPTER 5 BULK, THAA ISOTOPE DATA

Units are nmol ^{13}C or ^{15}N gdw^{-1}

Day	Pool	Bulk 15N	Bulk 13C	Dala 15N	THAA 15N	D/L-Ala 15N	Dala 13C	THAA 13C	D/L-Ala 13C	THAA/ BULK15N	THAA/ BULK13C	DALA/ BULK15N	DALA/ BULK13C	PLFA/ BULK13C
1	H1	33.15	21.50	0.11	16.75	0.06	0.06	13.16	0.06	50.51	61.23	0.32	0.29	
1	H3	17.17	22.51	0.03	8.07	0.04	0.02	9.30	0.04	46.97	41.33	0.16	0.11	3.30
1	H5	36.48	22.07	0.03	16.59	0.03	0.05	8.57	0.06	45.46	38.81	0.09	0.23	3.63
1	I2	151.28	105.67	0.15	56.89	0.04	0.10	52.83	0.04	37.61	49.99	0.10	0.09	4.50
1	I4	53.54	49.02	0.03	35.03	0.02	0.03	15.60	0.03	65.42	31.84	0.06	0.06	1.00
1	I6	34.01	33.61	0.05	15.27	0.04	0.03	9.88	0.06	44.91	29.39	0.14	0.09	3.06
2	H1	16.46	25.16	0.05	11.07	0.05	0.02	10.56	0.04	67.24	41.95	0.29	0.09	1.90
2	H3	35.14	38.25	0.08	22.09	0.04	0.05	20.85	0.05	62.86	54.51	0.22	0.14	3.09
2	H5	68.99	38.01	0.13	26.32	0.05	0.07	21.43	0.05	38.15	56.37	0.19	0.19	3.85
2	I2	58.38	87.97	0.08	30.90	0.04	0.06	29.09	0.04	52.93	33.06	0.13	0.07	1.18
2	I4	68.09	17.65	0.04	21.26	0.03	0.02	10.40	0.04	31.22	58.93	0.06	0.11	1.64
2	I6	27.32	32.30				0.00	7.98	0.02		24.71		0.01	3.22
7	H1	251.99	207.97	0.17	91.53	0.03	0.10	65.16	0.03	36.32	31.33	0.07	0.05	4.01
7	H3	1199.42	1137.17	1.07	493.69	0.03	0.43	413.00	0.03	41.16	36.32	0.09	0.04	4.93
7	H5	263.25	394.88	0.15	63.26	0.04	0.08	45.18	0.04	24.03	11.44	0.06	0.02	1.67
7	I2	76.65	96.16	0.04	19.68	0.03	0.03	20.24	0.04	25.67	21.05	0.05	0.04	3.19
7	I4	649.65	767.97	0.12	217.73	0.02	0.09	230.29	0.02	33.52	29.99	0.02	0.01	1.97
7	I6	72.52	65.34	0.01	23.79	0.02	0.01	26.00	0.02	32.80	39.80	0.01	0.02	3.99
14	H1	1198.61	929.53	0.49	523.11	0.02	0.15	396.64	0.02	43.64	42.67	0.04	0.02	1.72
14	H3	71.34	58.38	0.03	24.49	0.03	0.03	20.23	0.03	34.33	34.64	0.04	0.04	2.29
14	H5	84.40	29.20	0.07	33.19	0.03	0.04	22.01	0.04	39.32	75.37	0.08	0.13	3.11
14	I2	316.84	296.49	0.11	85.59	0.03	0.08	72.16	0.03	27.01	24.34	0.03	0.03	1.36
14	I4	69.31	39.02	0.04	29.35	0.03	0.02	16.45	0.03	42.34	42.15	0.06	0.06	2.56
14	I6	942.84	1213.61	0.36	285.39	0.03	0.25	332.27	0.02	30.27	27.38	0.04	0.02	1.41

APPENDIX I: CHAPTER 5 PLFA ISOTOPE DATA

Units are nmol ^{13}C gdw^{-1}

	Day 1	1	1	1	1	1	2	2
Component	Meso-H1	H3	H5	I2	I4	I6	H1	H3
12:0	0.01	0.00	0.00	0.00	0.00	0.00		0.00
13:0	0.01	0.00		0.00	0.00			
i14	0.06	0.00	0.00	0.01	0.00	0.00		0.00
14:1w9								
14:1w7								
14:0	0.44	0.08	0.08	0.29	0.02	0.08	0.03	0.11
i15	0.38	0.01	0.03	0.13	0.04	0.02	0.01	0.02
a15	0.17	0.00	0.01	0.03	0.02	0.03	0.00	0.01
15:1								
15:0	0.22	0.02	0.02	0.07	0.03	0.01	0.03	0.03
16:4*								
16:3*								
16:2*	0.01	0.01	0.00	0.01	0.00	-0.01	-0.01	0.00
i16	0.13	0.00	0.01	0.05	0.01	0.01		0.00
16:1w9								
16:1w7	0.61	0.18	0.14	0.54	0.11	0.07	0.10	0.22
16:1w5								
16:0	2.27	0.34	0.41	2.75	0.16	0.65	0.28	0.63
10Me17br			0.00				0.00	0.00
i17	0.05	0.00	0.01	0.03	0.01	0.01	0.00	0.01
a17	0.02	0.00				0.01		0.00
17:1	0.07	0.01	0.00	0.09	0.03	0.01		0.02
17:0	0.06	0.00	0.00	0.04	0.00	0.00	0.00	0.01
18:4								
18:3w6	0.01	0.00		0.01	0.00	0.00		
18:2w6	0.03	0.00	-0.01	0.06	0.00	0.01	0.00	0.00
18:3w3								
18:1w9cis	0.09	0.01	0.00	0.09	0.01	0.07	0.00	0.00
18:2w3								
18:1w9t	0.03	0.01	0.01	0.08	0.01		-0.01	0.01
18:1w7	0.02	0.00	0.00	0.01	0.00	0.00	0.00	0.01
18:1w5								
18:0	0.10	0.02	0.02	0.19	0.01	0.02	0.01	0.03
10Me19br								
i19*								
a19*								
19:1*								
19:0 i.s.	0.00	0.00	0.00	0.00	0.00	0.00	0.00	0.00
20:5w6								
20:4w6	0.02	0.00	0.01	0.03	0.00	0.01	0.00	0.01
20:5w3	0.03	0.01	0.03	0.07	0.01	0.01	0.02	0.03
20:3w6	0.02				0.00			
20:4w3	0.00	0.00		0.00				
20:2*								
20:3w3								
20:1w9	0.00	0.00	0.00	0.02				0.00
20:1w7								
20:1w5								
20:0 i.s.	0.02	0.01	0.01	0.03	0.01	0.00	0.01	0.02
21:0 i.s.	0.00	0.00	0.00	0.01	0.00	0.00	0.00	0.01
22:6w6*								
22:6w3	0.03	0.00	0.00	0.02	0.00	0.00	0.00	0.01

22:5w6*								
22:5w3*	0.00	0.00		0.01	0.00			
22:2*								
22:1w9				0.00	0.00			
22:1w7*								
22:0	0.02	0.01	0.01	0.03	0.00	0.00	0.01	0.01
23:0 i.s.	0.00	0.00	0.00	0.01	0.00	0.00	0.00	0.00
24:1	0.00	0.00		0.01	0.00			
24:0	0.04	0.01	0.01	0.04	0.01	0.01	0.01	0.02
Total	4.94	0.74	0.80	4.75	0.49	1.03	0.48	1.18
Sat FA's	3.16	0.48	0.55	3.42	0.23	0.77	0.37	0.83
Mono Unsat	0.82	0.21	0.16	0.85	0.16	0.15	0.09	0.26
Polyunsat	0.15	0.03	0.03	0.22	0.02	0.02	0.01	0.05
Br FA's	0.81	0.02	0.05	0.26	0.08	0.08	0.01	0.04
% Sat FA's	64.03	65.11	69.12	72.03	47.26	75.26	77.03	70.33
% Mono Unsat	16.68	28.27	19.82	17.87	33.16	14.72	19.59	21.98
% Polyunsat	2.97	4.38	4.22	4.59	4.07	2.11	2.15	4.16
% Br FA's	16.32	2.24	6.84	5.51	15.51	7.91	1.23	3.53
BrOdd FA	0.62	0.01	0.05	0.20	0.07	0.07	0.01	0.04
PUFA (3+)	0.12	0.02	0.04	0.15	0.01	0.02	0.02	0.05
%BrOdd FA	12.52	1.81	6.03	4.12	13.51	6.87	1.24	3.27
%PUFA (3+)	2.34	3.14	5.28	3.06	2.86	1.95	3.61	4.09
SCFA	2.72	0.42	0.50	3.04	0.18	0.73	0.31	0.74
LCFA	0.06	0.02	0.02	0.08	0.01	0.01	0.02	0.02
BoshkerBact	0.76	0.02	0.05	0.24	0.07	0.07	0.01	0.04
PUFA (20, 22 3+)	0.10	0.02	0.04	0.13	0.01	0.02	0.02	0.05
%SCFA	55.02	57.02	61.84	64.05	36.47	71.08	65.24	62.64
%LCFA	1.25	2.10	2.25	1.65	1.76	0.76	3.73	1.93
%BoshkerBact	15.38	2.56	6.49	5.06	14.69	6.33	1.84	3.61
%PUFA2022	2.05	2.82	5.28	2.75	2.38	1.99	3.61	4.09
TARFA	0.02	0.04	0.04	0.03	0.05	0.01	0.06	0.03
BrODD/PUFA2022	6.10	0.64	1.14	1.50	5.67	3.45	0.34	0.80
BrODD + PUFA	0.72	0.03	0.09	0.33	0.08	0.09	0.02	0.09
%16:1w7c	12.28	23.92	18.08	11.35	22.30	6.65	20.09	18.56
%205w3	0.67	1.96	3.32	1.45	2.07	0.84	3.28	2.75
%20:4w6	0.35	0.35	1.40	0.64	0.02	0.80	0.63	0.75
BoshkBact/(Boschk+PUFA)	0.88	0.48	0.55	0.65	0.86	0.76	0.34	0.47
PLFA/Bulk	0.23	0.03	0.04	0.04	0.01	0.03	0.02	0.03
PLFA/Bulk (%)	22.96	3.30	3.63	4.50	1.00	3.06	1.90	3.09
BrODD/Bulk (%)	2.87	0.06	0.22	0.19	0.13	0.21	0.02	0.10
BrODD/BrODD+PUFA	0.86	0.39	0.53	0.60	0.85	0.78	0.25	0.44
BrODD/20:5w3+BrODD	0.95	0.48	0.64	0.74	0.87	0.89	0.27	0.54
BrODD/16:1w7+BrODD	0.50	0.07	0.25	0.27	0.38	0.51	0.06	0.15
XS 13C BrODD/C16	0.33	0.06	0.13	0.09	0.46	0.10	0.03	0.07
XS 13C PUFA2022/C16	0.04	0.06	0.10	0.05	0.08	0.03	0.06	0.08
BrODD/SCFA	0.23	0.03	0.10	0.06	0.37	0.10	0.02	0.05
PUFA/SCFA	0.04	0.05	0.09	0.04	0.07	0.03	0.06	0.07
14+16:1w7+20:5w3	1.08	0.27	0.25	0.89	0.14	0.16	0.14	0.36

2	2	2	2	7	7	7	7	7	7	14	14
H5	I2	I4	I6	H1	H3	H5	I2	I4	I6	H1	H3
0.00	0.03	0.00	0.00	0.02	0.13	0.01	0.01	0.04	0.01	0.01	0.00
0.00	0.01			0.01	0.04	0.01	0.01	0.02		0.00	0.00
0.00	0.04	0.00	0.00	0.03	0.52	0.07	0.04	0.07	0.03	0.03	0.01
0.17	0.30	0.02	0.06	0.69	4.76	0.42	0.14	1.07	0.14	0.14	0.08
0.03	0.23	0.01	0.04	0.21	4.50	0.48	0.23	0.32	0.16	0.24	0.04
0.01	0.17	0.01	0.02	0.11	1.52	0.19	0.19	0.15	0.16	0.12	0.02
0.06	0.23	0.03	0.03	0.34	0.99	0.39	0.15	0.35	0.06	0.11	0.09
		0.00									
0.02		0.00	0.00	0.00	0.02	0.02	0.00	0.03	0.00		
0.01	0.03	0.00	0.00	0.05	0.96	0.17	0.04	0.09	0.03	0.03	0.02
0.29	0.38	0.07	0.17	0.94	4.07	0.70	0.21	1.23	0.20	0.21	0.14
	0.03									0.04	0.01
0.53	2.05	0.08	0.51	4.66	30.93	2.70	1.52	8.73	1.37	0.65	0.40
	0.03									0.01	0.00
0.01	0.07	0.00	0.01	0.02	0.89	0.13	0.04	0.07	0.03	0.02	0.01
0.00		0.00	0.01	0.01	0.15	0.05	0.03	0.50	0.02		
0.02	0.21	0.02	0.04	0.11	0.32	0.13	0.05	0.03	0.03	0.05	0.03
0.02	0.11	0.00	0.01	0.11	0.45	0.13	0.05	0.15	0.03	0.03	0.03
0.00		0.00	0.01	0.01	0.11	0.03	0.00	0.02	0.00	0.00	
0.01	0.04	0.00	0.00	0.01	0.22	0.03	0.01	0.03	0.00		
0.03	0.15	0.01	0.07	0.29	0.87	0.08	0.06	0.48	0.05	0.03	0.02
0.04	0.23			0.11	1.03	0.09	0.01	0.31	0.01	0.16	0.09
0.02		0.00	0.01	0.04	0.19	0.03	0.02	0.04	0.01		
0.06	0.16	0.00	0.02	0.23	1.30	0.21	0.10	0.45	0.08	0.06	0.06
	0.02									0.00	0.01
										0.00	
-0.01	0.05	0.00	0.00		-0.02	0.00	0.00	0.00	0.00	0.00	0.01
0.02	0.03	0.00	0.01	0.01	0.14	0.05	0.01	0.06	0.01	0.01	0.02
0.05	0.05	0.01	0.01	0.10	0.35	0.19	0.04	0.14	0.04	0.05	0.04
					0.11	0.02		0.06			
0.00				0.01	0.03		0.00	0.02			
											0.02
0.01					0.01	0.02	0.01	0.04		0.00	
0.04	0.17	0.00	0.01	0.06	0.30	0.06	0.02	0.14	0.02	0.02	0.01
0.00	0.03	0.00	0.00	0.00	0.04	0.03	0.01	0.02	0.00	0.00	0.01
0.01	0.01	0.00	0.00	0.03	0.24	0.07	0.01	0.05	0.02	0.01	0.01

0.00	0.01			0.00	0.02	0.02	0.00	0.01	0.01	0.00	0.01
	0.00									0.00	0.02
							0.00	0.02			
0.01	0.05	0.00	0.00	0.06	0.36	0.07	0.02	0.16	0.02	0.02	0.02
0.00	0.04	0.00	0.00	0.00	0.05	0.00	0.01	0.00	0.00	0.01	0.03
	0.02			0.02	0.14	0.01	0.01	0.11	0.01		0.01
0.01	0.09	0.00	0.01	0.09	0.66	0.08	0.05	0.25	0.05	0.04	0.01
1.46	4.76	0.29	1.04	8.33	56.01	6.59	3.07	15.12	2.61	2.10	1.20
0.87	3.03	0.14	0.65	6.21	39.62	4.01	2.04	11.22	1.77	1.07	0.69
0.41	1.01	0.11	0.28	1.51	6.62	1.07	0.38	2.26	0.32	0.50	0.30
0.12	0.14	0.02	0.04	0.17	1.24	0.43	0.09	0.43	0.09	0.08	0.10
0.06	0.58	0.02	0.07	0.44	8.53	1.09	0.56	1.21	0.43	0.46	0.10
59.44	63.68	49.15	62.17	74.57	70.74	60.81	66.45	74.20	67.83	50.69	57.47
28.08	21.18	36.54	27.29	18.09	11.81	16.21	12.42	14.95	12.09	23.75	25.37
8.10	2.86	7.08	3.57	2.09	2.22	6.51	2.90	2.84	3.61	3.82	8.55
4.37	12.28	7.23	6.97	5.25	15.23	16.46	18.24	8.00	16.48	21.74	8.60
0.05	0.46	0.02	0.06	0.35	7.06	0.85	0.48	1.04	0.36	0.38	0.07
0.09	0.09	0.01	0.03	0.16	1.01	0.38	0.07	0.36	0.09	0.08	0.07
3.63	9.63	6.82	6.23	4.24	12.60	12.88	15.64	6.89	13.94	18.17	6.02
5.98	1.95	5.13	3.13	1.93	1.80	5.83	2.39	2.40	3.56	3.81	5.83
0.70	2.38	0.10	0.57	5.36	35.82	3.12	1.67	9.84	1.52	0.80	0.48
0.03	0.15	0.00	0.01	0.16	1.01	0.15	0.07	0.41	0.07	0.05	0.03
0.07	0.47	0.02	0.07	0.44	7.68	0.94	0.51	0.68	0.39	0.42	0.08
0.08	0.09	0.01	0.02	0.15	0.90	0.36	0.07	0.34	0.09	0.08	0.07
47.65	49.98	34.47	55.14	64.35	63.97	47.32	54.36	65.06	58.36	38.00	39.90
1.73	3.04	1.66	1.17	1.88	1.81	2.33	2.15	2.70	2.79	2.45	2.54
4.98	9.80	7.26	6.58	5.32	13.71	14.30	16.58	4.50	15.04	20.12	6.82
5.68	1.95	3.97	2.02	1.81	1.60	5.39	2.24	2.23	3.41	3.72	5.83
0.04	0.06	0.05	0.02	0.03	0.03	0.05	0.04	0.04	0.05	0.06	0.06
0.64	4.95	1.72	3.08	2.35	7.86	2.39	6.99	3.09	4.09	4.88	1.03
0.14	0.55	0.03	0.09	0.50	7.95	1.20	0.55	1.38	0.45	0.46	0.14
19.87	7.87	24.09	16.11	11.31	7.26	10.62	6.79	8.11	7.64	10.17	11.45
3.70	0.97	3.54	1.29	1.24	0.62	2.90	1.27	0.95	1.40	2.29	3.30
1.03	0.56	0.43	0.84	0.17	0.25	0.77	0.39	0.36	0.57	0.64	1.29
0.47	0.83	0.65	0.76	0.75	0.90	0.73	0.88	0.67	0.82	0.84	0.54
0.04	0.05	0.02	0.03	0.04	0.05	0.02	0.03	0.02	0.04	0.00	0.02
3.85	5.42	1.64	3.22	4.01	4.93	1.67	3.19	1.97	3.99	0.23	2.05
0.14	0.52	0.11	0.20	0.17	0.62	0.21	0.50	0.14	0.56	0.04	0.12
0.39	0.83	0.63	0.75	0.70	0.89	0.70	0.87	0.76	0.80	0.83	0.51
0.50	0.91	0.66	0.83	0.77	0.95	0.82	0.92	0.88	0.91	0.89	0.65
0.15	0.55	0.22	0.28	0.27	0.63	0.55	0.70	0.46	0.65	0.64	0.34
0.14	0.23	0.26	0.13	0.10	0.25	0.35	0.33	0.08	0.29	0.65	0.21
0.16	0.05	0.14	0.04	0.03	0.03	0.13	0.05	0.04	0.07	0.12	0.18
0.08	0.19	0.20	0.11	0.07	0.20	0.27	0.29	0.11	0.24	0.48	0.15
0.12	0.04	0.12	0.04	0.03	0.03	0.11	0.04	0.03	0.06	0.10	0.15
0.51	0.72	0.10	0.24	1.74	9.18	1.31	0.39	2.44	0.38	0.40	0.26

14	14	14	14
H5	I2	I4	I6
0.00	0.00	0.03	0.01
0.00	0.00	0.02	0.00
0.02	0.00	0.07	0.01
0.28	0.02	2.19	0.19
0.13	0.03	0.65	0.13
0.06	0.02	0.36	0.03
0.34	0.05	0.70	0.03
0.02	0.01	0.19	0.01
0.42	0.06	2.24	0.18
0.03	0.01	0.14	0.01
1.42	0.19	10.36	1.22
0.01		0.04	0.01
0.02	0.01	0.20	0.02
0.11	0.03	0.51	0.03
0.07	0.02	0.28	0.02
0.01	0.00	0.07	
0.02	0.01	0.17	
0.06	0.02	1.07	0.09
0.22	0.07	1.21	0.21
0.12	0.03	0.93	0.11
0.01	0.00	0.05	0.01
		0.03	
0.02	0.01	0.08	0.00
0.02	0.01	0.20	0.01
0.09	0.03	0.35	0.05
0.02	0.01	0.14	0.01
0.03	0.02	0.14	0.03
0.01	0.00	0.09	0.03
0.02	0.01	0.05	0.01

0.01	0.00	0.04	0.00
	0.01	0.01	0.00
0.03	0.01	0.15	0.03
0.02	0.01	0.07	0.02
0.00	0.00	0.07	0.01
0.04	0.01	0.23	0.05
3.62	0.71	22.75	2.48
2.31	0.34	14.90	1.65
0.86	0.21	5.39	0.54
0.17	0.07	0.88	0.07
0.28	0.08	1.58	0.21
63.92	48.80	65.48	66.77
23.66	30.34	23.68	21.94
4.78	9.36	3.89	3.01
7.63	11.50	6.95	8.29
0.21	0.06	1.23	0.18
0.15	0.05	0.70	0.07
5.87	8.75	5.42	7.11
4.10	7.24	3.07	2.92
1.70	0.22	12.58	1.41
0.07	0.02	0.39	0.08
0.24	0.06	1.27	0.17
0.14	0.05	0.63	0.07
47.10	30.55	55.30	56.82
2.06	3.29	1.70	3.03
6.52	9.01	5.60	6.95
3.94	6.98	2.78	2.92
0.04	0.11	0.03	0.05
1.49	1.25	1.95	2.44
0.36	0.11	1.87	0.25
11.71	9.19	9.84	7.25
2.46	3.71	1.52	1.86
0.69	1.61	0.88	0.59
0.62	0.56	0.67	0.70
0.12	0.00	0.58	0.00
12.39	0.24	58.30	0.20
0.73	0.02	3.16	0.01
0.60	0.56	0.66	0.71
0.70	0.70	0.78	0.79
0.33	0.49	0.36	0.50
0.17	0.34	0.12	0.14
0.10	0.26	0.06	0.06
0.12	0.29	0.10	0.13
0.08	0.23	0.05	0.05
0.80	0.11	4.77	0.41